

ESTIMATION OF EPISODIC GROUNDWATER RECHARGE
IN SEMI-ARID FRACTURED HARD ROCK AQUIFERS.

By

ETTIENNE VAN WYK

Dissertation submitted in the fulfillment of the requirements for the degree
of

DOCTOR OF PHILOSOPHY

In the Faculty of Natural and Agricultural Sciences,
Department of Geohydrology
University of the Free State
Bloemfontein, South Africa.

August 2010

Promoter: Prof. G. J. van Tonder
Co-Promoter: Dr. P.D. Vermeulen.

ACKNOWLEDGEMENTS.

I would like to thank the following persons and institutions for the opportunity offered to me and for their consideration and support in making it possible to endure on a long and multi-faceted study to finally submit my doctoral thesis on episodic groundwater recharge in fractured hard rock terrains. I would therefore like to thank:

My Promoter, Professor Gerrit J. van Tonder, who has guided me over the years as a friend, colleague and advisor on episodic recharge principles and semi-arid livelihoods. My Co-promoter, Dr. Danie Vermeulen, who guided me on the framework of the script and practical and administrative matters. To all staff members of the Institute for Groundwater Studies, Univ. of the Free State who through the years treated me as a supporting colleague and for including me in many of their training support programmes.

The Department Water Affairs for the bursary and time, especially the Chief Director: Water Resources Information Management, Mr. Mbangiseni P. Nepfumbada and the Director: Hydrological Services, Mr. L. Zacharia Maswuma for their substantial support and interest in the subject.

My 'isotope' friends, Prof. Balt Verhagen and Mr. Siep Talma who guided me for many years in practical experience, interpretation of isotope hydrology and invaluable sources of information.

My personnel from the sub-Directorate: Groundwater Resources Assessment and Monitoring (Adaora Okonkwo, Thiru Chetty, Nico De Meillon, Theodorus Moolman, Frans Manamela and Sam Mmabatswa) who, on short notice, took over functions, helped with decisions, prepared data and still maintained the monitoring site Networks and equipment. DWA officials from the regional offices, Messrs. W du Toit (Limpopo Region) and P. Leon Havenga (Western Cape Region) and staff who supported me with downloading data, equipment and 'sommer' general support.

Thanks to Jaco de Lange (proof-reading) and Olga de Beer (construction of script framework) during the final preparations to the document.

Then my wife, Magriet, for her faithful companionship, typing 'here and there' and especially for her prayers; and

To my family who provided much needed emotional support and encouragement.

SUMMARY.

The semi-arid regions of southern Africa cover large portions of settled land where domestic and agricultural activities depends on isolated groundwater systems replenished by irregularly occurring rainfall events. Southern African rainfall patterns are regulated by the annual oscillation of winter-summer weather systems and most of all, abrupt changes in regional atmospheric patterns, which may result in either wet/dry cycles. Given the highly differential hydro-climatic conditions and hydrogeological environment in semi-arid regions, effective groundwater recharge events are episodic in nature and largely occur once in every five years.

Sustainable, medium-term management of local groundwater resources requires dynamic hydrological information to ensure a healthy supply-demand balance; thus requiring dedicated hydrological monitoring. High-level monitoring programmes on a few experimental sites have produced localised hydrological data, which illustrate how erratic groundwater resources are replenished. For many years, it was postulated that groundwater resources were recharged every time the total annual rainfall peaks a certain threshold. This postulation may hold in humid regions, but surely not elsewhere in the drier parts of South Africa.

Semi-arid regions portray a flattish regional landscape with occasionally elevated parent rock windows and mountainous regions. Soil cover is restricted to low-relief areas, and lacks the thick mature soils distinctive of the humid areas. Fractured hard rock windows with very little soil cover represent potential groundwater recharge terrains, allowing recharge-producing surplus rainfall to infiltrate directly into the underlying aquifer. The hydrogeological conditions of hard rock terrains in the same-arid environment do vary in terms of the rock types and their response on weathering processes. Nonetheless, an array of joints and fractures running from ground surface into the SZ represents fast and effective pathways when episodic high rainfall events occur. Mature soil/regolith profiles in plain areas enhances surface run-off and support local floods in rivulets where riparian vegetation and open-water evaporation intercepts most of the available bank storage and depression recharge.

Atmospheric moisture is, in principal, generated by warm, evaporating maritime waters, and is therefore marked by its hydrochemical signature. This signature changed abruptly during its continental migration, and finally manifests as cloud water. Winter rainwater specifically demonstrates the impact of oceanic aerosols, hence characterized by a prominent NaCl composition. Summer rainwater is a diluted version due to continental rainfall/evapotranspiration events, and is transformed by anthropogenic airborne substances peaking during the late-winter months. The hydrogeochemical composition of rainwater is therefore quite diverse, and needs logic

monitoring to understand its seasonal cyclic oscillation. Short-term hyetograph observations report episodic rainfall events, occurring mostly over the January-March period of wet hydrological cycles. These are spaced over a period of 4 to 8 days, of which at least one rain event exceeds ~45 mm, associated with a rain-rate intensity of $>1.5 \text{ mm}\cdot\text{h}^{-1}$.

Extraordinary depleted rainwater hydrochemistry and isotopic compositions are associated with these rain weeks, which are significantly different from normal seasonal concentrations. Wet Cl^- concentrations during these high rainfall periods are almost an order of magnitude lower than the average annual values.

Hyetograph-hydrograph sets confirm that extraordinary groundwater recharge occurs as the result of episodic rainfall events. Hydrogeochemical profiling in the upper section of the unsaturated zone verify the presence of different compositions which probably indicate different modes of recharged rainwater percolation in fractured, hard rock terrains. Hard rock profile sections below the rebound water table interface containing almost 50% less Cl^- than country-wide background values of $\sim 40 \text{ mg}\cdot\text{L}^{-1}$.

Isotopic compositions in a typical rain week period report similar depleted concentrations and resemble a prominent amount effect. Such depleted rainwater is merely linked to specific seasons, for example the rainfalls of 2003-2004, 2005-2006 and 2007-2008 hydrological years can be clustered as high rainwater input periods with notable lighter isotopic compositions; around $-7.5\text{‰ } \delta^{18}\text{O}$, $-41\text{‰ } \delta^2\text{H}$. The fact that most of the two (2) meter vertical profiles reported relatively negative isotopic compositions ($-8\text{‰ } \delta^{18}\text{O}$, $-44\text{‰ } \delta^2\text{H}$), indicates a high probability of preferential recharge with pristine rainwater with even more negative isotopic composition.

Direct groundwater recharge estimations from local, short-term rainfall and groundwater rebound stage hydrochemical data proposes a recharge value $<2\%$ in most flat lying, semi-arid regions. Although fractured hard rock terrains are isolated, it allows in the order of 4%, where as local mountainous areas are high at 14%; obviously enhanced by orographic rainfall development. Recharge on dolomitic terrains are highly variable due to diverse ground surface conditions, and may vary between 6% in flat lying plains to 13% in mountainous regions (Kuruman Hills at Kuruman).

Groundwater recharge varies significantly spatially. The control by prominent soil/regolith capings is that high that establishing realistic recharge figures for a particular area, will require a dedicated soil mapping programme to identify direct recharge terrains.

CONTENT.

Acknowledgements.....	ii
Summary.....	iii
Table of Contents.....	v
Tables.....	ix
Figures.....	xi
List of Symbols.....	xvii
List of Abbreviations.....	xxii

TABLE OF CONTENTS.

1. INTRODUCTION.....	1
1.1. GENERAL RESEARCH STATEMENT.....	1
1.2. RESEARCH OBJECTIVES.....	2
1.3. RESEARCH STATEMENT.....	3
1.4. METHODOLOGIES DEVELOPED AND APPLIED.....	4
1.5. DEFINITION OF TERMS.....	6
1.6. THESIS STRUCTURE.....	9
2. SOUTH AFRICAN HYDROLOGICAL INFORMATION SCENERY.....	12
2.1. INTRODUCTION.....	12
2.2. HISTORY OF HYDROLOGICAL DATA GENERATION IN SOUTHERN AFRICA.....	17
2.2.1. Hydrological Monitoring Programmes Implemented by the Department.....	18
2.2.2. International Water Resources Monitoring Obligations, SADC Region.....	18
2.2.3. Hydrological Monitoring by Water Users.....	19
2.3. MANAGEMENT FRAMEWORK FOR GROUNDWATER MONITORING PROGRAMMES.....	20
2.3.1. Chapter 14 of NWA (1998): Monitoring, Assessment and Information.....	20
2.3.2. Groundwater Monitoring Management Framework.....	21
2.3.2.1. Administrative Levels.....	23
2.3.2.2. Monitoring Programme Types.....	24
2.3.2.3. Linkages between Monitoring Levels and Types.....	26
2.4. GROUNDWATER QUANTITY MONITORING PROGRAMMES (WATER TABLE).....	27
2.4.1. Introduction.....	27
2.4.2. Attribute Configuration and Measurement Interval.....	27
2.4.3. Raw Data Generation and Quality Control.....	29
2.4.4. National Groundwater Level Monitoring Programme.....	31
2.5. GROUNDWATER QUALITY PROGRAMMES (HYDROGEOCHEMISTRY).....	32
2.5.1. Introduction.....	32
2.5.2. The National Groundwater Quality Monitoring Programme (NGwQMP).....	33
2.5.3. Analytical Requirements for Groundwater Research Investigations.....	35
2.6. HYDROGEOLOGICAL DATA BASES AND SUPPORTING SOFTWARE.....	35
2.6.1. Introduction.....	35
2.6.2. Data/Information Generation Procedures.....	36
2.6.3. Storage Processes and Facilities.....	38
2.6.4. Monitoring Site and Piezometric Level Information.....	39
2.6.4.1. National Groundwater Archive (NGA).....	39
2.6.4.2. Hydstra.....	39

2.6.4.3.	Hydras 3.	40
2.6.5.	<i>Hydrogeochemistry</i>	41
2.6.5.1.	Water Quality Management System (WMS)	41
2.6.5.2.	Collective Hydrochemistry Analysis and Reporting Tool (CHART)	41
2.7.	A DEDICATED GEOHYDROLOGICAL MONITORING PROGRAMME	42
2.7.1.	<i>Introduction</i>	42
2.7.2.	<i>Programme Objective and Network Design</i>	43
2.7.2.1.	Introduction	43
2.7.3.	<i>Climate Monitoring</i>	45
2.7.3.1.	Introduction	45
2.7.3.2.	The portable Davis Climate/Weather Station	47
2.7.4.	<i>Precipitation Depth Time-series Monitoring</i>	48
2.7.4.1.	Introduction	48
2.7.4.2.	Rainfall Depth Logging Apparatus	49
2.7.4.3.	Network Scope and Design	50
2.7.4.4.	Rainfall Depth Time-series Logging	51
2.7.5.	<i>Rainwater Quality Monitoring Programme</i>	51
2.7.5.1.	Introduction	51
2.7.5.2.	Rainwater Sampling Apparatus	52
2.7.5.3.	Rainwater Quality	52
2.7.5.4.	Bulk Periodic Rainwater Sampling	53
2.7.5.5.	Rainfall event sampling	55
2.7.6.	<i>Groundwater Table Time-series Monitoring</i>	56
2.7.6.1.	Introduction	56
2.7.6.2.	Theory	56
2.7.6.3.	Apparatus	57
2.7.7.	<i>Groundwater Hydrogeochemical Time-Series Monitoring</i>	57
2.7.7.1.	Introduction	57
2.7.7.2.	Theory	58
2.7.7.3.	Apparatus for sampling groundwater from saturation zone	59
2.7.7.4.	Sampling surface water runoff in a rivulet	62
2.8.	SUMMARY	62
3	SOUTHERN AFRICAN SEMI-ARID ENVIRONMENTS	64
3.1	INTRODUCTION	64
3.1.1	<i>Ground Surface Characteristics</i>	66
3.1.2	<i>Southern Hemisphere Weather Patterns</i>	67
3.1.3	<i>Southern African Climate Variability During the Late Quaternary Period</i>	69
3.1.4	<i>Modern-time Climate Variations</i>	70
3.2	HYDROMETEOROLOGY	73
3.2.1	<i>Introduction</i>	73
3.2.2	<i>Generation of Atmospheric Vapor Mass Over Southern Africa</i>	74
3.2.2.1.	Summer Rainfall Regions	74
3.2.2.2.	Winter Rainfall Regions	75
3.2.3	<i>Physical Characteristic of the southern African Maritime Waters</i>	76
3.3	SEMI-ARID HOMOCLIMATE STATE VARIABLES	77
3.3.1	<i>Temperatures and Atmospheric Humidity</i>	77
3.3.2	<i>Evaporation and Transpiration</i>	78
3.3.2.1	Estimation of Potential ET (ET_P)	80
3.3.2.2	Relationship between ET_P and Actual ET (ET_A)	82
3.4	SUMMARY	83
4	HYDROGEOLOGICAL PORTRAYAL	84
4.1	INTRODUCTION	84
4.2	THE SOUTHERN AFRICAN GEOMORPHOLOGICAL HISTORY	85
4.2.1	<i>The Late Mesozoic Era</i>	85
4.2.2	<i>Neogene Tectonic Uplift and Erosion Cycles</i>	86
4.2.3.	<i>Gondwanaland Fragmentation, Karoo Magmatism and Erosional Unloading</i>	87

4.2.4. Hard rock surfaces.....	89
4.2.5. The Unsaturated Zone Reservoir.....	92
4.2.5.1. Soil profile characteristics.....	93
4.2.5.2. Fractured and Weathered Hard Rock Profiles.....	95
4.2.6. The Saturated Zone.....	95
4.2.6.1. Upper fractured and weathered zone (UFWZ).....	97
4.2.6.2. Deep Bedrock Fractures.....	97
4.2.7. Karstic Profile and Plane.....	98
4.3. HYDRO-LITHOLOGICAL CHARACTERISTICS OF HARD ROCK FORMATIONS.....	101
4.3.1. Introduction.....	101
4.3.2. Vertical Jointing and Fracturing.....	102
4.3.2.1. Micro Jointing/Fracturing.....	105
4.3.2.2. Macro Jointing/Fracturing.....	105
4.3.2.3. Master Jointing/Fracturing.....	106
4.3.3. Horizontal Jointing/Fracturing.....	108
4.4. UNSATURATED-SATURATED ZONES FLOW REGIME.....	108
4.4.1. Introduction.....	109
4.4.2. The Unsaturated Zone Reservoir's Flow Path.....	109
4.4.2.1. The Upper Unsaturated Zone Reservoir (Including the Rooting Zone).....	110
4.4.2.2. The Lower Unsaturated Zone Reservoir (Excluding the Rooting Zone).....	112
4.5. BASIC HYDRAULIC CONCEPT OF UNCONFINED GROUNDWATER FLOW.....	113
4.5.1. Physics of Groundwater Flow: Darcy Principle.....	113
4.5.2. Hydraulic Concepts of a Water Table Accretion Case.....	116
4.5.3. Recharge Concept of a Simple (groundwater) Reservoir Model.....	119
4.6. SUMMARY.....	122
5. HYDROGEOCHEMICAL FEATURES OF THE RECHARGE CYCLE	124
5.1 RAINWATER HYDROCHEMISTRY.....	124
5.1.1 Analytical Criteria.....	124
5.1.2 Terrigenous Dust and Airborne Pollution.....	126
5.1.3 Hydrochemical Properties: Summer Rainwater.....	129
5.1.3.1 Hydrochemical Composition.....	129
5.1.4 Hydrochemical Properties: Winter Rainwater.....	131
5.1.4.1 Macro element compositions.....	131
5.1.5 Temporal Responses and Trends.....	136
5.1.6 Spatial Variations and Trends.....	140
5.2 ISOTOPE HYDROLOGY OF SOUTH AFRICAN RAINWATER.....	142
5.2.1 Standards and Isotopic Fractionation.....	142
5.2.2 The Meteoric Water Line (or Isotope Line).....	144
5.2.3 Temporal Responses and Trends in ESI Compositions.....	146
5.2.4 Summary.....	150
5.3 HYDROGEOCHEMICAL COMPOSITION AT THE WATER TABLE INTERFACE.....	150
5.3.1 The Origin of Traceable Dissolved Rock Salts in Groundwater.....	151
5.3.2 Groundwater Hydrochemistry of Typical Rock Formations in South Africa.....	153
5.3.3 Groundwater Hydrogeochemistry: Spatial and Temporal Variations.....	156
5.3.4 Groundwater Hydrogeochemistry - Aquifer Unit Context.....	161
5.3.4.1 Temporal Variations in Hydrogeochemistry Composition at Variable Water Table Elevations.....	162
5.3.4.2 Vertical (depth) Variations in Hydrogeochemical Composition.....	164
5.4 CHLORIDE MASS BALANCE APPLICATION.....	174
5.4.1 Background.....	174
5.4.2 Traditional Application.....	175
5.4.3 Application: Rainwater - Groundwater Cl ⁻ Balances.....	176
5.4.4 Atmospheric Chloride Depositions.....	178
5.4.5 Chloride Concentration in the Unsaturated Zone.....	179
5.4.5.1 Bypassing the Rooting Zone.....	180
5.4.5.2 Impact of Multi-Modal Flow on Chloride Load in Saturated Zone.....	182
5.4.5.3 Chloride Tracer Application in Hard Rock Terrains.....	183

5.4.6	<i>Conclusions</i>	184
5.5	CORRELATION BETWEEN RAINWATER AND GROUNDWATER HYDRO-TRACERS.....	185
5.5.1	<i>Premise</i>	186
5.5.2	<i>ESI Signals from the Saturated Zone</i>	187
5.6	SUMMARY OF HYDROGEOCHEMICAL FEATURES OF THE RECHARGE CYCLE.....	191
6	EPISODIC RECHARGE EVENTS IN SEMI ARID HARD ROCK ENVIRONMENTS.	193
6.1.	RAINWATER - GROUNDWATER INTERACTION.....	193
6.1.1.	<i>Introduction</i>	193
6.1.2.	<i>Temporal Variability of Episodic Rainfall and Groundwater Recharge</i>	194
6.1.2.1.	Frequency of Exceedance.....	194
6.2.	EPISODIC RECHARGE EVENTS.....	199
6.2.1.	<i>Introduction</i>	199
6.2.2.	<i>Spatial Variability of Groundwater Recharge</i>	200
6.2.2.1.	Direct Mode.....	200
6.2.2.2.	Indirect Modes.....	201
6.2.3	<i>Groundwater Table Hydrographs</i>	201
6.2.4	<i>Rainfall Intensities and Water Table Responses</i>	207
6.2.5	<i>Hydro-Lithologic Model of Hard Rock Recharge Terrains</i>	213
6.3	CONCEPTUAL FLOW REGIME AT DIRECT RECHARGE TERRAINS.....	216
6.3.1	<i>Introduction</i>	216
6.3.2	<i>Enhancement of Episodic Recharge in Fractured Hard Rock Terrains</i>	217
6.3.3	<i>Hydraulic Characteristics of Water Table Rebound</i>	219
6.3.4	<i>Hydrogeochemistry Characteristics of an Episodic Recharge Event</i>	225
6.4	RECHARGE ESTIMATES FOR DIFFERENT HYDROGEOLOGICAL TERRAINS.....	229
6.4.1	<i>Introduction</i>	229
6.4.2	<i>Quantification of Episodic Recharge Events</i>	230
6.4.2.1	<i>Recharge Estimations for Some Experimental Monitoring Terrains</i>	232
6.5	SUMMARY.....	239
7.	CONCLUSIONS AND RECOMMENDATIONS: EPISODIC GROUNDWATER RECHARGE	
	241	
7.1	BACKGROUND.....	241
7.2	HYDROMETEOROLOGY CONDITIONS CONTROLLING EPISODIC RECHARGE EVENTS.....	242
7.2.1	<i>Ground surface conditions</i>	242
7.2.2	<i>Rainfall</i>	243
7.2.2.1	The Narrative of Episodic Rainfall and Recharge Event(s).....	244
7.2.2.2	Frequency of Exceedance: Episodic Rain Events.....	245
7.2.2.3	Rainfall Rates and Design Rainfall Pattern.....	246
7.3	HYDROGEOCHEMICAL INDICATORS OF EPISODIC RECHARGE EVENTS.....	247
7.3.1	<i>Monitoring Natural Rainwater Tracers</i>	247
7.3.2	<i>Monitoring Natural Groundwater Tracers</i>	248
7.3.3	<i>Environmental Isotopes</i>	250
7.4	HARD ROCK HYDROGEOLOGY IN DIRECT RECHARGE TERRAINS.....	252
7.4.1	<i>Hard Rock Features</i>	252
7.4.2	<i>Matrix Flow and Hydrochemistry Signal from Matrix Storage</i>	253
7.4.3	<i>Bypass Flow Mode in Vertical Recharge Cases</i>	254
7.4.4	<i>Summary of Groundwater Recharge in Different Rock Types</i>	255
7.5	EPISODIC GROUNDWATER RECHARGE.....	259
7.5.1	<i>Application of the CMB Methodology in the case of Episodic Recharge Events</i>	259
7.6	RECOMMENDATIONS.....	260
8.	REFERENCES.....	264
9.	APPENDIXES.....	273

TABLES.

Table 2.1. Summary of active surface water monitoring sites 2009 (Source: DWA).....	13
Table 2.2. Climate variables logged by the Davis Instruments weather station unit	47
Table 3.1. Classification of arid environments (Thomas and Shaw 1991)	66
Table 5.1. Summer rainfall hydrochemical composition ($\text{mg}\cdot\ell^{-1}$ and $\mu\text{eq}\cdot\ell^{-1}$) in semi-arid/arid regions of South Africa	130
Table 5.2. Average LLHc compositions ($\text{mg}\cdot\ell^{-1}$ and $\mu\text{eq}\cdot\ell^{-1}$; harmonic means) in the winter rainfall, semi-arid regions of South Africa	133
Table 5.3. Summary of early seasonal rainwater hydrochemistry ($\text{mg}\cdot\ell^{-1}$) in semi-arid region of South Africa: 2002-2009.	138
Table 5.4. Summary of peak seasonal rainwater hydrochemistry ($\text{mg}\cdot\ell^{-1}$) in semi-arid region of South Africa: 2002-2009.	138
Table 5.5. Summary of dry seasonal rainwater hydrochemistry ($\text{mg}\cdot\ell^{-1}$) in semi-arid region of South Africa: 2002-2009.	139
Table 5.6. Rainwater Cl^- from six (6) monitoring sites in the semi-arid summer rainfall regions of South Africa, 2003-2009.	141
Table 5.7. Table of LMWL's from this study and from published literature.	145
Table 5.8. Groundwater hydrochemical concentration ($\text{mg}\cdot\ell^{-1}$) from selected areas in South Africa: Some historic (pre-1947) values compared with modern values from similar geological groupings.....	155
Table 5.9. Total Cl^- values in rainwater and groundwater observed at Beaufort West monitoring terrains with different elevations, maximum pan = 80 km	157
Table 5.10. Chloride values in rainwater and groundwater from different locations in the Stella area at similar elevations (1320m amsl) but different rock formations and recharge terrains (soil/regolith covered plains versus hard rock windows).	160
Table 5.11. Hydrogeochemistry skim sampling results at monitoring site G47584, Bokfontein, Upper Kuruman River Catchment. (Recharge Terrain Type: Dolomite, fractured hard rock terrain)	162
Table 5.12. Hydrogeochemistry skim sampling results at monitoring sites in the Beaufort West area (Recharge Terrain Type: Sedimentary, fractured hard rock terrains).	163
Table 5.13. Results of stage sampling programme at monitoring site G29870BE in De Hoop Poort (Type: Karoo sedimentary hard rock terrain).	173
Table 5.14. Total wet and dry Cl^- deposition ($\text{mg}\cdot\text{m}^{-2}\cdot\text{y}^{-1}$).....	179

Table 5.15. Illustration of altitude effect in two hard rock terrains in Beaufort West (statistics: $n \approx 7$ and used harmonic means of samples collected between 2003 and 2009)	190
Table 6.1. Monthly occurrences of rainfall events for a typical semi-arid region: Vryburg rainfall from 1913 to 2008 monitored at Station No. 468318.....	197
Table 6.2. Return periods (years) for three categories of rainfall depths for the Vryburg weather station (SAWS station no. 468318).....	198
Table 6.3. Rainfall intensities, duration and local water table responses calculated from hyetograph-hydrograph sets.	209
Table 6.4. Karoo fractured hard rock terrain, episodic recharge (2007-2008).....	233
Table 6.5. Karoo fractured hard rock terrain with soil/regolith cover on peneplain, episodic recharge (2007-2008).	234
Table 6.6. Karoo fractured hard rock terrain in Nuweveld Mountains, episodic recharge (2007-2008).	235
Table 6.7. Dolomite hard rock terrain in Ghaap Plateau, Kuruman District, episodic recharge (2007-2008).....	236
Table 6.8. Savanna peneplain with local hillocks consisting of Kraaipan Group BIF's (2007-2008).	238
Table 7.1. Chloride concentration in rainwater over a three tier interval of the HC for summer and winter rainfall in semi-arid regions, 2002 to 2009 (HARmean).....	248

FIGURES.

Figure 2.1. River flow at the Mooi River Gauging Station C2H001.....	12
Figure 2.2. The time-series flow response (cumecs) at the Mooi River gauging station C2H001 since 1904.	14
Figure 2.3. Dolomite spring water quality at the Rhenosterfontein spring (A3H0017) in the Northwest Province (S25.72110°; E026.13540°, 1435 m amsl).	15
Figure 2.4. Initial acid mine water decant from a decommissioned borehole next to the Twee Lopies Spruit in the West Rand (S26.11519; E027.72303, 1664 m amsl).....	22
Figure 2.5. Graphical presentation of the linkage between Monitoring Programme Levels (administration, funding and management) and Monitoring Programme Types (physical networks, instrumentation and operation and maintenance).	26
Figure 2.6. A typical time-series electronically-generated water level, temperature, and electrical (specific) conductivity datastring as recorded by a Schlumberger CTD data logging device	28
Figure 2.7. Spring-flow gauging weir (a 2' Parchall Flume) at Kuruman A-Spring with instrumentation housing for Ott Thalimedes water level logger	29
Figure 2.8. Borehole pair with a DWA rainfall logging/sampling unit on the LRAS, District Vredenburg, Western Cape	30
Figure 2.9. The current national coverage of monitoring sites in South Africa for obtaining groundwater level data	32
Figure 2.10. Illustration of a monitoring cycle showing the general processes required to generate hydrogeological information to satisfy the objectives of a specific monitoring programme	36
Figure 2.11. A Hydstra composite annual cumulative rainfall and waterlevel time-series plot of a monitoring site A2N0715, in the Bapsfontein – Delmas area.....	40
Figure 2.12. The De Hoop Dyke in De Jagers Pass, District Beaufort West, showing a ± 3 m thick, dolerite dyke intruded into late Permian-earlyTriassic Beaufort Group sediments.	44
Figure 2.13. A special purpose network configuration for monitoring the hydrological state variables required for groundwater recharge estimations at the De Hoop Poort monitoring site.	46

Figure 2.14. A DWA rainfall logger/bulk-sampler developed by the author and incorporated into groundwater monitoring networks in South Africa	49
Figure 2.15. The total hyetograph for the Spitskop monitoring site (G43988_RF) at Stella, District Vryburg for the 2000-2001 to 2008-2009 HCs.	51
Figure 2.16. Showing a column of rainwater collected in the acrylic collector tube of the DWA rainfall logging/sampler unit at G29870BB_RF, De Hoop Poort monitoring site, District Beaufort West.	54
Figure 2.17. The internal configuration of the RES unit with the integrated manifold and the 10 mm sample aliquots.	55
Figure 2.18. The Skim groundwater sampler used to sample the upper-most 19 mm of the SZ in a borehole.....	60
Figure 2.19. A fully retrieved 3m water column from borehole G29870BE, De Hoop Poort, District Beaufort West	61
Figure 2.20. A 120 ml aliquot (sample cell) with intake siphon and air outlet.	61
Figure 3.1. Boundaries of the climate zones in southern Africa based on the Meigs (1953) and Grove (1977) demarcations (cited in Thomas and Shaw 1991, p. 7).....	65
Figure 3.2. Topographical depressions in Kalahari Weissrand Plateau, Namibia showing low-lying pan surfaces and unique local drainage systems collecting infiltration-excess overland flows (Bar = 1 km)	67
Figure 3.3. Synoptic weather patterns over southern Africa during the summer and winter climax weather period showing the seasonal migration of prominent weather systems over southern Africa.	68
Figure 3.4. Long-term annual rainfall time-series log for Vryburg, SAWS Weather Station No. 468318, Northern Cape Province.....	72
Figure 3.5. Reconstructed groundwater table fluctuation in the Lower Kuruman River section between Van Zylsrus and Askham showing a dramatic recharge event following the 1976 flood period and long-term recession.	73
Figure 3.6. Observation of rainfall and ET values at the Stella, Appelkoosboom monitoring site between 14-12-2009 and 02-02-2010, including a rain week period recording 199 mm.....	81

Figure 4.1. Planar view of jointed Karoo-Beaufort Group mudstone, De Hoop, District Beaufort West, illustrating superimposition of a NNW and W-E set of master-joints	90
Figure 4.2. Vertical and horizontal fracturing in a Karoo-Beaufort Group sandstone lens overlying massive Karoo mudstones, Nuweveld Mountains, District Beaufort West (S32.04233° E022.71436°, 1514 m amsl)	91
Figures 4.3. Typical structural make up of an A-horizon with underlying fractured hard rock in moderate relief areas	96
Figure 4.4. Bushman Gat on the farm Mount Carmel (191), District Danielskuil. A funnel-shaped sinkhole in the Ghaap Plateau dolomites, (S27.92183°; E023.64161°, 1562 m amsl).....	100
Figure 4.5. A combination of micro and macro jointing with a prominent master joint/fracture in Karoo-Beaufort Group mudstone.....	102
Figure 4.6. Macro fracturing illustrated in Karoo-Beaufort Group sediments contact with a Karoo dolerite aureole in De Jagers Pass cutting.	103
Figure 4.7. A typical Karoo-Beaufort Group sandstone lens with even-spaced vertical fractures, Nuweveld Mountains, District Beaufort West	104
Figure 4.8. A close-up of sub-vertical joints in the Beaufort Group's, Teekloof Formation.....	106
Figure 4.9. Character of the rooting zone (brownish, soil zone: ≈0.75 m) and underlying regolith (> 1.5m) on the side of a rivulet in the Nuweveld Mountains, District Beaufort West.	111
Figure 4.10. Groundwater flow conditions with vertical accretion due to infiltration in an unconfined (gravity flow) aquifer resting on a horizontal, impervious basement.	114
Figure 4.11. Control volume to simulate the gravity flow conditions in an unconfined aquifer with a horizontal impervious basement and dipping water table plane on top.	116
Figure 4.12. The relationship between receiving and discharging sub-reservoirs of a total groundwater recharge model in fractured hard rock terrains (modified after Willemink 1988)..	120
Figure 5.1. Satellite image of a typical pan system in the Kalahari showing a Lunette dune system as described by Lancaster (1988).	127
Figure 5.2. The early, peak and dry (HARmean) Cl ⁻ concentrations in rainwater collected during 2003-2006 from summer and winter experimental monitor terrains in South Africa	132

Figure 5.3. Ration between Cl^- and Na^+ from the West Coast winter rainfall region in the Western Cape Province, South Africa.	134
Figure 5.4. Ratio between NO_3^- and Cl^- concentrations in rainwater from the West Coast winter rainfall region in the Western Cape Province., South Africa.	135
Figure 5.5. Positions of the national rainwater quality and quantity monitoring terrains in South Africa and the number of rainfall stations on each monitoring terrain.	137
Figure 5.6. Rainwater chloride profile across the Sandveld Region showing decreasing Cl^- values with increasing ground elevation away from the seaboard at E018.40°.....	140
Figure 5.7. Correlation between rainfall depths and $^{18}\delta$ (‰) at the Stella monitoring terrains for the period 2002 to 2009.	147
Figure 5.8. Isotopic composition of rainwater obtained from the Beaufort West monitoring sites (nine (9) rainfall sampling/logging stations) categorized in 2003-2004 to 2007-2008 HC's	148
Figure 5.9. Isotopic composition of rainwaters from the Pretoria East monitoring site illustrating the difference between bulk rainwater sampling (over a month) and individual rain sampling (RES unit)	149
Figure 5.10. In-situ chloride profiles (Cl , $\text{mg}\cdot\text{l}^{-1}$) taken from the Beaufort West monitoring terrains: (a) from the Nuweveld Mountain and (b) and (c) from a Karoo peneplane terrain	167
Figure 5.11. Hydrogeochemical profile from the Stella, Midkopreen monitoring terrain showing Cl^- and ESI profiles from below 16.9 m bgl.	168
Figure 5.12. The Harmon Craig diagram ($^{2}\delta$ - $^{18}\delta$) illustrating the ESI composition of a 2 m groundwater profile at the G44504 Midkopreen monitoring site in Stella,.	169
Figure 5.13. Hydrogeochemical profile from the De Hoop, G29870L monitoring site showing Cl^- and ESI profiles from below 22.4 m bgl.	170
Figure 5.14. Hydrogeochemical profile from the De Hoop, G29870L monitoring site showing Cl^- and ESI profiles from below 16.9 m bgl.	171
Figure 5.15. Illustrating the groundwater Cl^- trend in a 1.52 m water table rebound logged with the stage sampling procedure, De Hoop Poort, G29870BE.....	174
Figure 5.16. Isotopic composition of groundwater sampled using a 3 m column and 19 mm skim sampler in November 2008 in correlation with local rainwater sampled during the 2004-2008 period. Rainwaters containing the episodic events in 2006 and 2008 are marked specifically.	188

Figure 6.1. Illustration of extraordinary rainfall event (110 mm in 20½ hours) and responding groundwater table rebound (1.57 m over 35½ days) in Karoo fractured hard rock terrain, District Beaufort West.....	193
Figure 6.2. Illustration of extraordinary rainfall event (269 mm in 6 days 7 hours) on the Spitskopreen monitoring site on a Kraaipan fractured hard rock terrain, Stella, District Vryburg.	199
Figure 6.3. Combination of rainfall and groundwater hydrograph from monitoring sites G29870BB_RF(Rw) and G29870BE(Gw) at De Hoop Poort, District Beaufort West.....	203
Figure 6.4. Typical groundwater table hydrograph-hyetograph set at monitoring site G47600 (G47600 water level) and G46600_RF (Klein Boompie rainfall) in a dolomitic terrain.	204
Figure 6.5. Comparison between groundwater recharge mechanisms in an area with local infiltration on a hard rock terrain (G29870BE) and a nearby receiving flood plain area (G29899F), De Hoop Poort, District Beaufort West.....	205
Figure 6.6. Water table responses in two different recharge cases in the Karoo environment against the local rainfall input over two HCs.....	206
Figure 6.7. Hyetograph-hydrograph set for the 2005-2006 HC as observed on the Spitskopreen monitoring site, at Stella, Vryburg District.....	210
Figure 6.8. Hyetograph-hydrograph set for the 2002-2003 to 2008-2009 HC's as observed on the Greenfields monitoring site, at Taaiboschgroet, Alldays District, Limpopo Province.	211
Figure 6.9. Hyetograph-hydrograph set for the 2003-2004 HC as observed on the Greenfields monitoring site, at Taaiboschgroet, Alldays District, Limpopo Province.	212
Figure 6.10. Hydrochemical conceptual model of groundwater recharge and the Cl ⁻ flow path in an actual fractured hard rock terrain with adjacent soil/regolith cover area.....	214
Figure 6.11. The theoretical water level response, $\Delta(\Delta h)$ over a period of 365 days from a precipitation rate of 10 mm·d ⁻¹	223
Figure 6.12. Showing a simulated water level response, $\Delta(\Delta h)$ over a period of 365 days from a precipitation rate of 10 mm·d ⁻¹	224
Figure 6.13. Comparison between the stable isotope composition of the 2002-2009 rainfall period and groundwater sampled from local boreholes where a water table mound of 2.84 m was recorded.....	227

Figure 7.1. A rain-week scenario as it occurred from 29 - 31 Janaury 2009 (2 days and 15½ hours) in the Taaiboschgroet area, Limpopo Province with a total rainfall of 193 mm.	244
Figure 7.2. Chloride and ESI profile during steady state conditions in fractured hard rock terrain in Beaufort Group sandstone/mudstone at the De Hoop Poort monitoring site, Beaufort West District.....	250
Figure 7.3. Flow diagram illustrating the peak rainwater and corresponding groundwater rebound Cl^- concentrations, the ESI variation between rainwater and groundwater and the estimated groundwater recharge as a percentage of R_{eff}	256

LIST OF SYMBOLS.

Symbol	Description	Dimension	Units
General and Mathematical.			
A	Area, the area perpendicular to flow direction.	L^2	m^2
α	Constant, adopted from water table geometry, flat (≤ 1), parabolic ($\geq \frac{2}{3}$), De Vries (1974)	Dimensionless	
b	Saturated thickness above a datum line (base of aquifer).	L	m
b	Width of a fracture/joint (Cook 2003).	L	μm
B	Fracture/joint spacing (Cook 2003).	L	m
$\beta_{t,f,m}$	Porosity: total, fracture and matrix (Cook 2003).	ratio	
β	A constant = 1.12 (Gieske 1992).	-	-
$\beta_{w,a}$	Compressibility, water (w) and aquifer (a) medium.	$L^2 \cdot N^{-1}$	$m^2 \cdot N^{-1}$
$C_{P,G}$	Cl^- concentration in rainwater (C_P) and groundwater (C_G).	$M \cdot L^{-3}$	$mg \cdot l^{-1}$
C_{Gbp}	Cl^- concentration of bypass flow/macro fracture system.	$M \cdot L^{-3}$	$mg \cdot l^{-1}$
C_D	Cl^- concentration in rainwater collected during the 'Dry Period'.	$M \cdot l^{-1}$	$mg \cdot l^{-1}$
$C_{PP,EP}$	Cl^- concentrations in rainwater collected during the 'Early Period' ($_{PE}$) and 'Peak Period' ($_{PP}$).	$M \cdot l^{-1}$	$mg \cdot l^{-1}$
C_{Gm}	Cl^- concentration in rock matrix/micro fracture system.	$M \cdot l^{-1}$	$mg \cdot l^{-1}$
C_{Pd}	Cl^- concentration in rainwater based on effective input: dry period (summer: Apr_n to Sep_n).	$M \cdot l^{-1}$	$mg \cdot l^{-1}$
C_{Pep}	Cl^- concentration in rainwater based on effective input: early period (summer: Oct_n to Dec_n).	$M \cdot l^{-1}$	$mg \cdot l^{-1}$
C_{Ppp}	Cl^- concentration in rainwater based on effective input: peak period (summer: Jan_{n+1} to Mar_{n+1}).	$M \cdot l^{-1}$	$mg \cdot l^{-1}$
C_{Gd}	Cl^- concentration in groundwater based on background values: summer dry period.	$M \cdot l^{-1}$	$mg \cdot l^{-1}$
C_{Gep}	Cl^- concentration in groundwater based on event input: summer early period.	$M \cdot l^{-1}$	$mg \cdot l^{-1}$
C_{Gpp}	Cl^- concentration in groundwater based on event input: summer peak period.	$M \cdot l^{-1}$	$mg \cdot l^{-1}$
C_{Dd}	Cl^- concentration in atmospheric outfall based on daily input over summer dry period.	$M \cdot l^{-1}$	$mg \cdot l^{-1}$
C_{Dep}	Cl^- concentration in atmospheric outfall based on daily input over summer early period.	$M \cdot l^{-1}$	$mg \cdot l^{-1}$

Symbol	Description	Dimension	Units
C_{Dpp}	Cl^- concentration in atmospheric outfall based on daily input over summer peak period.	$M \cdot \ell^{-1}$	$mg \cdot \ell^{-1}$
δ	Relative deviation of an isotope ration from that of a standard (SMOW).		
d	Depth to water table interface.	L	m
d'	Deuterium excess: $d' = {}^2\delta - 8{}^{18}\delta$; Harmon Craig diagram.	-	‰
D	Dry chloride input from atmospheric 'out fall'.	$M \cdot L^2 \cdot T^{-1}$	$mg \cdot m^2 \cdot y^{-1}$
D_D	Mean areal discharge.	$L \cdot T^{-1}$	$mm \cdot y^{-1}$
D_{GWR}	Direct groundwater recharge.	$L \cdot T^{-1}$	$mm \cdot yr^{-1}$
δ^2H	Stable hydrogen isotope deviation from SMOW.	-	per mil, ‰
$\delta^{18}O$	Stable oxygen isotope deviation from SMOW.	-	per mil, ‰
ET, E, T	Evapotranspiration, evaporation or transpiration.	$L \cdot T^{-1}$	$mm \cdot d^{-1}$
ET_P	Potential evapotranspiration from UZR.	$L \cdot T^{-1}$	$mm \cdot d^{-1}$
ET_A	Actual evapotranspiration from UZR.	$L \cdot T^{-1}$	$mm \cdot d^{-1}$
ET_{INDEX}	Evapotranspiration index $\frac{C_P}{C_G}$ (Mazor 1997).	ratio	-
ϕ, n, ϕ_F	Porosity of porous media, or porosity of a fracture (ϕ_F).	ratio	-
Fa_i, Fb_i	Frequency interval (frequency of exceedance) between an upper (a_i) and lower limit (b_i) rainfall values.	Dimensionless	
g	Gravity acceleration	$(L \cdot T^{-1})$	$m \cdot s^{-1}$
H, h	Water table head above datum.	L	m
h_0, L, a	Water table head at watershed (h_0), discharge point (h_L) and annual fluctuation (h_a).	L	m
h_{max}	Maximum elevation of water table head (h_0) after a recharge-producing rainfall surplus.	L	m
h_Z, z_i	Water table head because of an instantaneous recharge event at time $t=t_i$.	L	m
K	Hydraulic conductivity.	$L \cdot T^{-1}$	$m \cdot d^{-1}$
K_F	Hydraulic conductivity of fracture/joint.	$L \cdot T^{-1}$	$m \cdot d^{-1}$
k_{ET}	Relative evapotranspiration rate $E_A = k_{ET} \cdot E_P$.	Ratio	na
km	Kilometer (1000 m).	L	km
L	Sectional length of a flow system from water table divide to discharge zone	L	m
m bgl	Meters below ground level	L	m

Symbol	Description	Dimension	Units
m asml	Meters above mean sea level.	L	m
m_i	Number of rainfall depths in a rainfall depth interval between an upper (a_i) and lower (b_i) value.	-	-
M_i	Number of rainfall events exceeding a_i	-	-
Ma	Geological age, million years before present, BP.	T	Yr ⁶
μ	Viscosity of water	poise	
η	Porosity of a flow medium.	Ratio	%
n	Number of events, observations, measurements or counts.	-	-
P, P _A	Precipitation (design rainfall), Annual precipitation.	L	mm
P _{EP}	Effective Rainfall during early period (EP).	L	mm
P _S	Precipitation surplus (or Recharge-producing rainfall surplus as per De Vries (2000)).	L·T ⁻¹	mm·yr ⁻¹
ppm	Part per million, concentration of the total dissolved solids in water (equivalent to total mg·ℓ ⁻¹).	M·ℓ ⁻¹	mg·ℓ ⁻¹
P _{PP}	Effective Rainfall during peak period (PP).	L	mm
P _D	Effective Rainfall during dry period (D).	L	mm
P _R	Rainfall depth.	L	mm
P _{Reff} bp	Recharge-producing rainfall surplus via bypass flow condition.	L	mm
P _{Reff} m	Recharge-producing rainfall surplus via matrix flow condition	L	mm
q	Darcy Velocity.	L·T ⁻¹	m·d ⁻¹
Q	Discharge, quantity of flow through a section	L ³ ·T ⁻¹	m ³ ·s ⁻¹
q _x '	Flow per unit width, in x-direction	L ³ ·T ⁻¹	m ³ ·d ⁻¹
Q _{DIS}	Discharge from sub-reservoir by means of base-flow, evapotranspiration or feeding deeper aquifers.	L ³ ·T ⁻¹	m ³ ·d ⁻¹
q _f	Flow rate of fracture system (Cook 2003).	L·T ⁻¹	m·d ⁻¹
Q _I	Acronym for groundwater/rainwater quality.	M·V ⁻¹	mg·ℓ ⁻¹
Q _{LAT}	Lateral discharge from a direct recharge terrain.	L ³ ·T ⁻¹	m ³ ·d ⁻¹
Q _n	Acronym for groundwater/rainwater quantity.	V·T ⁻¹	m ³ ·h ⁻¹ or ℓ·s ⁻¹ ₁
q _{sm}	Flow rate through soil/regolith matrix.	L·T ⁻¹	m·d ⁻¹
q _{pr} , q _{bp}	Flow rate through macro pores (preferential or	L·T ⁻¹	m·d ⁻¹

Symbol	Description	Dimension	Units
	<u>bypass</u> flow).		
$Q_{X,Y}$	Discharge in the x, y-direction.	$L^3 \cdot T^{-1}$	$m^3 \cdot s^{-1}$
R, r	Correlation coefficient or ratio (linear, exponential).	Dimensionless	
R_{eff}	Effective rainfall observed from hyetograph-hydrograph set.	L	mm
R_F	Rainfall event.	L	mm
R_{PR}	Recharge rate via macro pores (bypass or preferential paths).	$L \cdot T^{-1}$	$mm \cdot yr^{-1}$
R_R, N	Recharge rate to saturated zone, (N used by Gieske (1992)).	$L \cdot T^{-1}$	$mm \cdot yr^{-1}$
R_{RM}	Recharge rate via the rock matrix (micro fracture systems).	$L \cdot T^{-1}$	$mm \cdot yr^{-1}$
R_{RT}	Rainfall intensity (or rain rate).	$L \cdot T^{-1}$	$mm \cdot hr^{-1}$
R_{SM}	Recharge rate via the soil moisture (soil/regolith) media.	$L \cdot T^{-1}$	$mm \cdot yr^{-1}$
R_T	Total recharge rate (Ting et al. (1998) and De Vries (2000)).	$L \cdot T^{-1}$	$mm \cdot yr^{-1}$
R_{wl}	Rest water level (steady state).	L	m
ρ	Density of water.	$M \cdot L^{-3}$	$kg \cdot m^{-3}$
s	Slope of the Meteoric Water Line.	Dimensionless	
Sm_s	Soil/regolith moisture storage	Dimensionless	
Ss	Specific storage (conf.), $S_s = \rho \cdot g \cdot (\eta \cdot \beta_w + \beta_a)$.	L^{-1}	m^{-1}
S	Storativity, $S = S_s \cdot b$; b = confined thickness	Dimensionless	
S_y	Specific yield (unconfined storativity $S = S_y + h \cdot S_s$; h = unconfined thickness)	Dimensionless	
S_{ya}	Apparent specific yield (as applied by McWhorter and Sunada (1977)).	Dimensionless	
SW_R	Surface run-off.	$L \cdot T^{-1}$	$mm \cdot yr^{-1}$
T_D	Average thickness of a specified geological unit.	L	m
TC	Total atmospheric chloride deposition (Gieske 1992).	$M \cdot L^{-2} \cdot T^{-1}$	$mg \cdot m^{-2} \cdot yr^{-1}$
T	A specified time in which a series of events takes place (De Vries (1977) and Gieske (1992)).	T	year or day
t_0, t_i	Time = 0; at the onset of specific activity, or per unit of time (i)	T	days to years
v	Seepage velocity.	$L \cdot T^{-1}$	$m \cdot d^{-1}$
V	Volume, as in a volume of porous media.	L^3	m^3
V_w	Volume water.	L^3	m^3

Symbol	Description	Dimension	Units
V_{wf}	Fracture water-velocity (Cook 2003).	$L \cdot T^{-1}$	$m \cdot d^{-1}$
yr	Years as in ~10 000 yr BP.	T	years

Calculus.

$\Delta t, v, x, y, z$	Change over a period of time (t), volume (v) or length/direction (x, y and z).	-	-
$\Delta h, (\Delta h_z)$	Difference in head of water (z-direction) over a period.	L	m
dx, z, dl, dp	Difference in x-direction (x), vertical plane (z), distance (l) and pressure (p).	L, P	m, mBar
$\nabla, \nabla h$	Gradient Operator, Gwater flow driving force.	-	-
$h(x, t)$	Water head as a function of distance (x) and time (t) as per Figure 4.10.	L	m
Λ	Vertical Flow Resistance = b' / K'_v , where b' = thickness of the UZR and K'_v its Hydraulic Conductivity.	T	days
Υ or W	Horizontal Drainage Resistance (SDR) = $\Delta h / P_s$, where P_s = the Recharge-producing rainfall surplus.	T	days

LIST OF ABBREVIATIONS

AMD	Acid mine drainage; decanting of acidic water from re-watered mine voids.
ASWCL	Analytical Services Water Chemistry Laboratory (CSIR's).
ASR	Aquifer storage recharge. A condition when the storage status of an aquifer system is replenished by rainfall recharge to such a potential that medium-term utilization can be considered, (One (1) in five (5) years episodic recharge recurrence).
AQRL	Air Quality Research Laboratory (CSIR's).
ARC	Agricultural Research Council.
BIF	Banded ironstone formation.
BP	Years Before Present (Chronological geological time).
CFB	Cape Fold Belt.
CHART	Collective Hydrological Assessment and Reporting Tool.
CMA	Catchment Management Agency.
CMB	Chloride Mass Balance (a methodology used for groundwater recharge estimation).
CRC	Convectional rainfall cell
CSIR	Council for Scientific and Industrial Research.
CTD	Conductivity ($\mu\text{S}\cdot\text{cm}^{-1}$), temperature ($^{\circ}\text{C}$) and depth (m water head) probe.
DTH	Down the hole.
DWA	Department of Water Affairs (under the Ministry of Water and Environmental Affairs).
DWAF	Department of Water Affairs and Forestry (pre April 2009).
E.L.	Evaporation Line (on Harmon Craig diagram).
ESKOM	Electricity Supply Commission, South Africa.
GMWL	Global Meteoric Water Line, established from the GNIP, instigated by IAEA in cooperation with WMO, MWL with $d = 10 \text{ ‰}$ (Mazor 1997; Mook 2000a, 2000b).
GNIP	Global Network of Isotopes in Precipitation (Mook 2001).
GRAII	Groundwater Resources Assessment Phase II.
GRAM	Groundwater Resources Assessment and Monitoring (sub-Directorate in DWA).
GRES	Groundwater Resources Monitoring and Recharge Studies, Ministry of Mineral Resources and Water Affairs, Rep. of Botswana (MMRWA), 1987.
HC	Hydrological Cycle, Oct _n to Sep _{n+1} .
HYCOS	Hydrological and Climate Observation System.

IAEA	International Atomic Energy Agency.
IGS	Institute for Groundwater Studies, Univ. o/t Free State, Bloemfontein, RSA.
IH	Instantaneous hydrograph.
ISARM	Internationally shared aquifer resources management.
ITCZ	Inter-Tropical Convergence Zone, southern hemisphere.
KGAS	Kalahari Group (T-Qk) Aquifer Systems.
LLHc	Low level Hydrochemical analyses at CSIR's AQRL.
LMWL	Local Meteoric Water Line, derived from a local precipitation/rainwater stable isotope data set.
LRAS	Langebaan Road Aquifer System, Western Cape Region.
LUZR	Lower unsaturated zone reservoir. The unsaturated UFWZ and part of the fresh/fractured parent rock where no evapotranspiration takes place; below the rooting zone.
MAP	Mean Annual Precipitation (rainfall in mm).
MWL	Meteoric Water Line, a linear expression derived from the isotopic relation between ^2H and ^{18}O in precipitation.
NGA	National Groundwater Archive.
NGDB	National Groundwater Data Base.
NWRS	National Water Resources Strategy, Department of Water Affairs.
NGwQMP	National Groundwater Quality Monitoring Programme (also known as the ZQM network).
NRwQMP	National Rainwater Quality Monitoring Programme.
NWA	National Water Act, 1998 of the Republic of South Africa (Act No. 36 of 1998).
ORS	Orographic rainfall system.
QUADRU	Quaternary Dating Research Unit (CSIR's).
RH	Relative Humidity.
RES	Rain event sampler: A unit which individually samples rainwater during a series of rainfall events.
RSA	Republic of South Africa.
SACS	South African Committee for Strategy.
SADC	Southern African Development Community.
SAFARI	Southern African Regional Science Initiative.
SAWS	South African Weather Services.
SDR	Specific Drainage Resistance Υ (also Horizontal Drainage Resistance De Vries 1974; 2000).

SGWRM	Simple (groundwater) Reservoir Model (De Vries 1974 and Gieske 1992).
SHPZ	Southern High Pressure Zone, southern hemisphere.
SMOW	Standard Mean Ocean Water (Mazor 1997).
SZ	Saturated zone, below the water table interface.
TFZ	Taaiboschgroet Fault Zone (locale referenced as the Tshipise Fault Zone, Limpopo Province).
TMG	Table Mountain Group sandstone, c. ~450 Ma, ortho-quartzite.
TZ	Temperate Zone, southern hemisphere.
T-Qk	Acronym for a geological period spanning the Tertiary (T) and Quaternary (Q) Periods and name given to the region where the sediments occur; Kalahari (k).
UFWZ	Upper fractured (jointed) and weathered zone
UNESCO	United Nations Educational, Scientific, and Cultural Organization.
UUZR	Upper unsaturated zone reservoir. Soil/regolith/UFWZ zone containing the rooting zone. Adopted from Willemink (1988).
UZR	Unsaturated zone reservoir.
VFR	Vertical flow resistance - Λ (De Vries 1974).
WISH	Water Information System for Hydrologists, Institute for Groundwater Studies, University of Free State, Bloemfontein, South Africa.
WRC	Water Research Commission.
WMO	World Meteorological Organization.
WRIM	Water Resources Information Management (Chief Directorate in DWA, Rep. of South Africa).
WUA	Water Users Associations.
ZAB	Zaire Air Boundary, southern hemisphere.

ESTIMATION OF EPISODIC GROUNDWATER RECHARGE IN FRACTURED-WEATHERED HARD ROCK AQUIFERS IN SEMI-ARID REGIONS.

1. INTRODUCTION.

1.1. GENERAL RESEARCH STATEMENT.

Groundwater resources in the semi-arid regions of southern Africa are highly vulnerable in terms of annual replenishment as a result of rather intermittent rainfall occurrences. These resources are commonly used for local water supplies and being classified as the sole source for many users, their long-term sustainability becomes a critical management aspect.

Long-term water table observations in southern African water table aquifers located in semi-arid environments, report water table rebounds which are erratic in time and specifically linked to those wetter Hydrological Cycles (HCs) with extraordinary high rainfall events as described by Van Tonder and Bean (2003, p 25):

.....While recharge is diffused in these environments, the recharge pulse is only mobilized by extraordinary rainfall, and is thus episodic in nature.....

The interaction between rainwater and groundwater to estimate the actual recharge percentage has been addressed by many research efforts in southern Africa. Recharge estimations for aquifers with strategic importance in semi-arid terrains is limited, nonetheless, because of insufficient long-term financial backing and maintenance of monitoring programmes.

Several methodologies were applied and general lack of area-specific information has been put forward as the reason for unrealistic recharge estimates that do not comply when water balances are calculated. During the research process, efforts to obtain applicable information require research groups to relate on extrapolated base line data which do not always bear sustainable results. Although semi-arid regions portray complex hydrogeological concepts, continuous observations of the hydrological regime provide a finger print of how effective aquifer systems operate under intermittent climatic conditions.

The focal point of this study, therefore, was to go back to aquifers of South Africa to observe pristine hydrogeological conditions in nature. Research in hard rock aquifers postu-

lates that bare rock terrains may play a roll in groundwater recharge physics and chemistry (Lloyd 1999). Given the fractured hard rock nature of a large percentage of the aquifer systems in South Africa, fractured terra firma represents direct recharge zones supporting groundwater replenishment to surrounding sub-reservoirs (Willemink 1988).

The aspect of limited information quantifying the important components of the hydrological cycle may be partially to blame, especially the hydrochemical characteristic of southern Africa's rainwater and shallow groundwater system. Unfortunately, the most important attribute to groundwater recharge, the atmospheric input (rainwater) has not been thoroughly analyzed in terms of site-specific short-term hydrochemistry and isotopic composition and rainfall intensities.

1.2. RESEARCH OBJECTIVES.

Groundwater recharge estimations in southern Africa over the last few decades were based on a variety of methodologies (Bredenkamp et al. 1995), including multiple tracer profiling. Gieske (1992) and Beekman (1999) conducted detailed investigations in the Botswana Kalahari on rainwater and soil water Cl^- and environmental stable isotopic (ESI) compositions using multi-tracer profiling, but with mixed results. The complexities of these recharge estimations in terms of obtaining long-term time-series data, periodic rainwater chemistry oscillations during wet/dry cycles and the scaling factor were noted.

The objective of this investigation was focussed on the interaction between rainwater and groundwater in terms of qualities (hydrochemical) and physical responses (quantity impact) in phreatic, hard-rock aquifers. Specific terrains were selected where direct recharge represented the main recharge mechanism, by using fractured hard rock terrains. A new short-term approach for monitoring rainwater and groundwater based on rainfall and recharge events were developed and implemented. A review of conventional multi-tracer applications in hard rock terrain was finally embarked on, using a modern set of hydrological data.

As a first approach in addressing groundwater recharge utilizing environmental tracers like Cl^- and stable hydro-isotopes, short-term time-series monitoring of modern hydrometeorological conditions was initiated in semi-arid hard rock terrains over a period of nine (9)

years, starting in 2000. Both summer and winter rainfall regions in South Africa are included. Each monitoring terrain consisted of several individual sites covering control conditions like soil/regolith-covered areas, peneplanes and high relief zones (mountains) and rivulets/depressions.

These monitoring terrains generated a dedicated set of rainwater and groundwater state variables over the short-term (daily) which allowed the capturing the episodic nature of extraordinary rainfall events and subsequent recharge responses in local hard rock aquifer systems.

Finally, a review is presented of multi-tracer applications in different hard rock terrains for southern African, semi-arid conditions.

1.3. RESEARCH STATEMENT.

Application of hydrogeological concepts in support of groundwater recharge estimations requires a physical understanding of the interaction between incoming rainfall patterns and water table responses. It has been noted in several cases that annual average and sometimes above-average rainfall depths do not generate significant medium to long-term aquifer storage recharge (ASR) as hypothesized in applications like the cumulative rainfall departure technique under cyclic climate conditions.

Rainfall patterns in the southern African semi-arid environments can be classified as highly variable in time and space. In addition to the general southern African hydrogeological conditions, a sporadic soil cover underlain by a variable jointed/weathered hard rock unsaturated zone reservoir (UZR) with variable thicknesses, the actual groundwater recharge will be likewise intermittent, thus episodic in nature.

Multiple-tracer profiling presents dedicated rainwater and groundwater data for analyzing short-term rainwater-groundwater interaction between these two components of the hydrological cycle. Groundwater recharge research in Botswana (GRES) reports that hydro-atmospheric meta-data sets are relatively sparse in southern Africa. Valuable work was done in the past on algorithms describing recharge estimations for dolomitic aquifers. The physical responses portrayed by the remaining aquifers hydrogeological conditions are

quite diverse; however, and especially the recharge mechanisms and hydrochemical transformations are related to site-specific conditions.

Application of multiple tracers profiling in fractured hard rock environment is not feasible, due to the UZR's hard rock lithological composition. Conventional profiling to obtain soil moisture samples is therefore restricted, and the underlying saturated zone (SZ) is approached as receptor of the multiple tracers hydrochemically adjusted by physical processes at ground surface and the rooting zone (Xu and Beekman 2003).

Water table fluctuations, especially in the semi-arid environments, respond sporadically, and are linked to extraordinary rainfall events (Vogel and Van Urk 1975). It reports that (i) a specific rainfall event, in (ii) a specific wetting period, will (iii) drive a specific recharge pulse in (iv) a characteristic confined locale (a hard rock terrain). In phreatic or water table aquifer systems, a recharge event will lead to distinct conditions in the SZ itself. Firstly, the most elementary observation is the response of the water table interface, which report water table rebounds of variable magnitude over a specific period of time. Secondly, the hydrogeochemistry balance or mixture between infiltrated rainwater and *in situ* groundwater will be altered to such a level that differences can be measured.

To conclude, a dedicated methodology for capturing rainwater and groundwater quality and responses under steady state and recharging conditions are essential in order to generate a set of modern hydrological data sets from where it can be put into practice.

1.4. METHODOLOGIES DEVELOPED AND APPLIED.

Observations of water table fluctuations report variable responses to infiltrating rainwater on different hydrogeological settings throughout the semi-arid regions of southern Africa. This study therefore focused mainly on the total hydrological recharge aspects of (i) hard-rock terrains, and to a lesser degree to (ii) local rivulets and (iii) local depression-features. An attempt was made to monitoring recharge pans in the western arid-Kalahari, but the rainfall in the last decade did not generate any local runoff to fill these pan.

Given the lack of high-level hydrological information covering areas where sustainable decisions must be made in terms of economics and sustainability, many groundwater schemes have, in fact, failed, because of improper management and maintenance of

monitoring programmes/networks. In most cases, it was clear that limited monitoring data was generated to control abstraction, and the aquifers subsequently are over-utilized. One example is the Brandwag Groundwater Unit in Beaufort West, where the current steady state draw down after forty (40) years of exploitation is in the order of thirty (30) meters.

On a regional scale, generation of specific hydrological parameters within a highly variable hydrogeological scenery calls for an organised approach of generating data as required for estimating rainwater-to-groundwater interaction. A set of hydrological measures needs to be collected by dedicated instrumentation geared for operation under remote and extremely harsh environmental conditions, and represents the backbone of any intended groundwater recharge study.

The attributes requirement for estimating groundwater recharge from a quantity (levels) and quality (concentrations) perspective, collected under remote and robust environmental conditions, is rather complex. It can be divided into spatially-fixed attributes, namely: (i) hydro-lithological and flow-path hydraulic characteristics, (ii) topographic features and (iii) geo-ecosystems, followed by the time-series-related hydrologic impacts which drive the quantity and quality conditions in the HC. This requires a high level of state variable monitoring practices specifically designed for operating under extreme and robust climatic conditions.

For the purpose of regional presentation, a variety of hydrogeological type areas had to be identified. The starting point was to select regions where sufficient long-term groundwater information is available to pinpoint superior recharge spots in (i) Karoo-Beaufort sedimentary rocks, (ii) Chuniespoort/Ghaap Plateau dolomites, (iii) Swazian Granite Gneiss, (iv) Pretoria Volcanics/Sediments, and (v) Karoo-Letaba lava's/sediments.

Specific groundwater monitoring networks were established in these hydrogeological sceneries. These networks have been operational for several years now, but unfortunately do not yet cover the full hypothetical eighteen (18) year climate cycle-term (Thomas and Shaw 1991).

Sampling of the different hydrological attributes required for estimating groundwater recharge initiated under sporadic climatic conditions requires short-term observation intervals. These intervals were short-term (30 minutes, 1 hour or 2 hour) water table measurements, short-term (15 min. or 30 min.) rainfall depth measurements, medium term (monthly, quarterly, six-monthly) bulk rainwater sampling, and medium term (monthly, quarterly, six-monthly) groundwater sampling from boreholes/springs.

Although sampling of bulk rainwater requires only a shielded, airtight container, groundwater sampling from the SZ is not simple. During the onset of the study, only samples from the water table interface were drawn (500 ml), but indications from the hyetograph-hydrograph sets pointed out that the groundwater should in fact be sampled over a specified water column from below the water table interface. Similarly, it was realized that individual sampling of the rainwater is required to capture the individual extraordinary rain event which characterizes a particular hydrochemistry and isotopic composition.

Application of high-tech electronic data loggers for rainfall depth and water table monitoring considerably enhances the time-series value of the data due to the short programmable interval period and medium-term storage facilities. These applications therefore were applied to generate a refined and episodic guided modern hydrological data set which can be used in an upgraded version of the conventional multi-tracer recharge methodologies.

The final approach of this study is to assess a differential groundwater recharge estimation based upon the diverse rainfall pattern and recharge response over the hydrological cycle.

1.5. DEFINITION OF TERMS.

A series of terms/nomenclature were used in this document to express specific attributes and effects observed during the study. These are presented below in alphabetic order:

'Aquifer-storage recharge' (ASR) refers to a prominent water table rebound scenario after an extraordinary rainfall sequence, which lasts from a few months, to several years. This scenario, has in fact, altered the local aquifer systems to such an extent that the initial groundwater chemistry is significantly changed;

'Column sampling' refers to a groundwater sampling procedure where an *in situ* 2-3 m section of the groundwater below the water table interface is removed and sampled at surface.

'Depleted' refers to (i) extraordinary low Cl^- concentrations ($<0.7 \text{ mg}\cdot\text{l}^{-1}$) in rainwater and (ii) relative negative ESI values and plots on the Harmon Craig diagram ($<-6.0\text{‰ } \delta^2\text{H}$, $<-38.0\text{‰ } \delta^{18}\text{O}$).

'Direct/Indirect recharge' terrain/area/site refers to a specific zone where rainwater percolates almost directly (vertically) into the underlying aquifer. Indirect recharge refers to cases where surface run-off and/or interflow captures a portion of the rainfall and diverts it via rivulets to a distant depression/stream. Recharge then occurs along this route, but mostly where the remaining surface flow resides in a depression (pan or swallow in the case of karstic conditions);

'Experimental monitoring terrain/sites' refers to specially selected areas in the winter/summer rainfall regions used for rainwater-groundwater interaction monitoring. The terrain refers to an area like Beaufort West, which comprises of several monitoring sites. A site can be a single borehole or a cluster of boreholes with an onsite rainfall logger-sampler.

'Groundwater rebound sampling' refers to the physical sampling of a water column from the SZ during an episodic recharge event.

'Hard rock terrain' refers to areas with either bare parent rock outcrops on the one hand, or similar rock covered with a maximum of 0.25 m soil or regolith on the other hand. The bulk hard rock itself may have endured various phases of deformation (jointing to fracturing) or faulting. Limestone/dolomites represent the upper limit hard rock terrains in terms of effective recharge due to secondary solution and karstification at ground surface level;

'Hydrochemistry' or 'hydrochemical' refers to the macro constituent analyses for rainwater and groundwater. For the rainwater component, the hydrochemistry analysis comprises of sodium (Na^+), chloride (Cl^-), nitrate (NO_3^-), sulphate (SO_4^{2-}) and phosphate (PO_4^-). For the groundwater component it comprises the macro-analytical package;

'Geochemistry' or 'geochemical' refers to the stable isotope composition of hydrogen (^2H , deuterium or D) and oxygen (^{18}O) in rainwater and groundwater samples (Mazor 1997);

'Hydrodynamics' describes the physical responses of the underlying saturation zone when groundwater recharge occurs as reported in the water table responses (rebounds or mounding) following a recharge-producing rainfall event;

'Hydrogeochemistry' or 'hydrogeochemical' refers to the combination of the macro constituent analyses and the isotopic composition;

'Parent rock' refers to the underlying weathered and fractured rock mass from which a soil's/regolith's secondary material is derived;

'Rain-week' refers to a short-term wet period, estimated 3 to 8 days with consecutive rainfall events of which at least one of the rainfall events is regarded as extraordinary (episodic); a flush rainfall event ($R_{eff} > 45 \text{ mm}$) with a high rain rate ($R_{RT} > 1.5 \text{ mm} \cdot \text{hr}^{-1}$);

'Rainout' condition refers to a situation where a synoptic system (e.g. a convection storm cell) develops and produces condensates (cloud water) which physically departs from the system as precipitation (rainwater);

'Soil/Regolith' refers to cases where hard rock terrains are capped by a combination of soil and or regolith¹. This horizon varies between a few centimetres (mostly soil) to several meters (regolith).

'Skim sample' refers to a groundwater sample taken right at the water table interface in unlined boreholes. A special side valve sampler is required for this procedure;

'Stage sample' refers to a series of groundwater samples obtained during a water table rebound in a borehole by using a special framework of aliquots inserted into the borehole above the water table;

'State Variables' refers to a prescribed set of dynamic hydrometeorological variables observed during a hydrological monitoring programme. It includes for example, rainwater and groundwater depth measurements and water quality analysis;

'Underdrainage' refers to infiltrated rainwater moving into the UUZR (incl. rooting zone) and LUZR, it includes the local (site scale) interflow component;

'Term. (Short, Medium and Long)'. A general specification used for a period of time applicable to time-series-based observations. In this context, short-term implies days to several

¹ Mantle of fragmental and loose material of residual and / or transported origin, comprising rock debris, alluvium, aeolian deposits, soil and *in situ* weathered rock. It overlies or covers more solid rock, bed rock (Vegter 1995)

weeks (i.e. an episodic occasion to a specific HC interval), medium-term implies months to several years (interval to 4 HCs) and long-term implies several HCs (> 4 to 18 years²).

'The Act' implies the National Water Act of the Republic of South Africa, Act No. 36 of 1998;

'Three tier period' implies three intervals in the HC which coincides with periods of characteristic rainfall depths and hydrogeochemistry input. It applies to summer and winter rain fall regions and comprises of a *'early'*, *'peak'* and *'dry'* period;

'Water column' refers to an *in situ* section or column of groundwater removed from the SZ with a special sampling tube (viz. column sampling); and

'Upper fractured and weathered zone' (UFWZ) refers to specific profile in any hard rock domain stretching from ground surface, vertically into the underlying parent rock. This zone represents the majority of southern African shallow aquifer systems and its saturated thickness seldom exceeds a mean of 25 m (Vegter 1995).

All other frequently used abbreviations are listed in the Abbreviation List in the first part of the document.

1.6. THESIS STRUCTURE.

The thesis consists of seven (7) chapters containing 68 figures and 28 tables. An extensive appendix consisting of 12 chapters is attached in electronic format (DVD). The flow pattern runs from the introduction to the case of episodic recharge, the information requirements, methodologies applied, and review of groundwater recharge estimations applying multi-tracer technologies. A final conclusion/recommendation for future rain-water/groundwater monitoring methodologies and applications concludes the document.

Chapter One (1) provides an introduction to groundwater recharge under some typical southern African semi-arid hydro-climatic environments. The objectives of the study are stated in terms of site-specific recharge terrains in semi-arid regions. The need for generating modern hydrological data using dedicated monitoring equipment and the methodologies applied to review the approach to episodic groundwater recharge estimations are highlighted as the main objectives of the study.

² 18-Year rainfall oscillation over summer rainfall zone of southern Africa proposed by Tyson (cited in Thomas and Shaw 1991, p. 95).

Chapter Two (2) presents the status of hydrological information of the Department of Water Affairs (DWA) based on elementary monitoring programmes. The aim of this is to give the reader some background of the total package of qualified monitoring data generated, edited, stored, and made available for dissemination in various formats from the DWA information platforms. This chapter also describes the rainwater-groundwater monitoring programme, and equipment developed and implemented to generate short-term hydrological data.

Chapter Three (3) describes the background of the semi-arid regions where most of the experimental monitoring terrains were developed. Timely groundwater recharge in semi-arid regions is a critical issue and there are many factors impacting on this process ranging from episodic rainfall events to the condition of the ground surface in terms of vegetation and soil/regolith cover. The climate conditions of semi-arid regions are highly intermittent in terms of rainfall and the region is characterized by extreme evapotranspiration (ET) processes. The origin of rainfall is discussed in detail as this prescribes the hydrogeochemical composition of the rainwater tracers.

Chapter Four (4) describes the hydrogeological setting of the unsaturated profile consisting of soil/regolith/hard rock outcrop, the upper weathered and fractured horizon, to be followed by the first 3 - 4 metres of the saturated profile. The characteristics of hard rock terrains are discussed with reference to the hydrogeological background of the experimental monitoring terrains/sites. The chapter addresses the winter/summer rainfall generation over the African sub-continent, and introduces the flow dynamics of rainfall infiltration in direct recharge areas.

From Chapter Five (5) the thesis starts to focus on the hydrodynamics of groundwater recharge, and introduces the hydrogeochemistry of the atmospheric precipitate (rainwater) and the lithosphere (saturated profile); in terms of a local hydrological cycle. This section therefore displays the hydrogeological and hydro-climatic settings of the semi-arid regions in terms of the hydrogeochemistry, and serves as a preamble to episodic recharge events driven by intermittent rainfall sequences. Multi-tracer profiling in the saturated section of

hard rock terrains is specifically addressed, as this zones bears the most pristine ground-water recharge mechanisms.

Chapter Six (6) examines episodic recharge events in terms of the process and identification through dedicated monitoring and applying hyetograph-hydrograph data sets. This chapter describes a proposed methodology which correlates specific rainfall events and succeeding water table responses. It specifically addresses the quantification of episodic recharge events under semi-arid environs utilizing hydrogeochemistry state variables and hydrodynamic relations between rainwater and groundwater. Six (6) monitoring sites in the summer rainfall region are discussed in detail. The chapter concludes with preferential hydrological conditions required for generating a single or a series of episodic recharge events, and demonstrates the principles of hard rock terrain recharge with soil/regolith-covered terrains. Differentiation of the chloride mass balance (CMB) principle for rainwater-groundwater correlation into a three tier seasonal approach is demonstrated.

Chapter Seven (7) summarizes the hydrometeorological and hydrogeological aspects and results in terms of episodic groundwater recharge in the semi-arid hard rock terrains. It concludes with a set of principles which should be applied with modern rainwater-groundwater monitoring programmes and hydrological monitoring in terms of climate variability.

The Appendices.

Several appendices were produced, containing more detailed estimations and summaries of various aspects of the study.

Appendix 1 to 13 is written on a DVD storage disk attached to the document for references.

oooOOOooo

2. SOUTH AFRICAN HYDROLOGICAL INFORMATION SCENERY.

2.1. INTRODUCTION.

Quantification of surface and groundwater resources and their mutual contributing interaction requires basic parameters such as (i) rainfall events, (ii) ET, (iii) stream discharges, (iv) local aquifer recharge and (v) groundwater discharges (i.e. base flow), and necessitates the integration of hydrological monitoring programmes and compilation of a suitable information package to perform quantification of the water resources under variable hydro-climatic conditions.

Since the implementation of the National Water Act (the Act) in 1998, DWA's responsibility in terms of water resources has been focused particularly on information requirements to support water resources management b.m.o. policy and regulatory perspectives. From a surface water perspective, hydrological information relating to resource quantities is probably the best in the whole of southern Africa. Hydrological observations in the RSA, for example, started more than 100 years ago when the first surface water gauging station was erected on the Mooi River at Potchefstroom in 1904 (Figure 2.1).



Figure 2.1. River flow at the Mooi River Gauging Station C2H001.

Currently, high level monitoring programmes are running under the patronage of the Southern African Developing Country's Water Sector Group, such as the SADC-HYCOS programme, monitoring river flows in the major international transboundary basin's river systems, and provide valuable support in terms of flood warnings, which is crucial for the livelihood and environmental status of low-lying receptor countries such as Mozambique.

Generation of hydrological data in southern Africa has become a requirement for the development of large-scale surface water irrigation schemes such as the Vaalharts Scheme (1938-1939). The first irrigation water from the North Canal was delivered in 1946 and during 1950 from the West Canal. Abstractions from streams and rivers all over South Africa have increased since the expansion of ESKOM power supplies to rural areas since the implementation of specialized sprinkler irrigation systems. To provide in the water demand, high-capacity pumps abstracting water from streams and rivers necessitated the expansion of the surface water gauging station network to a maximum of 5721 river flow H-stations in 2009. The number of surface water related DWA gauging stations is shown in Table 2.1.

The current surface water data package consists of (i) time-series stage height data (<60 min interval of mm stage height flow data), which are transformed to volumetric flows (cumecs or $\text{m}^3\cdot\text{s}^{-1}$), (ii) full hydrochemistry time-series data (monthly, quarterly, bi-annually) at selected gauging stations, and (iii) climate data from dam sites to monitoring evaporation from open water bodies.

Table 2.1. Summary of active surface water monitoring sites 2009 (Source: DWA).	
Site Type	No. of Monitoring Sites
River Flow (H-stations)	5721
Reservoir (R-stations)	437
Evaporation (E-stations)	291
Rain (H,R and E-stations)	255
TOTAL	6704

The long-term flow stage at Station C2H001 is presented in Figure 2.2. The gauge measurements at this station reports the surface water flows in the Mooi River Loop and the

Wonderfontein Spruit. The contribution of the Wonderfontein Spruit Catchment has been impacted by gold mine dewatering in the catchment since the 1960's.

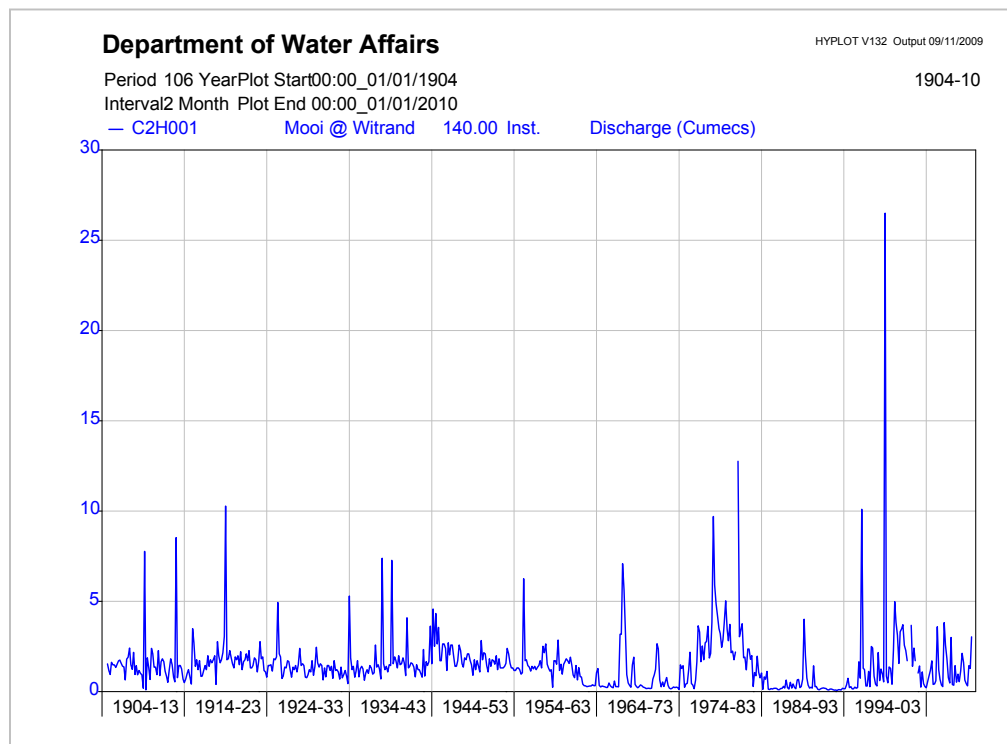


Figure 2.2. The Time-series flow response (cumeecs) at the Mooi River gauging station C2H001 since 1904.

Extensive dewatering of the deep gold mines in the catchment and heavy rainfall (re-charge and emergency dewatering) in the middle to late 1970's and middle 1990's has resulted in some of the highest reported flow heights in the flow history. Long-term changes in the flow dynamics of the Mooi River Loop gauging station since the 1960's is probably the result of large scale shifts in mining activities and methods applied underground to minimize ingress into the mine workings from surrounding water sources. For example, the erratic flows recorded since 1996 are probably the result of growing domestic wastewater spills into the Wonderfontein Spruit system and additional mine water releases from the decanting Western Gold Mining Basin towards the north (Keet 2009).

Groundwater monitoring initially focussed on the performance of local water supply schemes, mainly small municipal water supplies such as local water schemes at De Aar,

which supplied the town and the demand for water for the steam locomotives used on the Johannesburg-Cape Town railway line. Most historical monitoring programmes only focused on the status and trends of the piezometric levels in boreholes. No facilities for monitoring local³ rainfall were available in the medium-term for transformation into daily rainfall logs. Invaluable, long-term spring discharges in South Africa haven been recorded at dedicated of flow-gauging weirs equipped with sophisticated flow-gauging mechanisms like Parchall Flumes and Broad-Crested Weirs (Bredenkamp et al. 1995).

Hydrochemical monitoring generates a wide range of functional indicators supporting understanding and probably enhancing quantification of the interaction between rainwater, surface water, and groundwater modes. A good example of such long-term hydrogeochemical observations and their value in terms of groundwater quality behaviour due to anthropogenic activities can be seen in the Rhenosterfontein Spring Figure 2.3.

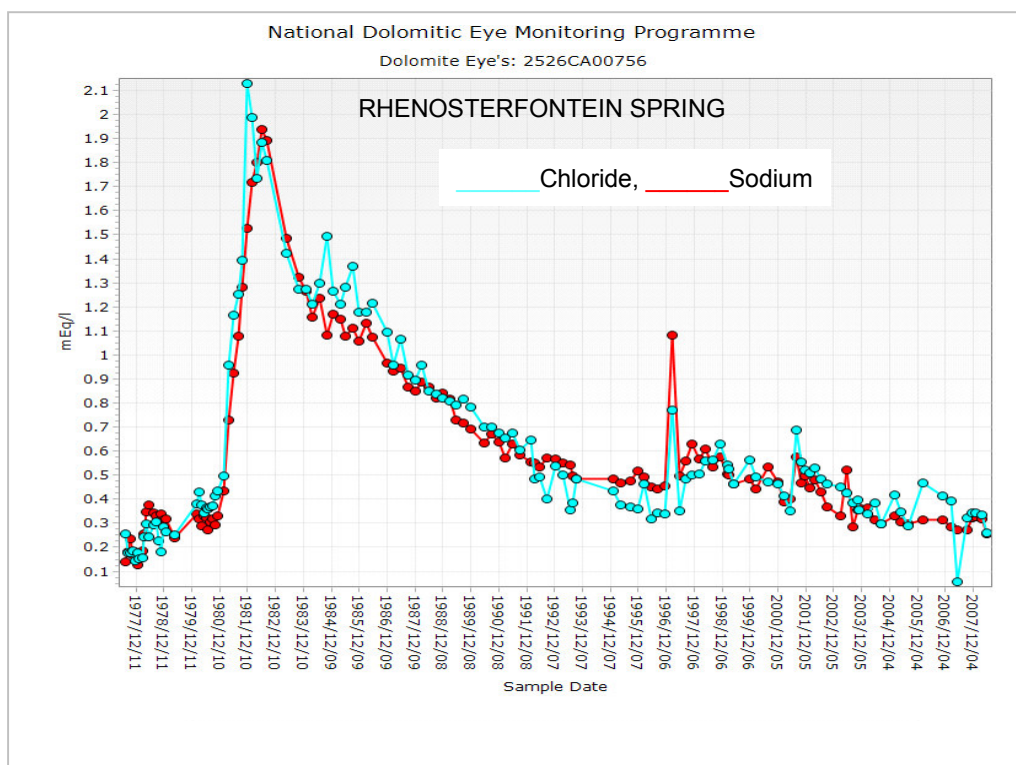


Figure 2.3. Dolomite spring water quality at the Rhenosterfontein spring (A3H0017) in the Northwest Province (S25.72110°; E026.13540°, 1435 m amsl).

³ Local implies within (<500 m radius) the immediate area of observation.

Water quality analyses by DWA monitoring teams at these springs have been conducted on a fairly constant interval since 40 years ago. The Rhenosterfontein spring drains a feldspar mining area. According to the nature of the pollution plume recorded in the long-term water quality log, a considerable amount of sodium chloride (NaCl) was probably dumped in the spring's upper catchment area which contains one of the older open pit mined areas. This feature is probably responsible for artificial recharging of the spring's catchment area in addition to natural recharge.

New developments and applications in field instruments, and specifically introducing capabilities for a wider spectrum of groundwater state variable logging, have enhanced the level of groundwater information, both spatially and chronologically. The correlation between the modern electronic groundwater information and climatic role players require further expansion, in order to enhance the quantification of critical decision making parameters, i.e. monthly/daily groundwater recharge values eventually on a $\text{m}^3\cdot\text{km}^{-2}$ level. This implies that modern hydrometeorological information needs to be monitored on a short-term basis, i.e. specific rainfall patterns (over hours-days), and episodic groundwater recharge event (days-weeks).

The scope of this study therefore was to design a series of experimental modern monitoring programmes to collect specific components of the HC and use these to upgrade the conceptual methods for recharge estimation by alterations to methodologies and applications. The semi-arid region of southern Africa were selected, as they are the most affected by irregular hydrometeorological patterns, thus impacting on the long-term groundwater recharge process and availability of sustainable water resources. Fractured hard rock terrains provide an effective interface between rainfall and groundwater, though, where with the aid of special monitoring techniques a unique set of hydrological state variables can be pooled.

Groundwater data is captured as basic information attributes and time-series data. Basic information covers a wide range of parameters about the monitoring site⁴ location and features and accumulates in the Department's National Groundwater Archive (NGA). Time-

⁴ A monitoring site includes a wide range of natural and/or man-made features, which allows one to observe groundwater in its many occurrences on earth, including springs, wetlands, boreholes, wells, burrow pits, mineshafts and even open-cast mines.

series data, consisting of water level data and hydrogeochemistry data generated through various monitoring programmes are stored in Hydstra and the Water Management System (WMS)⁵ respectively.

2.2. HISTORY OF HYDROLOGICAL DATA GENERATION IN SOUTHERN AFRICA.

Historical groundwater exploration was focused on developing groundwater supplies along the major railway lines in South Africa for supplying steam locomotives with water (Vegter, 2001). As local settlements expanded, developing of municipal and rural water supply schemes evolved into large-scale deployment of groundwater resources. Expansion of the national ESKOM power grid throughout the country instigated extensive groundwater irrigation systems where several million cubic meters of groundwater are abstracted annually. In addition, deep (>1 km) mining developments in the rural regions cause significant water-table depressions, which severely impacts on the shallow aquifer systems used by the local population.

Some of the earliest groundwater level records in the western Kalahari Region appear on drilling reports submitted by the Department of Irrigation in the Auob River⁶. Groundwater table values are by far the most abundant attribute of the observable groundwater sub-cycle of the HC, and can be found in many personal and official data bases at government departments, academic institutions and consultancies. Consolidation of this information has been the objective of the DWA, and special information systems were implemented during the last few decades to capture this and to secure long-term sustainability of these systems through continuous information technology maintenance and upgrading.

Groundwater quality information, on the other hand, can be classified as abundant, as about 20% of the borehole monitoring sites on DWA's National Groundwater Archive has at least one single macro analysis. In terms of groundwater quality time-series, the information package is disappointingly limited and chronologically highly irregular.

⁵ Water Management System (information base) for all water quality analysis data.

⁶ A water supply drilling project during 1914 to supply military horsemen and patrol horses with potable drinking water along an illegal horse-trading route between South Africa and Namibia.

The Act identifies DWA as custodian of national water resources for RSA, with a well-defined responsibility towards '*Monitoring, Assessment and Information*' as per Chapter 14 of the Act (Section 2.3.1). DWA has been the custodian for many hydrological monitoring programmes and networks development throughout South Africa and lately has been participating in monitoring programmes initiated under the Water Sector of SADC. These include the SADC-HYCOS programme and recently UNESCO's International Shared Aquifer Resources Management (ISARM) initiative, which will be discussed presently.

2.2.1. Hydrological Monitoring Programmes Implemented by the Department.

Through the last three (3) - five (5) decades, the utilization of South Africa's water resources has increased dramatically, especially in the food-production and industrial/mining sectors. To cope with these impacts of bulk abstractions from the resource and discharges, the requirement for impact-related information was already realized some 100 years ago. Large volumes of return/grey water discharged into many surface water drainages put an even higher responsibility on the maintenance and management of South Africa's potable water resources. As the impact on surface and groundwater resources widened, the DWA was obliged to expand and upgrade its monitoring programmes accordingly.

These monitoring programmes are still operated in isolation from one another, especially the surface water-groundwater programmes, and a process of amalgamation into a coherent and structured monitoring, assessment and information system is required (DWAF 2004).

2.2.2. International Water Resources Monitoring Obligations, SADC Region.

Most of South Africa's international boundaries are demarcated by river systems, (i) the Ramatlabama, Molopo, Nossob, and Orange drainage systems demarcating the Orange Senqu Basin in South Africa, Botswana and Namibia, and (ii) Crocodile-West, Limpopo drainage systems demarcating the Limpopo Basin in South Africa, Botswana and Zimbabwe. It is obvious that water use and more serious issues such as flood control need to be managed on an international level in order to manage extraordinary floods such as the

1999-2000 flood in the Limpopo Basin that caused a life-threatening situation in Mozambique.

For the surface water component, the SADC-HYCOS programme focuses on an international river-flow monitoring network consisting of 136 gauging weirs/stations in 14 countries. These stations are operated on real-time data transmissions using radio/satellite communication systems and have their main centre in DWA National Office, Pretoria.

The Groundwater and Drought Management Programme of the SADC's Water Sector focuses on the groundwater component, and several aquifers systems along the RSA international border were identified as potentially impacted systems for which special transboundary measures are required. One system, the Kalahari-Karoo Aquifer Systems, transcends between South Africa, Botswana, and Namibia. This system includes the well-known Stampriet Artesian Basin (Permian Karoo, Eccca Group sandstone/shale sequence), overlain by localized Kalahari Group Aquifers (Tertiary – Quaternary Kalahari Group (T-Qk) sediments). Subsequent to a recent re-assessment of the project in 2009, it was recommended and approved to add the Ramotswa Dolomitic Aquifer system shared between South Africa and Botswana as a vulnerable transboundary aquifer in need of assessment and long-term management.

2.2.3. Hydrological Monitoring by Water Users.

Implementation of the Act requires water users to report their water use activities on prescribed conditions as per a particular license application, issued for a specific period in time, with short-term reviews. In cases where bulk groundwater is abstracted, the Act promotes establishments of Water Users' Associations (WUA) who should manage the water resource and be responsible for the monitoring programmes. The attributes specified consist of (i) water abstraction figures (monthly to quarterly intervals), (ii) water levels from specified monitoring boreholes (continuous logging, weekly or monthly intervals) and (iii) total water quality analyses (monthly to quarterly, depending on the water use activity) which basically include an initial hydrochemical and trace element analysis at t_0 .

When one full hydrological year (Oct_n to Sep_{n+1}) has passed, the quality monitoring attributes/interval can be substituted by a site-specific configuration.

Unmanaged/uncontrolled local land use activities may have a long-term (10 years or more) impact on groundwater quality. A good example is in Figure 2.3, where it took almost 15 years before a local NaCl pollution incident has naturally drained out of a relatively small dolomitic groundwater unit.

2.3. MANAGEMENT FRAMEWORK FOR GROUNDWATER MONITORING PROGRAMMES.

DWA's National Water Resources Strategy (DWA 2004), states that no proper decision regarding water resource matters can be made without relevant, reliable and in-time information at hand. Information is therefore fundamental to the successful implementation of the Act and the strategies required for all aspects of water resources management.

2.3.1. Chapter 14 of NWA (1998): Monitoring, Assessment and Information.

The Act introduces several new concepts in the light of water resources management in South Africa (DWA 2000). It regulates all water-related aspects in South Africa based on the Constitutional Rights of the nation as stipulated in the Constitution of the Republic of South Africa Act, No. 108 of 1996.

Systems for water resources management should be established to generate appropriate data and information to assess, manage, and protect the national water resources of South Africa.

The following important concepts in the Act have direct relevance to monitoring, assessment and information:

- The issue of **resource protection** introduces the concept of **resource-directed** and **source-directed** measures which requires a dedicated hydrological information platform from where these measures can be implemented and maintained;
- The concept of **the Reserve** requires that before any water use is allocated, the water use requirement for basic human needs and protection of aquatic ecosystems needs to be secured. In the groundwater domain, springs are especially vulnerable, as a small drawdown (<1 m) instigated by upstream abstraction may significantly impact on the spring flows used by down stream users;

- After providing for the reserve, the remaining water supply needs to allocate for beneficial use in the public interest. Allocation should therefore be according to a system that promotes optimal use for the achievement of equitable and sustainable economic and social development;
- **Protection** of the resource is based on the constitutional obligation, and also reflects on the environment itself and *vice versa*. Water quality monitoring from a reference and compliance objective is required, as most of these cases will end up as court cases and water tribunal inquiries; and
- To conclude, the Act recognises that management of water must take place at **catchment** level, or for that matter in a **groundwater unit** context. Depending on the status of groundwater use in a specific groundwater unit, the monitoring programme should not only look at the impact water allocation alone. Resource reference conditions, such as groundwater recharge, needs to be part of the Act's implementation address.

The objectives of the Act therefore points to protection and sustainable use of the water resources of South Africa. It emphasises various aspects of the HC and provides regulations for the regulating authority (DWA), as well as water users to comply with. For the first time in South Africa's water legislative environment, groundwater in its many facets is recognized in the total water budget. Managing groundwater in terms of the regulations and conditions of the Act requires a dedicated approach for generating high-level information through dedicated observation networks and assessments.

2.3.2. Groundwater Monitoring Management Framework.

The Constitution of South Africa states clearly that '*Everyone has the right to have access to water and a healthy environment*'. The Bill of Rights highlights specifically that water resources management should (i) achieve sustainable use by adjustments, availability and legal requirements and protection by measures, and (ii) achieve efficient and effective water use by optimal social and economical benefits (DWAF 2000).

The 1956 Water Act did not recognized groundwater as a public entity. This resulted in a disregard for groundwater resources management, from both water quantity and water quality perspective. Because of this neglected obligation, serious deterioration in quality

due to anthropogenic activity became of problem in later years which imposes various threads to surface resources. For example, many redundant coal and gold mining operations have left vast systems of interlocked tunnels and mine voids which have been steadily filled with groundwater and ingress surface water to produce variable concentrations of acid mine water. A good example is the Witwatersrand Western Gold Mining Basin which started to decant via a decommissioned borehole, (to be followed by several shafts) and ultimately delivering in the order of $15 \pm 5 \text{ Ml} \cdot \text{d}^{-1}$ poor quality AMD (Figure 2.4).



Figure 2.4. Initial acid mine water decant from a decommissioned borehole next to the Twee Lopies Spruit in the West Rand (S26.11519; E027.72303, 1664 m amsl).

Support (i.e. funding, staffing and information technology) from the water resource managers (National, Regional and Catchment Management Agencies (CMA)) level is regarded as one the most important strategies to ensure a long-term successful sustainable management process which requires a sustainable monitoring infrastructure.

Water resource management in South Africa operates on (i) local government scale (District Municipalities), (ii) on a catchment scale (Water Management Area WMA) with its

CMA structure, currently the responsibility of DWA's regional offices), and (iii) on a national scale (DWA).

Monitoring programmes may be developed at various levels in the above-mentioned framework and depend on specific objectives. The current infrastructure framework of the department supports at least two levels of integrated operations on governance level, i.e. National Level and Regional Level. A third level, referenced as the Local Level focuses on the roles and responsibilities of the actual water use institution (water boards, water supply authorities and WUA). These institutions reports to the Department's regional offices in terms of water use license conditions and compliances thereof.

2.3.2.1. Administrative Levels.

The Act stipulates that the country's water resources should be managed on a three-tier system i.e. National-Regional-Local levels which correspond with the over-all governmental governance structure of National, Provincial and District/Local entities. It was experienced in the past, that important risk factors impact severely on the long-term sustainability of monitoring programmes. These are: (i) funding, (ii) human resources, and (iii) infrastructure support, which can only be sustained by committed governmental coordinated institutions and a set of regulations originating from the Act. The three tier structure functions as follows:

The National Level (Level One):

Advocating a policy and regulating function from a national office is required to ensure sustainable national and international water resources environment. Although DWA stands in for the national level responsibilities which includes scientific and technical support, its role is towards implementation of the Act and specifically responsible for its policy and regulation⁷ role aimed at the management of the country's water resources. DWA national office's responsibility in terms of the management of the water related components of the HC is in securing long-term observations for reporting on the status of resource in terms of the global/continental effects playing its role in the country's water budget. All na-

⁷ Water use allocations and long-term assessment of water resources resulting from natural effects and impacts.

tional monitoring programmes therefore reside directly under the custodianship of the Chief Directorate: Water Resources Information Management (CD: WRIM).

The Regional Level (Level Two):

To address the regional management of water resources in South Africa, 19 WMA's have been demarcated. Several regional offices were either established as new institutions, or existing regional offices restructured to represent the DWA's role as national protector and regulator. Regional offices have jurisdiction beyond the Provincial boundaries in terms of water resources management. These offices are responsible for the management of the impacted systems due to anthropogenic activities, and regulate the allocations of water resources to water users of all kinds. Quality and quantity impacts on the water resources as the result of water abstraction from and discharges to water systems need to be observed on an aquifer/drainage system level scale and require the regional offices to establish monitoring programmes for this purpose.

The Local Level (Level Three):

Quantification of abstraction from or discharge to water resources (especially the aquifer systems) requires dedicated monitoring at the level of boreholes and well fields. These points are licensed under the Act and water users are responsible for the data generation which mainly consists of hydrochemistry and abstraction figures. These water users may consist of an individual person or a group of local water users (WUA) or institutions (water boards or water supply authorities (WSA)). Specific water use license conditions in terms of the monitoring responsibilities are applicable to each water user. Funding water resource data acquisition and management comes from levies within the organizational structures of these institutions. Good examples of functional groundwater WUAs in South Africa are Tshiping WUA (Olifantshoek-Postmasburg-Kathu) in the D41J and D73A Quaternary Catchments and Tosca-Vergelegen WUA in the D41C and D41D Quaternary Catchment (De Villiers 2009).

2.3.2.2. Monitoring Programme Types.

Impacts generated by natural climate and anthropogenic events on the HC are time and spatially related. Given South Africa's diverse groundwater systems, monitoring pro-

grammes should be implemented to address various objectives for the purpose of obtaining applicable information. Groundwater monitoring programmes therefore consist of various types and scopes of monitoring; mostly driven by the monitoring objective.

Variations in the southern African HC, the scale of impacts and diversity in water occurrences and use, require monitoring programmes to be classified in at least four different types (Van Wyk 2003; Uil et al. 1999), and they are:

- ❶ **Basic/Reference (Type 1):** Background or reference conditions; to record ambient conditions, status assessment and long term variations (trends and status) required for long term water resource management, such as assessment of the impacts of large scale droughts/flooding on the water resources. This monitoring type also provides special data sets for national level resource studies, e.g. groundwater-rainwater interaction, piezometric-head recession rates, and aquifer water-retention abilities;
- ❷ **Regulatory Monitoring/Assessment (Type 2a):** Impacted or regional conditions specifically focussing on control management of the functions of the resource, and linked to regulations, laws, and directives related to the use of groundwater. A special subset of this level complies to **Local Regulatory** (Type 2b) monitoring specifically addressing the start-up and final delegation of compliance monitoring for well field and production borehole surveillance;
- ❸ **Specific Purpose Monitoring (Type 3):** Specific aspects/issues/functions during groundwater investigations and link to the surface water environment/components, the local water balance and recharge. Groundwater quality monitoring in areas where aquifer protection needs to be performed, implementation and evaluation of remediation and restoration measures resulting from specific land use activities, i.e. decanting of mine void seepages; and
- ❹ **Early Warning and Surveillance (Type 4):** A dedicated monitoring programme which addresses point source type impacts like accidental spills, determination of health hazard status of waste disposal sites, or determination of sources of groundwater quality deterioration.

The network of observation points can include, completely new developed monitoring sites or any monitoring site functioning under Types 1 to 4 for the period this monitoring action is required.

2.3.2.3. Linkages between Monitoring Levels and Types.

Although DWA at national level is responsible for policy and regulation, its hydrological services component has links throughout the whole administrative (Levels) and functional (Types) structure. Figure 2.5 illustrates a functional framework structure between managerial (Level) and physical stages (Type) of groundwater monitoring.

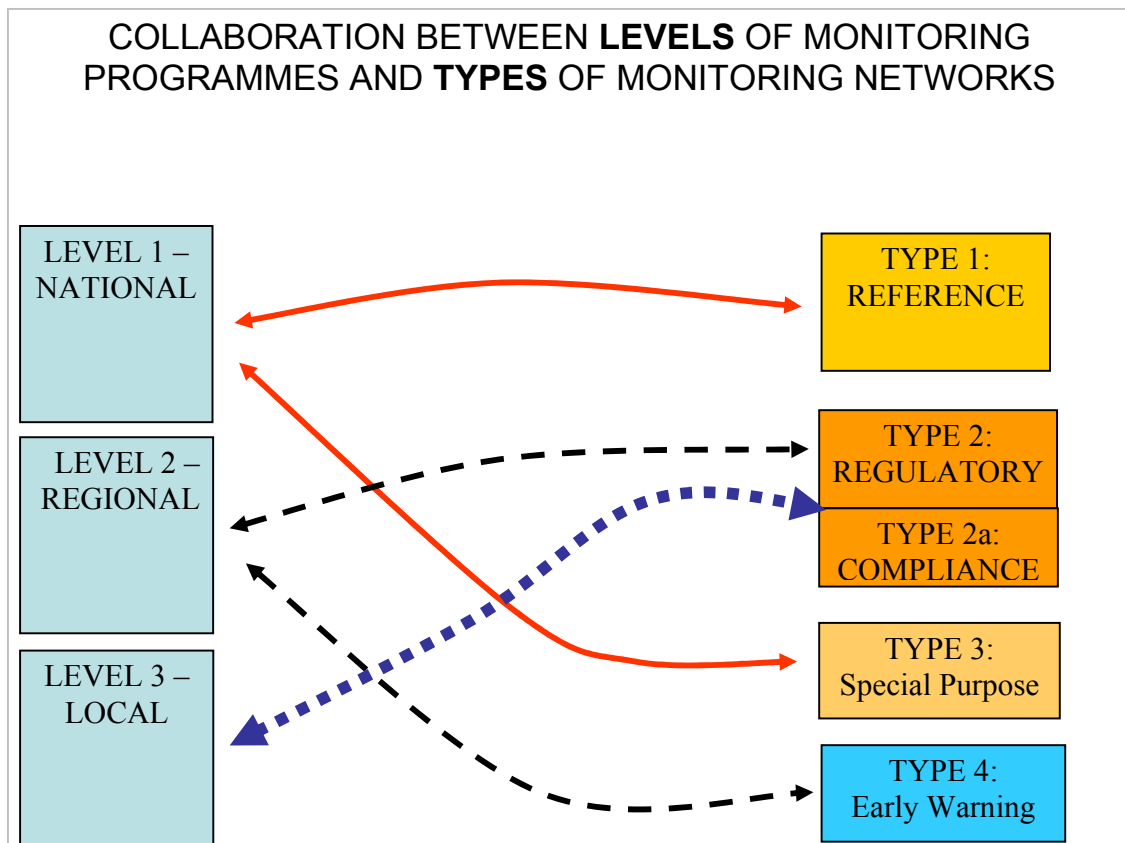


Figure 2.5. Graphical presentation of the linkage between Monitoring Programme Levels (administration, funding and management) and Monitoring Programme Types (physical networks, instrumentation, and operation and maintenance).

Environmental changes, naturally or anthropogenic driven, i.e. a flood situation, dry spell or mine water decanting, may require that a monitoring programme setup for Level One -

Type 1, may also support a short-term monitoring programme in a particular region, and the data generated may therefore satisfy the requirement of a Level 2 - Type 3 programme. In such cases, interaction between the managerial components (e.g. the national office and particular regional offices) of monitoring programmes is conclusive.

Figure 2.5 portrays the framework structure between managerial (Level) and physical stages (Type) of groundwater monitoring. The framework suggests that for example the Directorate: Hydrological Services (Level 1) is tied to monitoring functions and activities required to perform Reference Type Monitoring (long-term background information) as well as Special Purpose Type Monitoring (long-term dedicated monitoring, for example rainwater-groundwater interaction).

2.4. GROUNDWATER QUANTITY MONITORING PROGRAMMES (WATER TABLE).

2.4.1. *Introduction.*

Groundwater development programmes from 1970 onwards introduced the use of high capacity borehole pumps. Aquifer estimations were based on conceptual hydraulic parameter estimations. Many groundwater levels were recorded during yield tests and tabled into project reports.

Continuous time-water level recordings became possible as early as in the 1950's, by using autographic water level chart recording devices - an application of instrumentation used for monitoring surface water resources in canals, balancing dams and large reservoirs.

Modern electronic piezometric level logging devices opened a completely new perspective on recording and data processing of groundwater data. Real time (or in-time) logging facilities are just another feature which became available and substantially enhances the reporting lapse time for groundwater information.

2.4.2. *Attribute Configuration and Measurement Interval.*

Electronic data logging devices specially built for groundwater data logging applications can be programmed to measure and record basic attributes such as water head pressure,

temperature, and conductivity, through dedicated sensors in the logging units (Section 2.7).

A typical piezometric data string consists of Date-Time-Value configuration, and is illustrated in Figure 2.6.

```
Data file for DataLogger.
=====
User name: Application management >>
COMP.STATUS:Done
DATE       : 2007-05-23
TIME       : 18:53:05
FILENAME   : + D:\28_LDM-to-H3\G33327_May'07.MON
Created by : LDM VEI-edition version 4.0.0.3
===== BEGINNING OF DATA =====

[Series settings]
Serial number      =.N05-37130 309.
Instrument number  =G33327
Location          =LRAS_Chemfos
Sample period     =00 00:30:00 0
Sample method     =T
Start date / time =00:30:15 30/01/07
End date / time   =00:30:14 22/05/07
[Channel 1 from data header]
Identification    =NIVO
Reference level   = 0.000 m
Range            = 30.000 m
Master level      = -17.520 m
Altitude         =50 m
[Channel 2 from data header]
Identification    =TEMPERATUUR
Reference level   =-20.00 °C
Range            =100.00 °C

[Channel 3 from data header]
Identification    =2: Spec. Cond.
Reference level   =0.000 mS/cm
Range            =5.000 mS/cm

[Data]
5375
2007/01/30 17:00:00.0 -17.592 21.09 0.674
2007/01/30 17:30:00.0 -17.575 21.08 0.676
2007/01/30 18:00:00.0 -17.585 21.09 0.679
2007/01/30 18:30:00.0 -17.575 21.10 0.676
2007/01/30 19:00:00.0 -17.575 21.06 0.680
2007/01/30 19:30:00.0 -17.579 21.09 0.679
2007/01/30 20:00:00.0 -17.574 21.08 0.679
2007/01/30 20:30:00.0 -17.572 21.09 0.679]
```

Figure 2.6. A typical time-series electronically-generated water level, temperature, and electrical (specific) conductivity datastring as recorded by a Schlumberger CTD data logging device.

Comprehensive electronic logging apparatus is available that can measure several other physical and chemical constituents in groundwater. This is high-level technical equipment, which requires frequent calibration and care (i.e. on a weekly interval).

The logging interval varies from 0.5 seconds to 24 hours, and is programmable b.m.o. the instrument's interface software.

2.4.3. Raw Data Generation and Quality Control.

Hydrological data is generated at a particular monitoring site in a specific network establishment. A monitoring site may consist of a surface (spring water) flow gauging structure, (e.g. a Parchall Flume, Figure 2.7).

Additional devices for rainfall logging and weather attributes are incorporated to generate a more complete package of hydrological attributes.



Figure 2.7. Spring-flow gauging weir (a 2' Parchall Flume) at Kuruman A-Spring with instrumentation housing for Ott Thalimedes water level logger.

Infrastructures like these gauging stations are influenced by local land use and calibration of these structures forms the main part of the maintenance programme. Deterioration of

the channel side-walls changes the flow dynamics on the stream itself; thus the actual recorded measurements do not report the actual flow volume.

In the case of complex aquifer systems, like layered semi-confined and confined systems, monitoring both aquifers at the same spot is normally done (Figure 2.8). In this case the representative data quality requires dedicated boreholes for each aquifer system; not ignoring the special construction requirements for each monitoring point. The monitoring configuration shown in Figure 2.7, for example illustrates the borehole pair on the Langebaan Road Aquifer System (LRAS) where an upper and lower aquifer is monitored for quantity (Qn) and quality (QI) trends and variations. In this case the piezometric difference between the upper/lower aquifer at this sites is 5 m.



Figure 2.8. Borehole pair with a DWA rainfall logging/sampling unit, LRAS, District Vredenburg, Western Cape.

Most of the current groundwater level logging devices automatically transfer water head measurements (water level head above the sensor) to a depth to water level (water level

from borehole collar), hence adjusting the water level (m bgl) to actual piezometric elevation (m amsl).

Data quality filtering is a much-needed process to control and adjust the electronically generated data. As with the highly variable plotting quality of the older autographic chart recorders, the modern electronic units may also generate some erroneous data sets. These basic errors are (i) a electronic shift which causes a sudden step in the data set, (ii) a gradual, prolonged shift in the data string, and (iii) data spikes (those erratic single data points in an otherwise flattish configuration of data points). These errors can be corrected quite sufficiently b.m.o. control measurements⁸ and application software⁹.

2.4.4. National Groundwater Level Monitoring Programme.

Selection of monitoring sites (springs, borehole and mine shafts) for specific monitoring applications should undergo a dedicated site investigation - the best way is through down-the-hole (DTH) inspections using (i) geophysical, (ii) hydro-physical, and (iii) DTH-CC image logging applications.

The groundwater monitoring sites in South Africa total approximately 400 for quality (Type 1) and 2500 for water-table (Type 1-4). Compliance monitoring (Type 2A) required for local water users such as irrigation schemes, industries and mines, are not regulated by DWA, mainly due to the vast number of compliance monitoring sites involved.

During previous phases of groundwater development, drilling programmes produced a large number of boreholes of which only a fraction were eventually used for water supply. Many boreholes are therefore available for aquifer management purpose monitoring, but very few are situated in direct recharge terrains.

Most of these boreholes act actually as bypass links between ranges of possible smaller aquifer zones, which when purged for dedicated water samples, produces a whole mixture between shallower, recently recharged water and older, more stagnant, groundwater (Mazor 1997).

⁸ A water level control measurement taken at the monitoring site at least on a quarterly interval.

⁹ Hydras 3 application software by Ott Hydrometrie Pty Ltd, Germany and Hydstra by Kisters Pty Ltd, Australia.

Figure 2.9 demonstrates the skewed coverage of groundwater monitoring networks based on the most productive groundwater zones and areas where groundwater water development was initiated in South Africa

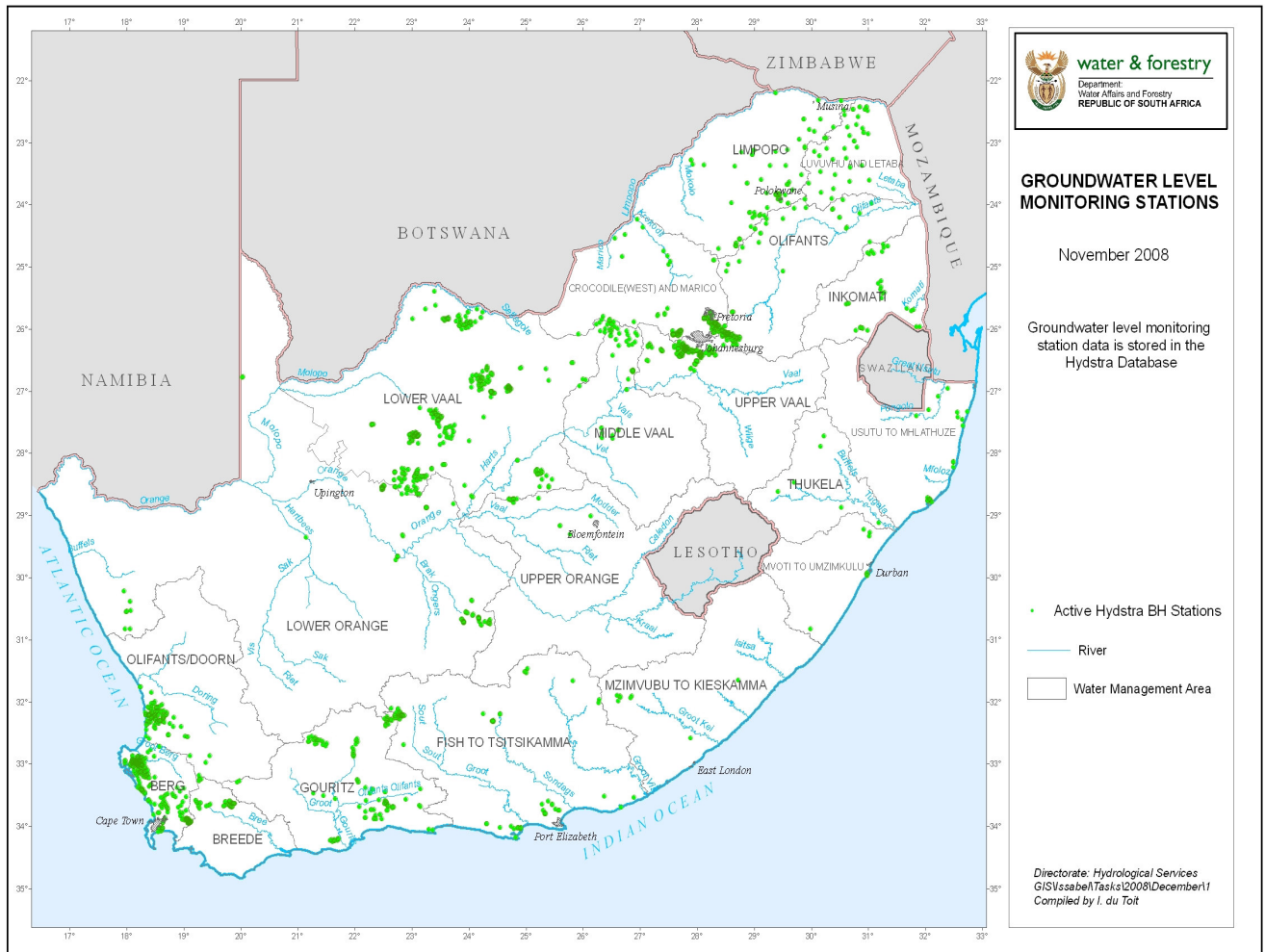


Figure 2.9. The current national coverage of monitoring sites in South Africa for obtaining groundwater level data.

2.5. GROUNDWATER QUALITY PROGRAMMES (HYDROGEOCHEMISTRY).

2.5.1. Introduction.

Prior to 1993, no formal groundwater quality monitoring programme operated by the Department was based on time-series and spatial coverage principles. DWA's water quality laboratory at Roodeplaat Dam started with macro-chemical analytical services in 1974.

Most groundwater samples submitted for analysis came from *ad hoc* projects, and consequently were once-off analyses. In a spatial context, these analyses are quite useful, and formed the basis for the groundwater quality assessments for the national 1:500 000 Geo-hydrological Map Series completed in 2003.

A National Groundwater Quality Monitoring Programme (NGwQMP) was initiated in 1994 with 131 monitoring sites and expanded to 410 monitoring sites over South Africa since 1996.

2.5.2. The National Groundwater Quality Monitoring Programme (NGwQMP).

In addition to long-term time-series observation of the country's groundwater quality, increasing usage of groundwater in the urban and rural domains, as well as the growing awareness of groundwater pollution by anthropogenic development, encouraged the establishment of the NGwQMP. A specific time slot was chosen, within four (4) weeks before and within four (4) weeks after the local¹⁰ rainfall season. This requires the monitoring sites to be visited for sampling twice annually. Two groundwater quality assessment projects utilizing the data generated by the NGwQMP as well as the long-term DWA WMS data base were conducted by Šimonič (2002).

The basic objective of this programme is to generate a long-term hydrogeochemical data set on a national scale which can be applied towards the optimization of groundwater quality and quantity management (Šimonič 1993), with specific goals i.e. to:

- Establish a spatial hydrogeochemical trend to identify variation in groundwater quality across South Africa. The outcome of this assessment portrayed the different hydrogeochemistry characteristics of the various aquifer systems, as mainly driven by the hydro-lithological composition of the aquifer itself. The initial areal rainwater input is probably one of the main drivers for the groundwater hydrogeochemistry regime, followed by the hydraulic flow regime from ground surface through the UZR reservoir to the water table interface and subsequently laterally to adjacent sub-reservoirs;

¹⁰ Summer and winter rainfall regions: April-May and September-October respectively.

- Establish a time-series hydrogeochemical trend assessment to assess how the groundwater quality changes with time; and
- Confirm that the proposed monitoring site spatially represents a conclusive groundwater quality terrain and specifically report changes caused by natural impacts only, i.e. as a result of long term dry spells or abnormal recharge events (for example the 1974-1976 abnormally high rainfall season, and the impact on the SZ water following episodic rain events considered in this study).

The infrastructure requirements for a groundwater quality monitoring programme, where water must be pumped from a borehole for a specified time to gain access to representative aquifer water, is quite challenging when dealing with a national monitoring network covering the whole of South Africa. In the case of non-equipped boreholes, a mobile pump unit must be available for purging the borehole. Using non-equipped boreholes for this programme therefore proved to be (i) time-consuming in terms of equipping/purging a monitoring site, (ii) impractical in terms of sampling representative aquifer water within a limited time slot, and (iii) uneconomical in the sense of dragging a heavy pumping unit over several tens of km from one monitoring site to the next one.

Using already equipped production boreholes situated in a non-affected environment seems to have the best advantage over a limited time slot and basic practices. In each region, a reconnaissance survey was conducted and ultimately about 410 monitoring sites were selected over almost 90% of South Africa. Monitoring started in 1995, and since then was operated on a mean annual coverage rate of 95% (Šimonič 1993; 2002).

Although many local operational problems¹¹ were encountered, redundant monitoring sites were immediately replaced by neighbouring ones, which in some cases has impacted on the spatial continuity of the site. In time, hydrogeochemical trends report small differences, which, as one should expect, come from local differences in the hydrogeochemistry regime.

The well-established infrastructure of the NGwQMP allows the operating institution (the Department's National Office's sub-Directorate: Groundwater Resources Assessment and

¹¹ Pump failures, electricity cuts, borehole failures and access restrictions.

Monitoring or GRAM) to add additional components of the hydrogeochemistry analytical spectrum to the bigger data package. For example, incorporating sampling/analyses for environmental isotopes (stable isotopes: ^{18}O and ^2H and radiogenic isotopes: ^3H) were accomplished on two sample runs in the last eight (8) years.

2.5.3. Analytical Requirements for Groundwater Research Investigations.

The majority of DWA's monitoring programme's hydrochemistry analyses are performed by the DWA laboratory at Roodeplaat Dam. Trace metal analysis forms part of the initial hydrogeochemical analyses package only when a new monitoring site or a replacement monitoring site is incorporated into the network.

In recent decades, as the estimation of groundwater recharge became a requirement for planning and management of groundwater resources, environmental isotope tracers in groundwater were analyzed utilizing external specialist laboratories such as the Council for Scientific and Industrial Research's (CSIR) QUADRU¹² Laboratory and iThemba Wits LABS.

Applying the CMB principle for estimating groundwater recharge, a special analytical procedure is needed for low level hydrochemical (LLHcs) analysis. Hydrochemical concentrations in rainwater are too low for detection by normal analytical processes as performed by water quality laboratories. These special analyses were done by the CSIR's Air Quality Research Laboratory (AQRL) in Pretoria, South Africa.

2.6. HYDROGEOLOGICAL DATA BASES AND SUPPORTING SOFTWARE.

2.6.1. Introduction.

The cost and integrity of hydrological data capturing and assessments necessitates the storage of data for future applications, using specific tools which vary from low level state variables time-series presentations (hyetograph-hydrograph) to high-level sophisticated (transient and particle transport) modeling exercises.

In DWA, three large hydrological related databases are in operation for the storage of collated and processed data and are used for high-level hydrological information dissemina-

¹² Quaternary Dating Research Unit.

tion, as will be discussed presently. This information is processed by different in-house tools developed for specific applications, for example the Groundwater Development toolkit and the Resources Directed Measure toolkit

2.6.2. Data/Information Generation Procedures.

Hydrogeological data consists of mainly basic (descriptive) and time dependant attributes. To achieve the objectives of any data generating process, a specific process cycle needs to be followed (Van Lanen 1998) as illustrated in Figure 2.10.

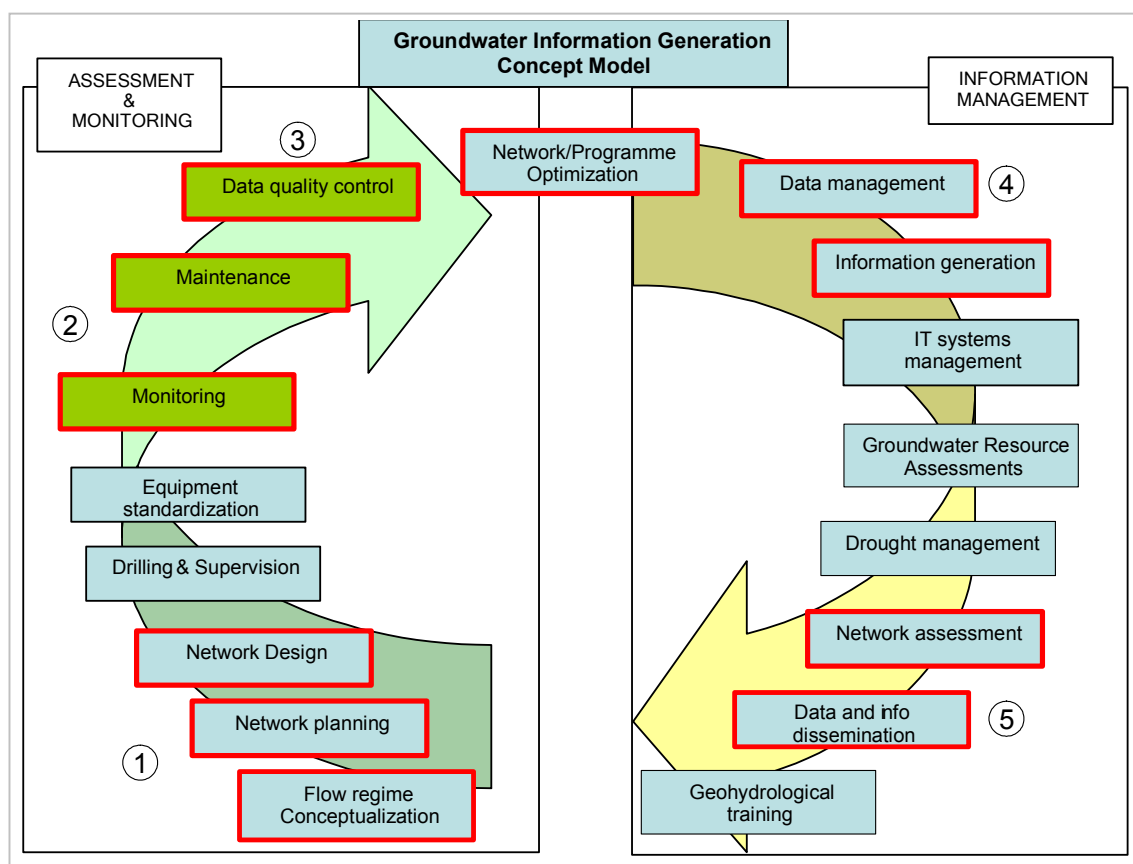


Figure 2.10. Illustration of a monitoring cycle showing the general processes required to generate hydrogeological information to satisfy the objectives of a specific monitoring programme.

Once-off information generation requires moderate to high specialist input, i.e. hydrogeological mapping and flow regime conceptualizing required for the establishment of specific groundwater-monitoring network design ①. These datasets are normally referred

to as basic information sets and characteristically fixed in time (monitoring site description, hydrogeological parameters/constants and construction features).

The actual data/information generation in any monitoring programme is time dependant; thus the data observed/collected is fixed to a time-series framework ②. This framework needs to be specified (specific monitoring intervals and state variables) as part of the monitoring programme with an appropriate storage facility due to the amount of data generated, especially with the modern electronic data logging devices.

The most important risks aspects of any monitoring programme lie with the maintenance and data quality control ③, followed by data management activity ④ as illustrated in Figure 2.10. All other sub-divisions in the monitoring cycle depend on the specific data generated during the monitoring programme, and assessment thereof.

Hydrological data needed to generate information for groundwater resources management is grouped into three major categories (WMO 1989):

- Constants: Primarily one-time data pertinent to the geometric pattern of the groundwater regime, the litho-stratigraphy of the groundwater unit, and technical characteristics of the observation network's facilities. Common constants are given below:
 - Co-ordinates of physical features like drainages, aquifer boundaries, catchment outline, monitoring sites, surface water gauging stations and springs;
 - Elevations of aquifer geometry, monitoring sites and catchment outlet and springs; and
 - Dimensions of boreholes, rain gauge funnels, pumping equipment, and gauging stations.
- Parameters: These are estimations of coefficients utilized in algorithms and equations which are used to generate hydrological information from the observed data. Examples of common parameters are:
 - Hydraulic parameters of groundwater flow models (hydraulic conductivity (K), transmissivity (T), effective porosity (n), storativity (S), and specific yield (Ss); and
 - Statistical parameters of these estimates.

- State Variables: Data changes over time, due to the dynamics of the hydrological regime under observation in a particular groundwater management unit. These are:
 - Variables pertinent to groundwater quantity (rainfall depths, water table fluctuations, spring flows, water use, surface water inflow/outflow and recharge rates; and
 - Variables pertinent to water quality as in rain water, surface water run-off, soil water moisture, and groundwater (hydrochemical and trace element constituents, environmental isotope compositions, and physical attributes such as temperature, pH, conductivity, redox potential and dissolved oxygen levels).

The processes and requirements for capturing appropriate and correct hydrological data to address a specific water resource evaluation, and assessment process during a preliminary monitoring design phase, need to be considered. It will be an insufficient exercise to parties involved in a monitoring programme to realize that one or more state variables required to perform a hydrological assessment, have not been captured during the observation period.

2.6.3. Storage Processes and Facilities.

Subsequent to the proposed criteria for generation of specific hydrogeological data as depicted in Figure 2.10, the ultimate success for any monitoring programme lies mostly with the continuity of data acquisitioning, management, and dissemination (③ to ⑤).

Before 1985, when only mainframe computer systems were available to perform limited calculations, and having poor storage facilities, groundwater data was stored in hard copy document format. In the current modern electronic age, micro-chip technologies enable storage facilities for large data sets in electronic format. Many initiatives such as the Hydrological Support Services project were initiated in 1989 by the Water Research Commission (WRC) and DWAF to start the process of physical capturing spatial and time-series data to specially developed data base systems (National Groundwater Data Base (NGDB), Hydrological Information, and the WMS).

Having stored in electronic format and with the ability to update stored data as new information is gathered, optimization of the data generating processes and systems becomes essential. Optimization of a costly data generation programme requires special assessment processes such as monitoring site (data point) clustering, data trend and spatial analysis, and finally reconciliation. Development of special hydrological tools required for data set assessments, generation of information sets, and special dissemination products produced a collection of useful software packages, i.e. Aquimon, Regis and CHART.

Capturing of autographic pen-recorded water level data from stacks of paper sheets required high-level assessment and processing prior to the physical digitizing and transformation to electronic data format. This process is rapidly replaced by the direct capturing of any type of calibrated data from a DTH electronic sensor to its associated data logging/storage device.

2.6.4. Monitoring Site and Piezometric Level Information.

Several different information databases are currently operational in DWA. This is due to the fact that field data is still generated by a complete diverse group of disciplines, i.e. surface water and groundwater monitoring. The main reason probably lies in the fact that at operational level, the data generation processes are high-level technical which requires dedicated training and applications.

2.6.4.1. National Groundwater Archive (NGA).

Initially developed as the NGDB, the NGA is an advanced information-technology-driven interactive system which allows external users to capture data in real time.

Very limited time-series information is captured on the NGA, thus it mostly caters for monitoring site descriptions, i.e. basic spatial information, hydrogeological information, construction data, and landowner information. No assessment facilities are available.

2.6.4.2. Hydstra.

A hydrological data storage and assessment software package developed and maintained by Hydstra Kisters Pty Ltd, Australia; applied in DWA for the capturing of spatial and time-

series data for surface water quantity monitoring programmes. Hydstra contains an advanced set of time-series data assessment tools, some specially designed for DWA to perform surface flow regime analyses and reporting (Figure 2.11).

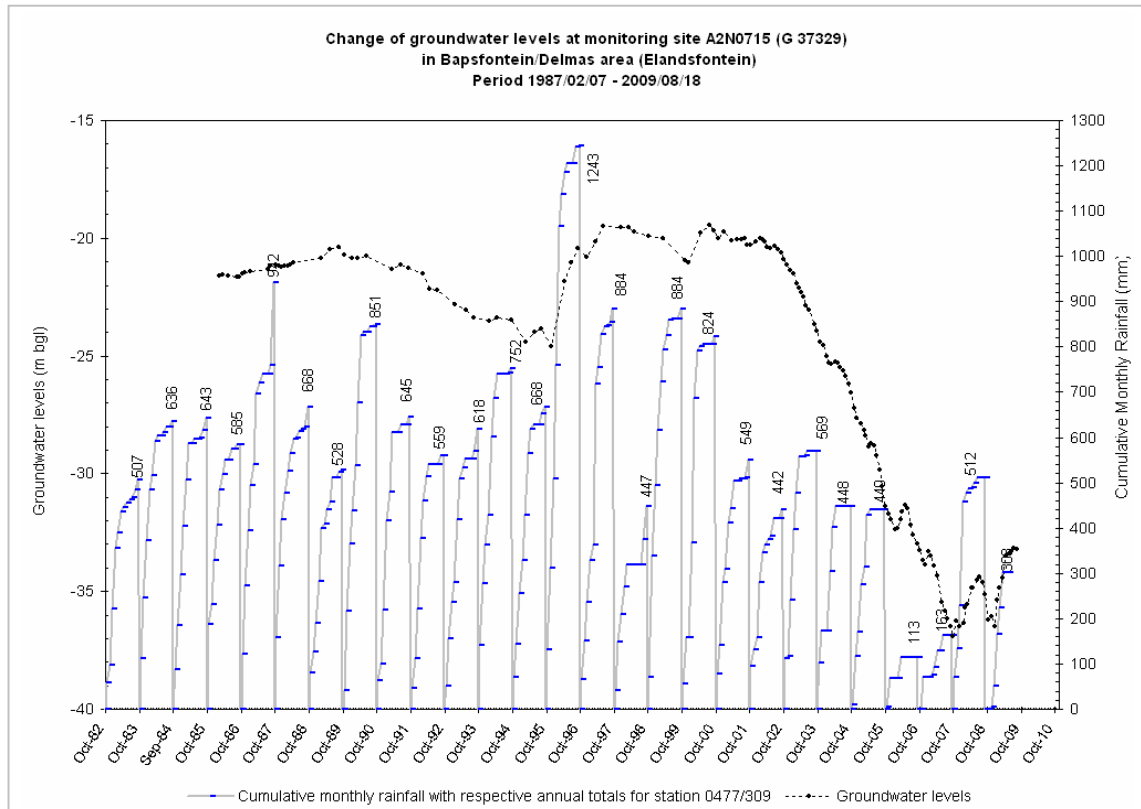


Figure 2.11. A Hydstra composite annual cumulative rainfall and waterlevel time-series plot of a monitoring site A2N0715, in the Bapsfontein – Delmas area.

Time-series groundwater level data, originally captured in NGDB has been transferred to the Hydstra platform. All newly generated groundwater level data is transferred directly to Hydstra from raw field data sets and subsequently edited.

2.6.4.3. Hydras 3.

Hydras 3 is a raw data storage and assessment software application which is solely used for Ott Hydrometrie instruments. The software is quite multipurpose, in terms of Ott Hydrometrie specification, although foreign data import facilities are easily performed. With limited manipulation of the Schlumberger and Solinst device's raw data text files, the data

can be imported and integrated into the Hydras 3 database. Hydras 3 are applied to edit/correct the data before it is uploaded to the Hydstra platform.

The data and graph matching facilities of Hydras 3 is applied throughout this thesis to produce composites of hydrographs (water table) and hyetographs (accumulated annual rainfall depths). Once the hyetograph and hydrograph match is established, all new data is automatically updated into the graphic presentation. These illustrations will be used presently as part of the data-assessment part of the thesis.

2.6.5. Hydrogeochemistry.

2.6.5.1. Water Quality Management System (WMS).

Water analyses done by various analytical units of the Roodeplaat laboratory finally resides in the WMS, which serves as the national data base for all water quality monitoring programmes operated by DWA. The data quality control at the Roodeplaat laboratory is of high standard and forms part of DWA's quality audit measures.

Special data storage facilities for the hydrological isotopes were added to the WMS's storage package; hence hydrogeochemistry data¹³ for NGwQMP monitoring sites can be populated in the WMS system.

2.6.5.2. Collective Hydrochemistry Analysis and Reporting Tool (CHART).

Interpretation of hydrogeochemistry data in spatial and time-series format requires the application of standard type diagrams, i.e. Piper, Durov, Schoeller and time related trend analyses. Application software like Aquachem™ by Waterloo or WISH by the Institute of Groundwater Studies (IGS) at University of the Free State, Bloemfontein, is not available at DWA. Data set preparation and transformation to these external software packages are time-consuming and create dead-end data base developments and storage.

A special software package, called CHART was developed in-house (DWA) with the following features:

¹³ Consisting of: macro/trace metals and environmental stable/radiogenic isotopes.

- CHART must be able to electronically retrieve hydrological data from within WMS, NGA and Hydstra;
- Any newly generated hydrogeological data uploaded to WMS and Hydstra must be automatically appended in CHART once per week;
- CHART must be able to generate specific monitoring programmes by selected groupings of monitoring sites and their relevant hydrogeochemical data, i.e. an interactive Monitoring Programme Generator;
- CHART must initiate hydrological integration, i.e. the ability to incorporate rainwater, groundwater and surface water analytical data in one work bench;
- A digital reporting facility for water management application and assessment of (i) a single monitoring site, (ii) a group of monitoring sites and (iii) a monitoring programme; and
- Have a special spatial (GIS driven) functionality to perform spatial assessment of hydrological information.

The basis for the CHART framework came from a comprehensive study of the NGwQMP 1993 to 2003 data set by Šimonič (2002). The need for an interactive assessment tool on the one hand and a dynamic water quality database on the other hand has been identified during this study period, because no facility was available in DWA.

The systematic links with other information systems and outputs of CHART are described in Appendix 1. One of the products is a time-series presentation of hydrochemical constituents which portrays hydrochemistry trends over time, as illustrated in Figure 2.3.

2.7. A DEDICATED GEOHYDROLOGICAL MONITORING PROGRAMME.

2.7.1. *Introduction.*

The *Estimation of episodic groundwater recharge in semi-arid fractured-weathered hard rock aquifers* requires a specific configuration of hydrological data consisting of rainwater-groundwater hydrogeochemical characteristics. Local runoff was also been identified as a

required condition to generate effective groundwater recharge. The above-mentioned state variable requirements cannot be satisfied by short-term observation periods. An observation period covering at least a few hydrological years (5-10 yrs) is needed in order to generate a realistic set of state variables. To meet this requirement, a dedicated monitoring programme and network setup is needed in the area where recharge estimation needs to be established. Optimization and rationalizing of the network should be part of a year-to-year programme assessment to achieve the most economical value from the exercise.

The magnitude of recharge-producing surplus rainfall (recharge into the UZR) is controlled by localized geomorphologic and hydrogeologic conditions (Section 4.3). Extrapolating to larger areas like Quaternary Catchments does not always produce the actual groundwater recharge value at this scale, due to the variability of the soil/regolith profiles over short distances (Willemink 1988; Gieske 1992). Hydrometeorological factors, especially in southern Africa's semi-arid regions, bring about even more variability in rainfall patterns and depths; thereby to a large extent changing the spatial distribution of groundwater recharge over an area of interest.

2.7.2. Programme Objective and Network Design.

2.7.2.1. Introduction.

A monitoring network consists of configuration of monitoring sites, equipped with dedicated instrumentation to monitoring state variables needed to generate a set of specified hydrological attributes (Section 2.6.2).

To be more specific on the study objectives (Section 1.2), it is required that a specific set of state variables be generate to:

- (i) identify a recharge-producing rainfall event with its unique rain rate configuration and hydrogeochemistry signature;
- (ii) monitoring the dynamic correlation between this recharge-producing rainfall event and water table responses in time and amplitude; and
- (iii) evaluate the responding recharge event in terms of Q_n and Q_l variation in the SZ.

As for the monitoring network in a potential recharge zone, a configuration of dedicated monitoring sites covering the most prominent hydrogeological features¹⁴ is required, and secondly, having dedicated instrumentation to monitor a configuration of determined parameters. The design criteria for a network that will satisfy the above-mentioned objectives, should allow for the physical construction of the monitoring sites, or evaluation of existing monitoring sites (boreholes) in a recharge terrain.

Not all monitoring sites response equally to recharge/discharge events in southern African hard rock aquifer systems, especially in the semi-arid regions due to the dissimilar fracture/matrix aquifer properties and spatial aquifer heterogeneities (boundary systems caused by intrusive dyke rock and faulting, as depicted in Figure 2.12).



Figure 2.12. The De Hoop Dyke in De Jagers Pass, District Beaufort West, showing a ± 3 m thick, dolerite dyke intruded into late Permian-earlyTriassic Beaufort Group sediments.

¹⁴Potential direct recharge features such as hard rock windows and indirect recharge features like rivulets and depressions.

Figure 2.12 shows a ≈ 3 m dolerite dyke in a sedimentary package in the lower Karoo Sequence consisting of late Permian-early Triassic Beaufort Group interbedded mudrock and lenticular sandstones. This vertical, dyke system will act as a groundwater flow path boundary. A high conductive flow path exists along side the dyke towards lower terrains where groundwater may issue as a spring and discharges into the surface water regime to sustain local baseflow.

A series of experimental networks, in this case a network classified as Type 3, were established and tested for reporting the required hydrometeorological state variables (Section 2.3.2.2). These networks comprise of the following components (i) a rainfall depth and bulk sampling unit, (ii) dedicated boreholes for sampling groundwater and allowing installation of special hydrological data logging devices, (iii) stream flow event/height loggers and sampler logging flash floods in rivulets, (iv) hydrometeorological variables, i.e. Davis weather station, and (v) *in situ* water sampling devices.

2.7.3. Climate Monitoring.

2.7.3.1. Introduction.

Weather patterns in semi-arid regions are highly variable, and probably bear the highest control over any groundwater recharge event. Hydrometeorological components such as rainfall depth, wind velocity, soil/regolith evaporation and temperature differences are the driving factors for creating a recharge-producing rainfall surplus condition, which will subsequently infiltrate into the UZR.

Depending on the status of vegetation water demand in the UUZr and the cyclic field capacity deficiency of the underlying LUZR, recharge-producing rainfall surplus may finally reach the water table and replenish the SZ. Preferential pathways, especially in fractured hard rock terrains, were identified as features promoting efficient and dynamic infiltration of rainfall-produced recharge (Johnston 1987; Willeminck 1988; Nkotagu 1997; Gehrels and Peeters 1998; De Vries and Simmers 2001).

These features may divert recharging surplus rainwater from the UUZr, and may cause such water to bypass the dried-out LUZR reservoir and flow directly to the SZ to illustrate

the bypass flow phenomenon in the hydrogeochemistry signature of fractured hard rock recharge terrains.

Special hydrometeorological monitoring equipment has been introduced as part of the trial monitoring networks to capture a wide range of hydrometeorological parameters (Figure 2.13). This monitoring set-up at the De HoopPoort experimental monitor site consist of (i) a DWA rainfall Logger/Samper, (ii) a DavisType weather station, (iii) the RES Unit and (iv) a Dry-Chloride Sampler.

The following sections describe the various components and methodologies followed to obtain the hydrometeorological state variables required for groundwater recharge estimations; under semi-arid and intermittent (episodic) weather conditions.

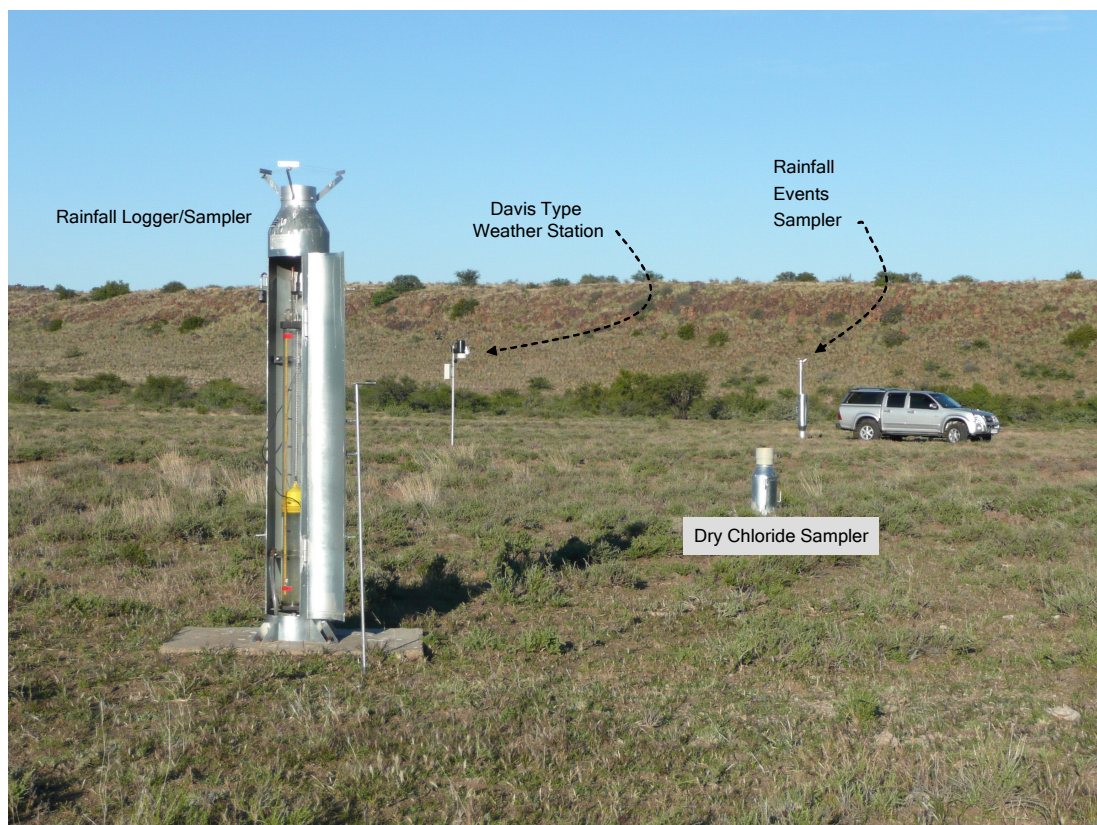


Figure 2.13. A special purpose network configuration for monitoring the hydrological state variables required for groundwater recharge estimations at the De Hoop Poort monitoring site.

2.7.3.2. The portable Davis Climate/Weather Station.

The Vantage PRO2™ manufactured by Davis Instruments, Hayward, U.S.A. supplies a wide range of time-series climate related state variables. The unit is supplied as a combined weather station set with an integrated data logging device. One unfortunate drawback of the unit is its limited data logging time-series facility of only fifty-three (53) days on a thirty (30) minute interval. Using it in remote areas is thus not practical.

All weather-related measurements are logged on a thirty (30) minute interval and stored in an Integrated Sensor Suite (Vantage Pro2 console unit) from where it is available for archiving and displaying. Climate variables logged and processes by the Davis weather station are shown in Table 2.2:

Table 2.2. Climate variables logged by the Davis Instruments weather station unit.		
Weather variable	Resolution	Source
Barometric pressure	0.1mm/.01mb	Sensor
Barometric Trend	1.5mm/0.5mm	Console
Evapotranspiration (ET-daily, monthly and yearly)	0.25mm	ISS and solar radiation sensor
Humidity Outside	1%	ISS
Dew Point (overall)	1°C	ISS
Rainfall (daily, monthly, yearly storm and rate)	0.25mm	Rain Collector
Solar Radiation	1W/m ²	Sensor
Temperature Outside	0.1°C	Sensor
Heat Index	1°C	ISS
Temp-Hum-Sun-Wind index (THSW)	1°C	ISS
Wind (direction and speed)	0.5m/s	Anemometer
Wind Chill	1°C	ISS
ISS: Integrated Sensor Suite		

The integrated sensor suite (ISS) is a solar powered unit containing a rain collector, temperature sensor, humidity sensor and anemometer. Additional solar and UV sensors were added to the ISS unit.

One of the useful parameters obtained with the Davis Type weather station is an estimation of the potential ET (ET_P). Although it is calculated indirectly from a set of state vari-

ables, it provides an estimate of the actual ET (ET_A). According to Chow (1964) ET_A varies around $0.78 \times ET_P$ for moderate climates (Chow 1946). The full effect of ET in semi-arid climate will be discussed in detail in Section 3.3.2.

2.7.4. Precipitation Depth Time-series Monitoring.

2.7.4.1. Introduction.

Groundwater resources in the arid and semi-arid zones of southern Africa represent the sole source for almost all the rural and farming communities scattered all over the region. It is ironical, to note that South Africa's two major perennial river systems originate on the eastern High Interior Plateau, but due to its westerly dipping geomorphological model, drain right through the driest western parts. Many rural towns situated on the banks of these river systems, are fortunate to have a permanent water resource at hand.

Distant areas not yet linked to the Vaal and Gariep River Systems via pipelines/inland waterways, depend on local groundwater resources. These resources are only replenished by local rainwater recharge. Estimation of groundwater recharge in these areas requires a comprehensive rainfall data set to support long-term water supply management (Van Tonder and Bean 2003).

Two (2) rainfall-quantity-related state variables are required to perform recharge quantification, and they are: (i) the actual amount of rainfall received and (ii) the rainfall-series pattern. The latter refers to the rainfall duration and intensities for each rainfall event. Rainfall depth data is normally collected by the South African Weather Services (SAWS) at manual and automatic stations all over South Africa and represent the national rainfall network. The spatial coverage is not so high as to support extrapolation of rainfall values required for local recharge estimations. Local geomorphological features have a remarkable influence on rainfall values and can be in the order of 100% as observed on and below the Great Escarpment at Beaufort West.

This study also incorporates the rainwater quality state variables which are not recorded by the SAWS. For the purpose of this investigation, special rainfall loggers/sampler units were constructed and installed within the monitoring terrains.

2.7.4.2. Rainfall Depth Logging Apparatus.

Recharge zones in the semi-arid regions of southern Africa vary in size and are mostly situated in remote areas. Manual measurements of actual precipitation values on a daily basis are therefore impossible, and a special rainfall logging device had to be designed, built and implemented as a continuous rainfall logger. The instrument resembles a large (1m * 100/90 mm OD/ID) acrylic tube equipped with a float/counter-weight water level type data logger; the Ott Hydrometrie Thalimedes stage height logger (Figure 2.14).



Figure 2.14. A DWA rainfall logger/bulk-sampler developed by the author and incorporated into groundwater monitoring networks in South Africa.

The acrylic tube/data logger unit is installed into a cylindrical mild steel housing, which was electroplated with a chrome base for internal heat control. The interior of the housing unit was painted black to extrude internal heat build-up. A 127 mm ID funnel right at the top of the housing collects the rainwater and diverts it into the inner unit where the rainwater drains into the acrylic tube and drives the Thalimedes float mechanism. The accuracy of the rainfall logger is 0.005 m.

In a literature study of rainwater-related studies in southern Africa, two sources describe sampling devices used. Mphepya et al. (2004) used an automated wet-only sampler (AeroChemetric); therefore only precipitation during a rainfall event was sampled. This unit, although collecting pristine rainwater during a particular rainfall event, ignores dry atmospheric fallout, which is important for the CMB application.

The second unit, an absolute rainwater bulk-sampling device, was developed by the CSIR and applied on various studies in southern Africa (Weaver and Talma 2005). To minimize evaporation, this unit was filled with silicon oil which unfortunately causes several negative effects in terms of analyses, and was therefore not used in this study for any comparisons with the DWA unit developed by the author.

2.7.4.3. Network Scope and Design.

The scope simply is to generate a time-series data set to record rainfall events and local water table responses in phreatic aquifer systems, in order to identify the hydrometeorological conditions prevailing for direct groundwater recharge. To evaluate this, it is required to have rainfall data collected as close as possible to water table monitoring points (<100m). A typical monitoring terrain for the purpose of groundwater recharge estimation should therefore consist of a spread of monitoring sites located in the area of interest, consisting of a borehole and rainfall logger/sampler unit at each site.

The rainfall monitoring network design should be based on a prescribed hydrogeological concept model of the research area. In this study, monitoring sites were specifically located in fractured hard rock regions where no permanent ponding of surface run-off occurs. In the plain terrains, surface water ponding manifests in superficial depressions, borrow pits and pans, especially after episodic rainfall events when surface run-off is generated in higher relief areas. The contribution to groundwater recharge in these cases is debatable, especially in areas with soil/regolith cover. Pan floors in semi-arid savanna ecosystems were compacted by animal hoof impacts as they are used for drinking sites. These mature pans are therefore merely evaporating all the surface run-off collected during high rainfall events.

2.7.4.4 Rainfall Depth Time-series Logging.

The rainfall data logger can be programmed to log the status of the water height (thus the accumulated rainwater from a HC period start) in the acrylic tube at any time interval from 1 minute. The resulting rainfall depth-time-series plot is called a total hyetograph (Figure 2.15).

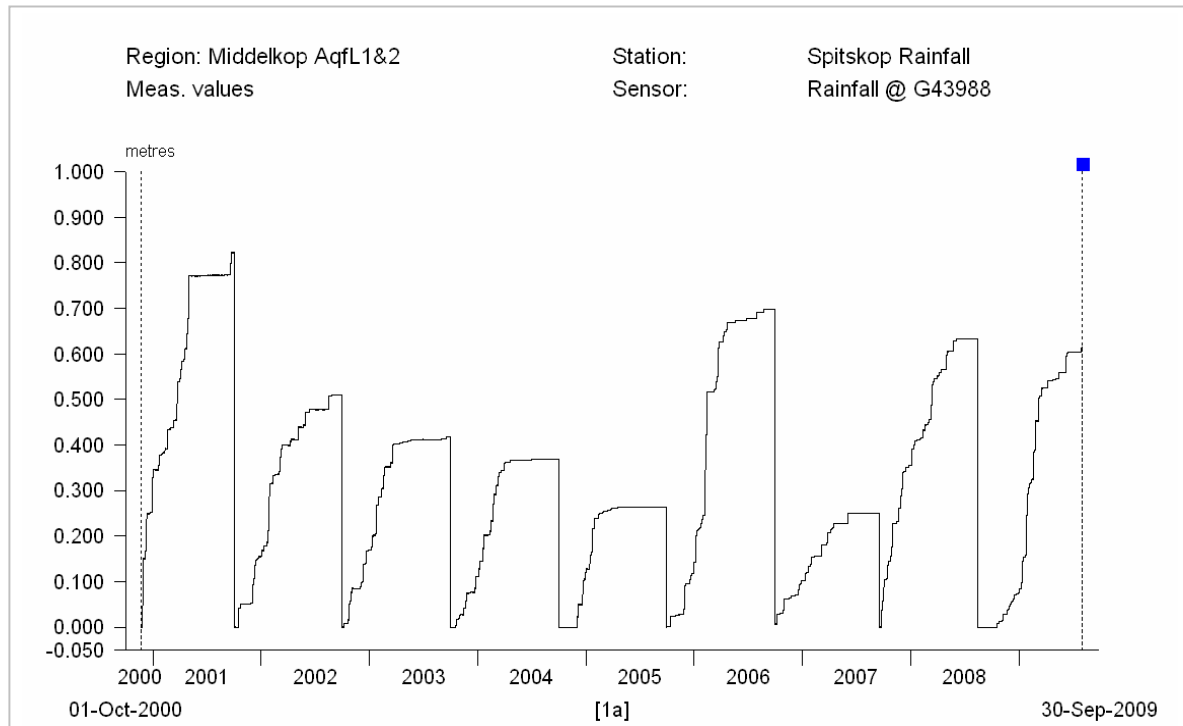


Figure 2.15. The total hyetograph for the Spitskop monitoring site (G43988_RF) at Stella, District Vryburg for the 2000-2001 to 2008-2009 HC's.

Over a period of one HC (01 Oct CCYY_n to 30 Sep CCYY_{n+1}), the data is edited into one annual accumulated data string using the Hydras 3 software application. It is then uploaded to the Hydstra platform where it is stored in daily and cumulative formats.

2.7.5 Rainwater Quality Monitoring Programme.

2.7.5.1 Introduction.

Rainwater contains a dynamic composition of natural tracers, i.e. specific hydrochemical constituents such as Cl^- , SO_4^{2-} , NO_3^- and Na^+ . In addition, rainwater holds cosmic altered water molecules containing environmental stable isotopes of oxygen (^{18}O) and deu-

terium (D or ^2H). These tracers are traditionally applied for estimating recharge-producing rainfall flux through the UZR, as well as imbedded in the saturated phreatic water column itself.

The CMB technique is highly dependant on the pristine and reliable rainwater chloride values. It is therefore necessary to collect rainwater samples under extreme controlled conditions, especially in remote regions. The interval of rainwater collection is also an important aspect as chloride input over the HC may vary (Van Tonder and Bean 2003).

2.7.5.2 Rainwater Sampling Apparatus.

Rainwater is collected in the above-mentioned acrylic tube and recorded in time-series as accumulated rainfall data. These rainfall-logging devices are installed in pristine regions; thus short-term sampling is not logistically feasible. Preservation of the rainwater is required for extended periods, monthly, quarterly and up to six-monthly.

Evaporation from bulk rainwater sampling units is a considerable risk in semi-arid regions; in this way, enrichment of the environmental tracer concentration levels may result. These logging/sampling units are equipped with a special water seal device, though, to prevent moisture escaping through the funnel systems during day-night temperature variations. The interior volume of the rainwater sampler is therefore sealed from the surrounding atmosphere at all times. Stable isotope analyses and the rainwater stage height values do not report any evaporation signal from this unit.

2.7.5.3 Rainwater Quality.

Hydrogeochemistry analyses of rainwater in South Africa were performed on an *ad hoc* basis prior to this study due to poor rainwater sampling facilities and inadequate analysis tolerances. Since the initiation of DWA's NRwQMP (2003), rainwater analyses became more frequently available.

Chloride concentrations in the rainwater collected from six (6) monitoring sites and eleven (11) regional monitoring networks report highly variable LLHc concentrations. Special care for secondary pollution of the rainwater has been taken but in some cases it was not possible to prevent secondary Cl^- enrichment from bird droppings (or similar) into the funnel

system of the rainwater collector. Larger birds, and specific owls and sparrows and primates (baboons) caused a few rainfall logger/sampling units to lose their classification as pristine rainwater sampling monitoring sites and were decommissioned. It was therefore decided to include LLHc concentrations of NO_3^- , SO_4^{2-} and PO_4^- in the rainwater hydrochemical analyses as a series of local pollution indicators. It will be demonstrated presently that NO_3^- and SO_4^{2-} form part of the continental savanna and anthropogenic pollution cycle captured by especially the summer synoptic systems.

Rainwater hydrochemical analyses from this study reported elevated PO_4^- concentration levels which correlate with cases where physical evidence of local rainwater pollution due to bird and animal droppings has been noted.

2.7.5.4 Bulk Periodic Rainwater Sampling.

The DWA bulk rainfall logging unit can sample a total of 450 mm rainwater (Figure 2.16). There is a 750 mm unit available, for high rainfall and remote areas.

The main drawback of the DWA rainwater-sampling unit is that bulk samples represent various different rainfall events with probably highly variable hydrogeochemical compositions. In the case of normal rainfall inputs during a season with no extraordinary rainfall events, it can be expected that the bulk sample is homogenic throughout the rainwater column in the tube.

Episodic rainfall events, which easily measure 150 to 250 mm over a rain-week period, feed a large volume of rainwater into the sample tube; normally with a total different hydrogeochemistry composition. Differential sampling from the sampler tube indicated some remarkable differences in the hydrogeochemical compositions. This observation was not expected as substantial mixing over time of new rainwater (with temperatures $<10^\circ\text{C}$) drains into older rainwater (with a settled background temperature of 30 to 35°C). It is expected that the piping system from the funnel and the float mechanism of the Thalimedes logger which collects the incoming colder rainwater, pre-heats the rainwater to almost the same temperature as the bulk sample in the tube. Thus, very little convection occurs over time, due to mild rainwater temperatures.

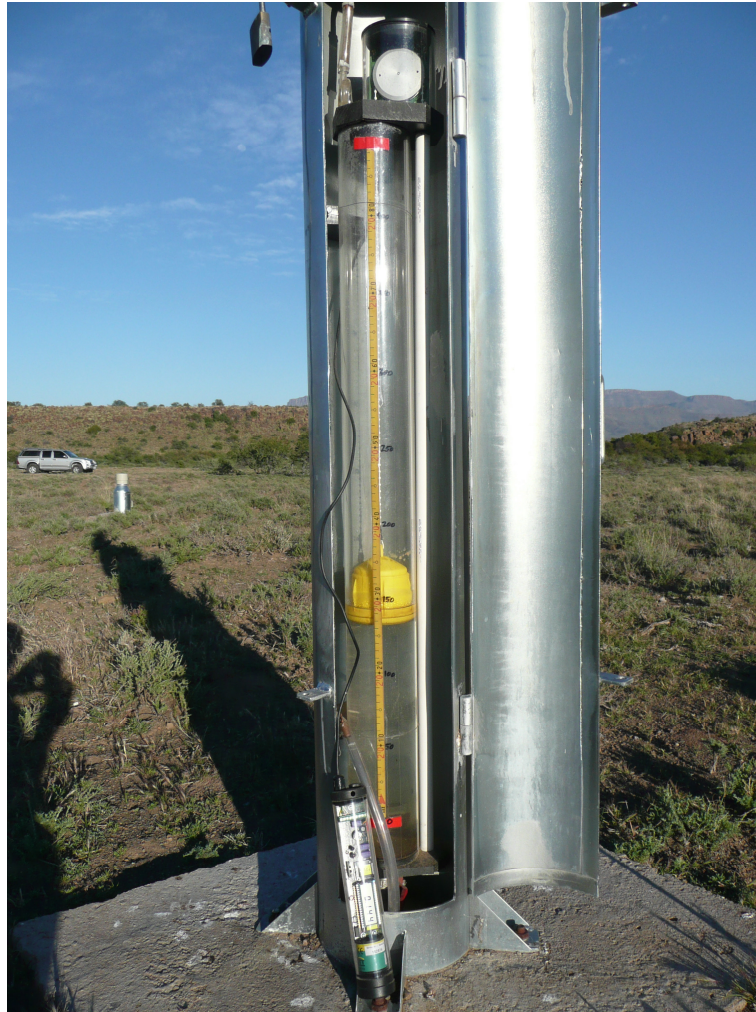


Figure 2.16. Showing a column of rainwater collected in the acrylic collector tube of the DWA rainfall logging/sampler unit at G29870BB_RF, De Hoop Poort monitoring site, District Beaufort West.

This observation has, in fact, instigated further investigations into the differences in rainwater hydrogeochemistry over the wet season of the summertime rainfall events. The observations indicated that the amount effect is undoubtedly an important factor in the southern African rainwater character, and imposes a useful signature of especially episodic high rainfall events.

To demonstrate the amount effect, the author has developed a rain event sampling (RES) unit and trial-tested it during the 2008-2009 summer rainy season.

2.7.5.5 Rainfall event sampling.

The RES unit was installed on 5 different sites in South Africa. The unit consists of an arrangement of individual sample vessels (18 vessels in one cradle unit), which can be pre-set to collect rainwater aliquots of 10 mm of rainwater at a time, and diverts it via a manifold to a sample vessel which automatically closes 45 minutes after the first aliquot was sampled (Figure 2.17).

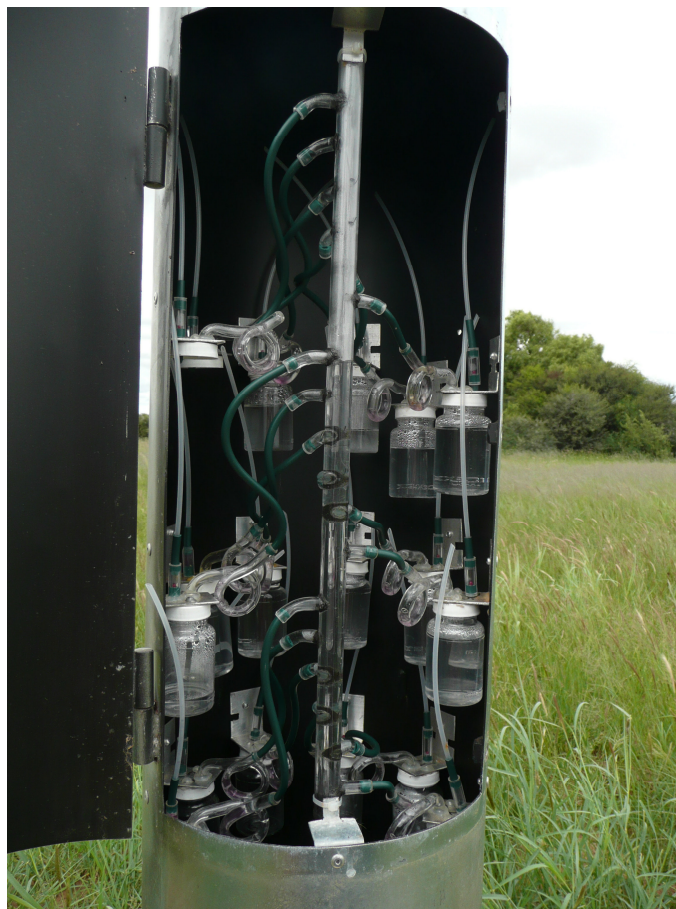


Figure 2.17. The internal configuration of the RES unit with integrated manifold and 10 mm sample aliquots.

The aim of this development was to obtain rainwater samples from individual rainstorm events as this should (i) provide a specific rainfall event's hydrogeochemical composition, and (ii) the changes in the rainwater's hydrogeochemical make-up in volume and over different the rainfall events.

2.7.6 *Groundwater Table Time-series Monitoring.*

2.7.6.1 Introduction.

Fluctuations in the groundwater table over time are clear indications of the saturation status of the responding aquifer system. Many forms of time-water table responses, whether the aquifer system is gaining, losing or holding its water content, can be reported and demonstrated empirically. As mentioned in Section 2.4, groundwater table hydrographs are complex data sets reporting the effect of what climate (rainfall and its time/spatial variability), environmental (evaporation and transpiration) and anthropogenic (water use and land use changes) impose on the saturation levels of aquifer systems.

2.7.6.2 Theory.

Data requirements for the estimation of *episodic groundwater recharge in semi-arid fractured hard rock aquifers* include detailed time-series observations of water table responses at monitoring terrains. Hydrometeorological information, derived from detailed time-series data sets is needed to estimate the time lapse between a specific rainfall event and the water table response. For aquifer supply-demand analyses, the total recharge-producing rainfall surplus input and long-term aquifer responses to recharge and abstraction are required.

International standards recommend that all groundwater-related hydrometeorological data should be collected at least at hourly intervals. For example, the influence of sun-moon tidal effects of deep confined aquifer systems reports piezometric head changes of up to 0.25 m over a period of 6 hours. If the water table is recorded with whatever device at any interval of >6 hrs, the data set will obviously miss these tidal effects and produce a set of potentially misleading measurements.

The application of electronic data logging devices for logging groundwater table responses at extremely short intervals (1 second to once every twenty-four (24) hours) generate valuable data sets that can be linked with many other data sets (water temperature, electrical conductivities and rainfall) to produce high level information. Mass data transfers via electronic media and remote real time observations are a few of many applications available.

2.7.6.3 Apparatus.

Various electronic water table logging devices were tested on the pilot monitoring networks developed for this study. They vary from the robust Ott Hydrometrie Orphimedes Bubbler water table logging unit to Schlumberger-Diver or Solinst-Levellogger CTD data loggers.

The accuracy of these instruments is remarkable, especially in terms of long-term drifting, which was a problem with the historical float-counter weight autographic logging systems. The straightness and plumbing of observations boreholes do not influence the readings as with the mechanical driven float-counter weight systems.

A short-coming in terms of short-term availability of groundwater level data is the remoteness of some of the monitoring terrains, which due to costs and logistical constraints only allows data downloads on a three or six-monthly interval. This unfortunately has resulted in some of the groundwater rebound sampling events being out of phase with episodic recharge events. Real-time reporting¹⁵ of logged groundwater data through utilizing national and rural cell phone network coverage in South Africa is now possible. Currently, only groundwater temperature, water table measurements, and rainfall depths are available.

2.7.7 *Groundwater Hydrogeochemical Time-Series Monitoring.*

2.7.7.1 Introduction.

A specific hydrogeochemistry signature of incoming rainfall will be transferred with the recharge-producing rainfall surplus percolating downwards to the water table interface. In the case of thick (>6 m) soil/regolith layers, the recharge-producing rainfall surplus will become part of the soil/regolith moisture zone once it has bypassed the rooting zone of the local vegetation on site. Analyses of soil/regolith moisture from the UZR are traditionally performed during hydrogeochemistry investigations.

Sampling of the recharge-producing rainfall surplus, which should reside in the LUZR and above the water table interface, is physically not possible due to semi-solid nature of the

¹⁵ Monitoring data is obtained via a SMS message or satellite system on prescribed intervals, i.e. hourly measurements from an Ott Hydrometrie Orpheus Mini data logger once per day and directly updates into the Hydras 3 information system.

regolith and the upper weathered and fractured UZR. In addition, the relatively thin (<1m) soil/regolith cover and extended rooting systems in the semi-arid regions, multi-tracer profiling can't be applied in its full significance for estimating groundwater recharge, especially with the conventional CMB application in fracture hard rock terrains.

An alternative application of the CMB was adopted where the Cl^- values from the underlying groundwater body are used instead. (Gieske 1992; Selaolo et al. 1994; Bean 2003; Xu and Beekman 2003).

2.7.7.2 Theory.

Time-lapse correlations between rainfall events and local groundwater table responses indicate that the SZ is replenished within hours to a few days after a particular rainfall event has occurred. During these events the hydrogeochemical composition of the groundwater and especially the associated groundwater mound is significantly altered. In theory, this is because recharge-producing rainfall surplus with a specific hydrogeochemical composition has entered the underlying groundwater body, carrying with it a different hydrogeochemical signature.

Therefore, it should be expected that a layered hydrogeochemical pattern exists from the water table downwards specifically in the direct recharge zones where prevalent vertical flow resides. Precise (0.1 m interval) DTH water chemistry¹⁶ logging indicates that significant changes occur in the first 3 to 4 m of the water column just below the water table interface (Venter 2003). Moving away horizontally from the direct recharge zones, the lateral flow regime becomes more dominant and may disturb this layered pattern and produces a mixture between recharge-producing rainfall surplus and older groundwater (Mazor 1997; Harrington et al. 2002).

On several occasions, sharp differences in these state variables were observed at depths which resemble individual and/or intersecting water bearing fracture zones. At these depths, one should also consider the contribution of groundwater that resides within the micro-fractures and probably have a completely different hydrogeochemical composition,

¹⁶ Temperature, pH, DOC and electrical conductivities with depth below water table.

i.e. those corresponding to extreme recharge events following periods of much lower saturation levels during past dry and/or high discharge cycles.

The only possible association which can be postulated between the hydrogeochemical composition of the rainwater and recharge-producing rainfall surplus, is therefore to look at the water table interface (i.e. unsaturated-saturated interface) given that observations is performed on a uncased borehole with sufficient well head protection. Sampling of groundwater at this interface is highly enterprising, and can only be achieved under controlled conditions.

Sampling must be performed at the correct timing of the water table rebound curvature as portrayed on the groundwater hydrographs, given that the recharge-producing rainfall surplus is forming a prominent layer on top of the water table interface and that no mixing occurs in the borehole itself.

2.7.7.3 Apparatus for sampling groundwater from saturation zone.

Two methods for sampling groundwater at water table interface and a 2-3 m *in situ* water column from the water table were developed by the author.

Firstly, for sampling groundwater at water table, a *skim sampler* was developed which is gently lowered into the water column. Sidewall apertures and level indicators with special water proof LED's guides the operator through the sampling procedure.

The sample holder can sample 0.5 l at the water table interface (about 19 mm in a 165 ID borehole), which is enough water for the required hydrogeochemical analyses¹⁷. Groundwater samples from as deep as 79 m bgl has been collected with this sampling unit (Figure 2.18).

The second sampling methodology was developed to capture and remove the upper 2 m to 3 m *in situ* section from below the water table interface; referred to as column sampling. A 2 m hollow acrylic tube is lowered into the SZ, sealed and retrieved to surface. Samples

¹⁷ Hydrochemical constituents and stable isotope composition

of each 0.25 m section, totaling 120 ml each, is removed from the tube and prepared for analyses (Figure 2.19).



Figure 2.18. The skim groundwater sampler used to sample the upper-most 19 mm of the SZ in a borehole.

A third method specifically developed for sampling groundwater at 0.25 m intervals during a water table rebound event has been used on a few of the pilot monitoring networks and is referred to as stage sampling. In this case a special cradle containing 120 ml aliquots (sample vessels) is lowered into the borehole and sustained just above the water table. In the event of recharge-producing surplus rainfall, causing a prolonged rise in the water table, samples will be collected from the rising water column in the borehole at the said intervals. Each individual sample cell will contain the water sample until the cradle is removed (Figure 2.20).

The circular inlet siphon is manufactured from a 10/6 mm OD/ID acrylic tube and contains a silicon gel locking device which seals any groundwater through flow within 45 minutes after sampling.



Figure 2.19. A fully retrieved 3m water column from borehole G29870BE, De Hoop Poort, District Beaufort West.



Figure 2.20. A 120 ml aliquot (sample cell) with intake siphon and air outlet.

2.7.7.4 Sampling surface water runoff in a rivulet.

A similar sampling cell has been used for sampling rainfall run-off once flow occurs in local rivulets. This network component was developed in the De Hoop Poort monitoring terrain where surface water runoff can be detected from a monitoring site. Sampling of surface run-off water using these isolated cells is problematic in the sense that it will sample the first water flush in the rivulet and all surface run-off generated by rainfall events in succession afterwards will not be sampled. The first run-off sample obtained should give an indication of the accumulated Cl^- deposited as dry deposition during the dry season. Flush flows in the rivulets generated by a particular rainfall event are isolated occurrences in the semi-arid environment, and one sample may thus report such an event's surface water hydrochemistry composition.

2.8 SUMMARY.

Monitoring of hydrological state variables in South Africa is done by various organizations. Dedicated legislation enforced by the national water act of South Africa puts a strict responsibility on government as well as water users to comply with policy and regulation requirements. Facilities for storage and management of hydrological information compare adequately with international standards, and may well serve as examples of semi-arid monitoring criteria.

Unfortunately, capturing of some state variables in the HC is not satisfactory, and need development. In a recent assessment of groundwater resources in South Africa, summarized on quaternary catchment scale from a groundwater management unit grid, it was reported that insufficient groundwater data was available to support the estimation of groundwater recharge on catchment scale based on the CMB application.

Probably the most critical state variable required, but not available on a regional scale, was the rainwater hydrogeochemical data. Rainwater quality monitoring in South Africa has been neglected by and large, and this now limits the application applied for groundwater recharge estimations based on multi-tracer profiling methods, CMB, and stable isotope applications. Groundwater hydrogeochemical data is more frequently available; time-series evaluation of long-term trends became available from the NGwQMP initiative.

The methodologies developed in this study to capture rainwater from different intervals in the HC and focusing on sampling groundwater during effective recharge events generate a modern set of state variables. These variables represent the actual rainwater and groundwater quality and quantity inputs at direct recharge terrains.

ooOOOooo

3 SOUTHERN AFRICAN SEMI-ARID ENVIRONMENTS.

3.1 INTRODUCTION.

Semi-arid regions are a direct result of weather pattern configurations caused by land-mass orientation in global atmospheric systems. South Africa is situated on the southern tip of the African Continent; delineated by the Great Escarpment (Khomas and Namaqua Highlands in the west, Kamiesberg and Nuweveld Mountains in the south, and the Drakensberg and Bankeveld Ranges in the east) surrounding a large interior basin (Kalahari/Karoo superimposed basins). The southern African land mass forms a prominent continental wedge between the Indian and Atlantic Oceans. A feature not only altering the subtropical southern hemisphere, but the warm southerly flowing Agulhas Current from the equatorial Indian Ocean zone and the colder northerly flowing Benguela Current from the Antarctic polar regions (Penver et al. 2001).

A very basic definition of semi-arid regions is those areas where the rainfall is sufficient for short-season crops, and grass is an important element of the natural vegetation (Chow 1964).

In the southern African context, the dry province (including extreme arid, arid, and semi-arid) demarcates the narrow elongated coastal desert of the hyper-arid Namib Desert, and the Kalahari-Karoo vegetated deserts and steppe uplands (the intervening areas of the Great Escarpment and the southern African Highveld). The boundaries of the arid and semi-arid climatic zones in southern Africa are shown in Figure 3.1. This zoning is based on demarcations by Meigs (1953) and Grove (1977) of arid and semi-arid regions in southern Africa (cited in Thomas and Shaw 1991, p. 7), as illustrated in Table 3.1.

Rainfall patterns in the semi-arid regions are irregular in terms of depths (mm), intensities ($\text{mm}\cdot\text{hr}^{-1}$) and footprints (km^2). Local summertime convection cells vary from 3 to 8 km in diameter (Van Heerden and Hurry 1992) and rainout occurs on a rain-line pattern over land which in many cases manifests as isolated rainstorms. During wetter seasons this system operates on a regional scale with a reasonable larger wetted foot print on land, which sporadically generates local flush flooding and depression storage. Indirect re-

charge in these cases is well-defined, although still occurring as point-source recharge zones in an otherwise low potential diffuse recharge domain (Arid Zone Hydrology 1980).

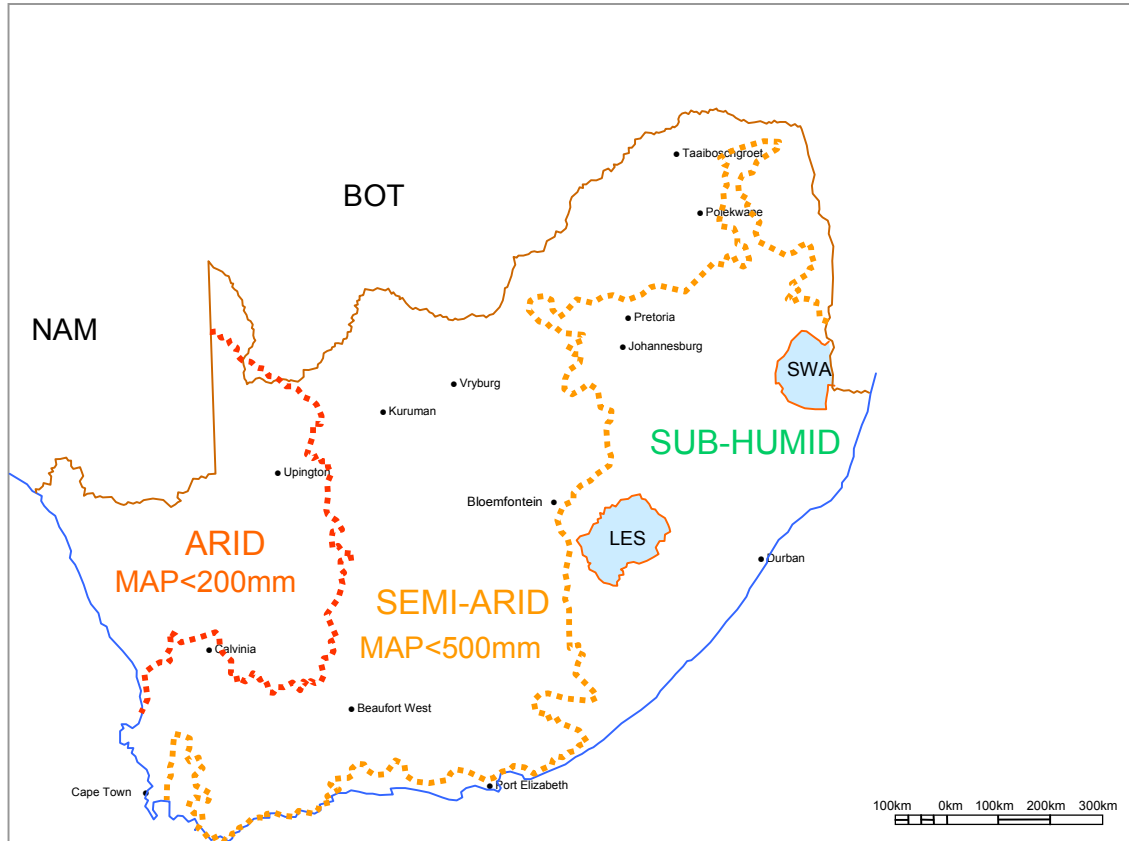


Figure 3.1. Boundaries of the climate zones in southern Africa based on the Meigs (1953) and Grove (1977) demarcations (cited in Thomas and Shaw 1991, p. 7).

Intermittent recharge events in semi-arid regions correlate with extraordinary rainfall patterns (Van Tonder and Bean 2003), and instigate medium-term aquifer replenishment. Low amplitude recharge events on the other hand, manifest as a pulse and once reporting to the groundwater flow domain, it dissipates within that specific HC.

Quantification of groundwater recharge in semi-arid regions is complex because of the extreme hydrometeorological conditions, for example the impact of ET during wet and dry cycles. The direct flow path between ground surface and the SZ is intermittent in both physical connectivity and wetted status (indicating that after periods of extreme drying-out of the UZR, the vertical flow regime requires a frequent rewetting phase to initiate recharge).

Table 3.1. Classification of arid environments (Thomas and Shaw 1991).

Ecosystems	Index (Im) ¹	Mean annual precipitation (mm) ²
Semi-arid	-20 to -40	200 - 500
Arid	-41 to -56	25 - 200
Hyperarid	<-56	12 consecutive months recorded without rainfall. No seasonal pattern.

¹ Im = Index of moisture availability

$Im = (100Sm - 60Dm) / ET_P$, where:

ET_P is the potential ET;

Sm is the annual moisture surplus, Dm is the annual moisture deficit (including stored soil moisture)

² Rainfall ranges suggested by Grove, 1977 (cited in Thomas and Shaw 1991)

3.1.1 Ground Surface Characteristics.

Soil/regolith development in arid and semi-arid southern Africa is insignificant compared to those deep (>6 m) soil profiles in the humid regions towards the north-eastern side of South Africa. Hard rock terrains or hard rock windows in the semi-arid region are therefore quite common as observed in the many roadside cuttings and shallow ravines.

Hard rock terrains in the semi-arid regions (particularly calcrete surfaces) enhance preferential recharge as observed on the Weissrand Plateau in Namibia (Figure 3.2). Local erosion processes developed their own unique local drainage systems for collecting water which infiltrate almost immediately into the UZR (Tredoux 2008). These features play an important role in regional groundwater recharge, and may be classified as the only areas where direct groundwater recharge manifests.

Soil development in semi-arid regions is limited to relatively thin coverages of a combination between fine silty soils and/or regolith consisting of a decomposed to jointed parent rock fragments. Average thicknesses are <0.6 m, although it may reach several meters in lowlying valleys where plant root systems stabilizes erosional degradation.

Detailed discussion of soil/regolith profiles in the monitoring terrains will follow presently (Section 4.2.5).

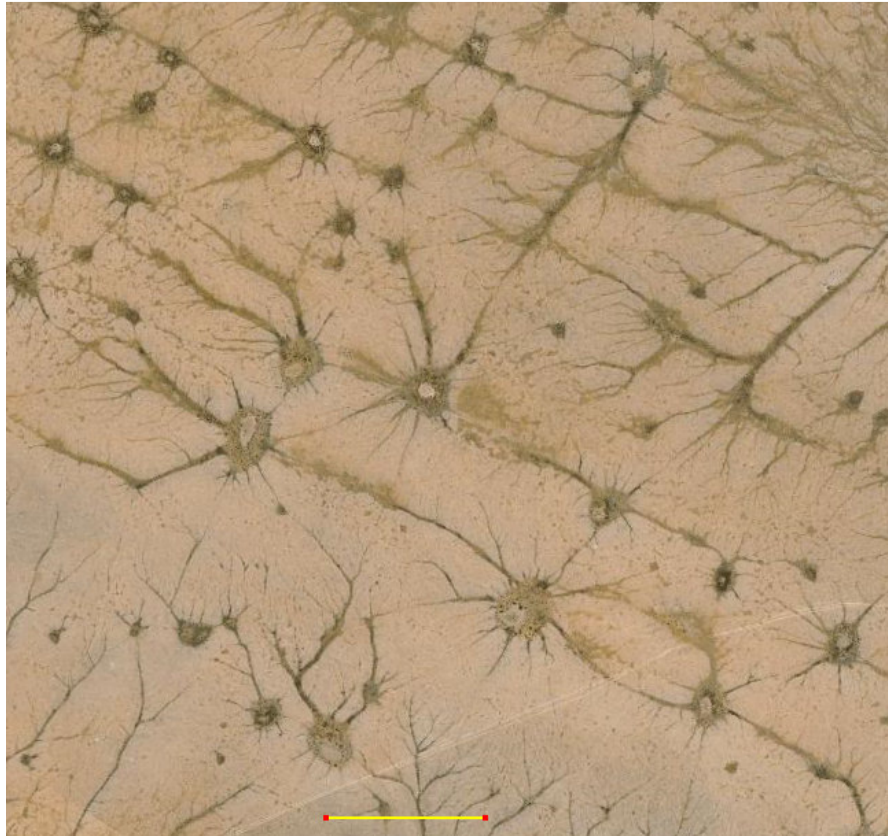


Figure 3.2. Topographical depressions in Kalahari Weissrand Plateau, Namibia showing low-lying pan surfaces and unique local drainage systems collecting infiltration-excess overland flows (Bar = 1 km).

3.1.2 Southern Hemisphere Weather Patterns.

Three major climate systems extend around the earth's southern hemisphere zone, i.e. (i) Intertropical Convergence Zone (ITCZ), (ii) Subtropical High Pressure Zone (SHPZ), and (iii) the southerly Temperate Zone (TZ). The annual north-south migration of these air circulation systems due to the earth's solar trajectory shapes the familiar seasonal weather pattern-shift across southern Africa (Mendelsohn et al. 2002; Thomas and Shaw 1991).

The differentiation between the summer and winter atmospheric conditions are illustrated in Figure 3.3. It illustrates the annual north-south-north migration of the three climate

zones and the pathway of synoptic systems during the winter and summer seasons. Summertime ($\text{Oct}_n - \text{Mar}_{n+1}$) and wintertime ($\text{Apr}_{n+1} - \text{Sep}_{n+1}$) rainfall is generated over completely different oceanic regions, (i) warm, equatorial West Indian maritime waters and (ii) cold, polar south Atlantic maritime waters, respectively. Detail discussion on the physical differences between hydrogeochemical compositions and rainfall patterns will follow presently (Section 5.1 and 5.2)

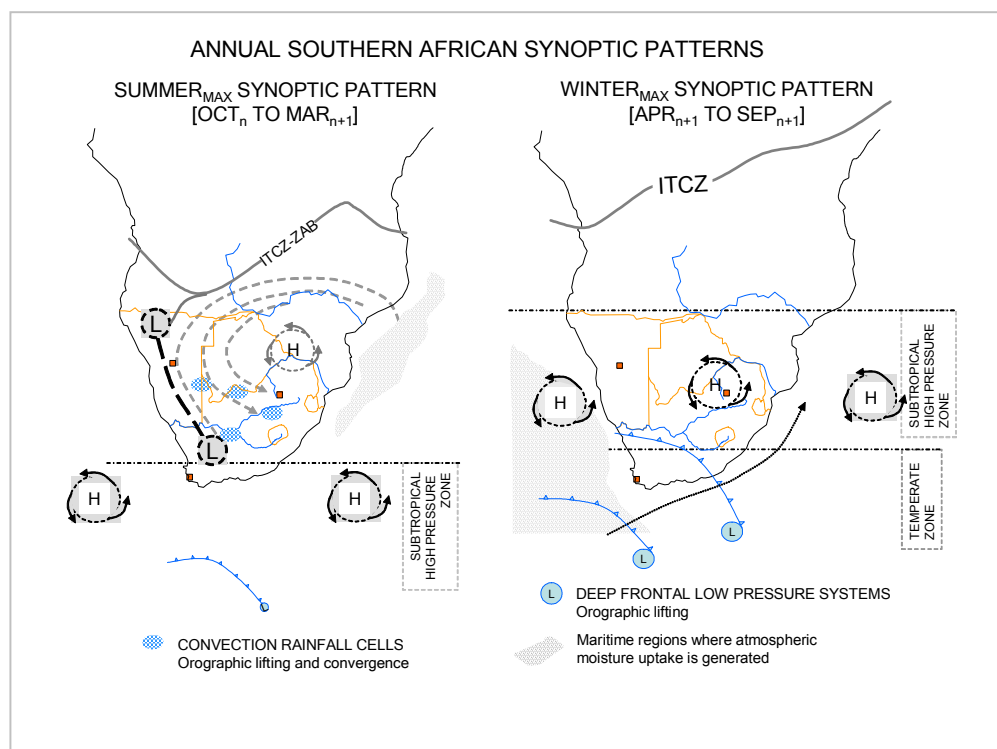


Figure 3.3. Synoptic weather patterns over southern Africa during the summer and winter climax weather period showing the seasonal migration of prominent weather systems over southern Africa.

The most prominent system dominating the southern hemisphere's weather pattern is the ITCZ, positioned across the equator. This system's existence is the result of vertical atmospheric circulation in the equatorial zone and generates an equatorial trough (low pressure) due to the thermally active north and south Hadley cells with a rising interior air mass (representing the low pressure trough, ITCZ). Just to the south, the Ferrel Cell is situated, forming the subsiding air mass at the interface with the South Hadley Cell, representing the nature and position of the SHPZ. This zone is characterized by a band of sev-

eral high pressure cells, lies south of the ITCZ and consists of dry air cascading downwards between the South Hadley and the southerly Ferrel cells (Tyson 1986)

The ITCZ forms a barrier between the hot and dry continental air coming from the Sahara Desert (Harmattan) and cooler and humid maritime air masses (monsoons) coming from the equatorial Indian and Atlantic Oceans (Galy-Lacaux et al. 2008). This is an area of extreme high rainfall and enhances physical processes of water vapor recycling due to ET produced airborne moisture with unique hydrogeochemical compositions (Mook 2001a).

3.1.3 Southern African Climate Variability During the Late Quaternary Period

Alternating wetter (humid) and drier (arid) weather patterns (an interglacial behavior) have been experienced in southern Africa from ~50 000 yr BP (De Vries 1984; Thomas and Shaw 1991; Tankard 1982). These authors provides evidence of extreme climate (hypothermal) conditions during the Late Pleistocene indicative of southern African Middle Stone Age hominids occupational hiatus from open coastal areas to caves and other natural shelters.

The last major pluvial period in southern Africa is estimated to have taken place ~12 000 yr BP. Several site investigations, cited by Lancaster (1988), Thomas and Shaw (1991) describes Holocene (~10 000 yr BP), enhanced dune mobility and dating of calcified sand and cave stalagmites respectively; all indicating several long-lasting, extremely humid and arid cycles in the Late Pleistocene-Holocene Epochs (<50 000 yr BP). De Vries (1984) describes a long-term piezometric table depletion since ~10 000 yr BP and suggests only occasional recharge events during the last ~4 000 yr BP, when wetter periods occurred, although not significantly enough to reset a dominant Holocene Depletion.

Several terrains were identified where indications of humid and arid conditions prevailed for several millennia, including short periods with extreme wet and dry hydrometeorological conditions. For example, observations at the Kathu Pan near the Khumba (former Sishen) Iron Ore Mine in the Northern Cape Province represent:

.....perhaps the best palaeo-environmental sequence from the Kalahari Basin... in Butzer's description (cited by Thomas and Shaw 1991, p. 173).

Fluctuations in the Kathu pan floor sediments, a palaeo-doline feature in the Kalahari environment, represents mega-term groundwater table trends spanning the Lower to Middle Pleistocene. Deposition of peaty organic material and fine sediments were disturbed during times with much lower water table conditions, and episodes of extraordinary groundwater recharges indicative of conditions wetter than present times. The presence of peat ash layering signifies periods of intense arid conditions during the mid-Upper Pleistocene as sedimentation were initiated by flash-flood deposits containing Middle Stone Age artefacts (Thomas and Shaw 1991).

Generation of depression storage (palaeolakes) in semi-arid southern Africa coincides with extraordinary rainfall periods occurring during palaeo times (Lancaster 1988). This has matured in extraordinary land/life forms in the arid/semi-arid regions of southern Africa, and provides a significant signature of historical climate variations and major groundwater recharge events. Evidence from cave sinter deposits in Drotzky's Cave, and palaeolakes in Northern Botswana report consecutive humid episodes at ~6000 to ~5000, ~4200 to ~3600 and ~2500 to ~2000 BP (Thomas and Shaw 1991). De Vries (1984) specifically uses the modern hydraulic gradient in central Botswana to indicate whether any replenishment of the Kalahari Group aquifer may have taken place during the Holocene Epoch. His prognosis indicates the present-day geometry of the piezometric surface is the result of groundwater depletion since the last pluvial period in southern Africa, ~12 000 yr BP and suggests a replenishment of less than $0.5 \text{ mm} \cdot \text{yr}^{-1}$ during the last ~4 000 yr BP.

These observations point towards the fact that the modern climate oscillations represent a much smaller window in an extreme climate oscillation pattern with a much larger bandwidth in time and humidity than modern man has ever experienced.

3.1.4 Modern-time Climate Variations.

Long-term rainfall observations in southern Africa indicate that even under current minute time scales compared to Late Pleistocene glacial and Holocene interglacial time scales, modern climate variations do occur although the amplitudes may still be too small to severely impact on the long-term endurance habits of life on earth. Modern technology allows dating of groundwater to at least ~5760 yr BP. Hence, indicating that groundwater that

has been effectively recharged several thousand years ago is still part of the modern HC. The Kalahari Group aquifer's groundwater cycles are good examples of these eternally flow regimes and emphasize modern recharge cyclicity (Verhagen et al. 2001).

Tyson, (1986) presented a statistically significant 18-year cycle of rainfall fluctuations occurring over the summer rainfall zone in Botswana. A similar long-term average rainfall departure for a SAWS weather station in Vryburg, Northern Cape, as illustrated in Figure 3.4. Although an 18-year cycle could be visualized up to 1970, it seems that there is a different oscillation in the rainfall pattern since then (personal observation). The annual rainfall departures are amplified and indicative of higher maximums and lower minimums during the last 40 years, thus expressing prominent wetter and drier conditions. The long-term (1913 to 2008) data set, indicates an increasing annual rainfall input, even though this might be a local phenomenon.

The Botswana 18-year rainfall cyclicity may hold significantly for the sub continental scale, i.e. $1\text{E}+6\text{ km}^2$ areas, Gieske (1992) concludes that on local scale ($1000\text{-}2000\text{ km}^2$), the 18-year cyclicity tends to disappear in the large variance of the stochastic processes leading to local, 25 km^2 rainfall cells. This suggests a significant difference in the actual point precipitation and spatial coverage on land itself; groundwater recharge in semi-arid regions is therefore episodic in time and space/coverage as well.

De Vries (1984) has investigated recent recharge in the Botswana Kalahari region and could not find any proof of diffuse recharge in thick ($>6\text{ m}$) sand covered Kalahari areas, probably as a result of the relatively low rainfall variability and deep-rooted thorn scrub vegetation utilizing all available soil moisture. Several other research papers were noted, suggesting extreme conditional recharge in this semi-arid region, provided:

.....situations of concentrated surface water and rapid infiltration in fossil river channels and nodular calcrete layers are suggested as a possibility by these authors (De Vries 1984, p.227).

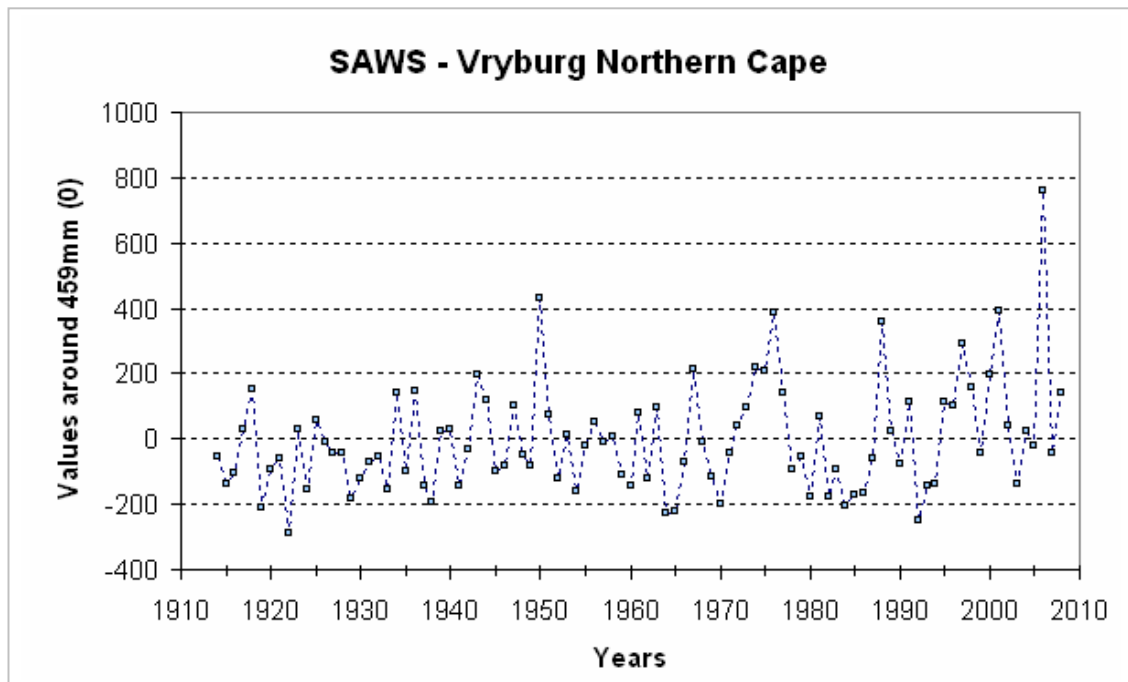


Figure 3.4. Long-term annual rainfall time-series log for Vryburg, SAWS Weather Station No. 468318, Northern Cape Province.

The most significant wet period experienced in the southern African semi-arid region has occurred in the early 70's. During three consecutive HC's, 1974-1975 to 1976-1977, the average annual rainfall was between 200 and 400 mm higher than the long-term average value. The Kuruman Spring, for example reported a high-flow of $\approx 2000 \text{ l}\cdot\text{s}^{-1}$ above the average 1959-1973 flow of $\approx 200 \text{ l}\cdot\text{s}^{-1}$. During significant flood event in the Kuruman River in 1976, the river flowed continuously for at least 6-months, resulting in a episodic recharge event in the local Kalahari Group Aquifer Systems (KRAS) as illustrated in Figure 3.5.

The borehole water table trend reported in Figure 3.5 represents the resulting recharge pulse. The borehole was drilled in 1927 with a rest water level of $\approx 47 \text{ m bgl}$. Three years after the 1976 flood, the water table was measured at $\approx 12 \text{ m bgl}$ which was already on a long-term recession trend(line); it is at 41.3 m bgl currently (01 January 2010).

In the last 83 years, several flash floods have occurred in the Kuruman river system, lasting only a few days in contrast to the six-month long, 1976 flood. This groundwater re-

charge event is therefore extremely episodic, although highly effective as the water table recession has still not reached the pre-1973 depth of 47 m bgl.

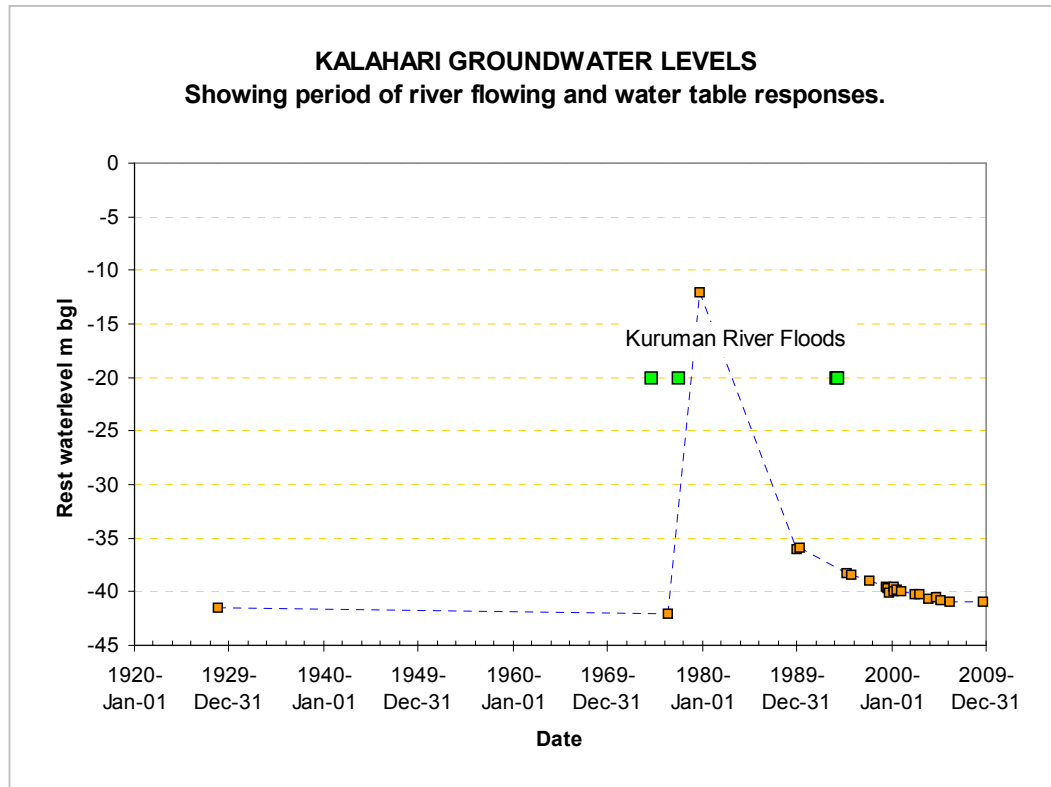


Figure 3.5. Reconstructed groundwater table fluctuation in the Lower Kuruman River section between Van Zylsrus and Askham showing a dramatic recharge event following the 1976 flood period and long-term recession.

3.2 HYDROMETEOROLOGY.

3.2.1 Introduction.

Three major seasonal demarcations occur in southern Africa resulting in cyclic rainfall patterns in (i) the summer period (Oct_n to Apr_{n+1}), (ii) the winter period (Apr_n to Sep_{n+1}) and, (iii) an all year zone along the southern coast of South Africa. The southern African semi-arid region falls partially in the summer and winter rainfall regions. Apart from the strong continental (seasonal) control over weather patterns, regional weather features dominate the rainwater balance considerably, and thus control recharge-producing rainfall surpluses, instigating long-term aquifer replenishment.

The origin of rainwater precipitating on southern African semi-arid land is generated by two extremely distinctive weather systems as described in Section 3.2.2. It is important to discuss these in more detail as the quantity (mm fall out) and quality (hydrogeochemical character) are coded by the initial moisture-generating systems.

3.2.2 Generation of Atmospheric Vapor Mass Over Southern Africa.

Precipitation on southern African land originates as evaporated water from the surrounding Atlantic and Indian Oceans. Migration from the evaporated maritime waters to reach the winter and summer rainfall regions in southern Africa are unique, thus resulting in a measurable difference between the hydrochemical signatures of rainwater condensates in winter and summer regions. Post-seasonal mixtures between wet and dry air masses over the interior of southern Africa alter the air mass's hydrochemical composition even more.

The pathways followed by the evaporated maritime waters, for example the summer rainfall occurring in the centre of southern Africa, is several thousand kilometers longer than the winter rainfall deriving from the south Atlantic Ocean. Significant changes in the hydrochemical composition from the original oceanic evaporate/aerosols occur due to sequential rainouts and introduction of terrigenous dust into the airborne moisture originating from the continent's eroding surface and atmospheric pollution (Mphepya et al. 2004; Mphepya 2006; Reason et al. 2006; Galy-Lacaux 2008). Winter rainwater precipitating along the western coastal regions of South Africa mimics the maritime waters' high salinity character that eventually are transferred to the local groundwater composition (personal observations from West Coast monitoring analyses).

3.2.2.1. Summer Rainfall Regions.

The most prominent system dominating the southern African atmosphere in summer time is the ITCZ positioned across the equator around the mid-summer period (Dec_n to Feb_{n+1}). This is a complex low-pressure synoptic system enhancing maritime evaporation over the warm Western Indian Ocean and probably the Eastern Atlantic Ocean during periods with above-normal seawater temperatures (Summer_{max} Synoptic Pattern, Figure 3.3).

During the peak summer rainfall season (Jan_{n+1} to Mar_{n+1}), the ITCZ is situated at its most southerly position just north of the Angola-Namibian border, where it is represented by the ITCZ's southerly extension, the Zaire Air Boundary (ZAB). The ZAB acts as a link between the ITCZ and a continental thermal low pressure system (the Kalahari Trough) developing around January to March over the western side of southern Africa, due to super heated land surfaces. Moist air is drawn in along the ITCZ-ZAB from both the equatorial Atlantic and Indian Oceans supported by convergent trade winds generated by an interior, moderate high-pressure system oscillating over the northeastern part of the sub-continent (Thomas and Shaw 1991; Mendelsohn et al. 2002).

The northerly continental anticyclone system drives both western and eastern airflow components. The upper, easterly moist air masses moves into the Kalahari Trough. This oscillating low-pressure system stretches from northern Namibia and passes the southern Cape coastal regions during its maximum domination. Rainstorms are in the form of localized thunderstorm activity instigated by convectional uplift. Regionally, these storm systems are associated in long trough lines, referred to as line storms and slowly migrate from northwest to southeast over southern Africa, depending on the consistency of the Kalahari low-pressure system (Van Heerden and Hurry 1992).

3.2.2.2. Winter Rainfall Regions.

Towards the winter season, the vertical and horizontal components of the equatorial and southern air circulation system migrate northwards ($\text{Winter}_{\text{max}}$ Synoptic Pattern, Figure 3.3). Southern Africa's weather pattern is then dominated by the SHPZ. This zone is characterized by three prominent high-pressure cells (anticyclones) situated across the sub-continent, i.e. (i) the South Atlantic, (ii) the Botswana/Kalahari and, (iii) the Indian Ocean Anticyclones. The southerly TZ has shifted substantially north, bringing deep Antarctic air masses to overshoot the southernmost tip of southern Africa. Westerly winds in this zone carry the cold Antarctic air masses as cold fronts to the western coastal and immediate inland regions of southern Africa.

Cold, polar air masses may migrate over large portions of southern Africa, depending on the physical position and strength of the Botswana/Kalahari Anticyclone. Cold fronts are

unstable frontal waves that occasionally mature into deep frontal low pressure systems, their centers commonly pass within 10° south of the South African coast. Cold frontal bursts over the South Atlantic Ocean generate *in toto* the winter airborne moisture (Figure 3.3). Conventional oceanic evaporative principles do not solely account for all airborne moisture generation in the TZ. Low altitude gale force winds could mechanically force maritime moisture directly into these low-lying dry air masses. Once on land, orographic uplift caused by rising land surfaces away from the seaboard, initiates precipitation.

3.2.3 Physical Characteristic of the southern African Maritime Waters.

The salinity levels of the western, equatorial Indian Ocean and southern, polar Atlantic Ocean differs slightly (SAWS n.d., p. 7-6). Salinity levels for the Indian Ocean varies between 34.5‰ to 37‰, with the southern Atlantic <35‰. Deep (600-800 m) Antarctic Intermediate water reports salinities of ~34.3‰

Sea surface temperature differences between the equatorial and sub-polar are high (~12°C). The southern Atlantic maritime waters, and specifically along the southwest African coastline, are influenced by the Benguela upwelling system (Penver et al. 2001). The Antarctic Intermediate water is extremely cold ($5^{\circ}\text{C} \geq T \leq 4^{\circ}\text{C}$) and blends the Benguela to approximately 15°C during the late summer period after the upwelling initiation in September-October.

The subtropical sea surface water along the east coast region of southern Africa temperature is warmer, $24^{\circ}\text{C} \geq T \leq 16^{\circ}\text{C}$. The southward flowing warmer Agulhas Current, at $27^{\circ}\text{C} \geq T \leq 16^{\circ}\text{C}$ forms a highly effective generator of airborne moisture and initiates most of the rainfall occurring on the eastern side of South Africa.

Although these physical water quality differences will probably not be that pronounced in the evaporated airborne moisture mass in summer and winter rainwater, the evaporation process is considerably enhanced by temperature differences between the two generations. The amount of evaporated moisture generated over warmer maritime water is probably much higher (Rouault et al. 2001; Rouault et al. 2003) and could contain less maritime aerosols than the rainwater generated over the southern Atlantic.

3.3 SEMI-ARID HOMOCLIMATE STATE VARIABLES.

3.3.1 *Temperatures and Atmospheric Humidity.*

The winter/summer temperature differences in the region are typically continental, and have a strong seasonal and diurnal trend (Thomas and Shaw 1991). During the wet season (Oct_n to Apr_{n+1}) both mean daily maximum and minimum temperatures are higher than during the cloudless dry season, because of nighttime radiation from the land surface. Diurnal temperature differences (max.- min.) usually run into double figures and can be as high as 21°C to 23°C. These high temperate characteristic of the semi-arid regions considerably influence the ET rate of open water, and the local vegetation water demand, and may drive the soil moisture field capacity during dry summer cycles to a total deficit (Willemink 1988).

Atmospheric humidity (logged as Relative Humidity, RH) is governed by (i) seasonal and diurnal temperature regimes, (ii) the moisture content of the surrounding air mass and (iii) distance from a source of humid air or water body supplying moist by means of evaporation (Thomas and Shaw 1991). Humidity and temperature variables follow an inverse pattern under fair-weather conditions. Humidity variations in the semi-arid region (used Monitoring site at Appelkoosboom (S26.58358°; E024.89777°, 1297 m amsl) at Stella, Northern Cape Province for comparison occur in conjunction with seasonal and diurnal temperatures.

At the Stella monitoring site, for a period of 29 days starting on the 29th of January 2009, the maximum diurnal humidity (% RH) ranged around 90±2.5% RH. The minimum range was fluctuating between 35% and 60% RH during drier periods. Rainfall occurred 17 days out of the 29-day observation period, and buffered the extreme diurnal lows by almost 25% RH for at least 24 hours after the extraordinary rainfall event, as a function of lower ambient temperatures and immediate ET (Willemink 1988). Normal temperature-humidity inverse returned after 2 days, thus indicating that actual ET (ET_A) is a significant, but short-lived process (Willemink 1988).

The spatial ranges of temperature and humidity over the semi-arid homoclimate region are significant. Humidity as an initial function of air temperature and wind speed tends to decrease considerably towards the southwestern part of the semi-arid regions and may reach levels as low as 10% RH to 13% RH during hot summer days (personal observations in southern Kalahari region by author). Plant transpiration during this almost daily ex-

treme atmospheric condition in the semi-arid environment is extensive and drains heavily on the available soil/regolith moisture content.

Humidity is the main driver behind the fractionation process of stable isotopes during large-scale evaporation from open water systems as well as pre-rainout events from cloud water. Low atmospheric humidity levels (say <15%) will adversely impact on the direct evaporation of cloud water during precipitation events as the atmospheric conditions effectively operate as open-system evaporation. Rainwater hydrogeochemical composition becomes significantly enriched during isolated rainout events in semi-arid regions.

3.3.2 Evaporation and Transpiration.

Evaporation (E) describes the removal of moisture from open water systems (lakes, pans, rivers, moist soil/regolith horizons or shallow aquifer systems) to the atmosphere and is a direct function of wind velocity, water/air temperature range and relative humidity. In semi-arid regions, all these factors are positively set to drive extreme evaporation ($>1000 \text{ mm}\cdot\text{yr}^{-1}$).

Transpiration (T) in semi-arid regions represents the water transport from the plants to the atmosphere via the leaves. Transpiration is a function of (i) the type of vegetation cover dominating, (ii) the spatial distribution of plants on ground surface, and (iii) meteorological conditions, of which heat and wind are the effective elevating factors.

One of the most characterizing scenes of semi-arid vegetation communities is the difference between grove and intergrove plants. Groves consists of typical desert type shrubs and trees with strong, deep rooting systems and special adapted leaf systems which can virtually diminish transpiration by closing the stomata pores and leaf diffusion. The intergrove cover is typically grasslands which can vary dramatically during periods of low rainfall and even disappear completely to leave a bare soil/regolith/hard rock terrain. Re-growth of grass and monocyclic shrubs may reset these areas within a few weeks after good rains and return the water balance to one with a dominant T-factor.

The impact of extreme temperatures in arid and semi-arid environments manifests in various ways from ground surface to the rooting zone. Both E and T variables are elevated during high temperature periods (daily and summer seasons) as observed in evaporation

pan and plant leaf transpiration observations (Davis weather station). The unsaturated zone moisture condition, especially in fractured hard rock terrains with limited soil/regolith capping, is significantly affected and undergoes a complete dry-out during early summer periods as well as prolonged dry summer seasons (De Vries 1984). Any remaining residual moisture from previous wetting cycle(s) is removed by deep rooting systems and an all-new wetting cycle is needed to establish rainwater flux between ground surface and the SZ.

The irregular (episodic) rainfall and subsequent wetting of a frequently dried-out soil/regolith zone in the semi-arid region in addition to T, may limit deep percolation of recharge-producing rainfall surplus. Actual E rates decrease dramatically after maximum of 5 days when E equals the rate of water vapor transfer to the atmosphere. Chow (1964) states:

However, the fact that falls of rain are frequently followed by long periods of dry weather means that much of the rain received in light falls is lost by direct evaporation even before a water vapor barrier is formed.

The effects of transpiration and evaporation are addressed as one entity in the HC, i.e. ET. ET is the combined effect of the evaporation of moist from the soil/regolith and the transpiration of water by growing vegetation, drawing its water supply from the rooting zone.

Plant transpiration is a factor of the development and depth of their rooting systems. In the semi-arid region, rooting systems of grass and small shrubs are most abundant between 200 and 650 mm below ground level, but drop to almost nil at 1m (Chow 1964). Specially adapted phreatophytes are fitted with a shallow and deep rooting system for storing and abstracting groundwater respectively. They are characteristic of streamline vegetation and areas of shallow water table. Because of the natural way these plants tend to cluster into dense communities in semi-arid regions, ET levels from these communities usually contain a large advective¹⁸ component, and according to Chow (1964), there is good evidence that phreatophytic ET may exceed free-water E.

¹⁸ Horizontal air flow component in regional air circulation systems.

Two specifications for ET manifest in the physical quantification (Chow 1964; Kijne 1974; Kessler and De Raad 1974):

- Potential ET (ET_P), maximum amount of water vapor which could be transferred from a well vegetated area to the atmosphere under existing meteorological conditions, given an adequate soil-moisture supply at all times. It is also referenced as the evaporative demand of the atmosphere; and
- Actual ET (ET_A), is the actual amount of water vapor transferred to the atmosphere, which not only depends on existing meteorological conditions, but also on the availability of moisture to meet the atmospheric demand¹⁹ and, in the case of vegetation, its ability to extract moisture from the soil/regolith zone.

3.3.2.1 Estimation of Potential ET (ET_P).

There are several physical applications to estimate ET_P – values ($\text{mm}\cdot\text{d}^{-1}$) which have not been considered in this study, due to the remoteness of the monitoring terrains. Logging of the evaporation data requires extreme sensitive logging devices, which were not available. The application of the Davis Weather Station, with a multi variable logging facility was used instead. The unit has a facility to log the state variables required for estimate potential ET from the following meteorological components:

- Air temperature;
- Relative humidity;
- Average wind speed; and
- Solar radiation.

Diurnal observations with a Davis Type weather station as used on this study, report the highest values for relative humidity (RH) around 03h00 to 06h00 in the mornings. The inverse correlation between the ambient air temperature and RH points out the role which the upward/downward heat flux plays in diurnal evaporation processes. During the diurnal upward flux period (incident heat radiation from the ET zone to atmosphere from 18h00 followed by RH peaking between 00h00 and 06h00) that moisture becomes available and precipitates as dew²⁰. During the sunshine period of the day, which in semi-arid regions

¹⁹ Physical condition of surrounding air mass in terms of humidity, temperature and wind velocity.

²⁰ Occurs when air temperature reaches Dew Point temperature - peaking at 03h00 to 06h00.

can be $10.5 \text{ hr} \cdot \text{d}^{-1}$ the moisture released overnight is quickly removed by wind runs and absorption into drier air in the early morning after sunrise. Willemink (1988) reckons that this process can reduce a single day's rainwater infiltration almost entirely.

An example of the daily ET_p and R_f data as logged by a Davis Type weather station is illustrated in Figure 3.6.

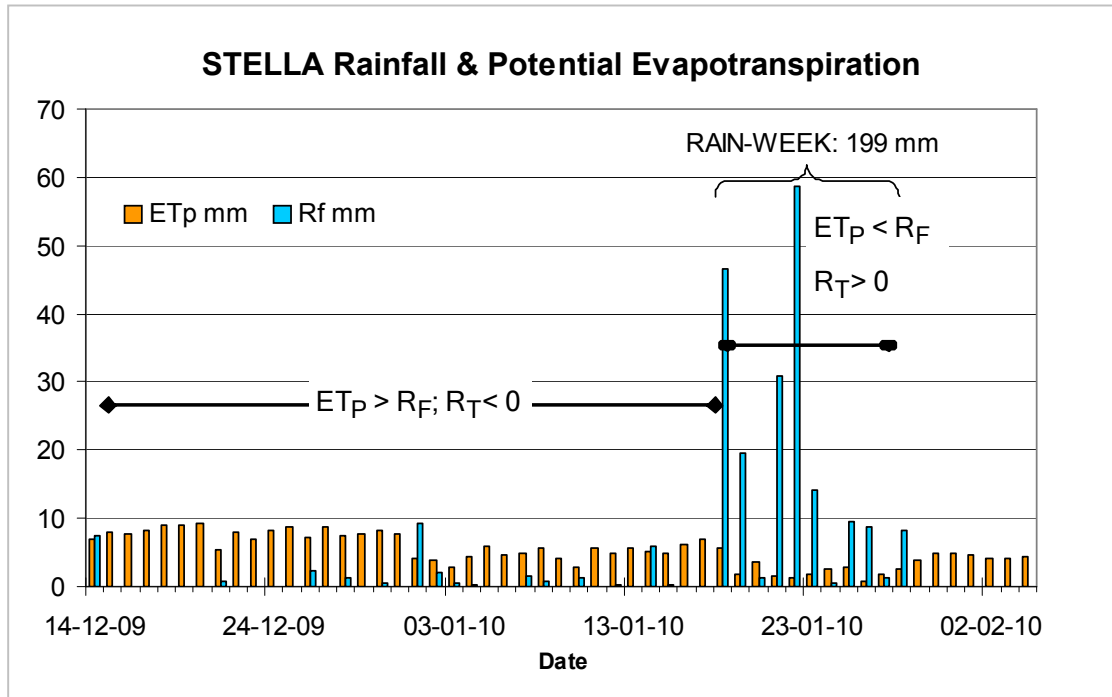


Figure 3.6. Observation of rainfall and ET values at the Stella, Appelkoosboom monitoring site between 14-12-2009 and 02-02-2010, including a rain week period recording 199 mm.

Observations with the Davies Weather Station report that ET_p is significantly less during rain-weeks due to lower air temperature, high RH-levels, minimum solar radiation and wind speeds. Three distinctive short-term periods can be visualized in the data. The first two weeks (14/12/'09 to 31/12/'09) recorded 12.2 mm of rainfall R_f , with a total accumulated ET_p of 143 mm (HARmean of $7.8 \text{ mm} \cdot \text{d}^{-1}$), the next two weeks (01/01/'10 to 17/01/'10) rainfall was 21.8 mm with a total accumulated ET_p of 82 mm ($4.5 \text{ mm} \cdot \text{d}^{-1}$). The next ten (10) days was a typical rain-week scenario with a rainfall of 199 mm, with two rainfall events of $>40 \text{ mm} \cdot \text{d}^{-1}$ at rain rates of between 60 and $100 \text{ mm} \cdot \text{h}^{-1}$. The accumulated ET_p over this period was 26 mm (HARmean of $1.8 \text{ mm} \cdot \text{d}^{-1}$).

The relationship between rainy days and the four main state variables influencing, and in these cases depleting ET_P by several mm, can be seen in the illustration. With in days after the rain week has passed, ET_P starts to increase from around $1.8 \text{ mm} \cdot \text{d}^{-1}$ to $4.5 \text{ mm} \cdot \text{d}^{-1}$ once the temperature increases and RH decreases.

The ET_P values calculated by the Davies Weather Station in the Stella area compares well with summertime Penman ET_P estimation calculated by Gieske (1992) in Botswana, i.e. $8 \text{ mm} \cdot \text{d}^{-1}$.

3.3.2.2 Relationship between ET_P and Actual ET (ET_A).

In comparison with moderate to humid homoclimate regions, where the soil moisture deficits exist only for short periods of time (matter of days), the monthly values for ET_A differ slightly from ET_P . In semi-arid and arid regions, where the interval between subsequent wetting periods is highly variable, thus causing alternating soil/regolith moisture deficits, the differences between ET_A and ET_P is significant, and the relation can be expressed as follows (Kijne 1974);

$$ET_A = k_{ET} \cdot ET_P \quad (3-1)$$

in which k_{ET} is a function of the soil/regolith moisture content and referenced as the relative ET rate ET_A/ET_P with $1 \approx k_{ET} \geq 0$. Some literature values for k_{ET} is reported to be in the order of 0.78 for temperate climates. In discharge area's where upward-rising groundwater provides continuous soil-moisture supply, k_{ET} will be significantly higher, and may even be larger than 1 if in vegetated regions (Kijne 1974; Freeze and Cherry 1979; Kendall and McDonnell 1998).

Once the soil/regolith moisture diminishes to the level of a field capacity deficit condition, the relative ET rate, k_{ET} decreases once more. Actual ET rate in semi-arid regions is therefore a function of the area, i.e. in a recharge area such as hard rock terrains, ET_A will be considerably lower than ET_P .

The Davis type weather stations used on three of the monitoring sites were not equipped with soil moisture sensors which would allow for the estimation of ET_A .

3.4 SUMMARY.

Hydrometeorological conditions in southern Africa have oscillated between extreme arid and humid conditions during the last 50 000 years. Drainage channels and depressions deployed by incisions and wind erosion in the humid/drier palaeo times still play an important role in the local spreading of especially modern time run-off events.

Semi-arid regions are characterized by extreme hydrometeorological conditions of which temporal extremes of temperature, precipitation, ET and vegetation vary to such a degree that water availability becomes critical for long-term socio-ecological wellbeing.

The effect of ET is significant in temperate climates, but is normally balanced by sustainable rainfall. In comparison, semi-arid regions with drastic climate changes, even over night, have a complex ET mechanism especially in areas with streamline vegetation which are normally larger types like scrubs and trees. Estimation of ET_P/ET_A still needs to be refined, and requires dedicated operations, and monitoring, methodical observations using representative monitoring terrains, and sophisticated equipment should satisfy high-level data requirements needed to quantify the rainwater-groundwater interaction and water budget. Estimation of the relative ET rate k_{ET} is a complex principle and requires dedicated meteorological monitoring and assessment.

The ET process plays an important role in the hydrogeochemical evolution of inland-downwind rainout events. Addition of moisture generated by terrestrially ET recycling to the atmosphere has been identified by Kendall and McDonnell (1998). This phenomenon alters the hydrogeochemical characteristics of downwind meteoric water and can either deplete or enrich the next rainout component. It is however expected that inland ET recycling from large forests and humid regions will deplete the hydrogeochemical composition of atmospheric moisture (Section 5.2).

oooOOOooo

4 HYDROGEOLOGICAL PORTRAYAL.

4.1 INTRODUCTION.

Ground surface conditions in the semi-arid region alter from terrains with hard rock outcrops to terrains with various thicknesses of soil/regolith masking the underlying parent rocks. These superficial conditions play an important role in the differentiation of surplus rainfall between direct infiltration and surface run-off, followed by contrasting underdrainage conditions differentiating flow between rooting zone capturing and bypassing infiltrated rainwater to the underlying SZ (Lerner 2003). In high relief regions²¹ the underdrainage may be captured almost completely by interflow which overpasses deeper percolation and discharges into local rivulets and subsequently drains out of the potential recharge terrain.

Shaping of the hard rock landscapes in semi-arid regions of southern Africa was initiated by Miocene (~18 Ma) and Pliocene (~2 Ma) uplift and subsequent Post African I and II erosion phases respectively (Partridge and Maud 1987). The impact of a semi-arid climate with occasional dramatic wet periods which initiate flash flooding, the landscape erosion process favors shallow mechanical weathering and erosion in contrast to the deep, *in situ* chemical weathering in the semi-humid to humid eastern parts of South Africa.

The hydrogeological characteristics of the unsaturated, hard rock interface between ground surface and the SZ controls the effectiveness of groundwater recharge in many ways. International and local research indicates that a multi modal recharge mechanism is possible. Fractured hard rock terrains where the rock matrix may still have primary porosity or have developed intense micro fracturing, probably classifies as a multi-modal flow regime which requires special monitoring procedures to capture the state variables needed to quantify groundwater recharge.

This chapter will address the hydrogeological flow path concept between ground surface (the semi-arid land surface) and the underlying groundwater table interface. It focuses on the development of fractured/weathered hard rock surfaces, conditions in the upper

²¹ Mountainous areas with steep slopes and deeply incised rivulets.

jointed/fractured and weathered profile followed by a fractured bulk rock, which all may yield variable matrix hydraulic characteristics.

To conclude, the hydraulic concept of unconfined flow with vertical accretion will be addressed with an analytical box model to demonstrate episodic rainfall recharge as depicted from groundwater table responses.

4.2 THE SOUTHERN AFRICAN GEOMORPHOLOGICAL HISTORY.

4.2.1 *The Late Mesozoic Era.*

During the Cretaceous Period (~142 to ~65 Ma) the southern African continent was mostly covered by Karoo Supergroup sediments and volcanics. The region has been elevated considerably since ~180 Ma, probably due to the presence of a mantle plume underneath southern Gondwanaland. The interaction between this feature, crustal fracturing/shearing and the late Karoo volcanism that produced the lavas of the Drakensberg Formation around ~190~180 Ma was noted in literature studies.

By ~120 Ma, rifting along the west and east coastal regions of southern Africa thinned the Gondwanaland continental crust and opened the ancestral Atlantic and Indian Oceans respectively. Extremely deep fractures during the final break-up have intersected kimberlitic magmas at 150 to 200 km depth. Several kimberlite pipes and fissures were emplaced around ~90~87 Ma in the interior of southern Africa. In many cases, kimberlite intrusions followed the same fracture path than those earlier feeder dykes associated with the final Karoo volcanism.

These dolerite dykes are linked with large sill-like intrusions, especially in the lower Karoo sedimentary Sequence (Ecca and Beaufort Groups) and play an important role in groundwater occurrences and flow control in the Karoo and older rock formations elsewhere in South Africa.

A prominent landscape feature in the southern African geomorphology initially started as a marginal, circum-country escarpment around ~120 Ma. The Great Escarpment of southern Africa was shaped during the African erosion cycle from Late Jurassic/Early Cretaceous to the end of the Early Miocene (Partridge and Maud 1987). Its landform became prominent

from the onset of the South America-Southern Africa-East Antarctica break-up (>~65 Ma) and already portrayed a gentle westward sloping high land from the newly formed coastal plains. Since its maximum domination during the Late Cretaceous Period, the escarpment still exhibits a large control over the climatic conditions over coastal as well as inland regions in southern Africa.

4.2.2 Neogene Tectonic Uplift and Erosion Cycles.

Intense erosion of the southern African shield has commenced since ~65 Ma producing the African erosion surface featuring hard rock landscapes in the semi-arid regions. Two phases of continental uplift (Miocene: 150-300 m and Pliocene: 100-900 m) has initiated two post-African erosion cycles, i.e. Post-African I and II, ca. ~18 Ma and ~2.5 Ma respectively. The combined uplift has resulted in a topographic anomaly of global significance and is referenced as the African Super Swell (McCarthy and Rubridge 2005). Most land surfaces in Southern Africa lie at 1000 m amsl, whereas regions around the globe with comparable geological compositions and history lie at elevations 600 to 700 m lower.

Both Miocene and Pliocene uplifts occurred along two axes in southern Africa, i.e. the central Griqualand - Transvaal Axis and the eastern Ciskei - Swaziland Axis. The position of the Griqualand - Transvaal axis shifted between 100 and 150 km during the two uplift phases, resulting in wide spread erosion along and inland of the Great Escarpment. Renewed sedimentation because of the Miocene uplift occurred on the coastal plains²² as well as a gradual filling of the inland Kalahari Basin from early-Middle Miocene to Late Pliocene (Partridge and Maud 1987).

The Post African II erosion cycle instigated by the 900 m Pliocene uplift resulted in a major downcutting phase, removing the older deep weather profiles and exposing shallow hard rock sub-outcrops. The Great Escarpment was eroded several kilometers inland, and this has continued ever since. The eroded material was transported from the continental plateau and was deposited on the continental shelf covering Late Jurassic continental shelf deposits. The resulting Post African II erosion surface exposed a landscape consisting of Pre-Cenozoic (>~65 Ma) landforms standing out above the African surface. These are the

²²Sedimentation on the southeaster, southern, southern and western and western coastal plains as well as major resurgence of sedimentation in deep oceanic basins (Partridge and Maud 1987).

Lesotho Highlands, major mountain ranges of the Cape Fold Belt (CFB) , Soutpans- and Waterberg ranges, Langeberg and Kuruman ranges, and extensive areas immediately inland from the Great Escarpment. Remnants of the African surface are still found in large areas of the Karoo inland of the Great Escarpment although being consumed by pedimentation to produce a landscape characterized by hard rock mounds²³.

4.2.3. *Gondwanaland Fragmentation, Karoo Magmatism and Erosional Unloading.*

Fragmentation of Gondwanaland took place in two phases between ~190 Ma and ~160 Ma (Partridge and Maud 1987). This fragmentation has produced an array of large shear zones (~500 km long) not only over the Karoo Basin (Woodford and Chevallier 2002b), but probably Early Gondwanaland fracturing all over southern Africa.

The geometry of Jurassic Karoo dyke swarms over southern Africa is an indication of the structural deformation and subsequent magmatic activity accomplished during some of the early stages (~20 Ma) prior to the break-up of Gondwanaland (Tankard et al. 1982; Woodford and Chevallier 2002b). They illustrate the mechanism of dolerite dyke emplacement, and indicate that these features, as well as the younger hypabyssal kimberlite intrusions, are the result of joints/fractures and faults instigated by early Gondwanaland break-up. Several non-intrusive tectonic features were classified as regional lineaments originating from the deeper basement. These features have a northwest-southeast orientation over southern Africa and are associated with late Gondwanaland shear fault detachment that took place along the Agulhas Falkland Fracture Zone (Tankard et al. 1982; McCarthy and Rubridge 2005).

It is evident that unloading of rock mass has occurred over southern Africa since the cessation of the Late Jurassic sedimentation process in southern Africa; including the final Jurassic Karoo volcanism at ~190 Ma. Most of southern Africa was covered with rocks of the Karoo Sequence excluding the CFB window in the south, whose orogenesis dated back to Permo-Triassic times (~278 to ~215 Ma). This orogeny has persistently deformed the southern margin of the Karoo Basin by episodic tectonism which deformed the (folded) the Ecca and Beaufort Group sediments.

²³ Mesas, buttes and bare rock landscapes with sporadic soil/regolith capping.

The Miocene and Pliocene erosion cycles has effectively removed between ± 300 m (Lesotho Highlands) and ± 1800 m (Kimberley, Northern Cape) from southern African topography since ~ 65 Ma (Partridge and Maud 1987). Burial releases of the underlying rocks due to erosional unloading have alleviated significant pressures (several hundred bars) and have initiated the disclosure of primary and secondary jointing in these hard rock masses to much lower hydrostatic pressures. The amount of overburden removed is indicated as relatively minor (± 1500 m), thus indicating that the observed secondary joint/fracture status could not be solely formed by erosional unloading (Woodford and Chevallier 2002b). They suggest that the initial crustal heat flow generated by the Karoo magmatic intrusives played a much larger role in the distribution of surface stresses than erosional unloading. It is to be noted that tremendous heat flows were generated by the Mid Jurassic Karoo intrusive phase (dolerite dykes/sills) and was responsible for the hydrothermal metamorphism and subsequent jointing of the Karoo Supergroup sediments.

Emplacement of several large dolerite sill and ring-complexes in the sedimentary package of the Karoo Supergroup are well-documented (Chevallier et al. 2001). During emplacement of these structures and subsequent cooling, several major types/sets of jointing/fracturing manifested. The country rocks in addition, were subjected to conjugate vertical jointing/fracturing (due to upliftment). Botha et al. (cited in Chevallier et al. 2001, p. 88) mentioned these type of dolerite intrusions could have contributed to bedding-plane fracturing; an observation frequently reported by Venter (2004) during DTH-CC image logging of deep exploration boreholes in the central Karoo region.

Erosional unloading surely will have caused differential pressure releases between rocks with different diagnostic compositions and instigated secondary jointing/fracturing originally formed by either hydrothermal metamorphism or bedding plane discontinuities. Near-surface stress fields (within 1000 m of the earth's crust) are induced by unloading leading to isostatic rebound and uplift. This process is accompanied by the formation of master jointing and fracturing (Chevallier et al. 2001; Woodford and Chevallier 2002a). They proposed several zones where re-organization of stress field resulted in closing of pre-Neogene open water-bearing joints/fractures, but reactivating a different geometry of master-joints and orthogonal joints/fracture sets. It is especially sedimentary formations, which

displays well developed jointing and fracturing in the upper jointed and weathered profiles in southern Africa.

To conclude, secondary jointing/fracturing, due to regional tectonism and magmatism since the Gondwanaland breakup and the Miocene and Pliocene denudation, is displayed in many road cuttings, quarries and ravines in southern Africa. It has to be acknowledge that many artificial fractures were created during excavations and blasting operations.

4.2.4. *Hard rock surfaces.*

The vertical flow regime (in time, volume and concentration) through the unsaturated zone, is governed by the characteristics of the geological profile. Shallow hard rock surfaces expose a wide range of fracture²⁴ heterogeneities, but more or less consequent orientations. Jointing/fracturing, showing various lengths and apertures, can be seen on superficial outcrops as parallel, angular or chaotic configurations. Superimposition of two dominant master-joint directions ((i.e. NW and W-E) are illustrated in planar view in Figure 4.1. This image is from a direct recharge terrain with <0.15 m soil/regolith cover. The origin of these abundant fracture systems in the Karoo environment is probably linked to the CFB orogenesis.

The impact of CFB orogenesis (Late Palaeozoic, ~300 to ~250 Ma) has had a prominent impact on the jointing/fracturing of the lower and middle Karoo Sequence formations in the southern Cape. Low angle folding can be observed in the Great Escarpment face just north of Beaufort West (observations by author). Campbell's study (cited in Woodford and Chevallier 2002b, p.136) of vertical joints in the Beaufort West area reported an average joint-density of 3 - 15 joints per m² in sandstone outcrops. Although joint apertures in the order of 1-2 mm have been observed, apertures of several millimeters were observed by the author in undisturbed ravine faces elsewhere in South Africa.

In profile, fracturing can be observed in several geometries and displays a virtual 3D dimension thereof. Rock faces in natural developed gullies/ravines provide a good indication of spacing and dimensions of joints/fractures in hard rock terrains. The three dimensional

²⁴ Or joints; where stress has caused partial loss of cohesion in the rock; as opposed to faulting, where some movement along the surface of the joint has taken place (Cook 2003).

context of these secondary features can be observed in detail in Figure 4.2, presenting vertical jointing in a lenticular sandstone lens and sub-horizontal fracturing at the contact zone with underlying mudstones as observed in the Nuweveld Mountain, District Beaufort West.



Figure 4.1. Planar view of jointed Karoo-Beaufort Group mudstone, De Hoop, District Beaufort West, illustrating superimposition of a NNW and W-E set of master-joints.

Once the fractured hard rock forms part of the SZ, the hydraulic classification (i.e. porosities) of the aquifer may alter between the two end members of (i) homogeneous porous media (e.g. immature sandstones) and (ii) purely fractured rock (e.g. fractured meta-quartzites), as per Cook (2003). Most hard rock aquifer systems in southern Africa fall between fractured porous media (e.g. Karoo rocks) and fractured non-porous media (e.g. Table Mountain Group (TMG) ortho-quartzite). Cook (2003) proposes that the total porosity (β_t) of a formation consisting of fracture systems (β_f) and its hard rock matrix (β_m), is as follows:

$$\beta_t = \beta_f + \beta_m(1 - \beta_f) \quad (4-1)$$

Several fracture (or joints) types have been categorized in structural geological literature; for this study we will focus mainly on those situated in the upper Fractured and Weathered Rock classification according to the National Geohydrological Map Series, DWAF (2003).



Figure 4.2. Vertical and horizontal fracturing in a Karoo-Beaufort Group sandstone lens overlying massive Karoo mudstones, Nuweveld Mountains, District Beaufort West (S32.04233° E022.71436°, 1514 m amsl).

These joint systems include the following geometric orientation in the hard rock mass as observed in the monitor terrains, viz.:

- Sheeting joints: Slightly curved and generally parallel to the topographic surface. These features developed in response to erosional unloading of horizontally layered sedimentary and granitic rocks; and
- Columnar joints: Generated due to shrinkage of rocks, either cooling of igneous rock or desiccation of argillaceous sediments and clayey surfaces.

Clayey surfaces, classified as Vertic A-horizons in soil classification literature are unique as their dimensions are changing depending on the moisture content. The latter joint systems play an important role for recharge where the soil/regolith areas are more clayey, i.e. the Vertisol soil type (Department of Agriculture Development 1991). These joints or cracks can reach a depth of 1.0 to 1.5 m after a prolonged dry-out process during the dry seasons and may therefore link directly to joints/fractures in the underlying fractured and weathered basement (King 1942).

Nkotagu (1997) recognized four (4) possible features at ground surface which enhances immediate infiltration of recharge-producing rainfall surplus once the limitations of rain intensity-depth are bridged. They are in order of efficacy (by the author):

- Highly permeable soil/regolith with limited evaporation in the UZR during high intensity rainfall and under depression storage conditions;
- Faults, fractures and joints available over the recharge area during high intensity rainfall and under depression storage conditions;
- Desiccation and tension cracks of micro-fissures in clays particularly in lowlands areas; and
- Numerous animal burrows, termite holes and tree root hollows.

4.2.5. The Unsaturated Zone Reservoir.

In an event of recharge-producing rainfall surplus during a rain event, that portion of the rainwater that does not flow away as overland flow has the potential to infiltrate directly into the soil/regolith zone where ET and/or deep-infiltration differentiation takes place. The lithological character of the soil/regolith therefore governs the storage and permeability, hence the spatial and temporal availability of moisture to ultimately replenish the underlying groundwater resource.

Some combinations of soil/regolith which will not allow any deep infiltration to take place under average climate conditions. Thick layers of aeolian sand are a good example. Smit

(1977) and De Vries (1984) noted that local groundwater recharge is limited to areas where the Kalahari Sand Formation (Late Pliocene to Early Pleistocene deposits) is less than 6 m thick²⁵. It is suggested that even during high rainfall events, this aeolian sand will retain the recharge-producing surplus rainwater where its thickness exceeds 6 m. Extraordinary rainfall events, like the Ulenhorst cloud burst in Namibia, recorded ≈ 450 mm in less a week, are exceptional cases and may generate significant ASR in enclosed desert terrains (Verhagen 2009; Talma 2009).

In soil profiles where durban/duripan (calcareous or siliceous cemented soil) horizons exists, as well as hardpan carbonate horizons, infiltrated rainwater might be rejected and transferred to become part of shallow through-flow regime instead, i.e. recharging rainwater will flow laterally and not vertically through the profile (Lerner 2003).

It is important, therefore, to observe the characteristics of soil/regolith profiles and underlying parent bedrock when investigating direct infiltration mechanism(s) of recharge-producing rainfall surplus, generated during episodic rainfall events.

4.2.5.1. Soil profile characteristics.

The alternating humid/dry, hot/cold and windy climatic cycles in semi-arid regions, hinder development of deep, mature soil profiles. The most important conservation factor for soil profiles is vegetation. Insufficiently thick vegetation in the semi-arid region cannot protect soil/regolith throughout the year, and hard rock terrains are continuously enlarged by the episodic nature of the rainfall (King 1942).

Diurnal and seasonal temperature differences run into tens of degrees; thus mechanical erosion of bare rock surfaces is common in semi-arid regions (King 1942). Bare landscapes open to high wind runs (6 to $8 \text{ m}\cdot\text{s}^{-1}$), are continuously swept clean of fine rock dust freed by mechanical erosion on the rock faces. In an event where surplus rainwater might bypass ground surface, high evaporation rates can easily remove up to 50% in the first 0.25 m profile, and lessening downward development of an *in situ* regolith solum (Chow 1964).

²⁵ Along current drainage channels, depressions, hard rock sub-outcrops within 6 m from surface and alongside the perimeter of the Kalahari Basin where the Kalahari Sand Formation tapers out.

Thicker (>6 m) profiles play an important role in the bulk storage of soil water and piston flow transport of during groundwater recharge events in sub-humid and humid regions. Complete soil horizon development is possible in isolated areas in the semi-arid region. For example, in drainage valleys, where shrub and tree coverage increases substantially, compared to the intergrowth areas where only savanna vegetation dominates. From surface to bedrock level, soil horizons A, B and R are most dominant. The R-horizon represents broken to fresh parent bedrock. Humic A-horizons, characterized by a well draining solum structure and loaded with organic material, may also allow drainage depending on the rainfall depths and bedrock composition.

Land surfaces in the semi-arid region portray a thin (<0.5 m) Orthic ↔ Melanic A-horizon (sandy ↔ slight clayey), observed by the author in roadside and crevasse sections. Vertic A-horizons (characterized by ≥30% clay with swell-shrink properties) may be found in semi-arid to sub-humid margins associated with a clay producing underlying parent rock like basalts (i.e. Letaba Basalt of the Karoo Supergroup volcanics is probably the best example in southern Africa).

Thin B-horizons are represented by (i) a reddish Apedal B-horizon (decomposed bedrock: basic igneous rock²⁶) or (ii) a yellowish Apedal B-horizon (decomposed bedrock: sandstone, quartzite, shale, mudstones and granite). The maximum root penetration depths of between 0.2-0.6 m bgl are situated in the B-horizon. The rooting system of many shrubs and trees may penetrate into the underlying jointed hard rock in open fractures which complicates the differentiation between the UZR and the LUZR (Van der Watt and Van Rooyen 1990; Gieske 1992).

The topography, soil/regolith and hydro-lithological properties of the UZR vary from area to area both vertically and laterally. There might be areas in a regional catchment where groundwater recharge is either inferior or enhanced due to gradual changing slopes of the surface and the slope of the boundary between the soil horizons and the fractured and weathered hard rock respectively.

²⁶ Dolerite, basalt, norite, gabbro and diabase.

Tightly packed soils in the B-horizon like hardpan calcretes, dorbank and Vertisols can act as infiltration barriers and any infiltrated rainwater is diverted laterally away from the area; even a slope steeper than 1% can form a capillary barrier and divert the infiltrated water laterally given the top layer has a high hydraulic conductivity (Balek 1988).

4.2.5.2. Fractured and Weathered Hard Rock Profiles.

Orthic A-horizons and Apedal B-horizons in the semi-arid region occur mostly in low-lying streamline zones; the thickness dissipates quickly towards higher ground where the soil/bedrock profile consists of thin/absent Orthic A-horizon directly on top of either a soft/hard carbonate (or calcrete), dorbank and/or broken bedrock. Merges between Orthic A-horizon and the underlying broken bedrock occur widely, and forms Lithocutanic B-horizons²⁷ and represent the typical arid/semi-arid soil/regolith composition.

Depending on the degree of calcification of the broken bedrock, the calcic enriched product is defined as the Neocarbonate B-horizon.

B-horizons are archetypical of regolith horizons in semi-arid regions (Figure 4.3). (note shallow rooting zone and transgression to hard rock with a few roots penetrating into open fractures (1 m scale).

The typical jointed character of the bedrock profile is the most common secondary feature and is a factor of the lithological composition of the bedrock itself and whatever tectonism the bedrock has passed through.

4.2.6. *The Saturated Zone.*

Over ninety percent (90%) of the southern African aquifer systems are classified as hard rock type aquifers (Vegter 1995)²⁸. These aquifers have a substantial secondary porosity potential, occurring as joints/fractures, developed after diagenesis through tectonism.

²⁷ >70% of the volume consists of fresh or partially weathered bedrock - distinctive affinities with the underlying parent rock into which it merges.

²⁸ Sediments, metamorphic and igneous rocks that were subjected to hydrostatic compressive stresses during deep burial in the crust, are slowly relieved by gradual erosion releases causing tensional stresses to dislodge and open various sets of joints and cleavages.

Groundwater tables in southern African and especially the semi-arid region itself, lies within the weathered and jointed zone. Water strikes in deep jointed zones below the latter zone result in immediate sub-artesian pressure equilibrium, which coincides with the water table in the jointed and weathered zone.



Figures 4.3. Typical structural make up of an A-horizon with underlying fractured hard rock in moderate relief areas.

Strike frequency analyses by Vegter (1995) of a selected group of geological formations in South Africa pertinently shows strike frequencies increase from around 5 m bgl and peaks around 30 to 50 m bgl depending on the lithological composition and diagenesis of the rock/formation.

4.2.6.1. Upper fractured and weathered zone (UFWZ).

During the diagenesis cycle of all rock formations, primary openings (i.e. those expressing primary porosity) are destroyed by either secondary cementing or grain fusion. New sets of joints form once the rock mass gets exposed due to erosional unloading, which may include those joints/cleavages introduced during the initial diagenesis process.

Semi-arid conditions characterized by high evaporation rates, intermittent rainfall events and limited wetting cycles, do not enhance the development of deep (>6 m) decomposed bedrock profiles. Observations made from several DTH-CC-image logging revealed that an UFWZ exists in virtually all hard-rock cases.

The major joint orientation in shallow (<30 m) jointed and weathered zones is horizontal and is the result of (i) near horizontal bedding plane jointing in Karoo Ecce and Karoo Beaufort Groups sediments of the Karoo Supergroup enhanced by vertical pressure relief due to erosional unloading, or (ii) sheeting joints in granites (e.g. Stella: Mosita Granite complex) and magmatic rocks (e.g. Taaiboschgroet: Karoo Letaba Basalt Formation).

Although vertical boreholes are not always intercepting all vertical/oblique fractures, some can be traced for several meters in depth. DTH-CC image profiling reports a lower fractured/weathered boundary from where all rock types portray a fresh and solid matrix; thus representing a fractured, secondary porosity media at depth.

4.2.6.2. Deep²⁹ Bedrock Fractures.

Below the upper jointed and weathered zone, there's a substantial decrease in strike frequencies. In some lithologies, the frequency may drop to less than 0.15 strikes per 10 m depth interval (Vegter 1995). DTH-CC image logging reveals that water strikes at these depths are related to (i) geological contacts between host rock and intrusions e.g. Mid Jurassic-Karoo dolerite sills or dykes intruded into Carboniferous-Triassic Karoo Basin sediments, (ii) horizontal bedding plane contacts between sandstone and underlying mudstones e.g. the large channel bar and point bar lenses in the Permo-Triassic Beaufort Group, and (iii) fractures (joints and faults) developed in or adjacent to regional fault

²⁹ That section of the hydrogeological profile where the associated strike frequency curve becomes vertical (Vegter 1995).

zones e.g. Triassic-Tshipise Sandstone Member and Letaba Formation basalt along the Taaiboschgroet Fault Zone (TFZ), southwest of Alldays, Limpopo Province.

Competent rock formations like ortho/meta quartzite exposed to orogenic deformation represent good examples in these cases, showing a heterogenic joint development generated by deep stress related deformation. Recent ultra-deep drilling (>800 m) in the TMG reported fracture zones with artesian and sub-artesian hydraulic conditions (e.g. TMG fracture zone was intercepted at 540 m bgl in the Blikhuis exploration borehole ($T_D = 802$ m), Citrusdal, Western Cape: S32.39507° E018.95978°, 158 m amsl). The Blossom deep artesian borehole ($T_D \approx 700$ m) south of Oudtshoorn, Western Cape, intercepted water at ~500 m bgl in a fractured, pressurized water bearing zone (S33.73412 ; E022.27920 , 421 m amsl). This borehole has a artesian pressure of 75 m.

The geometry of these deeper joints, especially the horizontal ones, are complicated in terms of hydraulic connectivity to the upper fractured and weathered system and probably all other fractures in the aquifer unit. DTH-CC image logging reports several oblique joint systems intersected by the borehole axis, although the fracture aperture (proportional to the fracture porosity β_f) is several orders of magnitude smaller than those of the horizontal fracture zones.

4.2.7. Karstic Profile and Plane.

Carbonate evaporates (primary limestone, dolomite and secondary calcareous duricrusts) in southern Africa represent a unique system with adverse hydraulic properties above and below the groundwater table zone. They represent a typical topographic character (karst) and the unsaturated/saturated profile and surface may vary considerably from local to regional scale.

Primary karst rock formations in southern Africa consist of limestone/dolomite belonging to the Chuniespoort/Ghaap Groups of the Vaalian Transvaal Supergroup consisting of carbonate evaporates.

Secondary carbonate rock formations in southern Africa consist of wide spread calcareous duricrusts, which normally represent the calcified upper horizons of the underlying parent

rocks of all types with a prominent hard or soft calcareous capping. These formations are formed at or close to the surface as evaporate from regionally dissolved carbonates in evaporating groundwater. It is therefore to be expected that these horizons will be enriched with ordinary rock salts like NaCl.

Soil/regolith cappings in mature karst regions are limited to low-lying depressions/doline structures. Extended soil horizons are not a common feature at all, especially in semi-arid regions. In the sub-humid regions, the A and B soil horizons consist of transported material from surrounding younger formations such as the lower Karoo Supergroup outliers occurring on the Chuniespoort dolomites in the Gauteng Province.

On the Ghaap Plateau, Northern Cape Province, soil horizons are limited, except in local depressions where it normally consists of residual chert rubble associated with/without wad (dolomitic residual clay); all *in situ* products of dolomite ($\text{CaMg}(\text{CO}_3)_2$) leaching/ weathering processes. Superficial bare parent rock faces are more the norm in these semi-arid dolomitic water areas. In many cases local overland flow systems have developed through natural weathering and erosion which discharges into local depressions or swallows (Wiegman 2006).

The ground surface conditions of the dolomitic water areas towards the semi-humid regions are different and exceptional deep leaching has taken place. Large cave systems like the Sterkfontein Caves, in the western Gauteng area, have been formed since ~5 Ma. The karst development is therefore much deeper in the Gauteng area and promotes direct recharge significantly.

These depressions were observed using high-end digital terrain mapping created during airborne geophysical surveys over the Northwest Province dolomitic water areas. The ultimate scale of these depressions represents swallows like the well-known Bushman Gat, on the farm Mount Carmel, some 55 km south of Kuruman in the Northern Cape Province of South Africa (Figure 4.4), which opens into a 274 m deep submerged cavity below water level.

The unsaturated profile characteristics of the karst groups portray its own diverse pattern and differ substantially between the hard-rock karst (limestone/dolomite) and the softer

duricrusts (i.e. calcretes, etc). Chemical weathering driven by high levels of carbonic acid (H_2CO_3)³⁰ in the rainwater normally creates unique sub-vertical chutes that completely bypass the unsaturated zone during recharge events. It is a well-known fact that recharge in karst regions in southern Africa occurs through these preferential pathways. The relative large diameters (several centimeters) of these chutes and non-existing primary porosity of hard rock dolomites implies that virtually no transmission of recharge-producing surplus rainfall into the rock matrix take place.



Figure 4.4. Bushman Gat on the farm Mount Carmel (191), District Danielskuil. A funnel-shaped sinkhole in the Ghaap Plateau dolomites, (S27.92183°; E023.64161°, 1562 m amsl).

Recharge mechanisms in karst terrains are therefore quite unique as the whole rock package consists of secondary openings with no consistency in terms of orientation, di-

³⁰ A weak acid formed by dissolving carbon dioxide (CO_2) in water (Hawley 1981). At an atmospheric partial pressure of $10^{-3.5}$ atm, rainwater has a pH of 5.65, H_2CO_3 dissociates to H^+ and HCO_3^- (Drever 1997).

mensions and secondary openings. The recharge mechanism is predominantly preferential flow driven with short (hourly) responses to rainfall events.

4.3. HYDRO-LITHOLOGICAL CHARACTERISTICS OF HARD ROCK FORMATIONS.

4.3.1. *Introduction.*

All hard rock formations in southern Africa have been subjected to one of more orogenic phases of different magnitude. Where the dolomites of the Transvaal Ghaap Group dolomites were subjected to regional fracturing, the Late Carboniferous (~310 Ma) to Mid Jurassic (~187 Ma) Karoo Basin sediments were mildly folded/fractured, and hydrothermally altered by Late Jurassic Karoo dolerite/basalt magmatism. The Karoo Drakensberg Group basalts, were subjected erosional unloading and local faulting³¹. The older hard rock formations went through several phases of deformation/metamorphosis, for example the Archaean Kraaipan Group rocks in the Stella area are tightly folded, in places isoclinally folded, sheared, and locally brecciated and cemented by siliceous compounds.

The lithological composition of the bedrock and whatever tectonic/orogenic cycles it has passed through, characterizes the hydraulic nature of the unsaturated profile in terms of recharge flux between ground surface and the SZ. Jointed bedrock with various stages of weathering is the most common secondary feature in hard rock profiles. In the Karoo Beaufort Group for example, master jointing manifests as orthogonal sets of fracturing, consisting of one systematic joint orientation accompanied by another non-systematic orientation (Woodford and Chevallier 2002b). The competent lenticular sandstone lenses portray a higher consistence of larger, vertical joint systems than the MDNS bulk.

In the case of the Karoo Beaufort Group³², the lithology consists of alternating argillaceous/arenaceous layers; each with its own jointing and weathering profile. Arenaceous sandstone layers under tectonic deformation may develop prominent master joint systems, whilst argillaceous formations may develop macro/micro joint systems.

³¹ For example along the TFZ in the Limpopo Province.

³² Sediments of this group were deposited under a fluvio-lacustrine environment consisting of massive grayish MUDSTONE and lithofeldspathic SNDS (late Permian Adelaide Subgroup) followed by the early Triassic Tarkastad Subgroup characterized by a greater abundance of SNDS and red MUDSTONE. (Turner 1979; Woodford and Chevallier 2002b)

Massive crystalline metamorphic rocks (thick dolerite sills, granites and granite-gneiss) display a complex array of jointing which is often a superimposing of more than two complete different phases of orogeny and deformation, e.g. cooling joints followed by tectonic deformation due to folding/faulting (Lahee 1952; Price 1966).

4.3.2. Vertical Jointing and Fracturing.

The concept of micro, macro and master jointing in the context of this study is illustrated in Figures 4.5, observed in a road cutting in De Jagers Pass (S32.07875°; E022.74762°, 1323 m amsl), District Beaufort West



Figure 4.5. A combination of micro and macro jointing with a prominent master joint/fracture in Karoo-Beaufort Group mudstone.

Figure 4.5 demonstrates a complex network of minuscule fractures in Karoo Beaufort Group mudstones³³ (image covers approximately 0.75 m across). These are probably a

³³ The Karoo Beaufort Group sediments in the study area north of Beaufort West consists of mainly massive and locally mudstone with occasional thin interbeds (<1 m) of ripple cross laminated and horizontally-laminated siltstones and fine-grained, tabular, sheet-like or lenticular sandstone horizons(<8 m).

product of internal clastic deformation because of erosional unloading. Individual joints occur within a few millimeters from each other and tend to present a rough grid of micro fracturing. The interconnectivity of these micro joints can be judged by the development of iron oxide staining on the joint faces (not very visible on the micro joints in this illustration).

Prominent joints/fractures occur as regional features that can be traced for several kilometers alongside faults or dykes as observed in De Jagers Pass, 36 km northeast of Beaufort West, Western Cape Province (Figure 4.6). These features represent a combination of micro, macro and master joints/fractures in the bulk hard rock media.



Figure 4.6. Macro fracturing illustrated in Karoo-Beaufort Group sediments contact with a Karoo dolerite aureole in De Jagers Pass cutting.

Micro joints occur on minute scale, and have no specific strike; thus they portray a blocky and interconnected appearance as shown in Figure 4.5. These are typical features in the upper jointed and weathered profile of the Karoo Beaufort Group mudstone.

Macro joints are classified as elongated, vertical features such as portrayed in Figure 4.5 with < 2 mm aperture according to Campbell's classification (cited in Woodford and

Chevallier 2002b). These macro joints may bifurcate and intersect adjacent macro joints or diagonal joint subsets to form a bulk trellis of interconnected joints.

Master joint sets, as the large (> 2 mm aperture) fracture shown in Figure 4.7, can be traced for many tens of meters, although they are confined to specific layers/horizons, e.g. the lenticular sandstone lenses found in the Karoo Beaufort Group formations.



Figure 4.7. A typical Karoo-Beaufort Group sandstone lens with even-spaced vertical fractures, Nuweveld Mountains, District Beaufort West.

In terms of groundwater recharge and ground surface conditions, these joints/fractures feature as indirect recharge mechanisms when Hortonian³⁴ overland flow is generated, setting off direct recharge where a rivulet crosses a fault zone or dyke (personal observations; Figure 4.7) in the Nuweveld Mountains (S32.042367°; E022.712045°, 1517 m amsl).

³⁴ Sometimes called Horton overland flows and occur when precipitation rate exceeds the local infiltration capacity of the underdrainage flow regime.

4.3.2.1. Micro Jointing/Fracturing.

Modern physical/mechanical forces on the underlying rock mass are probably still responsible for minute development of micro fracturing in hard rock formations. Mechanical weathering/erosion processes related to climate, mechanical (effect of lunar tides on the rock mass), root stem penetration, seismic activity and to a lesser degree chemical putrefaction under semi-arid conditions could enhance micro-joint/fracture development. Forces responsible for this development are probably the result of ongoing weathering and erosional unloading/uplift of the shield rock masses.

The joint/fracture configuration displayed in Figure 4.5 is probably a good example of this type of micro features present in hard rock formations.

4.3.2.2. Macro Jointing/Fracturing.

With reference to Figure 4.5, several vertical joints are visible cutting through the micro joints, with prominent iron oxide staining on the joint surfaces. These types of joints are especially visible with DTH-CC image logging in boreholes and they run vertically for a few meters below the weathered and jointed zone from where they dissipate within a few meters. In the upper UFWZ, these macro joints may enlarge because of erosional unloading and horizontal expansion close to the surface.

When intercepted by a borehole, these joints will form a perfect flat, iron stained surface on the bore sidewall and portrays a square borehole sidewall image. According to Woodford and Chevallier (2002b) these joints probably represent a subset of the larger master joint sets and do not particularly contribute to vertical groundwater fluxes, i.e. non-systematic orthogonal joint sets. Even at ground surface where erosional unloading effects should be at its maximum domination, these macro joints do not show substantial fracture/cleavage development (personal observations; Figure 4.1).

With reference to Figures 4.5 and 4.7, the joints/fractures on these images correlate with the systematic joint-sets model proposed by Woodford and Chevallier (2002b). These joints are probably related to regional orogenic deformation, prior to the Mid Jurassic Karoo intrusive phase. In the case of the Cape Karoo Basin, this is presented by the CFB orogeny (Section 4.2.2), and in the case of the Limpopo Karoo Basin, the TFZ orogeny.

4.3.2.3. Master Jointing/Fracturing.

In this study, master joints observed in the field displays various displacements along the joint plane and actually represent local and probably regional fracturing (Figure 4.8).



Figure 4.8. A close-up of sub-vertical joints/oblique slip in the Beaufort Group's, Teekloof Formation.

The configuration in Figure 4.8 illustrates a lenticular sandstone sheet overlying a sub-horizontal bedding plane contact with mudstone from the same formation. Joint/fracture mapping at the site indicated that some minor movement (slickenside) has occurred on this bedding plane causing the vertical joints to expand laterally. The large openings shown in Figure 4.5 and Figure 4.8 confirm fracture development in the master joint sets.

Slip surfaces are rough and contain irregularities which will create openings as soon as even minute movement takes place along these planes. This probably explains the large apertures observed in (sub-) horizontal bedding plane fractures

Fracture development instigated by Jurassic dolerite intrusions has been noted by Chevallier et al. (2001) and Woodford and Chevallier (2002a; 2002b) in the Karoo Basin as the

result of reactivation along the original dyke intrusion strike. The master joints reported above probably has no direct resemblance with the dolerite dyke intrusions, due to distances, and relates ostensibly to Neogene orogenic deformation which may have enlarged joints/fractures generated by the earlier Gondwanaland Break-up phase.

Large vertical fractures developed during the actual dyke intrusion phases form prominent macro fracture systems running from directly below the A- or B-Horizons to several tens of meters below ground surface. These features are likely enhanced during secondary movement along the primary feature, e.g. the dolerite dyke structures.

One extraordinary macro fracture system the author has observed was a vertical set developed in the contact aureole of a Karoo age (~140 Ma) east-west running dolerite dyke intruded into granite-gneiss of the Kokerberg Formation 14 km southwest of Kenhardt, in the Northern Cape. At this site, a set of parallel striking open fractures of several centimeters (5 to 10 cm) wide occurs within a 1-2 m wide contact zone at a depth of 228 m below ground surface (S29.45222°; E021.06611° Cape Datum, 900 m amsl).

The joint/fracture configuration in the dyke contact zones is unique and although they are related to the dyke emplacement, the large, open joints/fractures are situated away from the host rock-dyke contact, as illustrated in Figure 4.6. The contact aureole seems to be solid, whilst about 0.5 m away a high frequency of vertical fractures is visible. According to Woodford and Chevallier (2002b), who investigated distance-yield correlations of several hundred (594) cases and found a rather weak statistical correlation within the dyke contact aureole itself.

In terms of indirect groundwater recharge in favorable places (viz. rivulet crossings) along large fault and dyke features, the effect will probably be of local significance; all depending on the flow regime³⁵ of the surface water source. Special monitoring along the Brandwag-Tweeling dolerite dyke, north of Beaufort West where a rivulet intersects and meander across the dyke outcrops, is not reporting significant ASR conditions in the adjacent UFWZ aquifers.

³⁵ Whether the surface water flow is ephemeral (i.e. a flush flood) or a seasonal phenomenon.

Macro fracturing in the UFWZ is of interest here as these features represents the entrance permeable zones through which recharge-producing rainfall surplus enters and subsequently percolates towards the deeper SZ. These joint/fracture patterns, as observed from several excavated road cuttings/rock quarries/ravines throughout southern Africa portrays a simple sub-vertical and sub-horizontal joint/fracture configuration (Figure 4.7 and 4.8). Recharge-producing rainfall surplus will therefore flow according to a configuration of near horizontal and vertical flow patterns through the UZR until it reaches the SZ.

4.3.3. Horizontal Jointing/Fracturing.

Bedding plane jointing/fracturing in the UFWZ may develop significant openings for enhanced groundwater fluxes through fractured aquifer systems. Sedimentary rock formations are specifically favorable for development of horizontal jointing/fracturing, especially where erosional unloading occurred, i.e. unloading joints (Park 1983). DTH-CC image logging of the UFWZ in sedimentary rock formations shows a high probability for development of horizontal joint/fracture systems. This has been confirmed by onsite observations at road cuttings, quarry sites and ravines (Figure 4.8.).

Several examples of deeper horizontal fracture systems were noted in literature and observed on other areas during DTH-CC image logging. These include large bedding plane contacts between different formations (Brandl 2002), bedding-parallel fractures in Karoo Beaufort Group sandstone horizons (Van der Merwe 2008) and fracture zones in dolerite sill environments (Chevallier et al. 2001; Woodford and Chevallier 2002a; 2002b).

4.4. UNSATURATED-SATURATED ZONES FLOW REGIME.

These deep-seated fracture zones probably play a significant role in the regional flow regime where groundwater moves from direct recharge terrains to lower level sub-reservoirs according to the Willemink (1988) and Mazor (1997) flow regime models. Many hot water springs in southern Africa indicates that these flow paths can be several hundred meters deep as depicted from temperatures in the order of 45 to 55°C.

Recharge-producing rainfall surplus fluxes through the UZR at direct recharge terrains represent the initial entrance of rainwater into the subsurface from where several different processes alters the character in terms of volume and hydrogeochemical composition.

4.4.1. Introduction.

In Section 4.3, the occurrence and characteristics of joints/fractures in hard rock terrains, with special reference to the Karoo Beaufort Group formations has been discussed. These features will play a decisive role in groundwater recharge mechanisms. Once the recharged rainwater starts with its downward percolation through the UZR, the hydraulic characteristics of the soil/regolith and hard rock will control the rate of downward movement.

Hyetograph-hydrograph sets show that the actual time lag from the onset of a rainfall event and the onset of the underlying groundwater level response may vary from a few hours to several weeks. The storativity S , and hydraulic conductivity K , of the vertical and horizontal flow components through the UZR and SZ plays an important role in the dimensions and retention time of a water table mound after recharge has taken place.

A second important aspect which drives the rainwater recharge pulse through the UZR, is the rainfall configuration. It will be shown presently that under average annual rainfall patterns (duration and depths) effective ASR does not always manifests.

Considering the hydrogeological nature of the unsaturated zone in the hard-rock domains in southern Africa, the unsaturated flow regime can probably at best be approached as a dual flow system (Gieske 1992; Cook 2003). It is characterized by: (a) soil/regolith moisture flux (retarded, diffuse recharge - R_{SM}), (b) rock matrix flux (retarded, diffuse recharge - R_{RM}) and (c) preferred pathway flux (quick, preferential recharge - R_{PR}), all contributing to (c), a total recharge R_T .

4.4.2. The Unsaturated Zone Reservoir's Flow Path.

Recharge-producing rainfall surplus, or rainfall excess, at ground surface partially infiltrates downwards and becomes part of the unsaturated flow regime. A large portion (50% to 80% in semi-arid regions) of the rainfall excess not captured by interflow is intercepted

by plant rooting systems and returned to the atmosphere by plant transpiration (Chow 1964; Kendall and McDonnell 1998).

This process also generates a specific hydrogeochemical composition for the remaining water, termed soil/regolith water where applicable. During the next effective recharge event, new water is added to the upper portion of the soil/regolith water zone, and due to a downward pressure or piston effect, the soil/regolith water gets released under gravity feed and ultimately the water table interface if field capacity in the UZR is maintained (Willemink 1988).

The UZR can be divided into two zones, based on the effective thickness of the rooting zone, i.e. (i) an upper portion down to the base of the rooting zone (UZR) and (ii) a lower portion excluding the rooting zone down to the water table interface (LUZR). Under normal savanna type vegetation, this partition may hold. When larger scrubs and trees are present, this partition may become inferred, as tree roots may use vertical fracture systems to penetrate down to the water table interface and even beyond. In these cases demarcation of the UZR becomes complex and difficult to model (Gieske, 1992).

Under fractured hard rock conditions, the partition between (i) and (ii) above holds, although field capacity of both zones is seldom retained, because of the episodic rainfall patterns, extreme ET and multi-modal flow paths from ground surface down to the water table interface. The UZR therefore needs to be re-wetted after the dry season before field capacity in both partitions is achieved and the UZR operate as a temporary reservoir system.

4.4.2.1. The Upper Unsaturated Zone Reservoir (Including the Rooting Zone).

The thickness of plant rooting systems is generally a factor of the soil/regolith thickness above the underlying hard rock sub-outcrop (Figure 4.9).

Fractured hard rock terrains have very limited soil/regolith dressings; therefore vegetation is limited to scrubs, but mostly grass (Chow 1964). Although the rooting systems of the savanna type vegetation are well developed, the hard rock profile and the cyclicity in the

rainfall patterns tend to limit their root depths considerably. These plants go into a complete rest period during the winter season and may even die-out during a prolonged dry period. Hence, a new re-growth is required once the field capacity is partially/fully restored during a wet season (Figure 4.9).



Figure 4.9. Character of the rooting zone (brownish, soil zone: ≈ 0.75 m) and underlying regolith (> 1.5 m) on the side of a rivulet in the Nuweveld Mountains, District Beaufort West.

Photographic presentations from the Soil Studies Booklet of the Soil Conservation Group (Department of Agricultural Development 1991) indicates only limited root systems below 0.6 m from ground surface in soil profiles studied in semi-arid regions. During this study, some images taken from recently incised drainages illustrate this phenomenon quite

clearly (Figure 4.9). DTH-CC image logging also conforms relative shallow rooting development, although in local tree populated spots, roots were noted reaching the water table interface deeper than 6 m bgl. These are man-made cases whereby boreholes may act as free pathways down to the water table interface close to tree populations.

Although the UUZR in semi-arid fractured hard rock terrains is limited (<1 m) it acts as an effective interceptor of surplus rainwater. The storage capacity is limited, and any moisture excess above this zone's field capacity is assumed to drain out of the UUZR and thus bypassing the rooting zone's ET capture. This process, due to the limited thickness of the UZR's upper portion at hard rock terrains, may take place within a day (Willemink 1988). This surplus rainwater now enters the lower portion of the UZR (LUZR) and initiates downward percolation (viz. R_{PR}/R_{RM}).

4.4.2.2. The Lower Unsaturated Zone Reservoir (Excluding the Rooting Zone)

The LUZR drives the rainwater not taken up by (i) surface run-off, (ii) E from depression storage and (iii) the T from the UUZR. The surplus represents effective rainwater in excess of field capacity in the UUZR and bypasses the rooting zone the next time infiltrated recharge-producing rainfall surplus drains into the rooting zone from above, i.e. piston flow regime.

Vertical flow through the LUZR, especially in the case of fractured hard rock conditions can at best be described as a multi-modal regime. Water at the lower part of the UUZR is released (i) either deeper into the unsaturated profile, or (ii) directly into the SZ. Depending on the hard rock type and its degree of fracturing and weathering, this flow can be on the one hand (i) piston type flow, or on the other hand (ii) a bypass (macro pore) flows.

In the case of inherently fractured hard rocks like the Ordovician-Silurian TMG ortho-quartzite's, one can expect a significant short lag time (probably hours to days) between an effective rainfall event and a water table rebound (Van Tonder and Bean 2003).

Fractured and weathered hard rocks with some primary porosity, or being micro jointed like the Karoo Basin sediments, will report much differently and could be a site specific characteristic in terms of groundwater recharge estimations.

4.5. BASIC HYDRAULIC CONCEPT OF UNCONFINED GROUNDWATER FLOW.

The southern African aquifer systems, as mentioned, can be defined as local (10 to 100 km²) groundwater units with limited lateral interconnectivity and highly variable rock matrix hydraulic properties.

In the case of fractured porous hard rocks, the hydraulic characteristics are quite unique in the sense that fracture hydraulics is quantified by their dimensions (aperture, length and width), their location (orientation and spacing) and the nature of the fracture (wall roughness, secondary filling and weathering). The rock matrix, on the other hand, is characterized by its pore sizes, effective porosity distribution, which quantifies effective porosity (n) and hydraulic conductivity (K) (Cook 2003).

The local flow regime from ground surface through the UZR is based on the principle of discrete flow via a zone of (i) vertical downflow, followed by constant horizontal flow via (ii) a zone of lateral base flow and finally ends in (iii) a terminal base drainage (Mazor 1997). He concluded that the flow regime between recharge and discharge points resembles a model of L-shape through-flow path. This model describes the characteristic shallow (≤ 45 m) aquifer systems in Southern Africa, where an upper fractured and weathered flow zone overlies a sparsely fractured (>45 m to 100 m) zone, with the latter partially encapsulating an even deeper (>100 m), reserved and almost stagnant fractured aquifer system.

4.5.1. *Physics of Groundwater Flow: Darcy Principle.*

Henry Darcy's experiments with water transitory through porous media shows that quantity of flow (Q , m³·d⁻¹) are direct proportional to the hydraulic coefficient, (K , m·d⁻¹), a specified flow area (A , m²) and the hydraulic gradient (dh/dl) and is expressed as

$$Q = -KA \left(\frac{dh}{dl} \right) \quad (4-5-1)$$

Groundwater flow is a function of time and space and therefore the governing flow is usually described by partial differential equations, in which a 3-dimensional coordinates x , y and z , with time t are dependent. The effect of pressure differences, elevation difference, and hydraulic character of the unconfined medium generates a time and space related

groundwater potential which drives water from a higher to a lower potential; thus acting of a unit mass of groundwater (Walton 1970).

Groundwater-velocity, or Darcy velocity is defined as volume of discharge per unit measure of a bulk area (including space and solids) per unit of time (McWhorter and Sunada 1977; Wang and Anderson 1982; Fetter 1988). In the one-dimensional domain, the groundwater velocity (v^{36} , seepage velocity), is defined as

$$v = \frac{Q}{A} = -K \frac{dh}{dl}. \quad (4-5-2)$$

Application of the Darcy flow concept in unconfined aquifers (gravity flow) is complicated by the condition that the upper boundary of the flow domain be represented by a plane with different hydraulic gradient, viz. the water table interface $h(x,t)$ (Fetter 1989 and Figure 4.10).

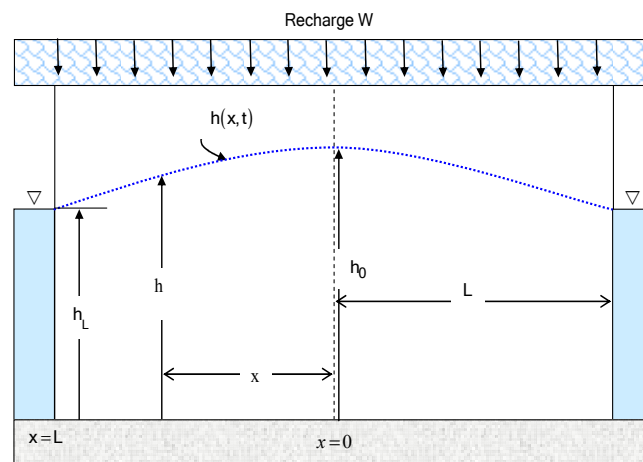


Figure 4.10. Groundwater flow conditions with vertical accretion due to infiltration in an unconfined (gravity flow) aquifer resting on a horizontal, impervious basement.

The saturated thickness (h , meters) of the unconfined aquifer varies, in contrast with the confined aquifer conditions where the aquifer thickness (b , meters) remains relatively constant in space.

³⁶ Seepage velocity is the average velocity of any fluid (water, oil or gas) through the rock matrix pores/channels.

The problem was solved by Dupuit³⁷ (cited in Muskat 1946; Fetter 1988), hence the groundwater flow per unit width (q' , $\text{m}^3\cdot\text{d}^{-1}$) of a gravity flow system can be approximated by

$$q' = -K \frac{dh}{dx} \quad (4-5-3)$$

where: K is the hydraulic conductivity ($\text{m}\cdot\text{d}^{-1}$), and dh/dx represents the water table gradient between any two points in the flow domain, e.g. h_0 and h_L (Figure 4.10).

To derive estimates for the total lateral flow Q_x over the water table elevation h_x (as a function of x above the aquifer basement) in a one-dimensional unconfined flow model, Q_x and h_x can be solved by integration of Eq. 4-5-3 over the following boundary conditions as per Figure 4.10,

- A discharge boundary [\Rightarrow], $x = L$ & $h = h_L$ and
- A recharge boundary [\Downarrow], $x = 0$ & $h = h_0$, thus

the Dupuit-Forchheimer³⁸ approximation $\left(q' = -Kh \frac{dh}{dx}\right)$ gives $\int_0^L Q dx = -K \int_{h_0}^{h_L} h dh$ and yields the following expression in terms of the total discharge Q_x to the flow boundary i.e.

$$Q_x = -\frac{K}{2L} (h_0^2 - h_L^2). \quad (4-5-4)$$

Consequently, the water table elevation $h(x)$ can be approximated at any point between $x = 0$ and $x = L$ by integrating the Dupuit-Forchheimer approximation

$$-\frac{1}{K} \int_0^x q' dx = \int_{h_0}^h h dh \quad (4-5-5)$$

which yields an expression for the water table h at any point between h_0 and h_L ,

$$h = \sqrt{h_0^2 - x \frac{(h_0^2 - h_L^2)}{L}}. \quad (4-5-6)$$

³⁷ Dupuit's assumptions for gravity (unconfined) flow conditions (i) hydraulic gradient equal to the water table slope and (ii) equi-potential lines are perpendicular to base boundary of the aquifer.

³⁸ Dupuit's assumptions valid for unconfined flow conditions in a radial system which was transferred by Forchheimer to a general equation for the free surface of any unconfined, or gravity flow regime (Dupuit-Forchheimer theory; cited in Muskat 1946).

The semi-arid climatic conditions at the experimental monitoring terrains do not comply with the steady-state flow regime in time, as the actual recharge input is episodic in nature. The vertical accretion (recharge-producing rainfall surplus input) in these cases is episodic in space and time; thus both h_0 (Eq. 4-5-4 and Figure 4-10) and Q (Eq. 4-5-4) varies significantly over time. With dedicated hydrological monitoring of the water table interface versus rainwater infiltration, over shorter periods, it will be able to observe the dimensions of water table accretions within a quasi-steady state period.

4.5.2. Hydraulic Concepts of a Water Table Accretion Case.

A small control volume (cell) of an unconfined aquifer system illustrated in Figure 4-11 will have the shape of a prism with the dimensions $dx \cdot dy \cdot dh$.

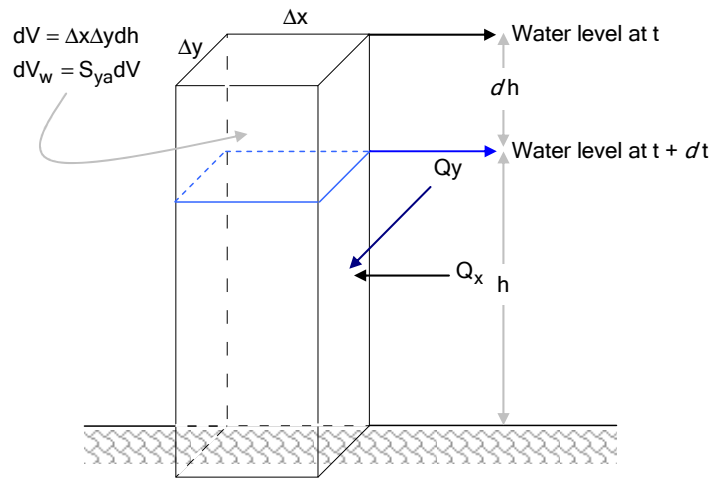


Figure 4.11. Control volume to simulate the gravity flow conditions in an unconfined aquifer with a horizontal impervious basement and dipping water table plane on top.

The saturated thickness, indicated by h , slopes in the direction of the groundwater flow (dx). Considering that the flow through the cell is in the x -direction only, the total groundwater inflow is described by Fetter (1988) as

$$q'_x dy = -K \left(h \frac{\partial h}{\partial x} \right)_x dy \quad (4-5-7)$$

The total outflow from the cell, q'_{x+dx} is:

$$q'_{x+dx} dy = -K \left(h \frac{\partial h}{\partial x} \right)_{x+dx} dy \quad (4-5-8)$$

The flow condition described by Eq. 4-5-8 simulates a steady state condition. Due to the water table gradient between the two faces (high to low), $\left(h \frac{\partial h}{\partial x}\right)$ is different at the in- and outflow faces. The change in the flow rate over dx (viz. the x -direction) is given by (Fetter 1988),

$$(q'_{x+dx} - q'_x) dy = -K \frac{\partial}{\partial x} \left(h \frac{\partial h}{\partial x} \right) dx dy \quad (4-5-9)$$

Any change in the inflow-outflow mass (water content) through the cell must be equal to a gain (viz. R_R) and loss (viz. ET). If $dx \times dy$ donates the basement of the cell, and R_R is the recharge rate, the volume change in the cell is $R_R \times dx \times dy$ and is given by

$$R_R \cdot dx dy = -K \frac{\partial}{\partial x} \left(h \frac{\partial h}{\partial x} \right) dx dy - K \frac{\partial}{\partial y} \left(h \frac{\partial h}{\partial y} \right) dy dx \quad (4-5-10)$$

which now includes the flow rate change in the y -direction (dy).

Both Fetter (1988) and Gieske (1992) refined Eq. 4-5-10 and presented a steady state expression for unconfined flow accretion

$$\frac{K}{2} \cdot \frac{d^2(h^2)}{dx^2} + R_R = 0 \quad (4-5-11)$$

With reference to the model presented in Figure 4.10, Gieske (1992) demonstrates that by

- (i) accepting the Dupuit Approximation and (ii) the flow regime described by the Boussinesq equation (McWhorter and Sunada 1977):

$$\frac{\partial^2 h}{\partial x^2} + \frac{\partial^2 h}{\partial y^2} + \frac{R_R}{K} = \left(\frac{S_y}{K} \right) \left(\frac{\partial h}{\partial t} \right), \quad (4-5-12)$$

two expressions describing the hydraulic concepts of infiltration in unconfined aquifer systems, (a) for steady-state conditions with $S_y \partial h / \partial t \approx 0$, and (b) when there is no recharge, thus $R_R = 0$. The boundary conditions in a two-dimensional model is given by $h(x, t) = 0$ and $x = 0$ and L respectively (Figure 4-10).

Gieske (1992) presents the basic equation for hydrogeological conditions in Botswana, as follows:

$$\frac{K}{2} \frac{\partial^2 (h^2)}{\partial x^2} + R_R = S_y \frac{\partial h}{\partial t}, \quad (4-5-13)$$

with $h(0,t) = 0$ and $h(2L,t) = 0$, and K is hydraulic conductivity ($m \cdot d^{-1}$), h is phreatic head (m), R_R is the recharge ($mm \cdot d^{-1}$) and S_y is the specific yield of the unconfined aquifer system. Eq. 4-5-13 can be used in two ways to derive expressions which can be used for calculate (i) the maximum water table rebound on an aquifer receiving direct recharge (a hard rock terrain) and (ii) the water table recession immediately after a recharge event.

Although certain constants in the derivatives of Eq. 4-5-13 are difficult to estimate without costly field investigations, observations of the state variables (time-series) such as rainfall input, water table responses and time lags between rainwater and groundwater events provide some of the unknown parameters otherwise depending on indirect assumptions through extrapolation/interpolation. Two manipulations of Eq. 4-5-13 will be demonstrated here:

- (a) The steady state condition with $S_y(\partial h / \partial t) = 0$; thus applying the boundary conditions in Figure 4.10 becomes

$$h(x)^2 = \frac{R_R}{K} \cdot (2L - x)x; \quad (4-5-14)$$

In the centre of the recharge terrain, i.e. the hard rock window area, where according to the reservoir model in Figure 4.10, $x = L$, an expression for the maximum head (H) is obtained, viz. $H = L\sqrt{R_R/K}$.

Observations in Botswana by Gieske (1992), gives values around 50 m which is much higher than the calculated (<20 m) maximum heads estimated at some of the hard rock monitoring terrains in South Africa. These values were tested against the hydrological state variables and parameters generated by the monitoring programmes developed for this study. The reason for these differences lies in the size of the exposed hard rock terrain ($L < 2000$ m) and specifically, effective recharge ($R_R < 10 \text{ mm} \cdot \text{yr}^{-1}$). Whereas the effec-

tive recharged used in Botswana was $20 \text{ mm} \cdot \text{yr}^{-1}$, the one used for the Karoo environment was $\approx 8 \text{ mm} \cdot \text{yr}^{-1}$.

- (b) For the second case, the recharge $R_R = 0$; thus Eq. 4.5-13 was solved by Boussinesq in 1904 (cited in Gieske 1992) in terms of $h(x, t)$ and becomes

$$h(L, t) = h_0(L) \left(1 - t \left(\frac{\beta K h_0(L)}{S_y \cdot L^2} \right) \right). \quad (4-5-15)$$

In the latter case where $R_R = 0$, the condition as with (a) above will change to a recession condition in the groundwater mound and the hydrograph will respond with a falling water table trend which may last for a few months, or even several years. In the case of the Taai-boschgroet area, one recession period was almost six (6) years. This recession rate, expressed as dh/dt is proposed by Gieske (1992) as

$$\frac{dh}{dt} = - \frac{\beta K h_0^2(L)}{S_y \cdot L^2}. \quad (4-5-16)$$

Values for dh/dt can be obtained from hydrograph recession curves ($\text{m} \cdot \text{yr}^{-1}$) from long-term, dry-condition ($R_{\text{eff}} = 0 = R_R$) water level time-series data. The recession rates are only possible in remote regions, given that long-term groundwater table observations are collated. The expression in Eq. 4-5-16 indicates that the natural groundwater recession dh/dt , is inversely proportional to the specific yield, S_y (Gieske 1992).

These expressions will be applied in Chapter 6 to illustrate the applicability of analytical problem solving in hard rock recharge estimations.

4.5.3. Recharge Concept of a Simple (groundwater) Reservoir Model.

The model proposed by Willemink (1988) to subdivide the total unsaturated zone into a series of linear, linked sub-reservoirs is probably the most practical conceptual approach in the case of semi-arid hard rock terrains. Four (4) linear reservoirs in a vertical configuration and one (1) lateral receiving sub-reservoir are visualized and illustrated in Figure 4.12.

The concept displayed in Figure 4.12 comprises of the following intermittent components:

- ①: Rainwater storage at ground surface from where surface run-off (Q_{RUN}) takes place in the case of a heavy rainfall/condition;
- ②: UUZR receiving rainwater through the underdrainage system. This zone represents the rooting and ET zone from where a variable portion of the recharged rainwater escapes the underdrainage system as water vapor. In this zone the CMB concept is developed and sustained under medium-term rainfall regimes.

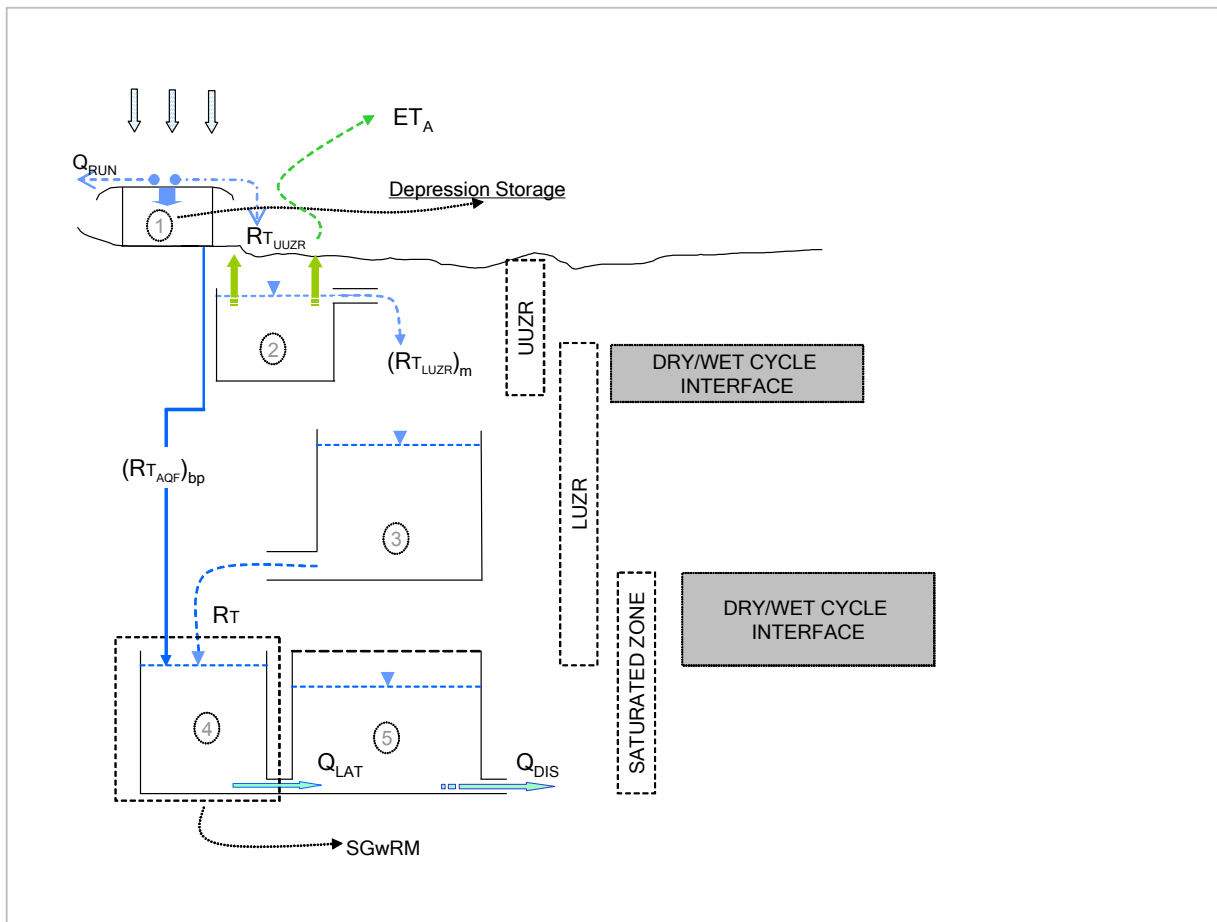


Figure 4.12. The relationship between receiving and discharging sub-reservoirs of a total groundwater recharge model in fractured hard rock terrains (modified after Willemink 1988).

- ③: The LUZR represents the unsaturated zone below the base of the rooting zone and the water table interface. It receives the residue of the total infiltrated rainwater, or the re-charge-producing rainfall surplus. The thickness of this zone varies over time as the phreatic aquifer goes through different phases of saturation. In fractured hard rock cases,

the LUZR contain the bypass flow network consisting of an array of joints/fractures. The LUZR was thoroughly observed by means of DTH-CC image logging and found to be notably dry, especially at the start of a new HC (Oct_n).

④: Representing the final phase of the direct vertical flux component in the LUZR as the recharge now starts building the recharge mound. Lateral flux (Q_{LAT}) is generated by the additional water head created by recharge mound and with the SDR flux control feeding into the surrounding sub-reservoirs (⑤). Q_{DIS} represents the final discharge from the total aquifer system either through base flow or spring flow support (or activated by abstraction).

Depending on the water budget losses in storage zones ① and ②, and the field capacity availability/retention in ③, storage zone ④ will get recharged via macro pore bypass flow and/or matrix flow through the bulk, rock formation above the water table interface. The effective porosity of the rock matrix and/or micro-fracture status, will govern the recharge flux.

Storage reservoir ④ represents the interface between what is recharged from the unsaturated zone and finally leaves the direct recharge area according to the simple L-shaped flow regime proposed by Mazor (1997).

Observations by Ernst (cited in De Vries 1974; Gieske 1992) propose a simple approach for complex aquifer systems with uniform thickness, and introduces a constant (α)³⁹ and a parameter (W) which gives an approximation for the groundwater recharge (R_R)

$$R_R = \frac{h}{W} + \alpha S_y \frac{dh}{dt}, \quad (4-5-17)$$

where W is called the total drainage resistance by Ernst (cited in Gieske 1992, p. 171) or specific drainage resistance (SDR) by De Vries (1974; 2000). They introduce a Simple (groundwater) Reservoir Model (SGWRM) with a storage coefficient S and an outlet drainage resistance αW which is described by Eq. 4-5-17 (Gieske 1992, p. 171). Under steady state conditions the solution of Eq. 4-5-17 is

³⁹ For parabolic water table interface, $\alpha \geq 2/3$ to an almost flat water table interface where $\alpha \leq 1$ (Gieske 1992, p.171).

$$h_0 = R_R \cdot W. \quad (4-5-18)$$

With reference to Dupuit's assumption (Eq. 4-5-13) and Figure 4.10, a groundwater recharge event will produce a maximum water table height (H, meters above baseline) in the SGwRM which depends on the recharge R_R ($\text{mm} \cdot \text{T}^{-1}$), the hydraulic conductivity K ($\text{m} \cdot \text{T}^{-1}$) and the SGwRM dimension, L (L).

Under no recharge conditions, i.e. when $R_R=0$, the water table tends to stabilize. Soon after ET and field capacity retention in storage zones ② and ③ respectively, prevents further replenishment of the SGwRM (storage zone ④), the water table starts with a recession phase which may last for several months/years until the next recharge event exceeds the ET losses in Zone ② and field capacity requirements in Zone ③.

Studies by Thiery (cited in Gieske 1992, p.171) using Eq. 4-5-17 as the governing equation for the SGwRM, defines the recession rate as

$$\frac{dh}{dt} = -h \cdot \frac{1}{\alpha S_y} \cdot W. \quad (4-5-19)$$

The SGwRM, with $\alpha = 1$, now provide an expression for the recession rate dh/dt given a long-term mean annual recharge (Eq. 4-5-18) is proposed by Gieske (1992) as:

$$\frac{dh}{dt} = -\frac{R_R}{S_y} \quad (4-5-20)$$

Dedicated monitoring of the groundwater recession rate at the hard rock terrains can now be used with groundwater hydrogeochemical information to estimate specific yields (S_y) for various hard rock terrains where rainwater data is not available.

4.6. SUMMARY.

Ground surface conditions in the semi-arid regions characteristically portray a relatively thin soil/regolith horizon. Hard rock terrains occurs frequently as low relief mounds surrounded by a low gradient rolling topography where the soil/regolith horizon reach its maximum thickness in valley floors.

Southern Africa, through its geological history beginning as far back from the Swazian Era (pre 3100 Ma) has been subjected to intense folding/fracturing during several tectonic cycles of which the Gondwanaland Break-up (~140 Ma) created an intensely jointed/fractured palaeo landscape. Two continental uplifts removed much of the Neogene Period (~24 Ma) landscape which was characterized by relatively deep weathering and prominent soil horizons. The semi-arid region of southern Africa was initiated exposing the underlying fractured hard rock characteristics.

The fractured hard rock terrains portrays an array of joints/fractures that act as flow paths for excess rainwater after interception, surface run-off, and depression storage capturing at ground surface. Due to the lithology and fracture composition, the flow regime through the unsaturated zone is probably of a multi-modal nature; varying from mostly macro fracture flow (crystalline and metamorphic rocks) to a combination of macro fracture bypass flows and micro fracture/porous rock matrix diffuse flow (viz. arenaceous and argillaceous sediments).

Describing unsaturated flow regimes in the fractured hard rock terrains is complex. Because of characteristic episodic recharge events and hard rock profiles, observations in the unsaturated zone are not feasible. Mathematical expressions describing the water table rebound during recharge events and subsequent water table recession during the dry seasons, allows evaluation of episodic recharge events, which will be supported presently with hydrogeochemical information.

These simplifications are difficult to apply especially in the medium/long-term context as R_R is an episodic event occurring over short periods. The multi-modal flow regime in fractured hard rock terrains is not specifically steady-state recharge conditions, but merely a pulsating response induced by a once-off extraordinary rainfall/recharge event. The UZR_s react differently in the semi-arid environment compared to a humid environment where field capacity in the UZR remains almost constant throughout the HC.

oooOOOooo

5. HYDROGEOCHEMICAL FEATURES OF THE RECHARGE CYCLE.

The groundwater recharge cycle is well imprinted in the HC and represents roughly 0.61% of the world's total free water volume of 1.3 Billion km³. Earth's fresh water component is almost 2.8% of the total free water volume, and groundwater accounts for 22%. Groundwater component is estimated at 40 times more than the surface water contained naturally and artificially by mankind's intervention (Miller 1994).

Subterranean flow duration is many orders of magnitude longer than the flowing surface water components, especially in confined aquifers, where to some extent groundwater can be classified as trapped, thus stagnant. In the UFWZ of the hydrogeological profile, groundwater fluxes are considered to be much more dynamic than the deeper portions of the flow regime, and report rather quickly as baseflow in surface water systems.

Infiltrating rainwater represents the most dynamic entity of the groundwater hydro-cycle as it is deposited in various quantities, each with a traceable hydrogeochemical composition. According to Fetter (1988) 0.001% (1.3E⁶ km³) circulates in the atmosphere at any given time.

5.1 RAINWATER HYDROCHEMISTRY.

5.1.1 *Analytical Criteria.*

Rainwater samples were collected in bulk format with the DWA rainfall logger/sampler unit during the logic-sampling intervals. Rainwater samples from the RES-units were sampled during episodic rain events, and provide a unique range of rainwater analytical data. These samples are then correlated with the RES's associated rainfall logger/bulk sampling unit (situated within a few meters from the RES-unit).

Full ionic (macro)-analyses of the sampled rainwater, unfortunately, is not available for both summer and winter rainfall regions due to costs and limited application. In most cases high-level analytical processes were applied due to the low rainwater Cl⁻ concentration levels in the episodic rainwaters (0.1 mg·ℓ⁻¹, tolerances are required for CMB application).

The hydrochemical composition of rainwater samples was determined by three (3) laboratories in South Africa, namely:

- CSIR's, Air Quality Research Laboratory (AQRL) for low level inorganic constituents (Na^+ , Cl^- , NO_3^- -N, SO_4^{2-} , F^- and PO_4^-), with a typical low level detection range of $0.1 \text{ mg}\cdot\ell^{-1}$ for Cl^- ;
- CSIR's, Consulting and Analytical Services Water Chemistry Laboratory (ASWCL) for high level inorganic constituents (Na^+ , Ca^{2+} , Mg^{2+} and HCO_3^- , Cl^- , SO_4^{2-} , NO_3^- -N and F^-), with typical low level detection range of $5.0 \text{ mg}\cdot\ell^{-1}$ for Cl^- ; and
- The DWA's Roodeplaat Laboratory for high level inorganic constituents (K^+ , Na^+ , Ca^{2+} , Mg^{2+} and HCO_3^- , Cl^- , SO_4^{2-} , NO_3^- -N, PO_4^- and NH_4^+), with low level detection ranges of $0.5 \text{ mg}\cdot\ell^{-1}$ for Cl^- .

Although DWA's Roodeplaat and CSIR's ASWCL did more comprehensive analyses on the rainwater samples, the analytical tolerances for Na^+ ($0.8 \text{ mg}\cdot\ell^{-1}$), Ca^{2+} ($0.4 \text{ mg}\cdot\ell^{-1}$), Mg^{2+} ($0.3 \text{ mg}\cdot\ell^{-1}$), Cl^- ($5.0 \text{ mg}\cdot\ell^{-1}$) and SO_4^{2-} ($5.0 \text{ mg}\cdot\ell^{-1}$) are just too high for rainwater quality assessments. For establishing the groundwater hydrochemical composition, the LLHc analytical tolerances are applicable.

A logic sampling interval is followed, due to the remoteness⁴⁰ of some of the monitoring sites i.e. early summer (Oct_n to Dec_n), peak summer (Jan_{n+1} to Mar_{n+1}), early winter (Apr_{n+1} to Jun_{n+1}) and finally dry winter (Jul_{n+1} to Sep_{n+1}). In some remote regions, only two sampling seasons were established, i.e. a summer interval (Oct_n to Mar_{n+1}) and a winter interval (Apr_{n+1} to Sep_{n+1}).

Environmental (radiogenic and stable) isotopes analyses were conducted on samples collected under specialized monitoring conditions. This data and especially the stable isotopes of Oxygen (^{18}O) and Hydrogen (^2H) form a substantial part of this script as it was used (i) for testing the endurance of the rainwater sampler/logger unit for evaporation and (ii) tracing episodic rain events with a particular stable isotope signal at the water table interface.

⁴⁰ Some monitoring terrains are specifically located in remote areas where hard-rock windows demarcate potential recharge zones.

All environmental isotope analyses were conducted by two specialist laboratories in South Africa, namely:

- CSIR's QUADRU Physics Laboratory in Pretoria for (^{18}O) - Oxygen and (^2H) - Hydrogen analyses and
- iThemba LABS, University of the Witwatersrand in Johannesburg for radiogenic isotopes ^3H - Tritium and (^{14}C) - radio-carbon. This laboratory is also used as a backup for stable isotope analyses and comparison.

5.1.2 Terrigenous Dust and Airborne Pollution.

Rainwater, as collected in the various samplers used in chloride-recharge studies, always contains a certain percentage of dust particles. It is therefore normal to find a layer of sediment in the pipes and sumps of rainwater sampling devices, which may also probably include a large portion of terrigenous dust⁴¹ originating from local and/or distant sources.

The arid homoclimate region, due to its intense dryness almost 80% of the year, produces immense amounts of dust which get integrated into the circulating air masses. Low-level wind runs are extremely powerful erosion agents and can lift superficial matter and aerated ocean water into transcontinental jet streams thereby charging air masses with high loadings in soil dust particles. These loads are referenced as the terrigenous contribution to rainwater chemistry composition (Mphepya et al. 2004; Mphepya et al. 2006; Galy-Lacaux et al. 2008).

Superficial terrigenous particles are supplied from (i) natural and (ii) anthropogenic sources, of which the latter can be highly variable due to land use activities at the monitoring sites.

Natural Sources of Terrigenous Dust: Lithosphere.

Natural sources of dust particles in the atmosphere can be the result of erosion processes in the superficial lithosphere producing terrigenous dust swept up by prevailing wind runs. Deposition of the heavier particles can be within a few hundreds of meters as ob-

⁴¹ In African semi-arid regions with rainwater generated via the ITCZ, the original marine hydrochemistry contribution gets muddled and may finally account for only 10% to 13% of the total rainwater hydrochemical composition (Galy-Lacaux et al. 2008).

served with the formation of numerous southeasterly sand dunes in the Kalahari Basin (Figure 5.1).

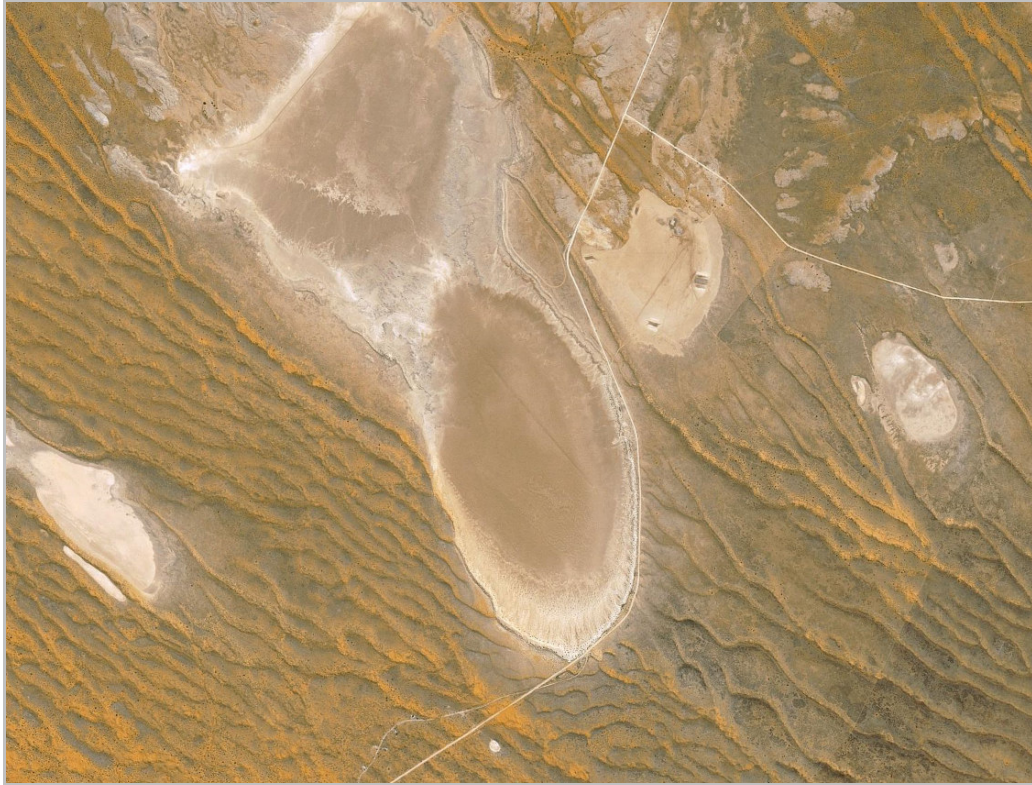


Figure 5.1. Satellite image of a typical pan system in the northern Kalahari region showing a Lunette dune system as described by Lancaster (1988).

The southeastern part of the pan perimeter is distinguished by high (10-15 m) whitish Lunette type dunes described by Lancaster (1988). Pan floor sediments, consisting of Kalahari Group limestones are mobilized by northwesterly trade winds. The heavier sand portion remains as mobilized dunes (The Rooi Pan: S26.671534°; E020.156052°, 826 m amsl)

The interior southern African semi-arid region is known for high ET_A levels. From a satellite view, a substantial number of depressions (pans) are visible which fall right in the migration zone of the traditional summer rainfall pathway. Some pans contain highly mineralized basements (pan floor deposits) fed by mineralized groundwater naturally discharged by

sun pond conditions; such as the salt pans in the Central Kalahari Basin of the Northern Cape Province.

The parent rock basements of these pans are Quaternary limestone (Kalahari calcretes) and a lesser occurrence of silcretes. The Hammada Plains of the Etosha Pan is a good example of bare eroded Kalahari calcretes which apparently cover large areas⁴² of the semi-arid region and are originally groundwater driven evaporates (Grunert 2003). The abundance of $\text{Ca}^{2+}\text{Mg}^{2+} - \text{HCO}_3^-$ dust is therefore significant.

The ionic concentrations of rainwater studied in the Sahelian region of Niger reported elevated levels of dissolved calcium and carbonates (calcite), and constitute about 40% of the total ionic charge of the Central African precipitation (Galy-Lacaux et al. 2008).

Anthropogenic Sources.

Since the discovery of fire, man has polluted the atmosphere with noxious gasses and soot (Masterton and Slowinski 1977). The composition of the aerosol load in the atmosphere over southern Africa has been found to consist of a composition of industrial dust, aeolian dust, biomass burnings, in addition to the natural background emissions from the oceans (Mphepya et al. 2004; Mphepya et al. 2006; Reason et al. 2006).

The Southern African Regional Science Initiative 2000 (SAFARI, 2000) has identified a significant air transport flow path over the subcontinent and reported that air masses from Zambia transport visible quantities of aerosols and trace gasses from biomass burning southward over the northeastern parts of southern Africa. Remote sensing investigations showed that a River of Smoke dominates the southern African atmospheric circulation especially in the late winter period, linking emissions from as far north as 10°S to the rest of southern Africa as reported by McGill (cited in Reason et al. 2006).

On local scale, it is a known fact that air masses close to areas with high industrial dust and smoke discharges get tagged by the emission's chemical signature. One particular example is the generation of acid rainfall (<5 pH) not only due to natural carbonic acid or

⁴² One-Third ($\frac{1}{3}$) of Namibia is covered by calcrete deposits (Grünert 2003).

CO₂ levels, but building a significant H₂SO₄ composition from SO₄ releases in coal fire furnaces containing iron pyrite (FeS₂) as reported by Mphepya et al. (2004; 2006).

Airborne aerosol contamination of air masses over the semi-arid regions of southern Africa has been proved by analyses of aerosol levels in the Okavango Delta in Botswana. It has been reported (Reason et al, 2006) that aerosols account for 52% of the required phosphates and 30% of the nitrates of this ecosystem.

5.1.3 *Hydrochemical Properties: Summer Rainwater.*

5.1.3.1 Hydrochemical Composition.

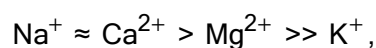
The origin of summer rainstorms in southern Africa is predominantly central Indian and occasionally Atlantic Ocean evaporated maritime water with a wide-ranging dose of terrigenous substances introduced into the atmospheric moisture column (Rouault et al. 2003; Mphepya et al. 2004; Mphepya et al. 2006). The composition is altered by consecutive tropic/sub-tropic forests regions rainouts and ET cycles that characterize the rainwater signature (incl. the isotopic composition), hence reporting a dynamic hydrogeochemical composition in time and space (Joseph et al.1992; Mook 2001).

In general, the hydrogeochemical composition of summertime rainwater in southern Africa will be of a depleted nature as the initial maritime/atmospheric moisture undergoes several rainout phases along the continental migration due to fractionation processes.

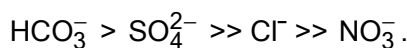
The anthropogenic impacts on the local summer rainwater composition are significant. Rainwater sampled as far west as Beaufort West and north in the Kalahari region (Van Zylsrus) reported occasionally SO₄²⁻ spikes as high as 10 to 15 mg·ℓ⁻¹. The rainwater collected from sampling units close to mining/industrial activities in the Free State, contains elevated levels of SO₄²⁻ (≈25 mg·ℓ⁻¹) and NO₃⁻ (≈44 mg·ℓ⁻¹), probably as a result of local coal burning furnaces and biomass incinerations.

Table 5.1 illustrates a typical summer rainwater composition from three (3) monitoring sites in semi-arid/arid regions of South Africa.

According to the hydrochemical analyses shown in Table 5.1, the summer rainwater displays a cation composition range of:



and an anion composition range of:



$\frac{2}{3}$

The hydrochemical composition of the rainwater collected from these three sites indicates the presence of terrigenous dust particles (high Ca^{2+} and HCO_3^- values). Although the data population is rather small ($n=3$), the regional correlation between high Ca^{2+} and Na^+ is an indication of high terrigenous input into the atmosphere by uplift wind drafts

Table 5.1. Summer rainfall hydrochemical composition ($\text{mg}\cdot\text{l}^{-1}$ and $\mu\text{eq}\cdot\text{l}^{-1}$) in semi-arid/arid regions of South Africa.

Attribute 1	Riemvasmaak		Central Kalahari		Korannaberg (Wit-sand)	
Attribute 2	Summer Period:		Summer Period:		Summer Period:	
<u>Cations</u>	$\text{mg}\cdot\text{l}^{-1}$	$\mu\text{eq}\cdot\text{l}^{-1}$	$\text{mg}\cdot\text{l}^{-1}$	$\mu\text{eq}\cdot\text{l}^{-1}$	$\text{mg}\cdot\text{l}^{-1}$	$\mu\text{eq}\cdot\text{l}^{-1}$
Ca^{2+}	9.9	494	7.3	364	0.0	0.0
Mg^{2+}	2.4	197	2.3	189	1.8	148
Na^+	9.9	431	8.8	383	10.2	444
K^+	0.5	13	0.4	10	0.3	8
<u>Anions</u>						
HCO_3^-	12.66	207	18.41	302	9.7	131
SO_4^{2-}	4.2	87	12.3	256	3.1	65
Cl^-	1.6	45	1.5	42	0.9	25
NO_3^-	1.3	21	2.2	36	<0.05	-
R.E. (%)	$\approx \approx$	1.75	$\approx \approx$	3.83	$\approx \approx$	2.2
R.E.: Reaction error or ionic balance (recommended to be $\leq 5\%$, Mazor 1997)						

The summer, semi-arid rainfall is therefore a $\text{Na}^+ \cdot \text{Ca}^{2+} - \text{HCO}_3^-$ type water, thus indicating a significant contribution from terrigenous dust (high input of Ca^{2+} , Mg^{2+} , K^+ , SO_4^{2-} and HCO_3^-) which can be as high as 52% of the total ionic content (Galy-Lacaux et al. 2008).

The high reaction error (RE) reported in Table 5.1 is probably due to a combination between analytical errors and to a lesser degree, in response to NO_3^- and SO_4^{2-} reduction. Detailed discussions of the summer rainfall region's hydrogeochemistry will follow under Section 6.4 when the rainwater character from the individual monitoring sites will be discussed. The three tier period summer rainfall Cl^- concentrations is reported in Figure 5.2

5.1.4 *Hydrochemical Properties: Winter Rainwater.*

5.1.4.1 Macro element compositions.

The winter rainwater is generated over the southern Atlantic Ocean and occurs as cold, frontal systems which migrate quite deeply into the interior of South Africa. Winter rainfall occurs along the Cape Province's West and South Coast regions during April to September. As described in Section 3.2.2.2, these frontal systems dominate the synoptic pattern of southern Africa, driving cold polar air masses deep over the region and generate sleet and light rainfall. Snowfall in the higher regions, such as the Cape Mountains and the Drakensberg Ranges, occurs from time to time, although the snowfall depths are not spectacular (King 1942).

Chloride, being one of the conservative tracers in the hydrochemistry domain can be used to demonstrate the variability in the winter rainwater composition. Long-term ranges for some of the coastal regions and inland rainfall regions are illustrated in Figure 5.2.

The three West Coast coastal monitoring terrains report almost the same average Cl^- values ($\text{HM} \approx 7.8 \text{ mg} \cdot \text{l}^{-1}$). The impact of terrigenous dust in the winter rainwater is limited to local impacts, i.e. industrial areas like the Cape Town Metropolitan area, as well as the industrial sites in the Langebaan Road area. The topographic higher Sandveld (towards the Cederberg mountains) and Dysselsdorp (towards the Swartberg mountains) areas report lighter hydrogeochemical compositions due to orographic and continental depletion⁴³.

The high-level of seaborne salts, a background characteristic in coastal regions, migrates inland for some distances due to onshore winds/rainfall, but soon becomes depleted as

⁴³ Because of rainout events from onshore areas along the inland, migration of the air mass producing cloud water, the remaining airborne moisture hydrogeochemical composition gets depleted. Mazor (1997).

the result of increasing altitude and hydrochemical fractionation due to consecutive rain-outs.

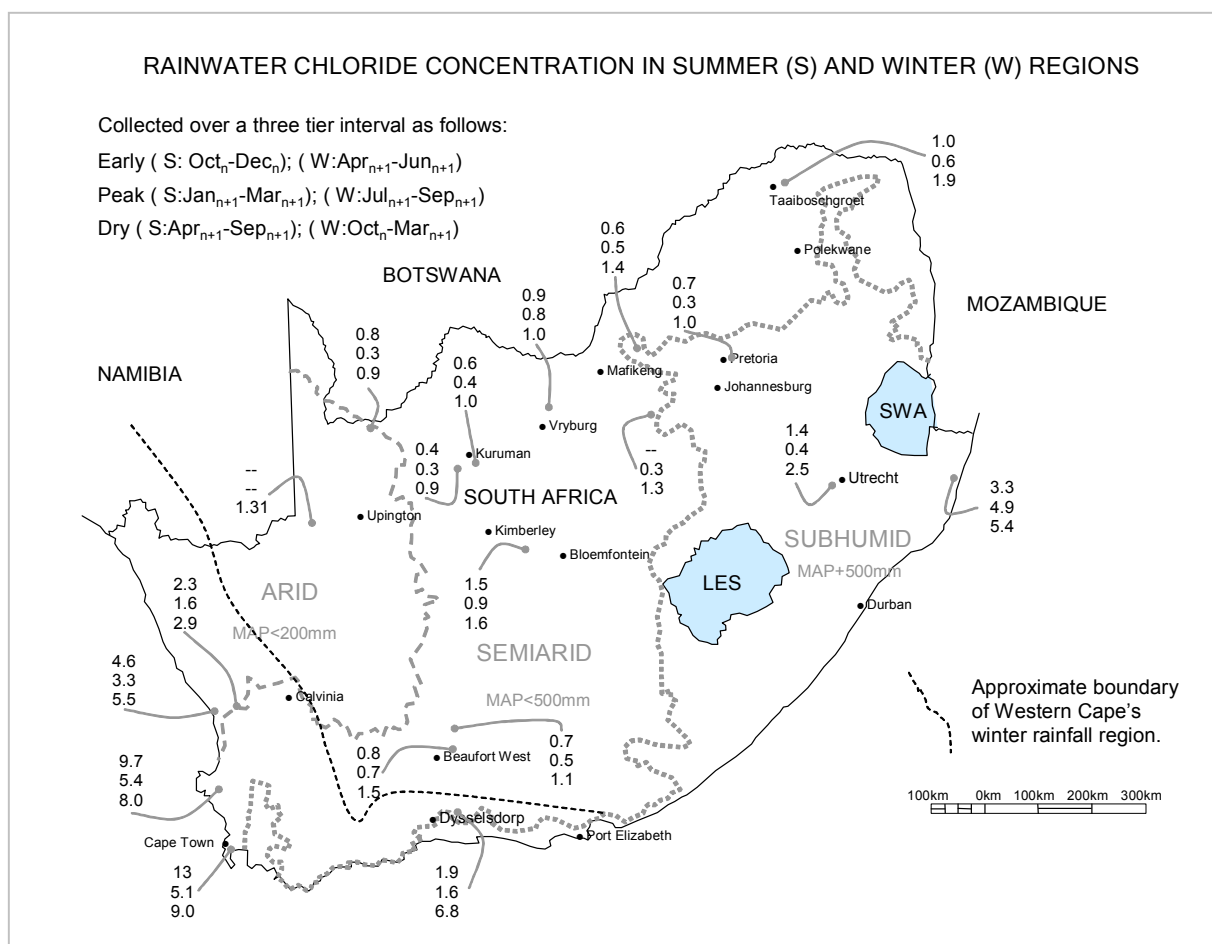


Figure 5.2. The early, peak and dry (HARmean) Cl^- concentrations in rainwater collected during 2003-2006 from summer and winter experimental monitor terrains in South Africa.

Hydrochemical analyses (LLHc) of winter rainwater from three Western Cape monitoring terrains in the winter rainfall region are shown in Table 5.2.

The impact of hydrogeochemical-loaded onshore maritime aerosols present in the atmospheric moisture is a general phenomenon in coastal regions. For example, along the South African North Coast regions, the effect of oceanic aerosols is shown between the onshore rainwater and those orographic rainwater further inland (Utrecht, Figure 5.2). Although this area does not fall in a typical winter rainfall region, the atmospheric processes

and orographic rainfall patterns are the same as in the Western Cape. This maritime moisture is generated by a warm Agulhas Current along the east coast of southern Africa (Rouault et al. 2003).

Table 5.2. Average LLHc compositions ($\text{mg}\cdot\ell^{-1}$ and $\mu\text{eq}\cdot\ell^{-1}$; harmonic means) in the winter rainfall, semi-arid regions of South Africa.

Attribute 1	West Coast Sandveld		Cape Peninsula		West Coast Sandveld	
Attribute 2	Sandveld		Univ. Western Cape		Langebaan Road	
<u>Cations</u>	$\text{mg}\cdot\ell^{-1}$	$\mu\text{eq}\cdot\ell^{-1}$	$\text{mg}\cdot\ell^{-1}$	$\mu\text{eq}\cdot\ell^{-1}$	$\text{mg}\cdot\ell^{-1}$	$\mu\text{eq}\cdot\ell^{-1}$
Na^+	2.1	91	1.7	73	3.0	130
<u>Anions</u>						
Cl^-	3.3	93	7.6	214	8.5	240
SO_4^{2-}	0.1	2	9.1	189	0.4	8
NO_3^-	0.9	3	1.8	6	1.8	6
PO_4^-	<0.05 ^②	-	<0.05 ^②	-	<0.05 ^②	-

Aliquots collected between 2003 and 2006 (Dyson (DWA) and Nel (DWA));

^② Analytical detection level; $0.05\text{ mg}\cdot\ell^{-1}$.

The impact of local industrial pollution is probably the reason for the elevated SO_4^{2-} concentration observed for example in the Cape Town and Langebaan Road areas. A few cases of extreme SO_4^{2-} contributions (20 to $45\text{ mg}\cdot\ell^{-1}$) were observed in rainwater collected at the University of Western Cape monitoring terrain (13 March 2006 to 28 August 2006).

The abundance of Cl^- in the hydrochemical composition as reported in Table 5.2 is evident and is illustrated in Figure 5.3 when for example compared with Na^+ .

The linear relationship between Cl^- and Na^+ (Cl^-/Na^+) in most of the winter rainwater monitoring terrains correlate well ($R^2=0.93$). The ratios for seawater and rainwater are 1.16 and 1.00 respectively as per Keene (cited in Galy-Lacaux et al. 2008). There are indications of Cl^- enrichment in the winter rainwater, though (some points plot on and above the seawater line trend of 1.16). These points are rainwater collected during the dry (Oct_n -

Mar_{n+1}) and early periods (Apr_{n+1} - Jun_{n+1}) and report extremely high Cl⁻ enrichment in relation to Na⁺.

Some of the winter peak rainfall ratios (Jul_n to Sep_n) fall just above the rainwater line which indicates a slight Cl⁻ enrichment. Some data points in Figure 5.3, plot even above the seawater ratio of 1.16 as proposed by Keene (cited in Galy-Lacaux et al. 2008) which is obviously maritime induced aerosols.

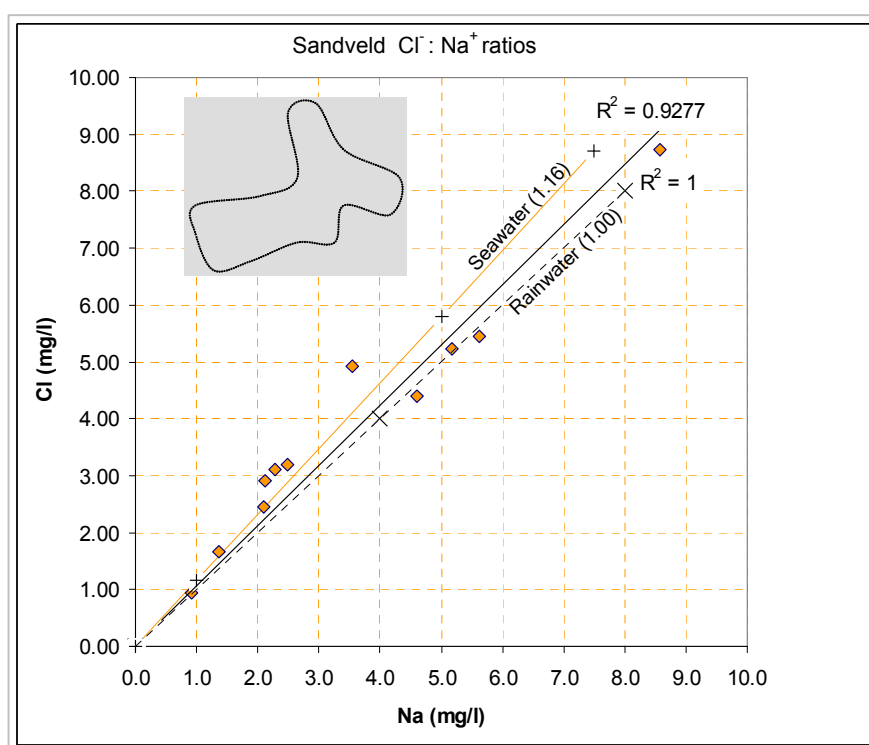


Figure 5.3. Ration between Cl⁻ and Na⁺ from the West Coast winter rainfall region in the Western Cape Province.

Correlation between NO₃⁻ and Cl⁻ emphasizes the abundance of Cl⁻ in the rainwater composition (Figure 5.4). The presence of elevated levels of NO₃⁻ in the winter rainwater is a matter of concern, as the nitrogenous contribution to rainwater hydrochemical compositions originates from a large spectrum of sources (Galy-Lacaux et al. 2008).

The relationship between NO_3^- and Cl^- as illustrated in Figure 5.4, is non-linear; thus an indication of secondary contribution of both constituents in an ad hoc manner. Sources familiar to the West Coast Region, are probably related to intense cash crop (dry land and irrigated cash crops) production which exposes deep soil and waste product burning. Another source of NO_3^- is bird droppings, although the PO_4^- concentration in the samples used in Figure 5.4 are all below detection level ($0.05 \text{ mg}\cdot\ell^{-1}$). This phenomenon indicates that rainwater from the coastal regions is impacted by substances probably relates to the environmental conditions/activities in these areas.

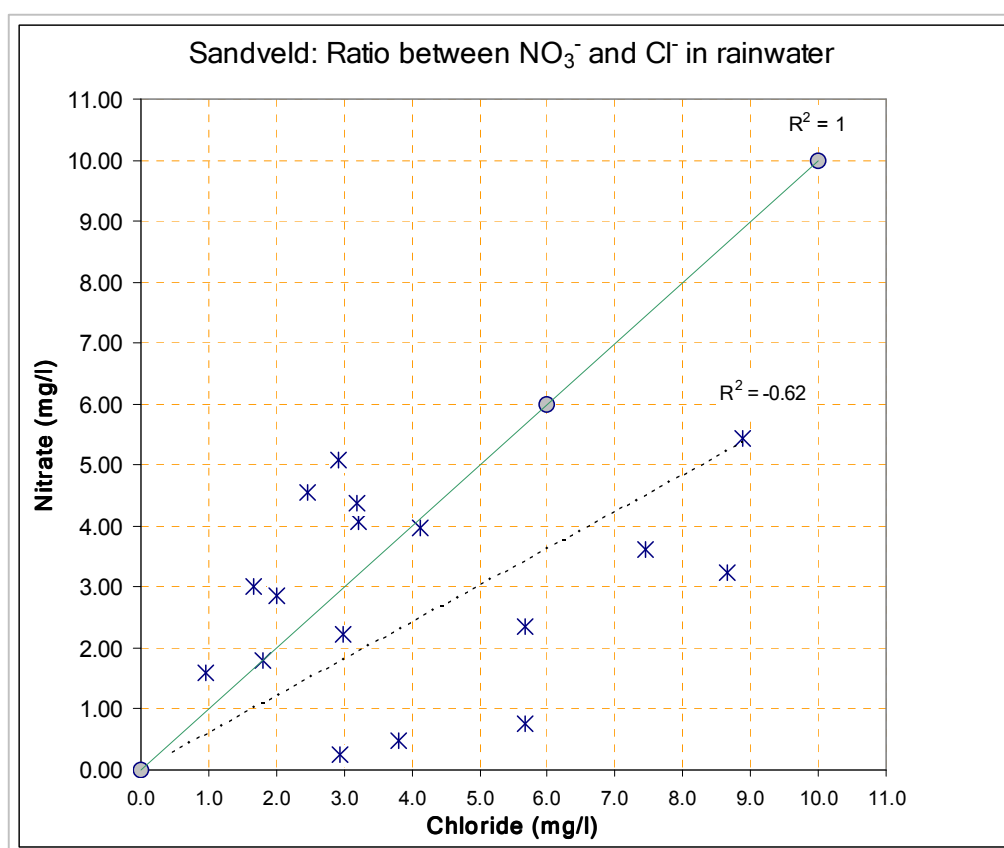


Figure 5.4. Ratio between NO_3^- and Cl^- concentrations in rainwater from the West Coast winter rainfall region in the Western Cape Province.

To conclude, the hydrochemical composition of South African wintertime rainwater is characterized by noticeable higher maritime aerosols, especially NaCl concentrations compared to the summertime rainwater. Nitrogen and sulphate contributions in winter rainwater are significantly less (1:0.17 and 1:0.04 respectively). Seasonal variations in the

hydrochemical composition of winter rainwater are extreme, and unfortunately limit the application of hydrochemical tracing applications like the CMB method, unless detailed, long-term monitoring is performed.

5.1.5 Temporal Responses and Trends.

Assessments of the hydrochemistry information obtained from the national rainwater monitoring network confirm cyclic variations in some constituents (Cl^- and Na^+), including irregular spikes in other constituents (NO_3^- and SO_4^{2-}).

The composition of NO_3^- and SO_4^{2-} are mostly related to natural (savanna soil and animal emissions) and anthropogenic conditions (intensive land use, biomass burning and industrial emissions). Due to this unfortunate condition, no fixed cyclic trend has been observed. In addition, hydrochemical destabilization of the water samples during on site accumulation storage/transport because of chemical reduction processes may also alter their compositions; although precautions are in place to control this process⁴⁴. Spatial variations were observed and will be discussed presently.

Although the range of hydrochemical constituents used in the hydrochemical assessments is biased to the LLHc collection, it is Cl^- in particular that indicates seasonal variations in both summer and winter rainfalls. Being classified as a relatively conservative tracer in hydrological applications, its application as an indicator for seasonal variability is therefore already verified (Mazor 1997).

The driving forces behind these seasonal oscillations are complex, as Cl^- also forms part of the local dry atmospheric input which is relatively elevated in semi-arid environments (Galy-Lacaux et al. 2008). Monitoring of rainwater Cl^- therefore requires high level monitoring protocols and apparatus. It will be shown presently that during the peak summer-time interval's rainwater Cl^- concentration is much lower than during the early wet seasons.

The national rainwater-groundwater monitoring network is illustrated in Figure 5.5. From an initial number of twenty-one (21) monitoring terrains, twelve (12) terrains were selected

⁴⁴ Protection from direct sunlight, extreme heat fluctuations and moisture losses (incl. evaporation).

for long-term monitoring of rainfall quantity and quality to support this study. Each monitoring terrain consists of several monitoring sites having a borehole and associated DWA rainfall logger/sampler unit.

The rainwater hydrochemistry analyses highlights three periods during the HC, each portraying a specific hydrochemical characteristic. The hydrochemical variation of Cl^- specifically, is so prominent depleted in the peak summertime (Jan_{n+1} to Mar_{n+1}) rainwater that this signal is carried as part of the recharge-producing rainfall surplus to the groundwater body.

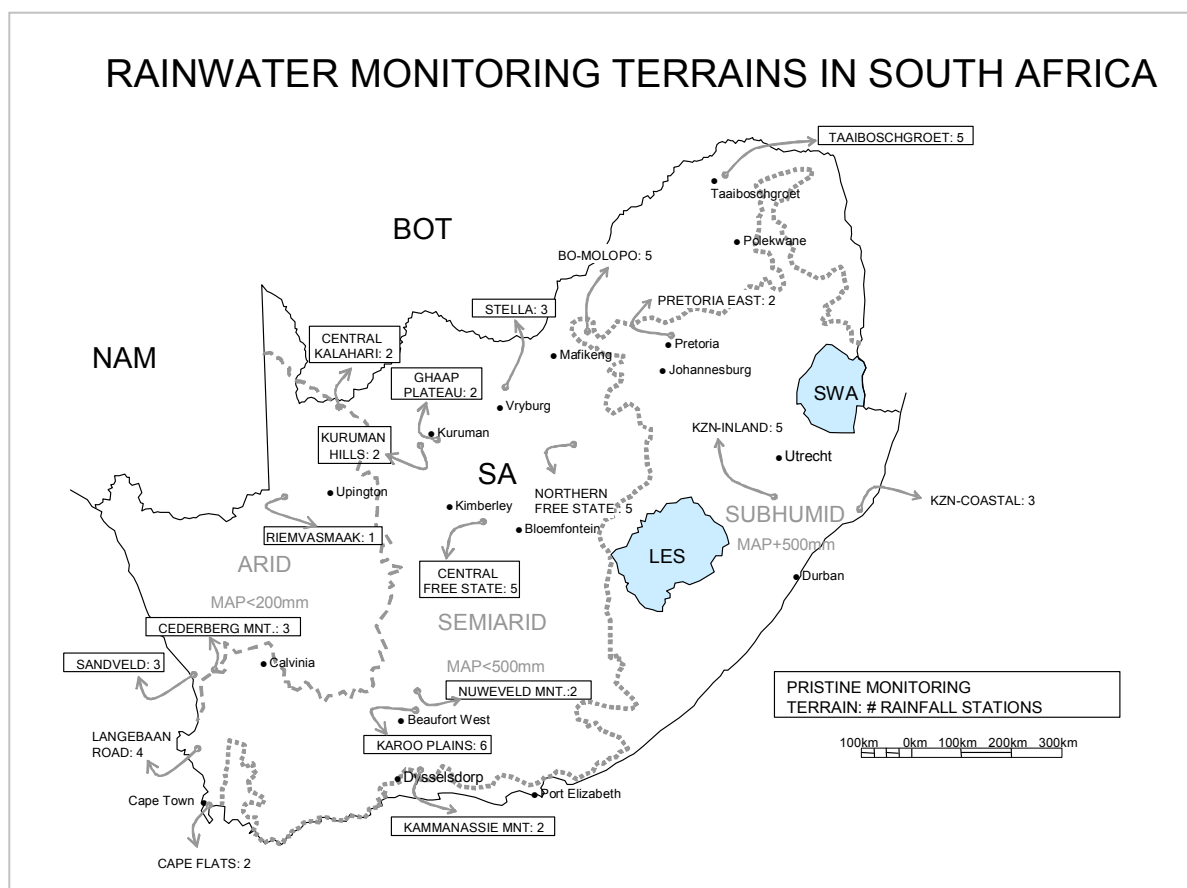


Figure 5.5. Positions of the national rainwater quality and quantity monitoring terrains in South Africa and the number of rainfall stations on each monitoring terrain.

These hydrochemistry-based periods are described in terms of specific time slots in the southern African HC (Oct_n to Sep_{n+1}) as follows:

- An early rain season input of moderate level dissolved substances, i.e. concentrations of Cl^- , NO_3^- and SO_4^{2-} in the winter and summer rainfall semi-arid regions (Table 5.3):

Table 5.3. Summary of early seasonal rainwater hydrochemistry ($\text{mg}\cdot\ell^{-1}$) in semi-arid region of South Africa: 2002-2009.

Regions	Element	HARMEAN	Std Dev.	AVERAGE	GEOMEAN
Summer rainfall: [O, N, D] (6 areas ⁴⁵ , n=71)	Cl^-	0.8	0.09	1.1	0.9
	NO_3^-	0.9	0.2	8.4	5.3
	SO_4^{2-}	0.2	0.43	3.3	1.7
Winter rainfall: [A, M, J] (4 areas ⁴⁶ , n=23)	Cl^-	3.6	0.35	7.2	5.2
	NO_3^-	0.1	0.3	1.5	0.5
	SO_4^{2-}	0.8	0.23	4.4	2.8

and

- A peak seasonal input of low level dissolved substances of Cl^- , NO_3^- and SO_4^{2-} in the winter and summer rainfall semi-arid regions (Table 5.4):

Table 5.4. Summary of peak seasonal rainwater hydrochemistry ($\text{mg}\cdot\ell^{-1}$) in semi-arid region of South Africa: 2002-2009.

Regions	Element	HARMEAN	Std Dev.	AVERAGE	GEOMEAN
Summer rainfall: [J, F, M] (6 areas, n=89)	Cl^-	0.4	0.06	0.7	0.6
	NO_3^-	0.7	0.27	7.5	3.2
	SO_4^{2-}	1.1	0.57	4.0	1.9
Winter rainfall: [J, A, S] (4 areas, n=24)	Cl^-	2.7	0.35	4.1	3.4
	NO_3^-	0.8	5.61	9.2	3.5
	SO_4^{2-}	0.07	0.01	7.2	0.8

⁴⁵Beaufort West, Stella-Vryburg, Kuruman, Pretoria East, Taaiboschgroet-Alldays and Central Kalahari.

⁴⁶UWC-Bellville, Langebaan Road-Vredenburg, Sandveld-Lambertsbay and Klein Karoo-Oudtshoorn.

and

- A dry seasonal input of dissolved substances of Cl^- , NO_3^- and SO_4^{2-} in the winter and summer rainfall semi-arid regions (Table 5.5):

Table 5.5. Summary of dry seasonal rainwater hydrochemistry ($\text{mg}\cdot\text{l}^{-1}$) in semi-arid region of South Africa: 2002-2009.

Regions	Element	HARMEAN	Std Dev.	AVERAGE	GEOMEAN
Summer rainfall: [A, M, J, J, A, S] (6 areas, n=66)	Cl^-	1.0	0.17	1.6	1.3
	NO_3^-	0.5	0.13	12.0	5.2
	SO_4^{2-}	2.1	0.64	4.6	3.5
Winter rainfall: [O, N, D, J, F, M] (6 areas, n=30)	Cl^-	6.8	0.8	8.8	7.7
	NO_3^-	0.2	1.2	8.0	1.2
	SO_4^{2-}	0.3	0.9	3.7	1.7

Rainwater hydrochemistry in the summer rainfall regions reports a prominent seasonal trend with 0.8, 0.4 and $1.0 \text{ mg}\cdot\text{l}^{-1}$ Cl^- concentration levels in the early, peak and dry periods respectively (n=226). The peak rain period from Jan_{n+1} to Mar_{n+1} emerging as the period with the lowest or most diluted Cl^- concentration input of $0.4 \text{ mg}\cdot\text{l}^{-1}$.

Atmospheric outfall, containing terrigenous dust during the dry period, represent in the order of 20% of the total chloride deposition (TC) (Gieske 1992). Although the rainwater Cl^- content during the peak period is low, the actual mass contribution varies between $200 \text{ mg}\cdot\text{l}^{-1}$ (high lands areas) and $310 \text{ mg}\cdot\text{l}^{-1}$ (plains areas). The highest input is during the early period, i.e. 55%.

The hydrochemistry of the winter rainwater, especially in the Western Cape varies between the early ($3.6 \text{ mg}\cdot\text{l}^{-1}$), peak ($2.8 \text{ mg}\cdot\text{l}^{-1}$) and dry ($6.8 \text{ mg}\cdot\text{l}^{-1}$) seasonal cycles (n=77). Irregular high inputs of Cl^- ($\approx 13 \text{ mg}\cdot\text{l}^{-1}$) renders the regional application of the CMB recharge estimation to become unstable (i.e., high standard deviations on harmonic mean values for winter rainwater as in Tables 5.3 to 5.5). Total Cl^- deposition on the other hand

is significantly high throughout the HC. The three tier period's TC input is $248 \text{ mg}\cdot\ell^{-1}$, $253 \text{ mg}\cdot\ell^{-1}$ and $267 \text{ mg}\cdot\ell^{-1}$ respectively for the early, peak and dry periods.

5.1.6 Spatial Variations and Trends.

With inland migration, the rainwater hydrochemistry becomes more stable in terms of seasonal cyclicity and the effect of maritime aerosols diminishes (Figure 5.2). Observations by international research programmes, report for example a rapid landward decrease in the Cl^- concentration from $6.0 \text{ mg}\cdot\ell^{-1}$ in an area a few km inland along the coast of New York, to $1.0 \text{ mg}\cdot\ell^{-1}$ at a spot 160 km inland (Hem 1959). This phenomenon was also observed by Hutton (1958) during rainwater analyses on the southern coastal regions of Australia (Victoria and New South Wales).

A good example of this distance/elevation effect has been observed in the semi-arid Sandveld area on the Western Cape Province's West Coast region. An NW-SE trajectory of the ground surface elevations and Cl^- values at six (6) monitoring sites is presented in Figure 5.6.

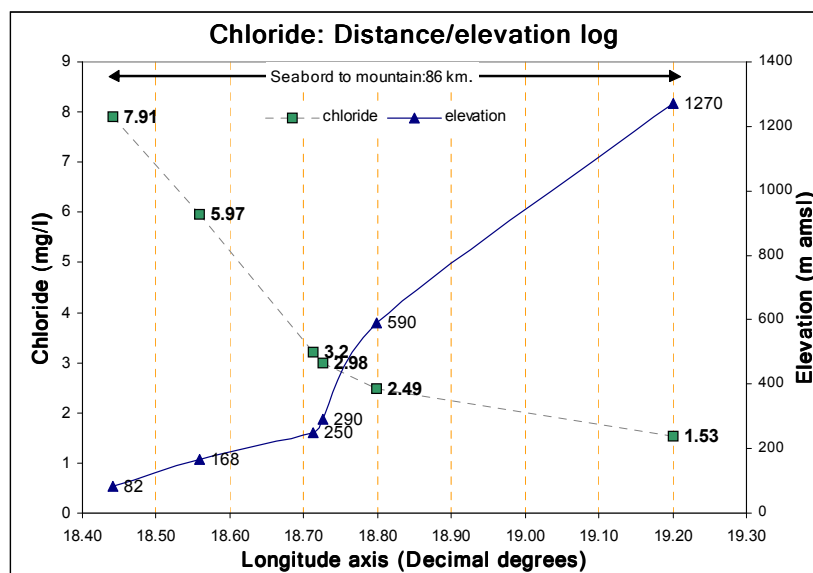


Figure 5.6. Rainwater chloride profile across the Sandveld Region showing decreasing Cl^- values with increasing ground elevation away from the seaboard at E018.40°.

On the seaboard section, rainwater analyses report Cl^- values⁴⁷ of $7.9 \text{ mg}\cdot\text{l}^{-1}$ (monitoring site G30F1_RF, Klein Klipheuveld, S32.24488°; E018.44212°, 82 m amsl). Moving some 86 km towards the southeastern highlands regions with an elevation increase of $\pm 1190 \text{ m}$, the harmonic mean value is $1.5 \text{ mg}\cdot\text{l}^{-1}$ (monitoring site E21H_RF, Roelofsberg, S32.74410; E019.20164, 1270 m amsl). The section in Figure 5.6; include rainwater Cl^- values in four (4) monitoring sites in between. A significant rainwater Cl^- decrease (7.9 to $3.0 \text{ mg}\cdot\text{l}^{-1}$) occurs and levels-off as soon as the topography starts to increase above 250 m amsl.

In the summer rainfall part of the semi-arid region, there is little difference in the LLHc's for respective monitoring sites, for example the Cl^- concentrations (Table 5.6).

Table 5.6. Rainwater Cl^- from six (6) monitoring sites in the semi-arid summer rainfall regions of South Africa, 2003-2009.

LOCATION	$\text{Cl}^- \text{ (mg}\cdot\text{l}^{-1}\text{)}$			
	Average	HAR Mean	Std. Dev.	Geo-mean
Summary: early rainwater input (71)	1.1	0.8	0.09	0.9
Summary: peak rainwater input (93)	0.7	0.4	0.06	0.6
→ Beaufort West: 8 monitoring sites (19)	0.7	0.8	0.04	0.8
→ Stella: 3 monitoring sites (14)	1.2	0.9	0.1	1.0
→ Kuruman Eye: 4 monitoring sites (11)	0.6	0.4	0.04	0.5
→ Pretoria East: 2 monitoring sites (16)	0.3	0.3	0.05	0.3
→ Taaiboschgroet: 5 monitoring sites (26)	0.8	0.7	0.04	0.7
→ Central Kalahari: 2 monitoring sites (7)	0.5	0.3	0.2	0.4
Summary: dry rainwater input (66)	1.6	1.0	0.16	1.3
(n): Implies population number in specific category.				

⁴⁷ Harmonic mean values from populations of 9 individual LLHc analyses.

Six (6) monitoring sites were used as demonstration of the Cl^- concentrations in rain-water. Although these sites are situated several hundreds of km apart, the statistical mean values and standard deviations show rather small differences.

Local deviations due to orographic effects were observed and should be acknowledged especially during CMB applications. For example, the Beaufort West monitoring terrain consist of three monitoring sites on the Nuweveld Mountains (± 1690 m amsl) reports rain-water Cl^- values around $0.7 \text{ mg}\cdot\text{l}^{-1}$, whilst monitoring sites on the southern Karoo pene-plane (± 850 m amsl) reports Cl^- values around $1.5 \text{ mg}\cdot\text{l}^{-1}$, i.e., 2-time higher.

The same has been observed at the Kuruman monitoring terrain where the difference between the Ghaap Plateau ($0.9 \text{ mg}\cdot\text{l}^{-1}-\text{Cl}^-$) sites and the Kuruman Hills ($0.3 \text{ mg}\cdot\text{l}^{-1}-\text{Cl}^-$) site is $0.6 \text{ mg}\cdot\text{l}^{-1}-\text{Cl}^-$, which indicate a recharge difference of 60% between the two areas.

Spatial variations in rainwater hydrochemical character in both winter and summer rainfall regions are significant and needs to be acknowledged. The orographic effect is the most significant factor altering the Cl^- composition to such a level that applying the CMB technique, even on a regional scale, is not advisable without having a representative monitoring coverage of the area under investigation.

Not only does the rainwater Cl^- vary over short distances, but the underlying groundwater hydrochemistry are affected accordingly. As with the rainwater hydrochemistry high-level monitor requirements, groundwater sampling requires even more dedicated procedures, due to the different background hydrochemical signatures in the SZ.

5.2 ISOTOPE HYDROLOGY OF SOUTH AFRICAN RAINWATER.

5.2.1 *Standards and Isotopic Fractionation.*

The initial investigations on hydrological isotopes were confined to rainwater to study meteorological patterns and seawater as the major source of atmospheric moisture. Isotope studies involved isotopic variations in global precipitation and the global 'isotopes-in - precipitation' network of the WMO and IAEA was initiated (Dansgaard 1964; Mook 2001)

Application of isotope hydrology for groundwater was started in the 1950s using radio-carbon (^{14}C in combination of $^{13}\text{C}/^{12}\text{C}$) as an indicator of groundwater movement). As

new analytical methods and equipment (mass spectrometry) developed, the hydrogeological application of isotopes with extreme low abundances in the environment became a sophisticated tool for hydrological tracer studies (Mazor 1997; Mook 2001).

In this study, the non-radioactive (stable) isotopes of hydrogen (^2H) and oxygen (^{18}O) will be applied for the following reasons:

- Stable isotopes in rainwater contain a unique signature which is marked by atmospheric processes (i.e. E), geographic positions (altitude and latitude) and time of the year. In addition, depletion of the heavier stable isotopes due to heavy rainout events which marks the rainwater stable isotope composition (^2H and ^{18}O) with respect to the most abundant rainwater molecule $^1\text{H}_2^{16}\text{O}$. This effect has been found to specifically mark the recharge-producing rainfall surplus in the arid/semi-arid regions of South Africa.;
- Once rainwater falls on to the ground surface, evaporation either at surface, depression storage, or from field capacity will alter the isotope composition and an evaporative composition may be established, which is a very useful tracer for estimating the groundwater recharge flow path from ground surface to the SZ.

The co-variance of $^2\delta$ and $^{18}\delta$ in natural waters is governed by two main processes in the global water cycle (Mook 2000):

- Evaporation of maritime water from the ocean surface; and
- Progressive raining out of the resulting oceanic vapor mass as it migrates into regions where orographic (higher latitudes and altitudes) or synoptic processes (frontal and convection systems) drives precipitation.

A specific standard value has been established, to which the isotopic compositions of all waters are expressed in comparison to the isotopic composition of maritime water, called the Standard Mean Ocean Water (SMOW) (Mazor 1997). The actual value for the stable isotopes of hydrogen (^2H) and oxygen (^{18}O) is determined by mass spectrometry and ex-

pressed as per mil (‰) deviations from the SMOW standard. The notations for hydrogen (^2H) and oxygen (^{18}O) isotopes are $^2\delta$ and $^{18}\delta$ respectively.

The evaporation process⁴⁸ fractionates the isotopically lighter water molecules ($^1\text{H}_2^{16}\text{O}$) more efficiently from the heavier ones ($^2\text{H}_2^{16}\text{O}$ and $^1\text{H}_2^{18}\text{O}$), thus leaving the residue behind as a heavier (or enriched) component ($^1\text{H}_2^{18}\text{O}$, $^2\text{H}_2^{18}\text{O}$). The partially evaporated vapor is enriched with the lighter molecules, and therefore reflects relatively negative $^2\delta$ and $^{18}\delta$ compositions. The remaining atmospheric moisture will have a more negative (lighter) composition; thus depleted of the heavier $1\text{H}^2\text{H}^{16}\text{O}$ (rare) and $1\text{H}1\text{H}^{18}\text{O}$ (rare) water molecules.

5.2.2 The Meteoric Water Line (or Isotope Line).

Studies by Craig and Dansgaard (cited in Mazor 1997; Mook 2001) of the changes in ^2H and ^{18}O in rivers, lakes and precipitation are fairly well synchronized. Graphing of $^2\delta$ ‰ versus $^{18}\delta$ ‰ isotopic compositions are aligned along a linear line that is referred to as a Meteoric Water Line (MWL). A best-fit approach of the global GNIP rainwater dataset produced a line with the expression:

$$\delta^2\text{H} = 8 \delta^{18}\text{O} + 10\text{‰} \quad (5-1)$$

and called the Global Meteoric Water Line (GMWL). Due to local kinetic fractionation during evaporation and associated effects (temperature, latitude and altitude), the covariance may be unique and may portray a Local Meteoric Water Line (LMWL).

LMWL's for each monitoring terrain were evaluated from the stable isotope dataset and were tabled with LMWL's for southern Africa cited in literature (Table 5.7).

The general relation for any MWL is:

$$^2\delta = s \cdot ^{18}\delta + d \quad (5-2)$$

⁴⁸ Physical process in which energy-loaded water molecules move from the water phase into the vapor phase (Mazor 1997).

The MWL is characterized by a slope of 8 and a specific intercept with the ^2H axis (the value of $^2\delta$ where $^{18}\delta = 0\text{‰}$) Mook (2001a). The slopes of the LMWL's of the southern African rainwater isotope compositions are <8 and vary between 5.4 and 7.7.

Table 5.7. Table of LMWL's from this study and from published literature.

Monitoring Terrain	Observation period	Co-variance (MWL)	Comments
GNIP (Global)	Since 1961	$\delta^2\text{H} = 8.0 \cdot \delta^{18}\text{O} + 10.0$	Craig (cited in Mazor 1997)
GNIP (Pretoria)		$\delta^2\text{H} = 6.5 \cdot \delta^{18}\text{O} + 6.37$	Mook (2000)
GNIP (Windhoek)		$\delta^2\text{H} = 6.6 \cdot \delta^{18}\text{O} + 7.04$	IAEA/WMO (2003)
Beaufort West	2003-2008	$\delta^2\text{H} = 5.4 \cdot \delta^{18}\text{O} + 2.6$	Western Cape, summer rainfall
Kalahari	2002-2009	$\delta^2\text{H} = 6.1 \cdot \delta^{18}\text{O} + 6.5$	Western Kalahari, summer rainfall
KwaZulu Natal	2003-2006	$\delta^2\text{H} = 5.6 \cdot \delta^{18}\text{O} + 6.7$	Northern KZN, summer rainfall
Langebaan	2003-2006	$\delta^2\text{H} = 6.5 \cdot \delta^{18}\text{O} + 6.6$	Western Cape, winter rainfall
Sandveld	2003-2006	$\delta^2\text{H} = 5.8 \cdot \delta^{18}\text{O} + 5.2$	Western Cape, winter rainfall
Kuruman	2002-2008	$\delta^2\text{H} = 5.5 \cdot \delta^{18}\text{O} + 0.6$	Northern Cape, summer rainfall
Pretoria East	2003-2009	$\delta^2\text{H} = 6.0 \cdot \delta^{18}\text{O} + 5.0$	Gauteng, summer rainfall
Stella	2002-2009	$\delta^2\text{H} = 6.4 \cdot \delta^{18}\text{O} + 4.4$	Northern Cape, summer rainfall
Taaiboschgroet	2003-2006	$\delta^2\text{H} = 7.7 \cdot \delta^{18}\text{O} + 8.1$	Limpopo, summer rainfall

With reference to Eq. 5-2, the slope s is determined by the ratio between the equilibrium H and O isotope fractionations during the rain condensation process, and d' is referred as the deuterium (^2H) excess (*d-excess*), representing the value where the MWL intercepts the $\delta^2\text{H}$ axis. The *d-excess* represents the process where oceanic vapor is evaporated under nonequilibrium (partly kinetic process) conditions resulting in a d' parameter shift of $+10\text{‰}$ (Kendall and McDonnell 1998; Mook 2000a, 2001). Regional values for $^2\delta$ differ from 10‰ , depending on relative humidity and temperature conditions during rainout evaporation processes, and differ during certain periods of the year.

The deuterium excess for this study's monitoring terrains varies between 0.6 and 8.1 (Average = 5.8). This phenomenon has been observed in southern African on various occasions (Butler 2010).

Mazor (1997) and Kendall and McDonnell (1998) specify the meteoric water line as a convenient reference line for tracing and interpretation of local rainwater-groundwater interaction in terms of origins and movement.

5.2.3 Temporal Responses and Trends in ESI Compositions.

Rainwater collected during a specific HC is contained in a bulk container in the rainfall logger/sampler unit and therefore represent an accumulation of several individual rain events with obviously different isotopic compositions. The instrument subsequently averages the results, especially during average rainfall seasons. Periodic sampling of the collected rainwater at the end of each of the three tier periods allows sampling over at least three different HC intervals. From this data some significant differences between the seasons was observed.

It was observed that the rainwater isotope compositions in the semi-arid regions are affected by the amount effect⁴⁹. Heavier rain events introduce a lighter ESI composition to the local rainwater budget, meaning more negative values for both ^2H and ^{18}O and are confirmed by observations by (Mazor 1997; Mook 2001; Van Tonder and Bean 2003). This will subsequently shift the isotopic composition to graphically plot more negatively along the MWL (Dansgaard 1964; Mazor 1997).

Negative shifts along the MWL correlates with high rainfall inputs (i.e. the amount effect) and were observed between the years 2006 (2005-2006 season), 2008 (2007-2008 season) and 2009 (2008-2009 season). In Figure 5.7, a correlation between rainfall depths and the $^{18}\delta$ composition from the Stella monitoring terrain is shown as an example of the isotope data set. A logarithmic trend line has been fitted through both datasets (i.e. Spitkopreen and Midkopreen) which indicates an increasing negative trend with higher rainfall depths.

⁴⁹ The amount effect is the result of evaporation (i.e. dynamic fractionation) during rain showers resulting in an enrichment of the isotopic composition of the cloud water during its descent, intercepting an atmosphere with low relative humidity. The effect becomes more pronounced during longer, wetter conditions when the evaporative effect is less because of a much higher relative humidity from the cloud base to the ground surface (Kendall and McDonnell 1998)

Two hydrological seasons containing episodic rain events that stand out are those of 2005-2006 and 2007-2008, specifically observed at the Beaufort West, Stella, Pretoria East and Kuruman monitoring terrains. The hydrogeochemical compositions reported this negative shift, probably related to the higher annual rainfall during 2006 and 2008 at the monitoring terrains having individual episodic rainfall events of 50 to 150 mm each. The monitoring sites recorded a 50 to 70% higher rainfall depth versus the long-term averages. The isotopic composition for these high rainfall events ($^{18}\delta=-10\text{‰}$, $^2\delta=-65\text{‰}$) shifted⁵⁰ the average isotopic composition towards the $^{18}\delta=-7(\pm 1)\text{‰}$ and $^2\delta=-40(\pm 4)\text{‰}$ and area on the Harmon Craig diagram.

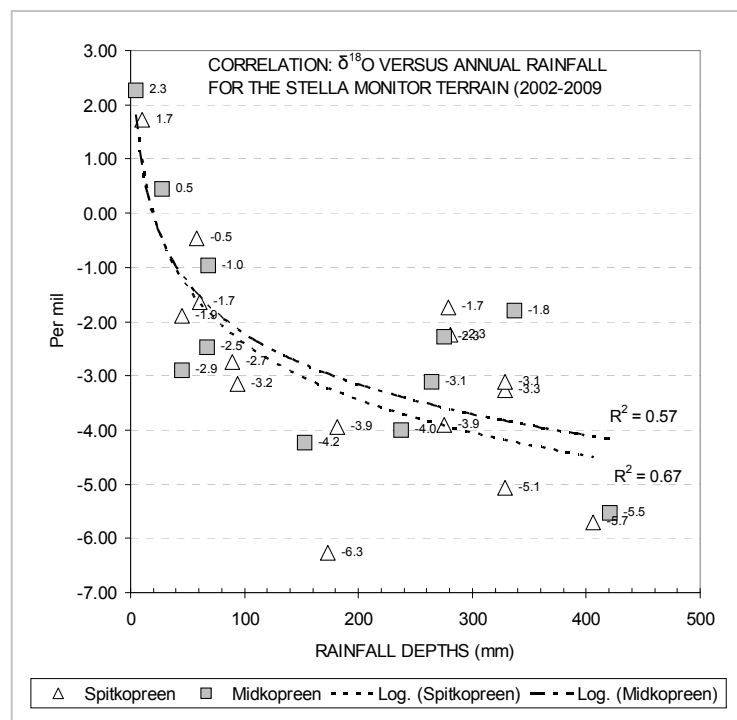


Figure 5.7. Correlation between rainfall depths and $^{18}\delta(\text{‰})$ at the Stella monitoring terrains for the period 2002 to 2009.

This phenomenon is illustrated in Figure 5.8 for Beaufort West monitoring terrains. The data shows that the isotopic compositions for those years with above-average rainfall depths (410 mm for 2005-2006 HC and 450 mm for 2007-2008 HC over a long-term average of 236 mm) falls in the region of $^{18}\delta < -7\text{‰}$ and $^2\delta < -30\text{‰}$. Except for the 2003-2004

⁵⁰ As observed with the RES units at Beaufort West and Stella (individual rainfall event sampling).

HC which tends to contains a few relatively depleted rainout events, the isotopic compositions of 2004-2005 HC and 2006-2007 HC plots around $^{18}\delta=-3\text{‰}$ and $^2\delta=-12\text{‰}$.

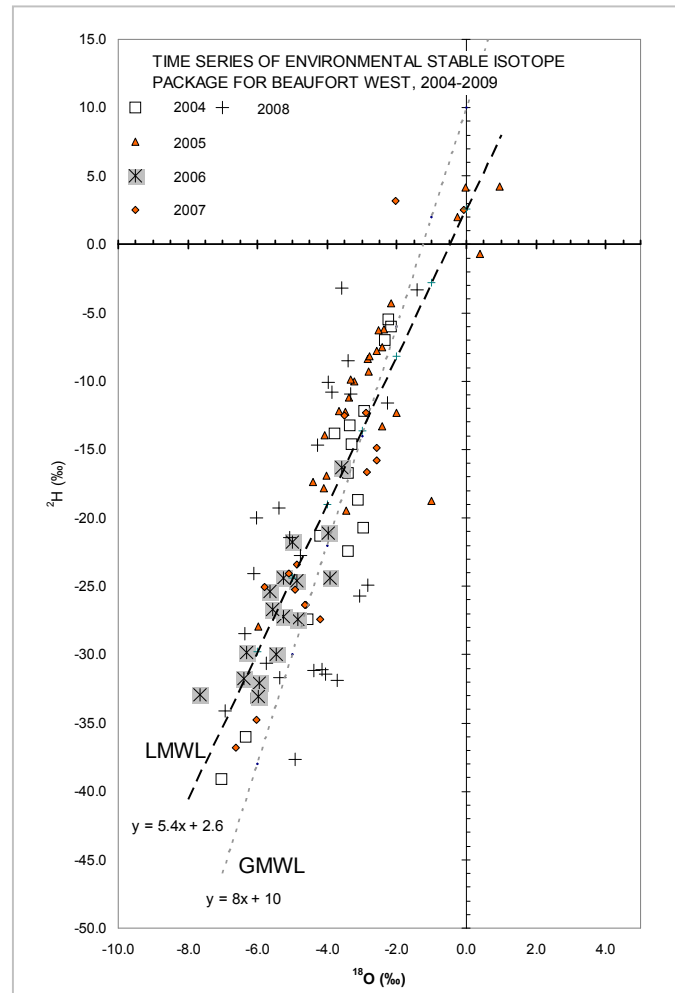


Figure 5.8. Isotopic composition of rainwater obtained from the Beaufort West monitoring sites (nine (9) rainfall sampling/logging stations) categorized in 2003-2004 to 2007-2008 HC's.

Physical sampling of these episodic, high rainfall events is quite challenging if a monitoring site is not manned by individuals (i.e. landowners, regional officers at regional offices or weather services officers). The RES unit solves this problem although it requires frequent maintenance and rainwater sample collections.

Unfortunately, only one of these units could be physically tested in Pretoria and Stella. The stable isotope data recorded reveals a significant lighter isotopic shift ($^{18}\delta=-11\text{‰}$, $^2\delta=-80\text{‰}$) from a series of nine (9) rain events (Figure 5.9).

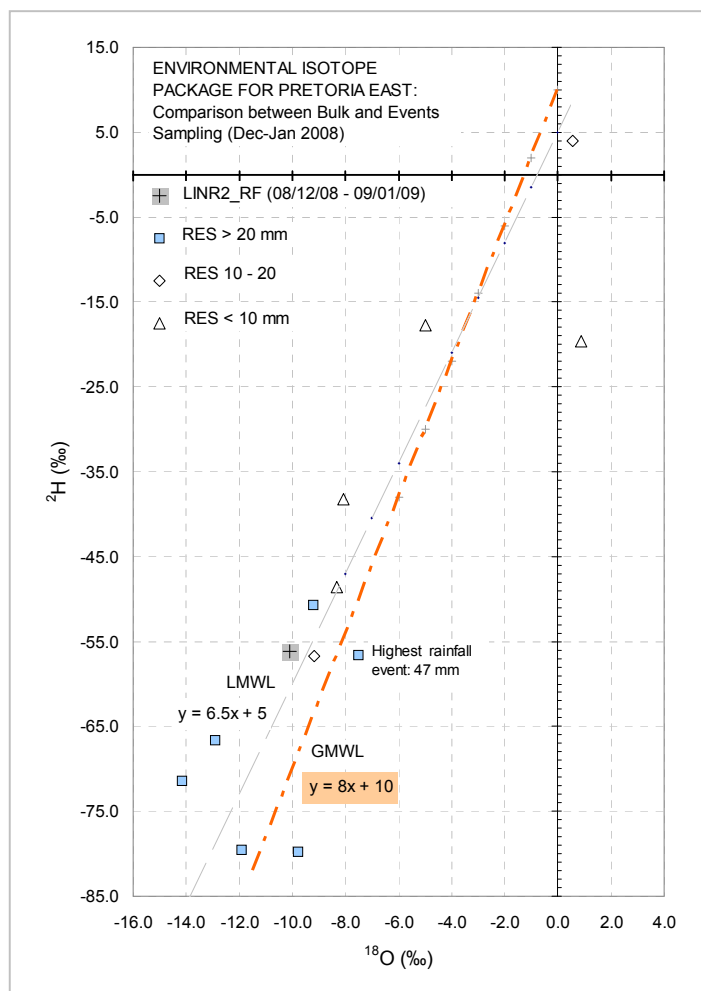


Figure 5.9. Isotopic composition of rainwaters from the Pretoria East monitoring site illustrating the difference between bulk rainwater sampling (over a month) and individual rainwater sampling (RES unit).

Stable isotope values presented in Figure 5.9, illustrates data obtained from the Pretoria East monitoring site, where the RES unit was tested over a period of thirty-two (32) days during the onset of the summer peak rainfall period.

The weather patterns were typical summer, thunderstorm activities with moist deriving from the ITCZ with a normal summertime synoptic pattern across southern Africa (Section 3.1.2 and Figure 3.3). The rainfall depth over the test period was 142 mm, of which three were rain events between 20 and 50 mm. The rainwater collected over the same period in the bulk rainwater sampler unit plots, in fact in the same region as the highest rain event of 47 mm or 33% of the volume (Figure 5.9). The isotopic composition of the rainwater does not vary much from the norm when referenced by the MWL for this rainout event ($\delta^2\text{H} = 6.5\delta^{18}\text{O} + 5.0\text{‰}$) versus the Pretoria GNIP (LMWL: $\delta^2\text{H} = 6.5\delta^{18}\text{O} + 6.4\text{‰}$).

5.2.4 *Summary.*

ESI composition of winter and summer rainwater collected over the period 2003 to 2009 from the eight (8) hydrological monitoring sites in semi-arid regions of South Africa varies from around $^{18}\delta = -0.3\text{‰}$, $^2\delta = +2.5\text{‰}$ to $^{18}\delta = -7\text{‰}$, $^2\delta = -38\text{‰}$.

These values represent quasi-average values, due to the accumulation effect of the bulk sampling process over the three-tier sampling intervals during average annual rainfall. Isotopic compositions within one HC can vary considerably; thus once-off sampling of rainwater to obtain representative rainwater isotope signature could lead to erroneous conclusion.

Short-term rainfall patterns, characterized by extraordinary high rainfall events occurring in an episodic manner, were observed in most of the monitoring terrains. It has been noted that once these events occur, the rainwater ESI composition of the bulk sample units are notably more negative, $^{18}\delta = -9.5\text{‰}$, $^2\delta = -53\text{‰}$.

Rainwater ESI compositions obtained from the RES unit, which samples individual aliquots during a rainfall event, demonstrate the reason for these negative shifts in the totalized samples. Individual rainfall ESI compositions are much lower and plots around $^{18}\delta = -12.5\text{‰}$, $^2\delta = -71\text{‰}$ on the Harmon Craig diagram.

5.3 HYDROGEOCHEMICAL COMPOSITION AT THE WATER TABLE INTERFACE.

The hydrogeochemical composition of the groundwater-saturated column of aquifer systems reports not only the background aquifer average water quality, but also the residue of

the recharged rainwater coming from a combination of vertical (unsaturated) to lateral (saturated) flow regimes.

Depending on where a groundwater sample is collected from the saturated column of an aquifer system, it probably is not feasible to analyze in-time rainwater samples and to take groundwater samples from a mixed flow regime which contains a mixture of resident aquifer water and younger recharged rainwater, if the local flow regime is not conceptualized. Aquifer hydrogeochemical characteristics should therefore be acknowledged if hydrochemical/isotopic tracers are to be used. Purging from the aquifer is not advisable, as deeper sections of the water column are also drained, which are probably not in phase with the modern hydrogeochemical signature of the hydro-climate and recharge regime.

It is essential to first consider the hydrochemical characteristics of the groundwater system to be investigated. In contrast with the isotopic signature in groundwater, variations in the hydrochemical composition also are a factor of the specific rock types. Initial sedimentary deposits driven by pluvial conditions tend to concentrate dissolved salts in certain formations such as, for example, the glacial ice-shelf deposits of the Late Carboniferous to Early Permian Dwyka Group and the marine shales of the Permian Ecca Group.

These salts are still part of the palaeo environmental salt balance and obviously get mobilized under modern wet-weathering processes. It may for example become part of the groundwater flow regime and may concentrate at places where the groundwater discharges via sun ponds, i.e. pans and modern playas. It has been noted by the author that groundwaters underlying surface calcrete deposits in the southern Karoo regions, Beaufort West for example, report extremely high salinities with Cl^- concentrations of several hundred milligrams per liter. These calcrete-capped areas probably represent historical evaporation ponds and contain elevated concentrations of palaeo dissolved connate salts.

5.3.1 The Origin of Traceable Dissolved Rock Salts in Groundwater.

On site observations by Clarke (1924), Rankama and Sahama (1949), Hem (1959) and more recently, Mazor (1997), presented Cl^- values for rock formations which are several orders of magnitude higher than the local, average rainwater Cl^- concentration. The hydrochemical composition of the groundwater logically depends on the nature of the rock

forming minerals dissolved during solution and hydration processes. This elevated Cl^- concentration therefore indicates rather poor recharge mechanisms and/or addition of connate Cl^- to the groundwater Cl^- balance.

Decomposition and subsequent leaching of the underlying rock mass is largely a surface phenomenon, and is driven by the presence of oxygen and carbon dioxide (Clarke 1924; Hem 1959; Mazor 1997). Therefore, apart from the mechanical breakdown of the upper rock mass, the second mechanism involved is driven by chemical processes, initiated by the presence of oxygen and carbon dioxide in the infiltrating rainwater. According to the analyses by Clarke (1924) and Hem (1959), the composition of air extracted from rainwater at 10°C contains:

Carbon dioxide (CO_2):	2.46 %;
Oxygen (O_2):	34.06 %; and
Nitrogen (N_2):	63.49 %.

Oxygen levels from shallow groundwater systems vary from 24.06% (at roughly 12 m bgl to 12.90% at 25 m bgl (Clarke 1924). These agents, both occurring in water and gas media, exert a solvent action on the mechanically disintegrating rock mass, thus charging the groundwater with products of rock mass solution.

Chloride is classified as part of the Halogen Group, and is regarded as a conservative tracer once ionized to Cl^- . It originates from dissolved solids such as rock salt (Hawley 1981). The Cl^- content in earth's lithosphere is highly variable due to the geological/geochemical nature of the rock mass. Chloride however occurs in great abundance in ocean water, 19 000 $\text{mg}\cdot\text{t}^{-1}$ (Clarke 1924; Hem 1959).

Chloride originates from the following sources (Hem 1959):

- Oceanic Cl^- : Only a small portion of Cl^- is leached from the weathering/decomposition of igneous rocks; the remainder of the relatively high Cl^- content of the ocean is believed to derive in the form of hydrochloride acid or volatile Cl^- salts added to the ocean directly by sub-marine and terrestrial volcanic emanations;

- Juvenile Cl^- : From hot springs resulting b.m.o. deep circulation from distant recharge terrains through different geological formations;
- Cyclic Cl^- : Transporting part of the dissolved salts in the ocean into the atmosphere from where it is carried to earth as dry and wet deposits. Windblown oceanic aerosols containing NaCl may be carried farther inland by prevailing winds from the seaboard.

Historic measurements by Clarke (1924) and Rankama and Sahama (1949) report the lowest primary Cl^- values (traces only) for dolomites and limestones. In comparison, basalts, granodiorites and granites on average contain 200, 540 and 330 $\text{mg}\cdot\text{l}^{-1}$ Cl^- respectively, pure sandstones report traces only, and argillaceous sediments on average 200 $\text{mg}\cdot\text{l}^{-1}$ Cl^- .

Flushing of the dissolved rock salts in the UZR is a rather common phenomenon in hard rock terrains and representing probably the best hydrogeological characteristics to estimate groundwater recharge. Jointing/fracturing resulting from the two Neogene (~18 to ~2 Ma) phases of uplifting and erosional unloading can be traced for several meters below the current ground surface. This allows fresh rainwater to percolate rather deep into the unsaturated and saturated profile, and subsequently to flush the upper fractured and weathered zones.

It will be demonstrated presently that when an episodic recharge event occurs, wherein the water table rises several meters, hydrogeochemical layering in the resulting new saturated profile has been observed. Considering the dynamic water table rebounds registered after episodic recharge events, it is possible that during these flushing events through the UZR, a high percentage of resident salts are mobilized and removed from the macro-pore flow network deposited during a previous diffuse flow infiltration event.

5.3.2 Groundwater Hydrochemistry of Typical Rock Formations in South Africa.

Rock formations in southern Africa's semi-arid regions are mainly of post-Swazian (<3.1 Ba) sedimentary/volcanic nature, deposited on a basement shield consisting of granite-gneisses and associated metamorphics. Detail mapping of groundwater quality data over southern Africa reports some correlation between fresh groundwater found in arena-

ceous rock types (e.g. Table Mountain Group ortho-quartzite), and brackish/saline groundwater found in argillaceous rock types (e.g. Karoo Supergroup). Dolomite (Chuni-espoort and Ghaap Groups) characteristically reports almost pristine rainwater hydrochemical composition due to direct rainwater recharge and virtually no traceable addition of secondary Cl^- to the flow regime.

The Late Carboniferous to Early Jurassic Karoo Supergroup in southern Africa, consisting of marine shales and diamictite in the Dwyka Group, carbonaceous shales in the Ecca Group and shales in the Elliot Formation contain connate rock salt. Groundwater found in the Dwyka Group's marine shales in the southwest Kalahari basin is characteristically saline. Extremely highly mineralized waters are quite common in this area, which in many cases exceed the total dissolved solids for oceanic waters.

Considering these high concentrations of palaeo rock salts imbedded in the primary rock matrix and using Cl^- as a modern time tracer, requires a good conceptual understanding of the local groundwater flow regime(s). Regional isotope investigations into the characteristics of the Karoo-Kalahari aquifer systems in the Northern Cape Province, demonstrated this phenomenon (Verhagen 1984). Hyper saline groundwater (>30 000 ppm) occurs in the Western Kalahari Salt Block⁵¹ area. The presence of radiogenic hydrogen (^3H) and carbon (^{14}C) classify this water as recently recharged. Extraordinary high values (180 000 ppm) has been observed by the author in brine from the Vry Soutpan (Free Salt Pan), a natural saltpan in the southwestern Kalahari (S27.34374°; E020.82958°, 842 m amsl).

Despite the fact that the groundwater may be recently recharged, the dissolved solids (containing NaCl) are in fact locally recycled and derive from high salinities during deposition in the Late Carboniferous to Early Permian period.

Groundwater quality assessments by Bond (1947) and Kent (1949) provide some basic groundwater hydrochemistry background collected over a period of several decades from different rock formations throughout South Africa (Table 5.8).

⁵¹ An area 130 km north of the town of Upington, Northern Cape, originally demarcated as a game reserve due to hyper saline groundwater with no surface water resources. The Vry Soutpan represents a large sun pond system where Dwyka groundwater evaporates at a rate of 2500 mm·yr⁻¹.

The relevant hydrochemical values from the different geological formations are highly variable. The historical values compare reasonably well with modern analyses obtained during the 2003-2009 period. Local variations especially between a hard rock window terrain (bypass, direct recharge) and a soil/regolith terrain (diffuse, piston flow recharge) are illustrated for the Beaufort West case (Table 5.8).

Table 5.8. Groundwater hydrochemical concentration ($\text{mg}\cdot\text{l}^{-1}$) from selected areas in South Africa: Some historic (pre-1947) values compared with modern values from similar geological groupings.

Formation at Area	Date sampled	Cl^-	NO_3^-	SO_4^{2-}	PO_4^-
Basement granite-gneisses at Mareetsane, N-Cape.	1907 [2009]	40 [44-100]	19 [0.4]	① [②]	① [①]
Ventersdorp Group lavas at Delareyville.	Pre 1947 [2009]	99 [75]	② [②]	21 [54]	3.0 [②]
Ghaap Plateau dolomites at Kuruman.	1939-04-19 [2002-'08]	7.0 [6.1]	3.5 [4.0]	0.05 [4.3]	② [①]
Beaufort Group sediments at Beaufort West.	1919-12-22 [2006-'08] ^γ	195 [169]	② [76]	130 [144]	② [①]
A hard rock terrain.	[2006-'08]*	[36]	[24]	[35]	[①]

[25.1] - Constituent concentration from this study, 2002-2009.

① - Constituent not analyzed.

② - Concentration level $< 0.05 \text{ mg}\cdot\text{l}^{-1}$, not detected by analytical procedures.

^γ - Beaufort West rural municipal area.

* - 'Pristine' monitoring site in remote hard rock terrain (De Hoop Poort, Dist. Beaufort West).

Background information regarding an area's groundwater hydrochemical character and flow regime should be acquired before comparisons between rainwater and groundwater are applied, i.e. CMB application.

To conclude, in southern Africa, the input of dissolved rock salts into the groundwater hydrochemical regime is a highly competitive factor when rainwater-surface water-groundwater chemistry is used for tracing a specific (episodic) rain event along the vertical flow path. The origin of dissolved substances in the groundwater regime is therefore legion. Both rainwater and rock matrix chemistry govern the final groundwater hydrochemi-

cal blend. The generation of solutes containing connate rock salts diluted by infiltrating rainwater may have reached an equilibrium stage as the current hard rock surfaces in southern Africa date from prehistoric time; thus leaching of newly released rock salts is probably minute compared to the modern atmospheric input.

5.3.3 Groundwater Hydrogeochemistry: Spatial and Temporal Variations.

In this section the variation in the groundwater hydrogeochemical composition because of rainwater infiltration into the SZ will be illustrated. Seasonal and spatial trends in the rainwater component of the HC have been discussed in detail in Sections 5.1 and 5.2. The hydrogeochemical characteristics of a prominent recharge event resulting from an episodic rainfall event gets imbedded in the groundwater part of the HC, especially in direct recharge terrains such as fracture, hard rock terrains.

Variations in hydrogeochemical composition of groundwater in the local HC could be due to (i) a short-term seasonal variation (a prominent rainwater signature) in addition to (ii) long-term climate variability (cyclic vegetation activity influencing ET). A third impact, i.e. regional pollution occurs over much shorter intervals, but its impact is severe. These aspects should be acknowledged in groundwater recharge estimations whereby hydrochemical tracers like Cl^- are applied, viz. the CMB application.

Background, full macro analyses of the regional groundwater quality in South Africa is generated through dedicated monitoring programmes like the NGwQMP, to estimate long-term hydrogeochemical trends in groundwater. A few long-term hydrochemistry time-series graphs from NGwQMP-sites located in the vicinity of this study's monitoring terrains are presented in the appendix section. Some long-term trends are not promising in terms of assuring a steady state Cl^- feed⁵² to the SZ, as the Cl^- concentration levels are slowly increasing. The phenomenon might be explained by (i) a gradual build-up of atmospheric-induced maritime salts, or (ii) domestic pollution, or (iii) changes in land use activities or (iv) climate variability. It is therefore necessary to perform a reasonably long groundwater

⁵² Under a steady-state groundwater recharge scenario and stable hydro-climate conditions, one would expect a quasi-stable groundwater hydrogeochemical character given a dynamic aquifer flow regime between recharge and discharge localities.

hydrochemical monitoring programme to establish Cl^- trends for a particular monitoring terrain.

In this study, groundwater sampled over a period of 5 years from a selected group of boreholes on each monitoring terrain, reported significant spatial variations in their hydro-geochemical concentrations (Table 5.9).

Table 5.9. Total Cl^- values in rainwater and groundwater observed at Beaufort West monitoring terrains with different elevations, maximum pan = 80 km

Monitoring Sites	Description	Date sampled: From - To (RF)	Elevation: m. amsl.	Chloride $\text{mg}\cdot\text{l}^{-1}$
Abrahamspoort	Rw Nuweveld Mnt.	07-11-2006_29-05-2008	1729	0.7
	Gw Sample: AT01	29-05-2007	1693	7.0
Welgevonden	Rw Nuweveld Mnt.			
	Gw Sample: G29862A	07-11-2006_29-05-2007 29-05-2007	1428 1090	0.7 27.8
Plaatdoorns	Rw Plaatdoorns River			
	(G29899F_RF):	06-11-2006_28-05-2008	991	0.8
	Gw Sample: G29899F	15-10-2008	992	100.1
Speelmanskul	Rw Speelmanskul			
	(G33551_RF):	08-11-2006_30-05-2007	938	1.2
	Gw Sample: G33551	30-05-2007	937	438.1
Beaufort West	Rw SAWS:	07-11-2006_29-05-2007	899	1.6
	Gw Sample: G29898TA	29-11-2007	874	30.4
De Hoop Poort	Rw Hard rock area	06-11-2006_28-05-2008	1031	0.6
	Gw Sample: G29870BE	28-11-2007	1031	35.7
	Gw Sample: W-pump	28-05-2007	1029	35.7

This phenomenon is probably the result of (i) geographic/elevation effects and (ii) differential spatial recharge mechanisms (i.e. direct/indirect mechanisms). Groundwater hydro-chemistry information from two monitoring terrains will be used to demonstrate this (Tables 5.9).

Table 5.9 display the local geographical influence over the rainwater and groundwater Cl^- values in a Karoo environment (Karoo peneplane along the Great Escarpment). Rainwater

Cl^- values on the Nuweveld Mountain are approximately 50% lower than the Plaatdoorns River plain south of the mountain; a typical orographic effect (Mazor 1997). These differences also manifest in the groundwater Cl^- values although differences between higher and lower elevated regions are more pronounced, average $7.1 \text{ mg}\cdot\ell^{-1}$ versus $30 \text{ mg}\cdot\ell^{-1}$.

The ET Index (ET_{INDEX}) for the mountain and plain area as per Mazor's (1997) equation is 10% and <5% respectively; thus indicting a significant loss of recharge on the Karoo peneplains due to ET processes and limited direct recharge terrains due to soil/regolith coverage and superficial, ostensibly saline limestone cap rocks.

The high Cl^- concentration ($\approx 440 \text{ mg}\cdot\ell^{-1}$) in the case of the Speelmanskuil monitoring site (G33551_RF and G33551) is included in Table 5.9 to demonstrate the spatial variance in groundwater quality and therefore complicating application of the CMB principle. This monitoring site is situated on a hard rock terrain consisting of surface limestone cap rocks, classified as nonpedogenic calcretes (Netterberg 1978; 1980). Calcrete is the product of shallow, evaporating groundwater solutions with high CaCO_3 solution levels.

Erosional remnants of these Late Pleistocene ($\sim 600\,000$ to $\sim 10\,000$ yr BP) calcrete cap rocks occur regularly in semi-arid regions. Calcrete capped areas are complex recharge terrains and its lithological character supports depression/slow infiltration type recharge mechanisms; evaporation from ground surface may substantially enrich the recharge-producing rainfall surplus.

It was observed at the Speelmanskuil monitoring site area, that although the rainwater ESI's correlates well with the GMWL, the ESI composition of some groundwater zones represents a prominent E.L. of $y = 0.45x - 33$. The reason for this phenomenon is not quite clear, but this ESI pattern and the extremely high Cl^- concentrations (360 to $529 \text{ mg}\cdot\ell^{-1}$) probably indicates ground surface conditions where evaporation enrichment manifests during local depression storage after high rainfall events.

The ratio $\text{rSO}_4^{2-}/\text{rCl}^-$ for the Beaufort West monitoring terrains report significant changes and indicate prominent recharge and discharge zones⁵³. For example that the Speelman-

⁵³ Observations indicate that recharge terrains have a $\text{rSO}_4^{2-}/\text{rCl}^-$ ratio of >1.0 and decreases away from recharge areas. Specified discharge areas report ratio's below 0.5 .

skuil site could probably represent a discharge zone having a ratio of 0.5, whilst the De Hoop Poort area's ratio varies between 1.2 and 1.4. The prominent hard rock sites, (Beaufort West hills and the Nuweveld Mountain) report ratios of 2.6 and 2.5 respectively. Surface water run-off at De Hoop Poort and on the Nuweveld Mountains, report values of 0.6 and 0.5 respectively, which are equivalent to the ratio of the incoming rainwater. This indicates that a relatively small component of the total chloride deposition resides at the ground surface in the Karoo hard rock environment.

Local variations in groundwater hydrogeochemistry were noted at most of the monitoring terrains and should be acknowledged, especially in the fractured hard rock domain. The reason for this behavior lies in the migration from direct to lateral recharge flow regimes. It is expected that the hydrochemical composition of groundwater, once part of the lateral flow regime, will blend with the background groundwater concentration (Eriksson and Khunakasem 1969).

In terms of deviating spatial recharge mechanisms, local variations in groundwater Cl^- values are reported in Table 5.10 as observed on the Stella monitoring terrain, District Vryburg in the Northern Cape Province (Figure 5.5). The data presented in this table illustrates the diverse direct/indirect recharge mechanisms occurring on a local scale in the vicinity of hard rock terrains.

At the Spitkopreen monitoring site (± 5 km south of Stella), the resident groundwater Cl^- varies from $109 \text{ mg}\cdot\ell^{-1}$ to $44 \text{ mg}\cdot\ell^{-1}$, probably due to differential recharge mechanisms on steeply dipping metamorphosed rocks (Swazian Kraaipan Group banded ironstone formations (BIF's)) and soil/regolith covered intrusive granite and gneiss rocks⁵⁴. Interesting to note is that the surface run-off collected in small depressions on the monitoring terrain has a Cl^- concentration of $30 \text{ mg}\cdot\ell^{-1}$ (Table 5.10).

The Noordreen monitoring site is situated just north of Stella, and is underlain by Ventersdorp lava with a prominent soil cover. A hard-rock window is located just northwest of the golf course consisting of Kraaipan Group metamorphic rocks.

⁵⁴ These values are predominantly influenced by the local geological model consisting of steeply dipping Kraaipan Group metamorphosed rocks, the intrusive Mosita granite body, once completely covered by flat lying Ventersdorp lavas (SACS 1980).

Table 5.10. Chloride values in rainwater and groundwater from different locations in the Stella area at similar elevations (1320m amsl) but different rock formations and recharge terrains (soil/regolith covered plains versus hard rock windows).

Rw and Gw monitoring site name	Description (Geological Form's)	Date Sampled	Depth to Rwl. m bgl.	Chloride mg·ℓ ⁻¹
Midkopreen	Rw: 199 mm	13-02-2008_27-05-2008	-	0.5
	Rw: 185 mm	14-08-2008_21-01-2009		0.7
G43988.....	Mosita Granite	14-08-2008	12.29 m	109.0
G44504.....	Mosita Granite	28-08-2008	16.92 m	75.7
G43991.....	Kraaipan relict	28-08-2008	9.57 m	59.9
	"	26-02-2009	9.58 m	46.0
G43997.....	Kraaipan relict	26-02-2009	9.84 m	43.9
G43989.....	Ventersdorp Lawa	26-02-2009	9.29 m	46.7
Spitkop Pans	Surface water in depression feature.	26-02-2009	0	30.3
Noordreen	Rw: 475 mm	26-09-2007_13-02-2008		0.4
	Rw: 176 mm	13-02-2008_27-05-2008	-	0.5
	Rw: 155 mm	14-08-2008_21-01-2009	-	0.8
G43982.....	Kraaipan relict	28-08-2008	7.61 m	13.5
G43623.....	Ventersdorp Lawa	12-04-2006	6.97 m	53.2
		21-01-2009	6.47 m	70.0

Note: All Kraaipan relicts are fractured hard rock terrains amongst soil/regolith covered Mosita GRNT and Ventersdorp Lawa sites.

The background Cl⁻ concentrations in this part of the monitoring terrain varies between 53 and 70 mg·ℓ⁻¹ (G43623, Table 5.10). The Cl⁻ value in borehole G43982 of 13.5 mg·ℓ⁻¹ reports the lowest Cl⁻ content which typically varies around 30 to 36 mg·ℓ⁻¹ for hard rock terrain in soil/regolith covered peneplane areas⁵⁵. This low Cl⁻ value is probably the result of the extreme groundwater recharge, following the high 2005-2006 rainfall resulting in a 22 m groundwater table rebound which took place over 138 days from 21 December 2005 in this part of Stella.

The groundwater rSO₄²⁻/rCl⁻ ratio for the hard rock terrain at G43982 is 2.2, whilst the surrounding areas report values of ≈0.8. In areas where the soil/regolith cover is promi-

⁵⁵ Observation from Beaufort West (Western Cape Province), Taaiboschgroet (Limpopo Province), Stella (Northern Cape), Van Zylsrus (Northern Cape) reports Cl⁻ concentrations around 30 to 36 mg·ℓ⁻¹.

nent, i.e., the Spitskop/Middlekop monitoring sites, this ratio is <0.5 . The ratio for the rainwater on the Stella monitoring terrains is 2.2 over the monitoring period 2002 to 2009.

To conclude, the importance of possible local variations in hydrochemical concentrations, and especially the Cl^- values, should be acknowledged. Local land use activities and even some natural processes may alter Cl^- concentrations in the groundwater body not solely derived by the CMB process. The $r\text{SO}_4^{2-}/r\text{Cl}^-$ gives a realistic indication of recharge and discharge, although the input of SO_4^{2-} in the rainwater should be evaluated carefully (Section 5.1.3.1).

Vertical variations in the hydrogeochemical composition are equally important as the water column below the water table interface reports some observable changes with depth. This will be addressed presently.

5.3.4 Groundwater Hydrogeochemistry - Aquifer Unit Context.

The UFWZ of the typical phreatic aquifer systems in South Africa represents the most dynamic section of the groundwater recharge cycle due to (i) the fractured hard rock nature and (ii) shallow water table conditions. According to Vegter (1995), by excluding the folded quartzitic sandstones of the TMG, the largest volume of groundwater available for exploitation, occurs between 30 and 50 m bgl. In context to this recharge investigation, and considering the fact that water table depths in most of the monitoring terrains are less than 20 m bgl, recharged rainwater at direct recharge terrains should reside in the UFWZ just below the water table interface. Once the lateral flow component starts to drain the recently recharge water towards the surrounding sub-reservoirs, one should expect mixing between newly recharged and older, resident groundwater along the lateral flow path (Willemink 1988).

Considering the model sketched above and the rather quick response time (hours/days) between rainfall and water table rebound, the recharged rainwater characterized by a specific ET signature should reside within the water table rebound. In this study, sampling at the water table interface was performed, followed by sampling of a 2-3 m profile below the water table interface using the column sampling technique once a water table rebound status developed. Sampling of this upper recently replenished water should theoretically

contain the recently recharged groundwater component and portrays the ET signature from ground surface and the UZR.

5.3.4.1 Temporal Variations in Hydrogeochemistry Composition at Variable Water Table Elevations.

During the operational phase of the investigation, groundwater samples were taken from a series of boreholes located in the rainfall monitoring sites. In this particular category, 500 ml aliquots at the water table interface were sampled in time-series which included rising (shallow) and falling (deeper) water tables. This was to observe the hydrogeochemical character at the water table interface at different saturation levels of the aquifer. As mentioned above, this groundwater should correlate hydrogeochemically with recent recharge-producing rainfall surplus inputs, as the traditional piston flow mechanism will deliver different layers of recharge water on top of a quasi-stagnant saturated interface (Mazor 1997).

The results confirms temporal changes in the hydrogeochemical composition of groundwater at shallow depths (say <10 m bgl) versus those with deeper water tables are observably different. The dolomite (DLMT) aquifers reported the largest variation in this regard (Table 5.11)

Table 5.11. Hydrogeochemistry skim sampling results at monitoring site G47584, Bokfontein, Upper Kuruman River Catchment. (Recharge Terrain Type: DLMT, fractured hard rock terrain)

Date	Rwl m bgl	$\delta^{18}\text{O}$ ‰	$\delta^2\text{H}$ ‰	Cl^- $\text{mg}\cdot\text{l}^{-1}$	Na $\text{mg}\cdot\text{l}^{-1}$	NO_3^- $\text{mg}\cdot\text{l}^{-1}$	SO_4^{2-} $\text{mg}\cdot\text{l}^{-1}$
08-02-2006	3.05	-6.75	-46.61	1.8	3.6	24.8	19.0
15-08-2006	3.24	-3.08	-21.29	24.8	106.9	6.6	48.3
06-02-2007	7.93	0.67	-11.42	22.8	13.8	64.1	32.5
14-08-2007	8.85	-1.43	-5.78	24.8	14.1	74.7	28.6
13-08-2008	3.66	-3.99	-18.82	19.8	-	8.4	61.0

Site coordinates: S27.55555°; E023.54000°, 1430 m amsl.

The water table interface at the G47584 site in the catchment of the Kuruman A-Spring reports drastic variations in the hydrogeochemistry, especially on 8 February 2006. This water sample was taken a few days after a series of episodic rainfall events from the 6th of December 2007. The rainwater hydrogeochemical compositions of this recharge event are

significantly depleted/lower than values from the other rainfall periods (late 2006 to late 2008).

Hydrogeochemistry time-series variation in the Karoo Group sedimentary terrains were noted, although the variation is much smaller than the dolomite terrains as (Table 5.12).

Table 5.12. Hydrogeochemistry skim sampling results at monitoring sites in the Beaufort West area (Recharge Terrain Type: Sedimentary, fractured hard rock terrains).

Date	Rwl m bgl	$\delta^{18}\text{O}$ ‰	$\delta^2\text{H}$ ‰	Cl^- $\text{mg}\cdot\text{l}^{-1}$	Na $\text{mg}\cdot\text{l}^{-1}$	NO_3^- $\text{mg}\cdot\text{l}^{-1}$	SO_4^{2-} $\text{mg}\cdot\text{l}^{-1}$
(i) Monitoring site G29870BE in De Hoop Poort area.							
02-04-'06	5.50	-5.2	-26.9	35.0	98.3	9.3	29.2
08-05-'06	5.71	-5.5	-31.0	34.9	99.7	8.6	28.1
08-11-'06	6.30	-4.6	-25.6	35.2	74.2	9.7	29.2
28-05-'07	7.38	-5.2	-24.8	35.7	28.9	5.1	36.6
15-10-'07	7.50	-5.2	-34.8	36.6	26.5	7.5	37.3
18-02-'08	5.90	-5.6	-25.9	39.5	-	32.0	34.9
03-06-'08	6.32	-4.8	-36.7	35.4	-	8.9	40.9
04-11-'08	6.83	-7.6	-39.3	35.5	-	8.5	40.5
28-01-'09	7.46	-5.9	-32.6	41.4	57.00	2.0	50.1
(ii) Monitoring site AT01 on Abrahamspoort, Nuweveld Mountains.							
07-11-'06	5.88	-4.69	-25.08	7.6	9.5	1.0	8.7
29-05-'07	6.87	-6.86	-39.68	6.9	9.9	1.8	15.3
16-10-'07	6.70	-5.63	-25.91	7.1	6.0	3.7	16.7
04-06-'08	7.00	-7.87	-43.47	6.4	-	1.9	15.3
05-11-'08	7.21	-7.81	-41.19	9.5	-	3.0	26.6

Time-series data from the Ghaap Plateau and the two monitoring sites in the Karoo environ (in Tables 5.11 and 5.12 respectively), report the following hydrogeochemical responses in terms of water table (i.e. aquifer saturation level) variations:

- After a series of episodic rainfall events instigating individual water table rebounds totaling ≈ 9.7 m, the hydrogeochemical composition at monitoring site G47584 is significantly different compared to average periods. The Cl^- variation, for example, is $21.1\text{mg}\cdot\text{l}^{-1}$ lower than the medium-term background value of $22.9\text{mg}\cdot\text{l}^{-1}$ for the period 2006-2008. The rainfall ESI's for that specific rainfall period ($^{18}\delta=-41.2\text{‰}$, $^2\delta=-7.2\text{‰}$;) correlates with the groundwater ESI composition of $^{18}\delta=-46.6\text{‰}$ and $^2\delta=-6.8\text{‰}$;

- The groundwater hydrogeochemistry seems to change significantly in cases where the aquifer saturation levels increases substantially after extraordinary (episodic) rainfall events. For example, in the Kraaipan hard rock terrain just north of Stella (Northern Cape Region), a water table rebound of ≈ 22 m has changed the local aquifer Cl^- content from $\approx 53 \text{ mg}\cdot\text{l}^{-1}$ to $\approx 14 \text{ mg}\cdot\text{l}^{-1}$ after a receiving 267 mm over 5 days; and
- Hydrochemistry values in the Karoo sedimentary environment tend to vary insignificantly probably due to a retarded lateral discharge from the direct recharge areas to the surrounding sub-reservoirs. Time-series Cl^- variations in the Karoo peneplain (1021 m amsl) and the Nuweveld Mountains (1691 m amsl) at Beaufort West were observed as $37.2 \text{ mg}\cdot\text{l}^{-1}$ (SD=2.2) and $7.3 \text{ mg}\cdot\text{l}^{-1}$ (SD=1.0) between 2006 and 2009 respectively.

To conclude, these temporal hydrogeochemical fluctuations are neither specifically cyclic, nor seasonal, and respond merely as erratic changes with different retention factors⁵⁶; some of which can last several years. These hydrogeochemical fluctuations in aquifer systems as observed following on high rainfall events, are indicative of significant amounts of surplus rainwater recharge stored in the UZR for some time. The hydrogeochemistry retention factors of the newly recharged groundwater in dolomitic aquifer systems is much shorter than that of aquifer systems consisting of clastic sedimentary rocks types, like the Karoo Supergroup sediments and basement granites/BIF's (Table 5.12).

5.3.4.2 Vertical (depth) Variations in Hydrogeochemical Composition.

The previous section deliberated the on groundwater hydrogeochemical fluctuations at the water table interface over time; thus reporting the effect of direct rainwater recharge at fluctuating upper boundary of a SZ. Water table rebounds of several meters following episodic rainfall events, points to the premise that in a hard rock environment any local, vertical percolating recharge-producing rainfall surplus rainwater should accumulate for some time as a distinctive layer and forms a new, shallower water table interface.

⁵⁶ A phenomenon where the hydrogeochemical composition of the groundwater remains in its altered state for a period before it mixes with the surrounding resident groundwater during the water table rebound recession period or blending during diffuse lateral flows.

The effect of multi-modal recharge mechanisms in a fractured-weathered unsaturated zone will probably report a complete mix of different recharge-producing rainfall surplus events with depth (Sami 1992). The storativity of the UZR plays an important role in the hydrogeochemical evolution of the infiltrating recharge-producing rainfall surplus. Van Tonder and Bean (2003) noted that in the case of inert fractured hard rock terrains such as the quartzites of the Aus Mountains (Windhoek, Namibia) and most likely the Table Mountain Group (Western- and Eastern Cape), the unsaturated zone has minute storage capacity. Rooting zones are not well developed and limited to isolated small valleys. The downward flux could therefore be radically enhanced through macro-pores under gravity feed. In this extreme case, the newly recharged groundwater's hydrogeochemical signature should bear little resemblance to (i) effective run-off and depression evaporation (rapid recharge via preferred pathways) and (ii) transpiration processes (bypassing the limited rooting zone).

In a rock matrix where bypass flow (via macro-pores) and diffuse flow (via micro-pores) occurs simultaneously, the hydrogeochemical signature may be muddled, and needs to be acknowledged when groundwater Cl^- is used as a tracer. The vertical hydrogeochemical trends, for example, should highlight on the one hand (i) retarded, matrix type recharge, allowing a smooth blending with the resident aquifer water, and on the other hand, (ii) a fast, preferential pathway recharge mechanism, which will probably injects the recharge rainwater into both unsaturated and SZ and will form a zone with complete different hydrogeochemical characteristics.

Research by the Department of Geohydrology at the Institute for Groundwater Studies (IGS) test site at the University of the Free State, suggests groundwater Cl^- concentrations vary between the matrix and open fractures. Matrix Cl^- concentrations are about four times (4x) higher than those measured in the fractures (mainly horizontal bedding plane jointing) on the same site (Van der Merwe 2008). Vertical fracturing, which is very difficult to identify in vertically drilled water boreholes, is the only possible link from surface down to these horizontal features. These fractures allow recent low Cl^- rainwater to flow directly to the deeper bedding plane joints as bypass flow. The elevated Cl^- concentrations in the matrix flow component could be the net Cl^- deposition introduced through diffuse recharge after evaporation from depression storage and the effect of the rooting zone transpiration.

Research literature suggests that the actual recharge-producing rainfall surplus only arrives at the water table interface once the water table trend shifts to a recession phase (Gieske 1992). This is probably the case when soil/micro-fracture moisture under renewed field capacity situation from earlier infiltration events, migrates under piston flow conditions. In fractured hard rock cases, a significantly larger bypass flow regime overrides the former flow mechanism. It is therefore possible that even the first recharge-producing rainfall surplus during the onset of the rainy season could reach the water table interface through a sufficiently dried-out unsaturated zone in non-porous crystalline rock formations (i.e. hypabasal and quartzitic rocks).

When profiling below the water table interface is performed, a series of hydrogeochemical different horizons are intercepted which represent previous recharge-producing rainfall surpluses. Hydrogeochemical profile sampling was therefore performed at hard rock terrains utilizing the column sampling technique (Figure 5.10).

These vertical groundwater profiles were analyzed to study the integrity of the vertical hydrogeochemical character below the water table interface. The Cl^- tracer and ESI's were used as indicators.

The results were quite surprising and reported basic three different types of Cl^- profiles (Figure 5.10). It should be noted that the Cl^- detection level for these analyses is $0.1 \text{ mg} \cdot \text{l}^{-1}$; thus differences as high as $\pm 45\%$ versus the background mean values, are most likely an indication of recently recharged rainwater through multi-modal (bypass) flow mechanisms.

These chloride profiles can roughly be classified in three potential flow mechanisms in direct recharge terrains as follows:

- (C1): Chloride profiles showing a prominent increase with depth (Figure 5.10(a)), probably indicating a mixing process between recently recharged water with deeper, mature type aquifer water. These conditions were observed during declining water table behavior.

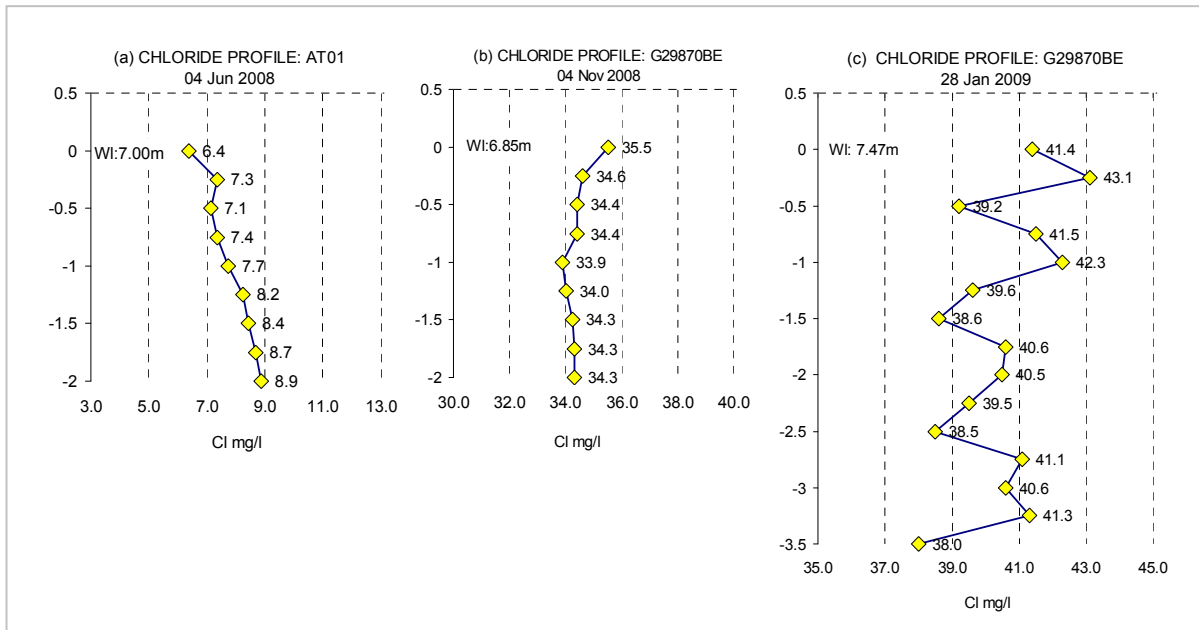


Figure 5.10. In-situ chloride profiles (Cl^- , $\text{mg}\cdot\text{l}^{-1}$) taken from the Beaufort West monitoring terrains: (a) from the Nuweveld Mountain terrain and (b) and (c) from a Karoo peneplane terrain.

- (C2): Chloride profiles almost stagnant with depth; thus a final mixture between newly recharged and resident water in the upper SZ (Figure 5.10(b)). These conditions were observed during periods with almost stagnant water table trends and occurred towards the end of the dry period (summer rainfall regions).
- (C3): Chloride profiles report slightly decreasing concentrations with depth, but with superimposed lower/higher curvatures (Figure 5.10(c)). These Cl^- profiles probably report multi-modal recharge events which during effective recharge periods generate different layers of recharged water in the upper saturated aquifer levels, and they coincide in time with prominent water table rebounds.

The Cl^- profiles presented in Figures 5.10(b) and 5.10(c) is from the very same borehole, but different periods.

The Cl^- profiles from monitoring site G29870BE for November 2008 and January 2009 are quite different and coincide with C2 and C3 respectively. The January 2009 profile is

probably a typical example of pulsating recharge events resulting in several different zones with lower Cl^- concentrations. The background Cl^- shift from $\approx 34 \text{ mg}\cdot\text{l}^{-1}$ in November 2008 to $40 \text{ mg}\cdot\text{l}^{-1}$ is probably the addition of the dry Cl^- deposition from the previous season washed down by the first rainfalls of the new season.

Several profiles with sharp spiky behaviors were observed (Figure 5.11). In this case a prominent low ($-23.8 \text{ mg}\cdot\text{l}^{-1}$) Cl^- zone occurs 1.25 m below the water table interface sitting at 16.9 m.

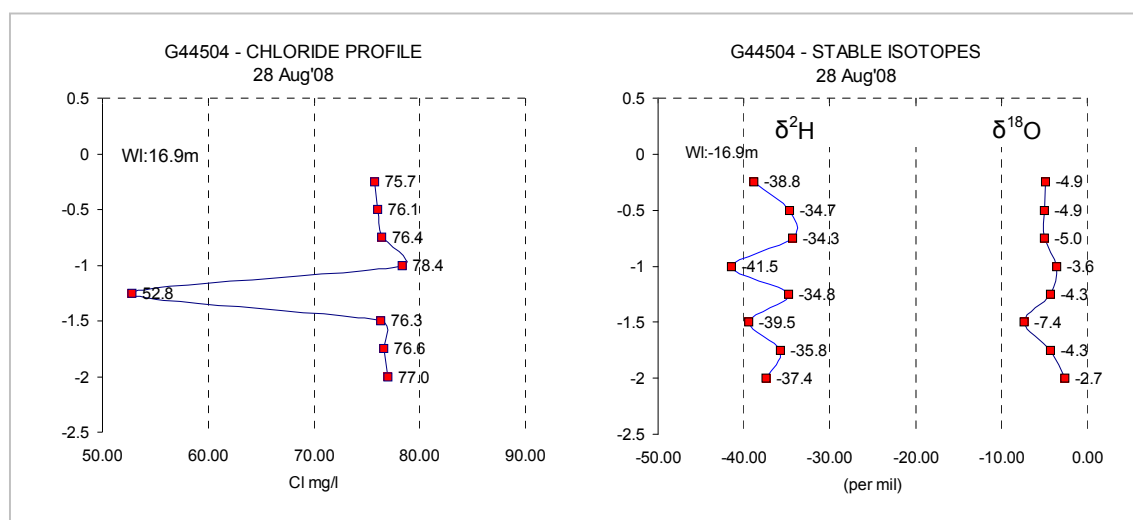


Figure 5.11. Hydrogeochemical profile from the Stella, Midkopreen monitoring terrain showing Cl^- and ESI profiles from below 16.9 m bgl.

Vertical hydrochemistry profiling enables examination of the upper transient flow regime, especially in direct groundwater recharge terrains, and demonstrates multi-modal recharge mechanisms in the fractured hard rock environment. In the case of high intensity, episodic rainfall events where the recharge-producing rainfall surplus can be several centimeters, it resets the groundwater hydrogeochemical profile accordingly.

The ESI's for this particular profile plots as slightly evaporated water except for the sample just below the low Cl^- spike (Figure 5.12).

The $\delta^{18}\text{O}$ (‰) profile reports a slightly depleted isotopic character for the water at this depth (1.5 m) which is rather difficult to explain as there is a unique relationship between depleted Cl^- and depleted ESI's in rainwater (observations by author in this study).

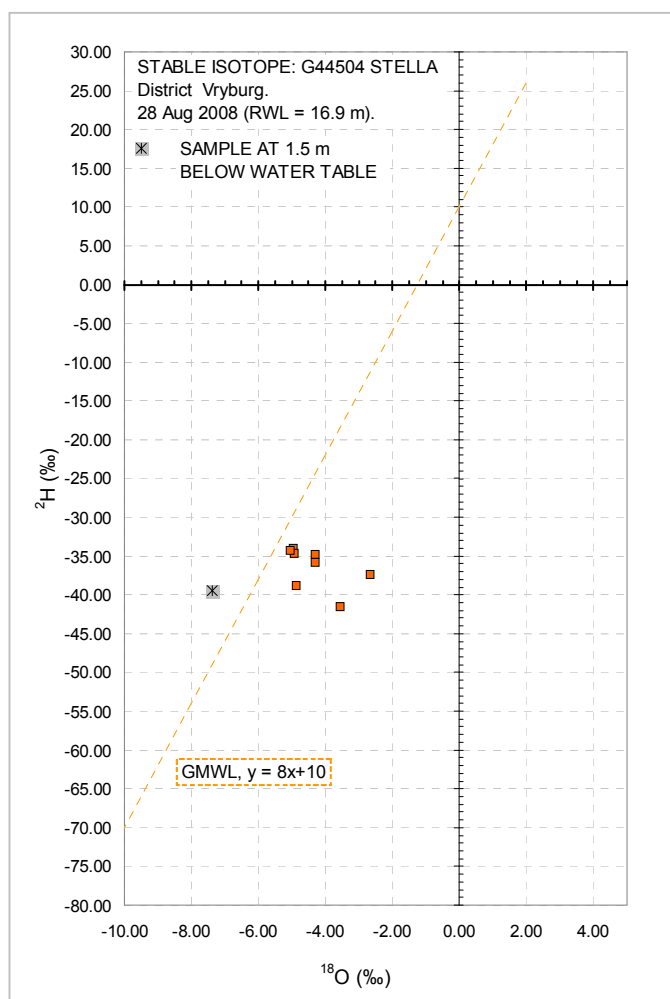


Figure 5.12. The Harmon Craig diagram ($\delta^2\text{H}$ - $\delta^{18}\text{O}$) illustrating the ESI composition of a 2 m groundwater profile at the G44504 Midkopreen monitoring site at Stella.

This shift was also observed in several other Cl^- - ESI profiles, especially areas with thicker (>10 m) unsaturated zones, and is probably the result of residual Cl^- residing in these thicker, unsaturated zones. What is unique about this site is that it is situated adjacent one of the many local depressions (± 20 m diameter pans); thus it is expected to portray a dominating evaporative-background hydrogeochemical signature.

The Cl^- and ESI profiles in an area with a thick (± 21 m) unsaturated zone consisting of fractured and weathered Karoo Supergroup sediments on the peneplain just below the Nuweveld Mountain escarpment at Beaufort West are illustrated in Figure 5.13.

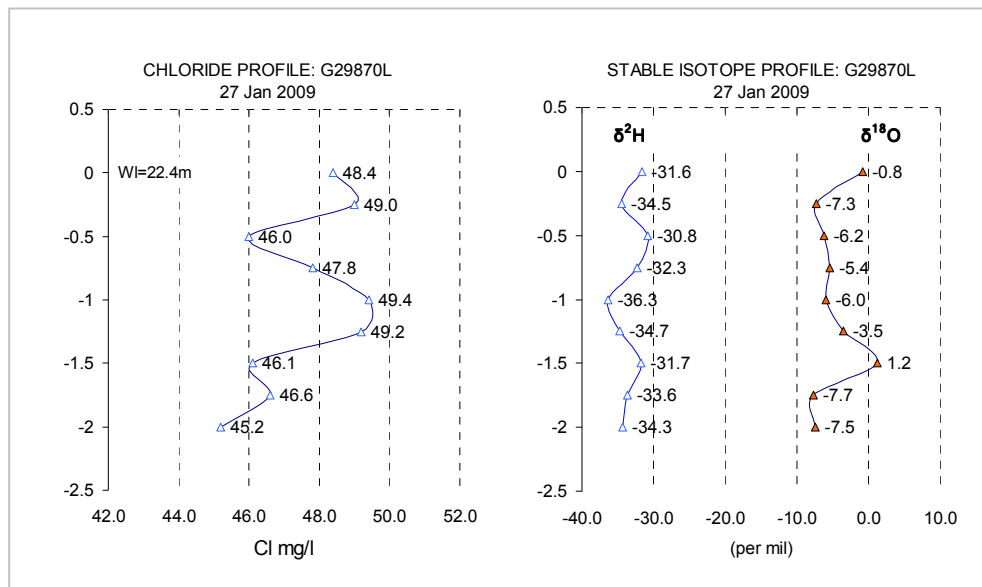


Figure 5.13. Hydrogeochemical profile from the De Hoop, G29870L monitoring site showing Cl^- and ESI profiles from below 22.4 m bgl.

The water table interface oscillation at this monitoring site is high (up to 7.8 m) for the Karoo hydrogeological environment, and indicates a considerable timely vertical migration of a Cl^- front, regardless of what Cl^- -values is introduced by the infiltrating recharge-producing rainfall surplus. ESI's, on the other hand do not have a memory in conditions where the UUZR significantly dries-out during dry seasons, in contrast to Cl^- which tends to build up and to become remobilized once newly recharged rainwater moves through the unsaturated zone.

The Cl^- profile for the G29870L monitoring site reports a relatively higher concentration around 1.0-1.25 m below the water table interface (22.4 m bgl). From this depth, the Cl^- pattern behaves according to the C3 condition mentioned above (i.e. depleting with depth). The ESI profile from -1.0 m reports a strong evaporative signature up to -1.5 m and is quite prominent on the $^{18}\delta$ profile. The isotopic composition of the groundwater from -1.0

to -1.5 m bgl signifies a strong evaporation signature with a d -access of -32. The $^{2}\delta$ versus $^{18}\delta$ plot for the above-mentioned data set is illustrated in Figure 5.14.

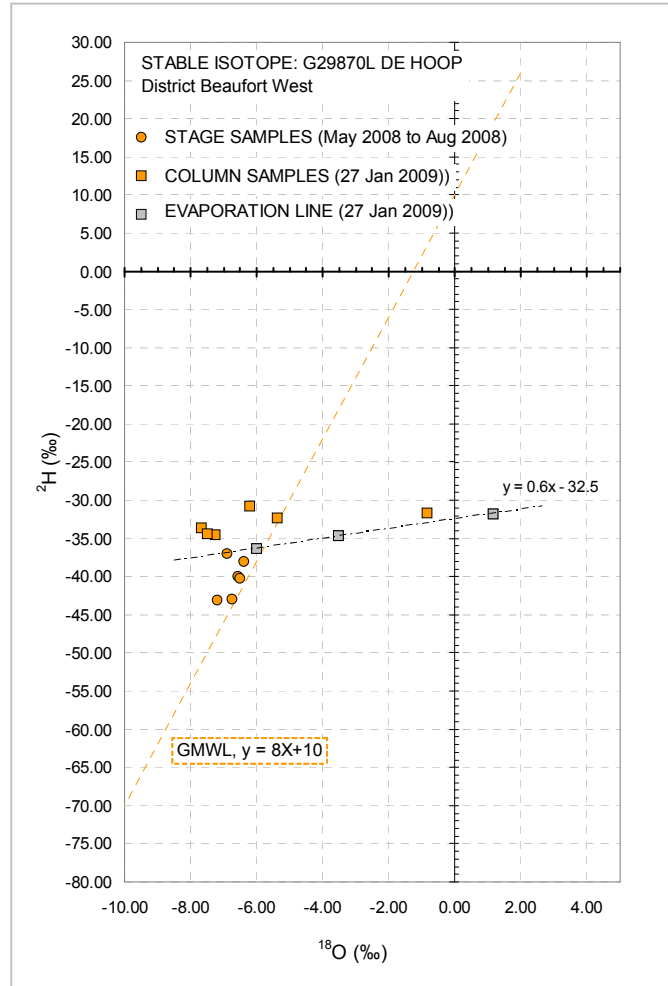


Figure 5.14. Hydrogeochemical profile from the De Hoop, G29870L monitoring site showing Cl^- and ESI profiles from below 16.9 m bgl.

A rational explanation for this extreme evaporative component in the groundwater profile lies in the recharge mechanism driven by the pattern of the incoming rainfall. Episodic rainfall events portray extreme depleted isotopic compositions ($^{18}\delta = -10\text{‰}$, $^{2}\delta = -65\text{‰}$). In contrast, the average rainfall's isotopic composition plots around $^{18}\delta = -5\text{‰}$, $^{2}\delta = -30\text{‰}$, which almost indicates the departure of the E.L. as observed on some of the monitoring terrains in this study.

The evaporated component of the groundwater profile obviously represents recharge-producing rainfall events of a series of lower and probably intermittent rainfall events recharging in these fractured hard rock environments but under high evaporative climate conditions.

The vertical profiles (Cases 2 and 3) indicate that the hydrogeochemical character differs over time as well. Timing of the groundwater sampling process to assess episodic recharge events is important and should be performed when the actual recharge mode is activated. This is difficult to achieve under physical sampling conditions as the recharge events are episodic and occur in rather short pulses. A sampling programme should therefore be initiated where a water table rebound scenario can be sampled automatically without requiring time consuming manual sampling.

The stage sampling technique was developed and tested on areas where multi-modal recharge is expected to take place according to the hyetograph-hydrograph information. One specific site is the De Hoop Poort monitoring terrain, in the Karoo peneplain northwest of Beaufort West. The hydrogeochemical analyses of this sampling event, which cover a ≈ 33 day period during January-February 2008 following an episodic rainfall event that occurred in the area is presented in Table 5.13.

It also includes some skim sample analyses from pre- and post January-February 2008 to illustrate the background trends taken over a longer period.

The analysis indicates that a significant depleted Cl^- recharging groundwater (≈ 37.7 to $21.8 \text{ mg}\cdot\text{l}^{-1}$) was sampled around the 6th of February 2008 by the stage sampling unit after two 50 mm rainfall events occurred on the 14th and 27th of January 2008 respectively. Both rainfall events occurred within a period of 24 hours, and reported rain rates in the order of 8.0 and $2.0 \text{ mm}\cdot\text{hr}^{-1}$.

This particular case demonstrates the groundwater recharge response initiated by an episodic rainfall event in direct recharge terrains. In the case of episodic rainfall events, the preferential component of the multi-modal recharge mode is most likely the biggest due to the volume of recharge-producing rainfall surplus and the high rain rates associated with these events.

Table 5.13. Results of stage sampling programme at monitoring site G29870BE in De Hoop Poort (Type: Karoo sedimentary hard rock terrain).

Date	Rwl m bgl	$\delta^{18}\text{O}$ ‰	$\delta^2\text{H}$ ‰	Cl^- $\text{mg}\cdot\ell^{-1}$	NO_3^- $\text{mg}\cdot\ell^{-1}$	SO_4^{2-} $\text{mg}\cdot\ell^{-1}$
28-05-'07	7.38	-5.2	-24.8	35.7	22.5	36.6
15-10-'07	7.50	-5.2	-34.8	36.6	33.2	37.3
14-01-'08	7.40	-6.0	-34.7	39.2	170.2	50.1
26-01-'08	7.10	-5.6	-34.1	39.9	45.5	48.1
31-01-'08	6.80	-4.9	-34.7	37.7	46.4	43.2
06-02-'08	6.50	-4.8	-36.1	21.8	110.5	21.9
10-02-'08	6.20	-4.0	-36.7	39.8	42.0	59.7
18-02-'08	5.90	-5.6	-25.9	39.5	141.4	34.9
03-06-'08	6.32	-4.8	-36.7	35.4	39.3	40.9
04-11-'08	6.83	-7.6	-39.3	35.5	37.6	40.5
28-01-'09	7.46	-5.9	-32.6	41.4	8.8	50.1

The shaded section represents the water samples collected with the stage sampling technique (Section 2.7.7.3).

The analytical package presented in Table 5.13 indicates a corresponding lower value for SO_4^{2-} at -6.50 m bgl and as with Cl^- marks the lowest value recorded over the whole monitoring period between 2006 and 2009. The elevated NO_3^- concentration does not correspond logically as these spikes could be the result of surface contamination in the Karoo environment. Both Cl^- and SO_4^{2-} do not indicate this; in fact the $r\text{SO}_4^{2-}/r\text{Cl}^-$ ratio's for the monitoring site are above 1.00 (HARmean = 1.14, STDEV = 0.2), which indicate direct recharge conditions. The high NO_3^- values reported in Table 5.13 are not clear, as the PO_4^- concentration did not report any secondary pollution (bird droppings, etc).

The Cl^- concentration of the water table rebound is illustrated in Figure 5.15. This illustration portrays the saturated profile containing a section of recharge groundwater with a characteristic depleted Cl^- concentration of $\sim 21 \text{ mg}\cdot\ell^{-1}$.

Although the isotopic signature of the recharge-producing rainfall surplus is not altered by a fractionation process due to transpiration only passing through the rooting zone, the infiltrating rainwater may intercept a higher concentration of residual Cl^- in the LUZR and appear to be out of phase with the original depleted hydrogeochemical composition.

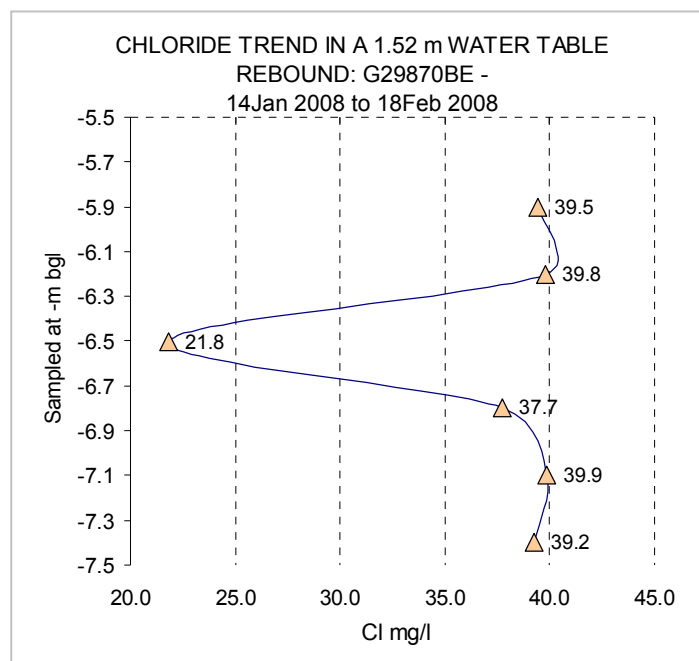


Figure 5.15. Illustrating the groundwater Cl^- trend in a 1.52 m water table rebound logged with the stage sampling procedure, De Hoop Poort, G29870BE.

To conclude, timing of the groundwater profile sampling is quite important to capture the actual recharge-producing infiltrating rainwater. Alteration to the original recharge-producing rainfall surplus manifests during the water table rebound. Under a multi-modal recharge mechanism, it could be argued that the contribution of the bypass flux manifests during the early part of the rising water table interface, to be followed by the slower matrix flux in the later part of the rebound. Sampling of the saturated zone water column should therefore cover the three tier intervals of the HC.

5.4 CHLORIDE MASS BALANCE APPLICATION.

5.4.1 Background.

The Cl^- ion has been applied as a successful tracer in multiple tracer profiling during the GRES⁵⁷ I and II studies in Botswana. In the previous century, the application of the CMB application was limited to isolated research projects, due to the lack of specifically local rainwater hydrogeochemical data. The accuracy of rainwater Cl^- concentration tolerances

⁵⁷ GRES: Groundwater Recharge and Resources Assessment in the Botswana Kalahari, Rep. of Botswana.

was roughly $1 \text{ mg} \cdot \ell^{-1}$ which could result in significant errors when applying the CMB principle.

One of the objectives for this study therefore was to initiate a monitoring programme to address the backlog on wet and dry Cl^- deposition on South African soil, by (i) logging the actual wet and dry Cl^- input during rainy and dry seasons on a national scale and (ii) investing in dedicated sampling of groundwater during recharge and recession periods.

5.4.2 Traditional Application.

The basic principle of the CMB application⁵⁸ is that any tracer introduced by the initial infiltrating rainwater will remain at that concentration when infiltrated into the unsaturated zone. Natural processes (viz. ET) distill water from the UUZR and the hydrogeochemical composition gets enriched. The ratio between the initial rainwater Cl^- concentration and the soil/regolith moisture Cl^- concentration provides a measure of ET (Mazor 1997).

Moisture samples can be obtained by using auger or hollow-stem-auger drilling technique to collect moisture from the vadose zone (gravitational/pellicular water) and analyzed (after vacuum distillation) for the required tracer or other particular hydrogeochemical constituents (stable or radiogenic isotopes (Gieske 1992)).

In the semi-arid and arid regions of southern Africa, the aquifer systems are classified as hard rock formations and with limited soil/regolith development on moderate to high relief zones. Application of the CMB principle in its traditional format therefore is not possible due to the limitation of auger or hollow-stem-drilling in hard rock terrains. By substituting the Cl^- content in the soil moisture (C_{SM}) with the Cl^- content in the groundwater C_{G} , the total recharge rate ($\text{mm} \cdot \text{yr}^{-1}$) can be estimated (Xu and Beekman 2003).

The typical vegetation model for the semi-arid to arid regions of southern Africa is grassland savanna with intense shrubs invasion, which have developed intense, deep rooting systems (Section 4.4.2.1). Two effective horizons were classified by Willemink (1988), (i) UUZR containing the rooting zone which is fully imbedded into the unsaturated portion of the UFWZ and (ii) LUZR representing the unsaturated zone between the rooting zone and

⁵⁸ Based on conservation of mass: In any isolated system the total mass remains constant in time.

the water table interface. The dimensions of the latter zone are highly variable in the semi-arid hard rock cases, due to the large water table fluctuations following a major recharge event.

The application of the CMB principle in this study has therefore been limited to the straightforward application of an ET_{INDEX} as proposed by Mazor (1997) and groundwater recharge (R_T) as applied in the literature (Eriksson and Khunakasem 1969; Johnston 1987; Nkotagu 1997; Sukhija et al. 2000 and Ting et al. 1998). All these applications start from the basic assumption that there exists a balance between total Cl^- deposits (TC) at ground surface and what Cl^- concentration finally resides in the groundwater (C_G).

5.4.3 Application: Rainwater - Groundwater Cl^- Balances.

Considering the vertical distribution of Cl^- concentrations from ground surface to the groundwater table, the total vertical flow of recharge-producing rainwater surplus with the condition that no *in situ* Cl^- is added from the aquifer itself, the rate of recharge R_R can be estimated from the groundwater Cl^- concentration C_G by

$$R_R = C_G C_P - \frac{dC_G}{dx} \int_0^x \frac{C_P (dx)}{C_G^2} \quad (5-3)$$

where C_G = the groundwater Cl^- concentration ($mg \cdot l^{-1}$), C_P = the rainwater Cl^- concentration ($mg \cdot l^{-1}$), dC_G/dx is the change in the groundwater Cl^- concentration from the intake area to the sample area.

This expression (Johnston 1987) applies strictly where the aquifer model is subjected to a horizontal flow regime as can be expected when having a borehole as the only access to the aquifer down gradient from a direct intake zone, the hard rock window area. The latter region operates under the condition that no lateral Cl^- from adjacent vertical intake areas is added to the horizontal flux, thus from a Cl^- input point of view C_G is uniform in terms of the multi-modal concept (C_{Gm} and C_{Gbp}); a condition proved by the time-series logging of C_G (Section 5.3.4). In this case,

$$R_R = \frac{C_P}{C_G} \approx ET_{\text{index}} \quad (5-4)$$

which is the same ET_{INDEX} relation proposed by Mazor (1997).

It has been observed (Section 5.1.5) that the weighted average Cl^- input from summer rainwater over the HC varies significantly, with the peak rainfall period (Jan_n to Mar_n) reporting the lowest (viz. depleted) Cl^- concentration levels ($\approx 0.4 \text{ mg}\cdot\ell^{-1}$), especially those episodic high rainfall events which generate recharge-producing rainfall surpluses.

It will be demonstrated presently that the most effective groundwater recharge takes place during the peak rainfall period as indicated by the hyetograph-hydrograph sets. It is to be expected, therefore, that the actual Cl^- dosing to the groundwater system will take place during this period, and should be a significant flushing of the total wet and dry deposition from the previous early and dry intervals.

The recharge estimation, R_R is calculated according to the following expression (Nkotago 1996):

$$R_R = P_R \left(\frac{1}{n} \right) \left(\sum_{1}^n \left(\frac{C_P}{C_G} \right) \right), \quad (5-5)$$

where P_R = the rainfall depth (mm), n = the number of observed incidences, C_P = Cl^- concentrations ($\text{mg}\cdot\ell^{-1}$) in the rainwater and C_G = Cl^- concentrations ($\text{mg}\cdot\ell^{-1}$) observed in the groundwater. All Cl^- values are harmonic mean values.

The Cl^- concentration in groundwater is a factor of the multi-modal flow regime of a particular study area and is rather difficult to average over large areas. The Cl^- concentration of that portion of the aquifer receiving its recharge from adjacent aquifers (Willemink 1988), is governed by Eq. 5-3. Its application requires sufficient sampling of the lateral flow regime, though, along a known trajectory, which was not the scope of this study.

On a national scale, rainwater hydrochemical data represents only a fraction of what is currently available for groundwater. Since the CMB application has been applied as one of the methods for groundwater recharge estimations in southern Africa, unrealistic extrapolations from a few isolated point observations were the only solution to generate a large

enough spatial coverage necessary for regional groundwater recharge estimations. These statistically derived Cl^- values could differ significantly from the actual Cl^- input in the recharge terrains.

5.4.4 *Atmospheric Chloride Depositions.*

The Cl^- cycle in the HC is considered to be relatively conservative as the only primary source for this ion is from the evaporated maritime water. The atmospheric moisture load varies significantly over the HC's wet/dry periods which influence the time-series concentration of Cl^- on meteoric water and the airmass. During the dry, winter/summer seasons, Cl^- will still be part of the atmospheric mass load, providing a continuous feed of substances settling on the earth's surface. During recharge-producing rainfall surplus, this dry-fallout will be captured and fed into the underdrainage.

For the CMB application, one should consider the total Cl^- deposition (TC) which includes the dry atmospheric outfall occurring during the dry periods of the HC. Estimation of this component of the Cl^- algorithm is quite complex, especially the sampling procedure. Literature references revealed that by using the same sampling devices under controlled conditions (sampling procedures), provides an acceptable value for the dry Cl^- deposition (Gieske 1992).

The results of the calculated dry Cl^- deposition for the South African monitoring terrains is illustrated in Table 5.14 and accounts for $\approx 25\%$ of the TC which correlates with values proposed by Gieske (1992) of 20% for studies done in the Botswana Kalahari Region.

Total Cl^- input, ($\text{mg}\cdot\text{m}^{-2}\cdot\text{y}^{-1}$) estimated for the semi-arid monitoring sites correlates well with values obtained by Gieske (1992) in the Botswana studies. Average wet Cl^- depositions vary from $113 \text{ mg}\cdot\text{m}^{-2} \text{ y}^{-1}$ (Maun Airport) to $645 \text{ mg}\cdot\text{m}^{-2} \text{ y}^{-1}$ (Jwaneng (A1)). Gieske (1992) also mentions two TC values observed by Eriksson (cited in Gieske 1992) for Pretoria ($330 \text{ mg}\cdot\text{m}^{-2}\cdot\text{y}^{-1}$) and Bloemfontein ($510 \text{ mg}\cdot\text{m}^{-2}\cdot\text{y}^{-1}$) which correlate fairly well with individual modern values from the different hard rock monitoring terrains in this study, i.e. 400 to $600 \text{ mg}\cdot\text{m}^{-2}\cdot\text{y}^{-1}$.

Collection of the airborne dry Cl^- component during the winter and summer dry periods was done by using the same apparatus for logging and sampling the rainfall and rainwater

during the wet seasons. Although there are cases of rain events occurring during the dry period, the principle adopted by Gieske (1992) and Selaolo et al. (1994) was used in a similar way, i.e. using the rainwater collectors for collecting TC.

Table 5.14. Total wet and dry Cl^- deposition ($\text{mg}\cdot\text{m}^{-2}\cdot\text{y}^{-1}$).

Season	KRM ⁽¹⁾	KRM ⁽²⁾	B-West ⁽³⁾	B-West ⁽⁴⁾	Stella ⁽⁵⁾	Pta East ⁽⁶⁾
2002-'03		338	161	269	500	319
2003-'04	331	394	170	289	298	338
2004-'05	167	208	318	384	507	427
2005-'06	145	608	197	213	381	238
2006-'07	339	310		285	283	197
2007-'08		256			185	
H-Mean ⁽⁷⁾	212	314	197	278	318	282
Dry ⁽⁸⁾		80	56	61	186	90

⁽¹⁾ Kuruman, Asbesberg on the farm Carrington (mountain region);

⁽²⁾ Kuruman, Ghaap Plateau on the farm Bokfontein (peneplane);

⁽³⁾ Beaufort West, Nuweveld Mountains on the farm Highlands (mountain region);

⁽⁴⁾ Beaufort West, De Hoop Poort on the farm De Hoop (peneplane);

⁽⁵⁾ Stella area (peneplane, combination of two monitoring sites);

⁽⁶⁾ Pretoria East, Lynnwood monitoring site (high relief area).

⁽⁷⁾ Includes the dry component during the wet season i.e. these figures are the TC.

⁽⁸⁾ Harmonic mean of Cl^- deposits during dry season (A, M, J, J, A and S).

5.4.5 Chloride Concentration in the Unsaturated Zone⁵⁹.

Observations by Sharma and Hughes (1985) in deep sandy soils in Western Australia, illustrated that water flux through the unsaturated profile does not occur uniformly. This observation subsequently applies for southern African hard-rock systems as well, and could eventually be considerably enhanced due to the fractured nature of the unsaturated profile in the hard rock terrains (viz. UZR).

In the above-mentioned study, it was stated that Cl^- concentrations in deep profiles below the rooting zone are much higher in comparison with the average C_G , which suggests that low Cl^- containing water is injected directly to or close to the phreatic surface.

⁵⁹ Refer to the interface or zone between the base of the rooting zone and the groundwater table interface, viz. the LUZR.

As previously mentioned, obtaining moisture samples from the hard rock section of the UZR is not possible. In addition, a large portion of the recharge-producing rainfall surplus enters the unsaturated/saturated zone as bypass flow. The only way to capture whatever surplus⁶⁰ rainwater is bypassing the rooting zone, is to sample regularly at the water table interface by using the skim sampling methodology (Section 2.7.7.3). Obviously, and as observed on the hydrograph sets, water table rebounds of several meters occur, which indicate a reasonable change in the aquifer storage, containing the newly recharged groundwater.

Interpretation of the hyetograph-hydrograph sets actually indicates that the interaction between rain events and water level responses fall into the category of hours/days. It is therefore quite possible that a large fraction of the recharge-producing rainfall surplus in fact runs down the macro pores and recharges the aquifer within hours after a rain event.

This phenomenon is a characteristic of fractured hard rock terrains and represents the bypass flow component. The CBM application should therefore address this component as an addition to the algorithm as will be demonstrated presently.

5.4.5.1 Bypassing the Rooting Zone.

Bypass flow, according to Ting et al (1998) the total recharge rate (R_T , in $\text{mm}\cdot\text{yr}^{-1}$) can be approximated by:

$$R_T = \frac{P_{\text{Reff}}^{\text{bp}} C_P}{C_{\text{Gbp}}} + \frac{P_{\text{Reff}}^{\text{m}} C_P + D}{C_{\text{Gm}}}, \quad (5-6)$$

where P_{Reff} = effective rainfall input, viz. the episodic rain event, C_P = Cl^- concentration in rain event, C_{Gbp} = Cl^- concentration of bypass (macro-pore) flow component and C_{Gm} = Cl^- concentration of diffuse flow from hard rock matrix (micro-pores), and D = the dry Cl^- input from the previous dry cycle.

⁶⁰After evapotranspiration has altered the hydrogeochemical composition of the recharging rainwater.

Bypass flow complicates the estimation of the total recharge rate R_T considerably, as the rainwater Cl^- concentration, C_P is in fact of the same order as the Cl^- flux entering the groundwater C_{Gbp} , $C_{Gbp} \approx C_P$, thus the recharge rate could be as high 100%. It is required, therefore, that the bypass flow mechanism should be addressed as part of a discrete multi-modal flow regime.

Long-term recharge rates were estimated from the three tier seasonal climate zones on which the rainwater-groundwater monitoring interval is based. The following algorithm was adopted from Selaolo et al. (1994) and applied using data from the summer semi-arid monitoring sites⁶¹ categorized in three intervals, (i) early, (ii) peak and (iii) dry:

$$\overline{R_T} = \frac{(\overline{P_{EP}} \cdot \overline{C_{EP}}) + (\overline{P_{PP}} \cdot \overline{C_{PP}}) + (\overline{P_D} \cdot \overline{C_D})}{\overline{C_G}}, \quad (5-7)$$

where,

P_{EP} = mean rainfall depth during the early rainfall season, 165 mm;

C_{EP} = rainwater Cl^- concentration during the early rainfall input, $0.76 (\pm 0.09) \text{ mg} \cdot \ell^{-1}$;

P_{PP} = mean rainfall depth during the peak rainfall season, 206 mm. this portion of the groundwater recharge represents a significant portion of the total bypass flow contribution;

C_{PP} = rainwater Cl^- concentration during the peak rainfall input, $0.44 (\pm 0.06) \text{ mg} \cdot \ell^{-1}$;

P_D = mean rainfall depth during the dry rainfall season, 89 mm;

C_D = mean rainwater Cl^- concentration during the dry period, $1.04 (\pm 0.16) \text{ mg} \cdot \ell^{-1}$;

C_G = mean groundwater Cl^- concentration; and

R_T = mean recharge rate, $8 \text{ mm} \cdot \text{yr}^{-1}$ or 1.7% effective recharge.

(note, all values are harmonic mean values from 71 early, 89 peak and 111 dry individual values obtained from rainfall depth logging and LLHc analyses).

It should be noted that the recharge rate R_T is based on the long-term mean groundwater Cl^- concentration, $C_G = 39 \text{ mg} \cdot \ell^{-1}$. In the case of an episodic recharge event, the total recharge in this case is 1.7% higher in the hard rock terrains as on the adjacent soil/regolith peneplane areas.

⁶¹ Beaufort West, Kuruman, Stella, Taaiboschgroet and Kalahari West monitoring terrains.

The application of Eq. 5-7 has been adopted for all fractured hard rock terrains where the monitoring configuration allows the generation of this three-interval approach.

5.4.5.2 Impact of Multi-Modal Flow on Chloride Load in Saturated Zone.

Considering the hydrogeological nature of the UZR in the hard rock domains in southern Africa, the direct recharge flow mechanism can probably at best be approached as a multi-modal flow system. The unsaturated flux is characterized by (a) a soil/regolith/rock matrix flux (retarded, diffuse recharge: R_{SM}), (b) bypass flux (quick, preferential recharge: R_{PR}), all contributing to (c), the total recharge R_T .

In terms of a conservative hydrochemistry tracer such as Cl^- , it can be assumed that its concentration at water table (C_G) during non-recharge periods consist of a mature mixture between C_{Gm} and C_G . Thus, any water sample collected from the upper SZ could have hydrochemical tracer concentrations (C_G) represented by the following flow components, $C_G > C_{Gm} \gg C_{Gbp}$. This configuration is illustrated in Figure 5.10(b) (Section 5.3.4.2).

During effective groundwater recharge phases, characterized by significant water table rebounds, a portion of the unsaturated zone is saturated with newly recharged groundwater introduced directly via bypass flow; thus the hydrochemical tracer concentration of groundwater (C_G) could be represented by the following flow components, $C_{Gbp} \gg C_{Gm} \gg C_G$. This configuration is illustrated in Figure 5.10(c) (Section 5.3.4.2).

It is important, therefore, to consider the correct timing for sampling the components of the CBM attributes in rainwater as well as groundwater. To reconcile the various Cl^- inputs in the groundwater (C_G) sampling should be performed during the three basic phases of aquifer status, (i) stagnant water table periods (no-recharge occurring with $C_G \rightarrow$ a background value), (ii) effective recharge phase with prominent water table rebound and peak (direct bypass recharge with $C_G \approx C_{Gbp}$) and (iii) water table recession periods ($C_G \approx C_{Gm}$).

A good indicator when the recharge condition $C_G \approx C_{Gbp}$, pertains is to consider the groundwater isotopic composition. It was observed that in cases where episodic rainfall events are the main driver of aquifer recharge, the groundwater isotopic composition correlates with the depleted isotopic composition of the rainwater (Section 5.5.2).

5.4.5.3 Chloride Tracer Application in Hard Rock Terrains.

Differential Cl^- concentrations in groundwater due to the multi-modal flow regime through the vadose zone were observed in the monitoring sites, and are debated in Section 5.4.5.1. It is a requirement for the application of Eq. 5-7 above to obtain values for C_{Gbp} and C_{Gm} which can only be obtained through special monitoring of (i) the correlation between the isotopic composition of the rainwater and groundwater⁶², and (ii) the Cl^- concentrations of the unsaturated zone moisture, Cl^- groundwater and Cl^- rainwater.

Obtaining an unsaturated zone Cl^- concentration value is problematic in fractured hard rock terrains. The skim sampling technique was used instead as it was argued that due to the fractured nature of the UFWZ⁶³, any water retained in the unsaturated zone below the rooting zone has rather similar hydrogeochemical compositions. DTH-CC image logging did not confirm this situation although it could be identify as a slightly different hydrogeochemical composition between the skim sample (sampling 19 mm of the water table interface) and the topmost column sample (sampling 250 mm below the water table interface).

The Beaufort West, De Hoop Poort monitoring site will be used as an example with the following measured variables obtained from field observations and application of Eq. 5-6:

- P_{Reffbp} = recharge-producing surplus rainfall during episodic recharge events reported as bypass recharge interpreted from hyetograph-hydrograph combination, 145 mm;
- P_{Reffm} = recharge-producing surplus rainfall during normal rainfall events reported as medium-term (weeks-months) matrix recharge interpreted from hyetograph-hydrograph, 77 mm;
- C_P = harmonic mean Cl^- concentration in collected rainwater for the 2007-2008 season, $0.6 \text{ mg}\cdot\ell^{-1}$;
- D = harmonic mean dry Cl^- deposit from the previous dry season (April 2007 to October 2007) from bulk sampling in DWA logger/bulk sampler unit, $67 \text{ mg}\cdot\text{m}^2\cdot\text{y}^{-1}$;

⁶² To qualify multi-modal flow mechanism at recharge area.

⁶³ Expect to have a relatively high permeability coefficient (K) which enhances vertical draining.

- C_{Gbp} = Cl^- concentration of the bulk bypass macro pore recharged rain(ground)water as sampled during an episodic rain event between 14 January 2008 and 18 February 2008, with a stage sampler unit, $22 \text{ mg}\cdot\ell^{-1}$; and
 - C_{Gm} = harmonic mean of the medium-term groundwater Cl^- concentration sampled with the skim and column sampler units over two hydrological seasons, $39 \text{ mg}\cdot\ell^{-1}$.
- R_T = mean recharge rate, $6.5 \text{ mm}\cdot\text{yr}^{-1}$ which represent 3.7% of the effective rainfall between April 2007 and May 2008, but only 1.4% of the total mean annual precipitation (MAP) of 463 mm.

The episodic rain event in this case represents around 50% of the total annual recharge. In this application, a 100% dry Cl^- input from the previous dry season (April 2007 to October 2007) was applied for the dry period before any rainfall occurred. This deposit was added to the matrix flow component during the period from October 2007 to January 2008. From January 2008 until May 2008, no additional dry Cl^- was added, as it was included with the incoming rainwater, as per definition by Gieske (1992).

5.4.6 Conclusions.

Application of the Cl^- ion as a conservative tracer can be applied in the case of hard rock terrains to estimate the direct, vertical groundwater recharge component. With dedicated sampling the actual effect of dilution of the groundwater following an effective episodic rain event can be quantified in terms of additional recharge to the aquifer system.

The resulting Cl^- value of the groundwater (C_G) varies considerably in the case of multi-modal recharge flux. Variations like those used in Section 5.4.5.3 for the macro-pore and micro medium Cl^- contributions, respectively 21 and $39 \text{ mg}\cdot\ell^{-1}$, can influence the final calculated recharge percentage by almost 50%. The influence of multi-modal fluxes in hard rock terrains and correct timing of groundwater sampling needs to be considered when macro-chemistry based assessments are performed.

Although the application of the CBM principle for groundwater recharge estimations is based on long-term (9-10 years plus) averaged (harmonic mean) values, the turnover of recharge water in some hard rock intake areas is probably much shorter as seen on the

hyetograph-hydrograph diagrams. This is also confirmed by the application of the De Vries (1974; 2002) application. It will be illustrated presently that the specific drainage resistance (SDR) is much less than 100 days (Section 6.3.3); thus indicating that hard rock regions are in fact a highly effective recharge terrains and may be solely responsible for recharge to adjacent sub-reservoirs (Willemink 1988), during episodic rainfall events.

5.5 CORRELATION BETWEEN RAINWATER AND GROUNDWATER HYDRO-TRACERS.

The temporal variations in the groundwater Cl⁻ data set is ommissibly small and do not indicate any specific trend. As mentioned, no soil/matrix water from the vadose zone could be collected, due to the pre-selected hard rock terrains. In addition, many DTH-CC image logging from the DWA borehole video bank were viewed for evidence of any moisture occurring above the water table interface. Although these images are once-off recordings all year around, it seems however that the matrix flow component in semi-arid regions are intercepted by transpiration which can be as high as 80% of surplus rainwater entering the rooting zone (Le Maitre et al. 2000).

Observations from several road/ravine cuttings and DTH-CC image logging show that in a majority of outcropping hard rock cases, open joint/fractures are present in a complex geometry of vertical/horizontal joints (bedded rocks) and a crisscross jointing/fracturing structure (massive sedimentary/crystalline rocks). According to Section 4.3.1 and Price (1966) the majority of these joints developed from a combination of vertical/horizontal extension during erosional unloading. DTH-CC image logging, reports that horizontal jointing occurs at a much lower interval/depth ratio than the vertical ones, although the aperture of the former one is more than 10-times larger. Price (1966, p.117) comments that:

‘many fractures, especially in horizontally bedded series, have vertical, or near vertical dips’.

Effective matrix porosities, whether it is still in a semi-primary state as with the Triassic-Jurassic Tshipise sandstones in the Taaiboschgroet terrain, or micro-fractured Permian-Triassic Beaufort sandstone/mudstones, a bulk matrix flow mechanism are probably driving mostly the long-term, slower recharge contribution b.m.o. diffuse gravity flow.

Considering the short lag times (hours/days) between rainfall events and water table responses, direct recharge on local scale by means of bypass flow (via macro-pores) instigated by a high rated rainfall event, is probably the most effective way for groundwater is recharge in semi-arid regions. Although the volumes of rainwater directly recharged through bypass flow could be site specific, fractured hard rock terrains are in fact covering large areas; thus the spatial spread of these bypass terrains in especially the Karoo Environment is sufficient to sustain aquifer potential for extended periods.

5.5.1 Premise.

The hydrograph-hyetograph sets indicate an effective short-term aquifer recharge mode where the water table rises several meters a few hours/days after an episodic rainfall event.

The newly recharged water column in the local aquifer should contain almost all of the recharged rainwater which has bypassed the local rooting zone, in a combination of faster bypass flow (macropore) and slower diffuse drainage (matrix flow based on the piston flow principle).

The difference between matrix flow recharge and total recharge (fracture flow plus matrix flow) is at maximum in the case of fractured hard rock regions (Sukhija, et al. 2000). They consider the input from bypass flow to be as high as 50 - 65%, although in spatial context in South Africa, bypass flow regimes are actual site-specific cases, as has been observed in the monitoring terrains used in this study. Differentiating between these recharge components, using rainwater hydro-tracers as indicators, is complex, especially when tracer concentration may be influenced by accumulated superficial concentrations of the same type, i.e. when dry Cl^- gets washed down the macropores during early season infiltration (Verhagen et al. 2001).

These different inputs will have to be isolated by means of dedicated monitoring of the dry Cl^- cycle. Remote sampling of a local runoff event in a rivulet has been achieved at the De Hoop Poort monitoring site, District Beaufort West. It confirms dry Cl^- enrichment from bulk rainfall Cl^- input at 0.58 and 1.14 $\text{mg}\cdot\text{l}^{-1}$ to the first overland flow at 1.70 and

2.29 mg·ℓ⁻¹ respectively. No measurable enrichment due to evaporation was detected, as the stable isotope values for these two (2) samples confirm no evaporative signal considering their plot position on the Harmon Graig ²δ and ¹⁸δ diagram (plots on the GMWL).

In another observation, in the Spitskopreen monitoring site at Stella, ponding of local surface water run-off in small pan-like features, report Cl⁻ concentration of 30.3 mg·ℓ⁻¹ after some weeks of evaporation.

In those areas where the flow path through the vadose zone is governed by bypass flow mechanisms, the hydrogeochemical compositions of the groundwater column will surely approach the composition of the surplus rainwater, especially in quartzitic and dolomitic parent hard rock windows (Van Tonder and Bean 2003). According to Nkotagu (1997), cases where bypass flow dominates, the ²δ and ¹⁸δ values of the surplus rainwater and the groundwater are almost similar, thus indicating no fractionation of the stable isotope signal due to superficial or UUZR evaporation has taken place.

5.5.2 ESI Signals from the Saturated Zone.

Once rainwater accumulates at ground surface and starts to infiltrate into the under drainage, a certain portion (volume) will be gradually diminished, due to ET. The isotopic signal of the infiltrated rainwater can only be significantly altered by the E component; though plant T has little impact on the isotopic composition (Sharma and Hughes 1985). The degree to which the isotopic composition will be changed depends on the duration/intensity of the physical E process; thus given the speed with which the rainwater enters the under-drainage. If bypass flow conditions exist it can be expected that the recharge water, once it reports at the water table interface, to carry an isotopic composition that will closely resemble the original rainwater's isotopic composition.

Isotope compositions in local groundwaters at the monitoring sites at Stella, Kuruman and Beaufort West plot on a relatively low (more negative) section of the Harmon Craig diagram. This phenomenon is illustrated in Figure 5.16 from the De Hoop Poort monitoring site, at Beaufort West. The water samples presenting this isotopic composition were in fact sampled from the recent (2007-2008 HC) water table rebound; thus it can be expected this

water to represent recently recharged groundwater. The recurrence rate of this modern recharge event will be demonstrated presently.

Some observations from Figure 5.16 need to be debated for clarity. First, the majority of groundwater isotope compositions plot above the GMWL, which indicates a LMWL, as has been observed with most of the other monitoring terrains (Figures 5.8 and 5.9)

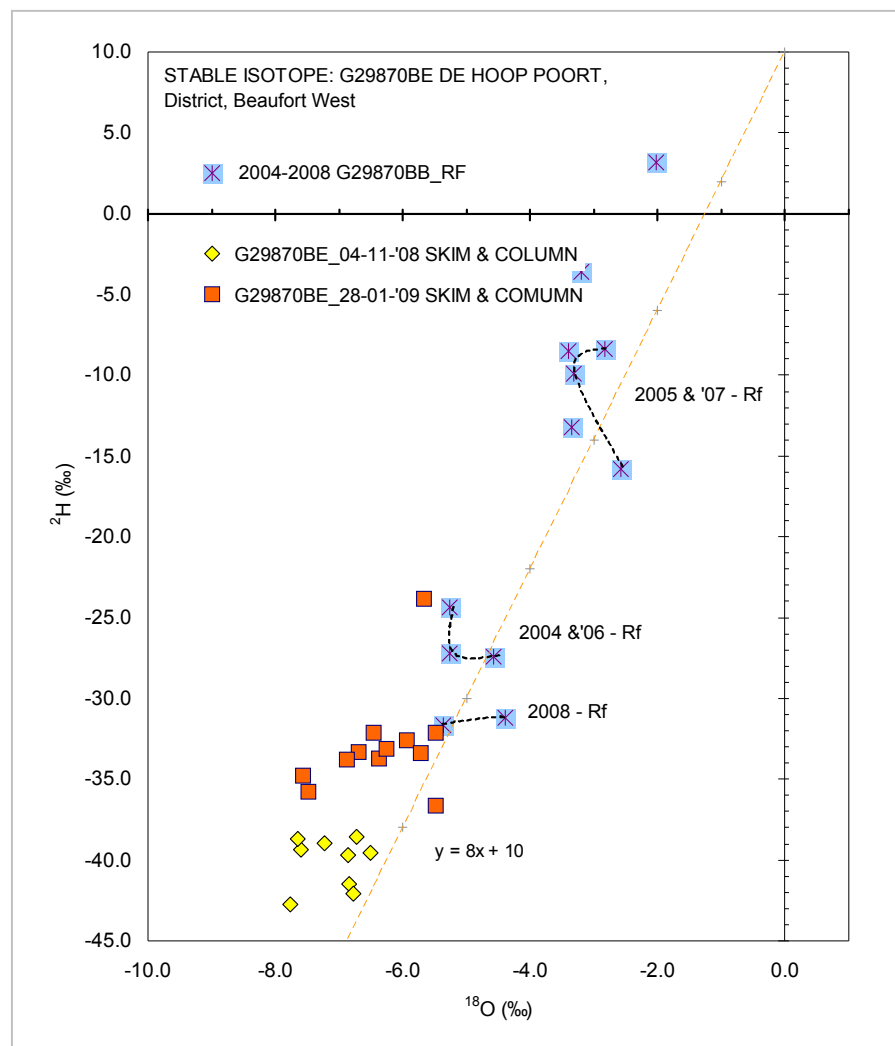


Figure 5.16. Isotopic composition of groundwater sampled using a 3 m column and 19 mm skim sampler in November 2008 in correlation with local rainwater sampled during the 2004-2008 period. Rainwaters containing the episodic events in 2006 and 2008 are marked specifically.

It seems that this LMWL, with a *d-access* around 5.0‰ is a general phenomenon in southern African waters (Butler 2010; Verhagen 2010). The physical reason for this shift has not yet been fully investigated, but contribution of domestic recycled water to the groundwater resources is out of question, as the waters analyzed in this study is pristine water. The slope of these LMWLs varies between 5.4 and 7.7.

The general negative characteristics of the groundwater at the G29870BE monitoring site can be explained by the observations made between the bulk rainwater sampler and the rainfall event sampler. The latter reports isotopic compositions in the order of - $^{18}\delta=12.5\text{‰}$, $^{2}\delta=-75\text{‰}$ and correlates with the higher rainfall events which generates recharge-producing rainfall surpluses; thus shifting the groundwater isotopic signature more negatively along the LMWL.

It was observed that some of the local groundwater isotopic composition falls at levels lower ($^{18}\delta=-6.5\pm2.5\text{‰}$, $^{2}\delta=-38\pm5.0\text{‰}$), than the bulk rainwater isotopic composition, which simply mean that the recharged water responsible for this plot originates from a series of relatively depleted rain events, with individual isotopic compositions, even lighter than the bulk sampled rainwater. The groundwater samples reporting this extraordinary lighter composition represents a water table rebound which has occurred after an episodic rainfall scenario. This means that this groundwater was recharged directly from the episodic rainfall event (bypass recharge mechanism).

As discussed above, the actual bulk sample collected in the rainwater collector represents a mixture of individual rains over a period of one (1), three (3) or six (6) months. Natural variations in the rainwater isotope composition due to (i) the amount effect as a result of higher rain events (Mazor 1997), or (ii) a complete different isotope configuration in the atmospheric moisture, will therefore be suppressed by the heavier rainwater from the average rainfall events.

The physical infiltration process through the UZR is rather complex. Nkotagu (1997) has observed in a crystalline hard rock environment in Tanzania that (i) $^{2}\delta$ and $^{18}\delta$ values in shallow groundwater correlate with surface and rainwater isotopic composition, indicating that local rainwater recharges the shallow groundwater with little evaporation, possibly

during flash floods, and (ii) isotopic values for groundwaters are more depleted than the local rainwater and surface runoff. This means that the local aquifers are recharged by rainwater originating from a higher altitude (the altitude effect), or episodic, local, heavy (depleted) rainfall events are responsible.

The altitude effect has been specifically tested in the Beaufort West area by comparing rainwater sampled from the Nuweveld Mountains on the farm Grazplaatz 113, at 1729 m amsl and groundwater on the southern peneplane area (monitoring site G29870L - S32.16450°; E022.72585°, 1022 m amsl). The short lag time between the rain events and the water table responses as observed at the G29870L site, do not confirm this mechanism, nor does a pressure migration effect due to the elevation difference between these direct hard rock infiltration sites seem to be possible. The correlation between the lighter local groundwater signature and the episodic rainwater is probably more a local, direct recharge event made possible by fractured hard rock terrains.

The isotopic rainfall data in Table 5.15 illustrates the altitude effect on the rainwater input although the groundwater compositions is similar; indicating a strong blending with aquifer water in the upper SZ. The differences in the hydrochemical composition are between the higher mountain area and the lower peneplane should be noted. This difference implies a significant variation in the recharge figures based on the CMB (13% versus 3%).

Table 5.15. Illustration of altitude effect in two hard rock terrains in Beaufort West (statistics: $n \approx 7$ and used harmonic means of samples collected between 2003 and 2009).

SITE	$^2\text{S}\text{‰}$	$^{18}\text{O}\text{‰}$	Cl^-	Na^+	NO_3^-	SO_4^{2-}
				$\text{mg}\cdot\text{l}^{-1}$		
Nuweveld Mountain rain-water (at 1729 m amsl).	-5.2	-24.1	0.79	0.07	4.1	0.54
Plains Area rainwater (at 992 m amsl).	-3.7	-18.5	1.02	0.71	3.4	0.95
Nuweveld Mountain ground-water (at 1729 m amsl).	-5.4	-33.4	8.00	9.09	11.8	4.61
Plains Area groundwater (at 992 m amsl).	-5.6	-31.8	36.43	59.22	12.2	48.99

5.6 SUMMARY OF HYDROGEOCHEMICAL FEATURES OF THE RECHARGE CYCLE.

Rain events referenced as episodic events form part of the annual rainfall pattern and occur during a sequence of rain events over a period of three (3) to eight (8) days or a rain-week. The rainfall hydrogeochemical character during these periods portrays a distinctive lighter composition. This effect is due to the amount effect although smaller (<25 mm) rainfall depths also report these depleted signatures which are probably affected by the position of the convection cells (rain cloud) in terms of the rainwater logger/sampler position.

The hydrogeochemistry of the upper section of the SZ varies considerably. Several cases exist in the semi-arid hard rock terrains where the upper section (2-4 m below the water table interface) of the SZ contains layers of water with a lighter isotopic composition than the bulk rainwater collected over the rainfall intervals (dry, early and peak). These incidents indicate that certain synoptic systems are highly depleted due to previous rainout events along their migration paths.

The hard rock monitoring sites consisting of Karoo sedimentary/volcanic (Beaufort West and Taaiboschgroet) and older crystalline (Stella) formations, have groundwater Cl^- concentrations in the range of $35 (\pm 5) \text{ mg} \cdot \text{l}^{-1}$ which probably represent a mean value for the combined bypass (preferential) and matrix recharge contributions, the total long-term Cl^- dose at the water table interface. Spatial effects however rules as these values can double/triple within a matter of 500 meters especially where the soil/regolith becomes thicker and vegetation communities thrive because of evaporation taking place in the rooting zone.

The hydrochemical composition of dolomitic terrains and specifically dolomitic springs fundamentally provides the best-integrated hydrogeochemical signature in terms of recharge ratios (ET_{INDEX}). These cases are rare, and the principles for estimating groundwater recharge should be limited to well known cases as the actual drainage basin for these springs is not that well demarcated. In the case of the Kuruman A-Spring, the flow is balanced between groundwater flowing from the Kuruman Hills BIF's with a Cl^- concentration of $\pm 5 \text{ mg} \cdot \text{l}^{-1}$ and groundwater from the Ghaap Plateau Dolomites with a Cl^- concentration

of 20 to 25 mg·l⁻¹. The spring itself has a mean (harmonic) Cl⁻ concentration of 6.1±1.8 mg·l⁻¹, as logged between 2002 and 2008.

To conclude, this chapter elaborated on the hydrogeochemical characteristics of rainwater and groundwater and the interaction in terms of groundwater recharge. The occurrences of episodic rainfall events and the impact on the groundwater hydrogeochemical character were elaborated in terms of the flow conditions (multi-modal fluxes). Only a few results from the six (6) experimental monitoring terrains were discussed. Abrupt changes in the groundwater hydrogeochemistry as the result of episodic rainfall events, accompanied by in some cases drastic water table rebounds, were observed at these sites, and are influenced by the rock type (i.e. dolomite versus mudstones).

oooOOOooo

6 EPISODIC RECHARGE EVENTS IN SEMI ARID HARD ROCK ENVIRONMENTS.

6.1. RAINWATER - GROUNDWATER INTERACTION.

6.1.1. *Introduction.*

Hyetograph-hydrograph observations from the rainfall/groundwater monitoring sites in the hard rock experimental monitoring terrains in South Africa, report a realistic correlation between specific rainfall events and local water level responses. Where a combination of a thin (<0.25 m) or totally absent A- and/or B-horizon cover over a fractured and weathered hard rock platform exists, the water table response following an extraordinary rainfall event is within hrs/days (Figure 6.1).

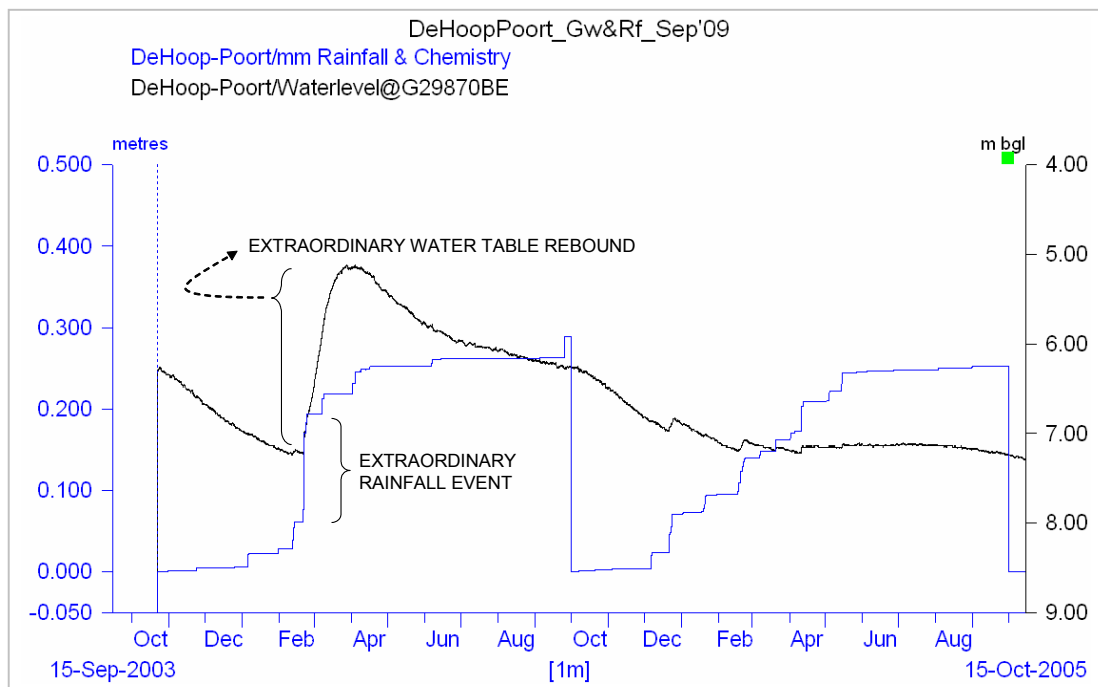


Figure 6.1. Illustration of extraordinary rainfall event (110 mm in 20½ hours) and responding groundwater table rebound (1.57 m over 35½ days) in Karoo fractured hard rock terrain, District Beaufort West.

An interesting observation made in Figure 6.1 is the rainfall patterns over the two HC's which are virtually the same (2003-2004: 257 mm and 2004-2005: 253 mm), although groundwater recharge occurred only in the HC containing the extraordinary rainfall event in February 2004. Observations made at other monitoring terrains report similar responses and highlight the importance of variability in rainfall patterns versus groundwater recharge.

In some cases the actual time lag between an episodic rainfall event and dynamic water table rebounds, are quite long, several succeeding HC's. It is therefore important to investigate the variability in the rainfall depths and frequency of exceedance of these episodic rainfall events.

6.1.2. *Temporal Variability of Episodic Rainfall and Groundwater Recharge.*

Rainfall patterns in the semi-arid climates may be described as occasional rainfall events that are separated by long periods of drought; thus classed as periodic or episodic (King, 1942). Episodic rainfall, described by the latter as non-seasonal events, opposed to the regular occurrence of rainy seasons classified as periodic cases under temperate climate conditions.

In addition to orographic and ground surface temperatures, rainfall input in semi-arid regions differs spatially and temporally due to high variability's in (i) seasonal/spatial weather patterns and (ii) residual moisture levels of air masses. The balance of recharge-producing surplus rainfall once passed the UUZR may not be sufficient to establish field capacity in the LUZR. This is where the infiltration ceases until a next phase of infiltrating water manage to bypass the UUZR. In the case where fracturing, animal burrows or plant roots have created specific bypass pathways, most of the recharge-producing rainfall surplus bypasses the rooting zone within a matter of days without losing too much to ET (Gieske 1992).

Observations of hyetograph-hydrograph responses from the semi-arid region clearly show that water levels respond only after a certain rainfall threshold has been overcome. This threshold can be (i) a series of individual rainfall events which forms part of a prevailing regional weather system, and/or (ii) a single, heavy rainfall event over a short period in time like the rain-week patterns.

6.1.2.1. Frequency of Exceedance.

The above-mentioned threshold can be quantified through an assessment of the rainfall-water level responses and a design rainfall can be modeled to match groundwater re-

charge events (Kessler and De Raad 1974). During this procedure, three critical components need to be selected i.e.:

- **Critical Season:**
That time of the year when an episodic rainfall event may be sufficient to generate recharge-producing rainfall surplus, i.e. the first six weeks and the last three months of the wet cycle, when ET^{64} is at a lower level.
- **Critical Duration:**
Rainfall patterns in the semi-arid region indicates that 85% of effective rain events during the wet cycle, occur in clusters over periods of 3 to 8 consecutive days with rains of 50 mm to 270 mm. Dry inter-rain events vary from 7 days to 25 days apart. The critical duration could be expressed as a rain-week scenario (3-8 day period).
- **Area under study:**
In the case of limited spatial coverage of observation/monitoring sites on the interested area due to logistics or financial constraints, the estimated area-average rainfall for a particular study area appears to be less than actual point rainfall values with high return periods. In this study where specific terrains were selected for hydrometeorology observations, sufficient rainfall logging devices were installed; thus the problem of area-coverage does not influence the assessment practice.

Frequency of recurrence based on rainfall depth intervals.

Rainfall data from seven (7) SAWS offices with weekly data ranging from as early as 1913 was used as representative data. The data from the SAWS weather station No. 468318 at Vryburg, Northern Cape was analyzed using the following algorithm (Kijne 1974):

$$F(a_i < P \leq b_i) = \frac{m_i}{n} \quad (6-1)$$

⁶⁴ Vegetation demands for soil moisture is at its lowest levels during the late dry cycle; there is a 1-2 month overlap on either side of the wet cycle when (i) re-growth depends on successive moisture availability during the onset of the wet cycle and (ii) following the mature-growth period after production of seeds has stopped (Chow 1964).

where a_i and b_i are the lower and upper limits of an appropriate number of rainfall depth intervals (P), m_i is the number of daily rainfall depths per interval and n , the total number of data points ($\sum m_i$). F represents the frequency of occurrence of precipitation in a specific interval. The analysis was done for each calendar month since 1913 of the Vryburg SAWS weather station.

The assessment indicates that weekly rainfall events, with rainfall depths greater than 38 mm, are intermittent (episodic) in nature. It can imply that even with average annual rainfall input, no effective recharge of aquifer systems may happen, when an episodic rainfall event like those incorporated in a rain-week scenario occurs (Figure 6.1).

The design rainfall for semi-arid regions is obtained by applying the following algorithm:

$$F(P > a_i) = \frac{M_i}{n} \quad (6-2)$$

where a_i is the lower limit of the depth interval i , M_i is the number of all rainfalls exceeding a_i , and n is the total number of rainfalls. Table 6.1 reports the number of monthly rainfall occurrences of specific rainfall depths over the annual HC.

Several estimations for groundwater recharge using a specified daily, monthly or annual total rainfall input requires that a threshold or minimum rainfall value is specified, meaning that only when this value⁶⁵ is bridged by the annual totals, groundwater recharge manifests (Bredenkamp et al. 1995). Threshold values for annual rainfall though, is not that simple, and is rather site specific than the norm.

Close observations of hyetograph-hydrograph sets generated in this study illustrates that individual rain events of moderate rains, i.e. 40 to 50 mm per event, may not generate a recharge-producing rainfall surplus once infiltrated to the underdrainage system. It seems that the rainfall intensity ($\text{mm} \cdot \text{hr}^{-1}$) plays an important role here as will be demonstrated presently.

⁶⁵ Values between 360 mm and 500 mm is mentioned in literature.

Many hyetograph-hydrograph sets from hard rock surface indicate that during a short sequence of rain events, a rain-week, rainfall in the order of 40 to 60 mm can generate ASR which resets aquifers' storage potential. The significance of these rain-weeks for generating ASR is quite pronounced in the semi-arid summer rainfall region

A statistical analysis of information supplied by the SAWS reports daily rainfall extremes in southern African semi-arid regions. These daily rainfall depths are noticeably higher than the long-term average monthly rainfall, but their return periods are in the order of decades.

Table 6.1. Monthly occurrences of rainfall events for a typical semi-arid region: Vryburg rainfall from 1913 to 2008 monitored at Station No. 468318.

Months	30-40 mm	41-50 mm	51-60 mm	61-70 mm	71-80 mm	81-90 mm	91-100 mm	> 101 mm	>150 mm
Oct _n ⁽³⁰⁸⁾	3	1							
Nov _n ⁽⁴⁴⁰⁾	5	4	1					1	1
Dec _n ⁽⁵¹¹⁾	7	6	6	3					
Jan _{n+1} ⁽⁶⁴³⁾	9	8	9	6	3				
Feb _{n+1} ⁽⁵⁸⁵⁾	18	15	2	5	1	1	1		
Mar _{n+1} ⁽⁵⁵³⁾	20	18	9	4	3			1	1
Apr _{n+1} ⁽³⁴³⁾	12	2	3		2				
May _{n+1} ⁽¹⁶⁷⁾	4	3							
Jun _{n+1} ⁽⁶²⁾	2		1						
Jul _{n+1} ⁽⁴⁰⁾	2								
Aug _{n+1} ⁽⁵²⁾	3	1			1				
Sep _{n+1} ⁽¹⁰⁶⁾	3	1		2					

⁽¹⁰⁶⁾ The total number of daily rainfall events per month over the period 1913 to 2008

Sequences of rain-weeks have also been noticed on most of the monitoring sites i.e. 3 days-111 mm, 4 days-80 mm, 5 days-158 mm and 8 days-109 mm. Rains like these are noticeably episodic and initiate accumulation of storm run-off in local rivulets and accumulation of rainwater in local depressions.

Long-term (at hourly logging intervals) summer and winter rainfall data reports a random configuration of individual events with highly variable rain values. The design rainfall report an expected huge population of rain events falling in the <1 mm to 40 mm range with the higher ranges (>40 mm rain) occurring as extreme outliers. Rain events larger than 50 mm

over periods of a day (24 hours) can thus be regarded as episodic in nature with a frequency of exceedance of 0.04, 0.03 and 0.06 for the three months in the peak summer interval (viz. January, February and March).

A statistical analysis of the rainfall data from the Vryburg weather station provides a sufficient long-term assessment of the rainfall pattern in terms of (i) frequency of rainfalls exceeding a design value and (ii) return periods of specific rainfall depth. These analyses are shown in Table 6.2 and were structured to report the return periods for three slots of rainfall depths during the months of the HC.

Table 6.2. Return periods (years) for three categories of rainfall depths for the Vryburg weather station (SAWS station no. 468318).			
Month in H.C.	50 mm's on	100 mm's	150 mm's
October _n	4	53	♣
November _n	3	11	50
December _n	2	8	27
January _{n+1}	2	4	8
February _{n+1}	2	5	10
March _{n+1}	2	4	8
April _{n+1}	1	4	8
May _{n+1}	-	-	-
June _{n+1}	-	-	-
July _{n+1}	-	-	-
August _{n+1}	-	-	-
September _{n+1}	-	-	-
♣ Maximum October rainfall depth over 105 years was 105 mm.			

According to Table 6.2, the months of January to March contains the highest probability to include a rain event of 100 mm (with a return period of ± 4 years) and a 150 mm rain event with a return period of ± 9 years.

The case of the 2006 prominent recharge event in the Stella area is an example where a few single rainfall extremes under a normal average annual rainfall pattern (600 mm yr^{-1}), generated sufficient Hortonian run-off which flooded the Stella Pan and most of the smaller depressions situated on the Middelkop Aquifer System. This year also stands out

as an extraordinary year in terms of rainfall depths and characteristically depleted hydro-geochemistry signature (Figure 6.2).

The statistical analysis of the Vryburg SAWS rainfall data, rate a rain-week of $270 \text{ mm} \cdot \text{d}^{-1}$ during this HC at a recurrence rate of one (1) in fifty-three-years (53). The occurrence of these rain-weeks throughout the history of rain events in the semi-arid regions is quite significant in the quest for groundwater recharge events.

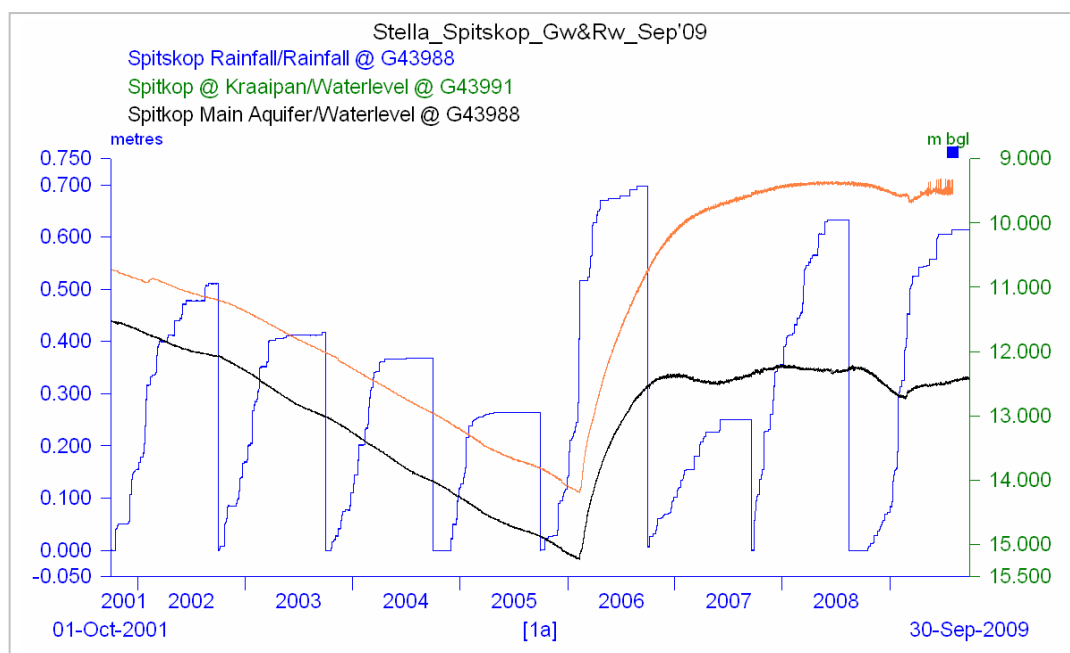


Figure 6.2. Illustration of extraordinary rainfall event (269 mm in 6 days 7 hours) on the Spitskopreen monitoring site on a Kraaipan fractured hard rock terrain, Stella, District Vryburg.

6.2. EPISODIC RECHARGE EVENTS.

6.2.1. Introduction.

The narrative of an episodic recharge event is contained in a sequence of natural events driven mainly by (i) the actual rainfall pattern as the incoming variable and (ii) given suitable surface conditions which can absorb the rainwater once surplus rainfall conditions manifest. The most critical variable for generating surplus rainfall seems to be the rain rate ($\text{mm} \cdot \text{hr}^{-1}$).

The hydraulic parameters (K and S) of the aquifer system have a significant influence on the water table rebound range. A good example is illustrated in the hyetograph-hydrograph set presented in Figure 6.2 showing the water table responses of two monitoring boreholes, i.e., G43991 (Kraaipan BIF's) and G43988 (Mosita granite). Although the rainfall input were the same over the area, there is almost an 2.00 m difference in the long-term water table response between the fractured Kraaipan hard rock terrain (G43991 - 4.82 m rebound) and the adjacent fractured and weathered Mosita granite aquifer system (G43988 - 2.95 m rebound). The storativity of the weathered Mosita granitic aquifer is probably much higher than the Kraaipan BIF aquifer which is the recharge intake area in this case study.

6.2.2. *Spatial Variability of Groundwater Recharge.*

In semi-arid regions with a moderate relief (hard rock terrains, rivulets, depressions and flats), two basic recharge modes are recognized - direct and indirect (Arid Zone Hydrology 1980). Rainfall patterns in arid/semi-arid regions sometimes instigate extremely high rainfall rates (R_T), resulting in local depression recharge as well as Hortonian run-off. The run-off component may enhance to such an extent that flash flooding occurs which is carried along the local drainage systems to places where the rainfall did not even occurred, i.e. the lower Kuruman River flood for example.

6.2.2.1. Direct Mode.

Refers to recharge by infiltration of recharge-producing rainfall surplus at the place where the rain occurs and is only possible where the rainfall event, less surface retention, surface runoff and immediate evaporation is greater than the soil moisture deficit.

The direct groundwater recharge (DGw_R) for recharge regimes estimation for semi-arid regions per interval Δt is specified by:

$$DGw_{R\Delta t} = P_{A\Delta t} - Sw_{R\Delta t} - ET_{A\Delta t} \pm \Delta Sm_{S\Delta t} \quad (6-3)$$

where P_A is the actual rainfall event depth, Sw_R is the surface runoff, ET_A is the actual ET from the UUZR) and ΔSm_s is the soil/regolith moisture storage-change (Arid Zone Hydrology 1980).

6.2.2.2. Indirect Modes.

Refers to recharge which first become surface runoff and later infiltrates through streambeds or the floors of local areas of concentration, depressions or flats. The area over which water is concentrated is much smaller than that available for direct recharge. Depressions and flats are areas where water-borne sediments accumulate and are characterized by high soil moisture capacities, thus producing conditions highly suitable for vegetal growth and higher ET losses.

In the case of karst systems, indirect groundwater recharge occurs where a surface drainage system overruns or ends in a swallow. These systems are instantaneous coupled with surface run-off during storm events and result in significant groundwater level response (several meters) per day. The recharge amounts are enormous, for example in the classic case of the Rietspruit system close to the Sterkfontein Caves, Mogale City District, where anything between 5 and 30 $MI \cdot d^{-1}$ feeds into a swallow (S26.051901°; E027.707657°, 1493 m amsl) and recharge of a local dolomite compartment.

To conclude, although indirect groundwater recharge areas may represent extremely small surfaces relative to the direct recharge areas, their contribution during episodic rainfall events supersedes local direct recharge.

6.2.3 *Groundwater Table Hydrographs.*

Time-series combination of water table and rainfall depth logs provide a unique presentation of groundwater recharge/discharge regimes which resemble the typical hydrographs generated in watershed hydrology instigated by run-off/overland flooding after rain events.

The groundwater hydrograph reflects recharge-producing rainfall surplus and groundwater discharges over a much longer time span than the surface water equivalent. In compari-

son with verified hydrographs (the Unit Hydrograph)⁶⁶ generated for a specific watershed catchment, groundwater table hydrographs come in a multitude of shapes and configurations (Kirchner 2003). These differences commence from factors and variables:

- (i) The hydrometeorological status of the preceding HC and its impact on the soil/regolith conditions and plant life;
- (ii) Hydraulic property of the vertical flow pathway (vertical flow resistance, VFR - Λ), how fast does the recharge-producing surplus rainfall percolate down to the water table interface to start recharging the aquifer;
- (iii) Hydraulic property of the surrounding horizontal flow regime (SDR - Υ), governed by the potential of the waterlevel mound to overcome the lateral flow resistance and force the newly recharged water to the surrounding sub-reservoirs; and
- (iv) The saturation status (levels) in the recharge zone and the receiving aquifer.

The shape of any groundwater hydrograph is a reflection of the local aquifer condition and its role in the regional groundwater flow regime. If sufficient head (Δh_{\max} , m) is created in a recharge mound to initiate the L-shaped lateral flow condition described by Mazor (1997), a steady-state condition between recharge and the underlying long-term recession rate may be reached (Figure 6.1, last week in March 2004 to first week in April 2004). The turn-over period (± 15 days) from a recharge mode to a discharge mode resembles a steady-state condition between recharge still from the UZR matrix and aquifer loss, due to local ET or lateral discharges. This condition will sustain for a limited period before a long-term recession of the water table starts. This recession rate dh/dt is inversely proportional to the storage coefficient S and can be expressed by the following formulae (Gieske, 1992):

$$\frac{dh}{dt} \approx -\left(\frac{1}{\alpha S \Upsilon}\right) \cdot h \quad (6-4)$$

⁶⁶The *Unit Hydrograph* is an expression used for a method of calculation which allows rainfall values to be converted to stream flow for a specific catchment (Dooge 1959).

where α is an indicator for a parabolic/flat (0.66 or 1.0) waterlevel mound respectively, S is the storage coefficient, T is the SDR (T , time) and h is the total thickness of the aquifer above its decanting level.

Figure 6.3 illustrate examples of a few episodic groundwater table responses (rebounds and recessions) which can be linked to specific episodic rain events in the Karoo Supergroup, Beaufort Group sandstone/mudstone hard rock environment over a period of six (6) consecutive years (monitoring site G29870BB_RF and G29870BE (S31.16276°; E022.78463° CapeDatum, 1031 m amsl) in De Hoop Poort, District Beaufort West).

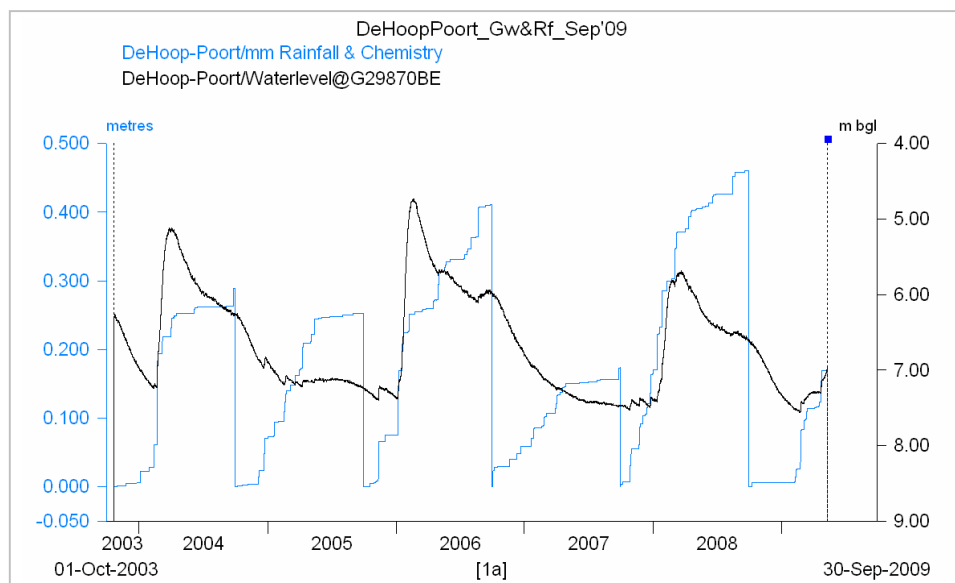


Figure 6.3. Combination of rainfall and groundwater hydrograph from monitoring sites G29870BB_RF(Rw) and G29870BE(Gw) at De Hoop Poort, District Beaufort West.

Three unique instantaneous hydrographs (IH) are superimposed on what can be described as a long-term, low trending natural draining water table mode, governed by the hydraulic and geometric dimension of the local aquifer unit underlying the hard rock terrain. HC's reporting low annual rainfall depths with no episodic significant rainfall event do not report these prominent instantaneous hydrographs; thus indicating significantly lower or probably no replenishment of local aquifer system(s) through recharge-producing rainfall surplus.

Hard rock windows consisting of dolomite rocks will probably report the most straightforward cases of singular-modal flow mechanisms as the rock itself is highly indurated; thus the matrix flow component of the total recharge-producing rainfall surplus will be a minimum/non-existing.

A monitoring site was selected for observations in a typical dolomite hard rock terrain in the upper Kuruman River catchment (dolomitic area catchment of the Kuruman A-Spring). The IH resulting from an episodic rain event is illustrated in Figure 6.4 (Geosite G47600: S27.48305°; E023.47305°, 1350 m amsl).

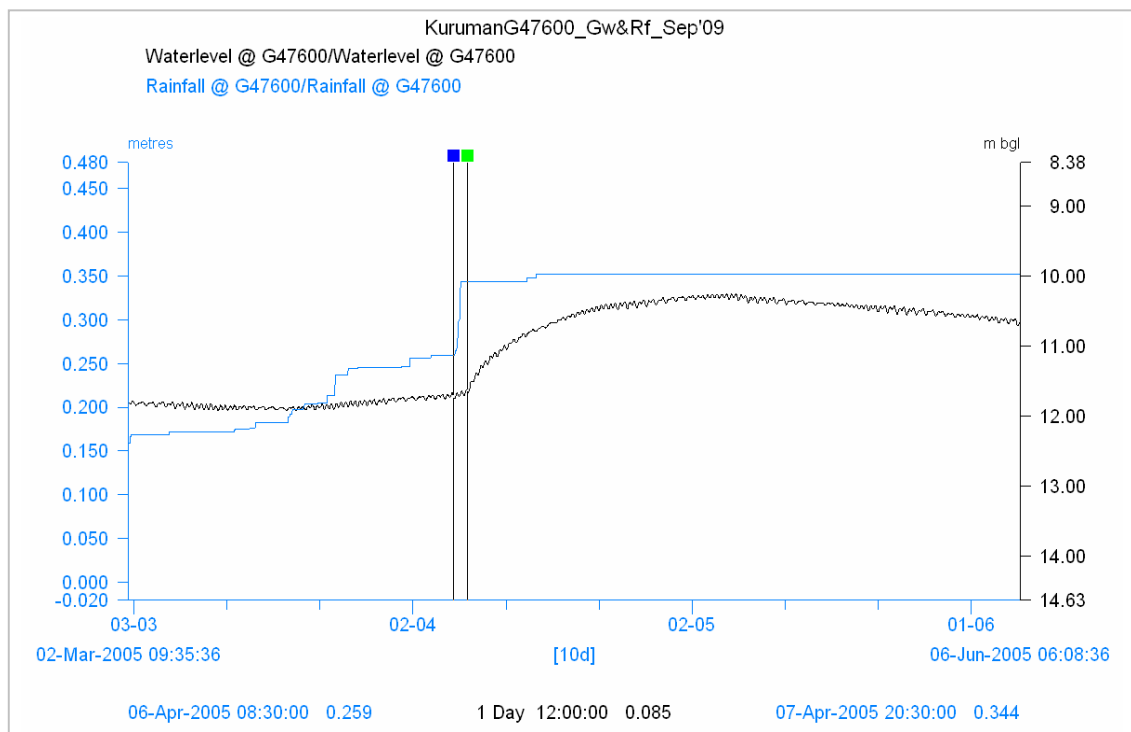


Figure 6.4. Typical groundwater table hydrograph-hyetograph set at monitoring site G47600 (G47600 water level) and G46600_RF (Klein Boompie rainfall) in a dolomitic terrain.

The surface area around G47600 constitutes a flattish bare dolomite hard rock terrain with several vertical solution channels. The time lag between the rain event of 85 mm and the onset of the water level mound was 1 day 12 hours (time lag between two vertical lines as indicated on figure).

A second type of hydrograph with a substantial longer lag time between the rain event and the onset of the water table mound is illustrated in Figure 6.5.

This type of hydrograph corresponds characteristically with sub-reservoirs situated on low-lying regions. These regions are uncharacteristically hard rock terrains having a prominent soil/regolith cover and most of the times a healthy vegetation community. Vertical recharge has a negligible contribution in these cases and aquifer replenishment depends on lateral discharge from adjacent hardrock terrains being recharged directly during recharge-producing rainfall surplus events (Willemink 1988).

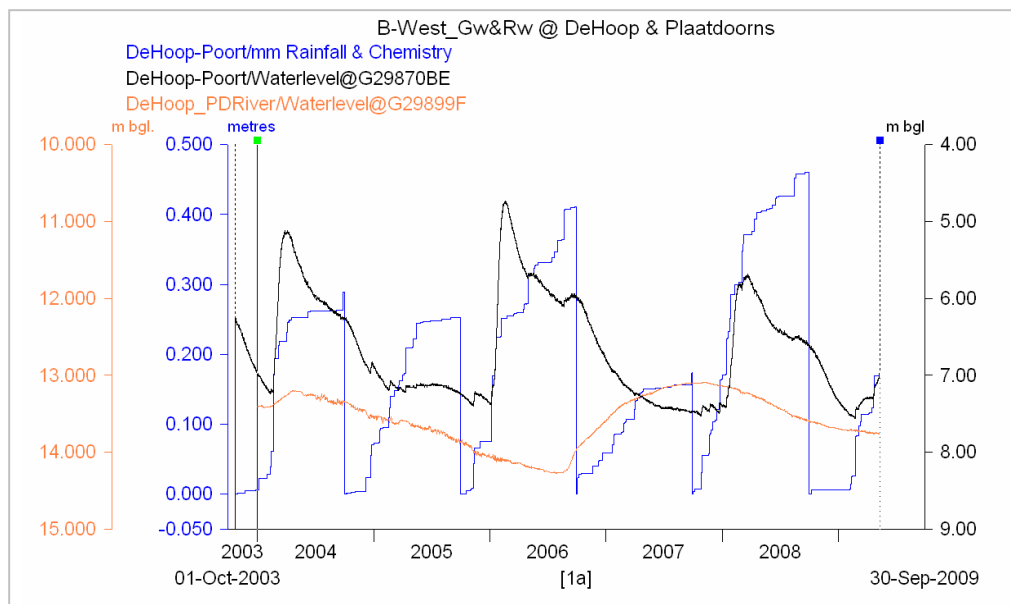


Figure 6.5. Comparison between groundwater recharge mechanisms in an area with local infiltration on a hard rock terrain (G29870BE) and a nearby receiving flood plain area (G29899F), De Hoop Poort, District Beaufort West.

The actual groundwater table responses in the case presented in Figure 6.5 emphasizes the complexities of recharge mechanisms and the difficulty to apply techniques to quantify the recharge mode. Although monitoring sites G29870BE and G29899F are situated 4.35 km from each other, their hydrogeological concepts in terms of the recharge mechanism are quite different. Where monitoring site G29870BE (the De Hoop Poort area) is situated in a moderately elevated hard rock terrain, G29899F (S32.19803°; E022.76556°, 992 m amsl) is situated in a large flood plain (part of a Karoo peneplane) of the Plaat-

doorns River. The underlying rock is Beaufort Group sandstone/mudstone. In the case of monitoring site G29899F, the ground surface consists of a soil/regolith cover.

The water table responses in what obviously are two different recharge mechanisms significantly illustrate the time lag between recharge events under different hydrogeological conditions (Figure 6.6). The time lag between the two vertical bars represents 202 days and demonstrates the delayed reaction in the case of G29899F (soil covered peneplane area,)

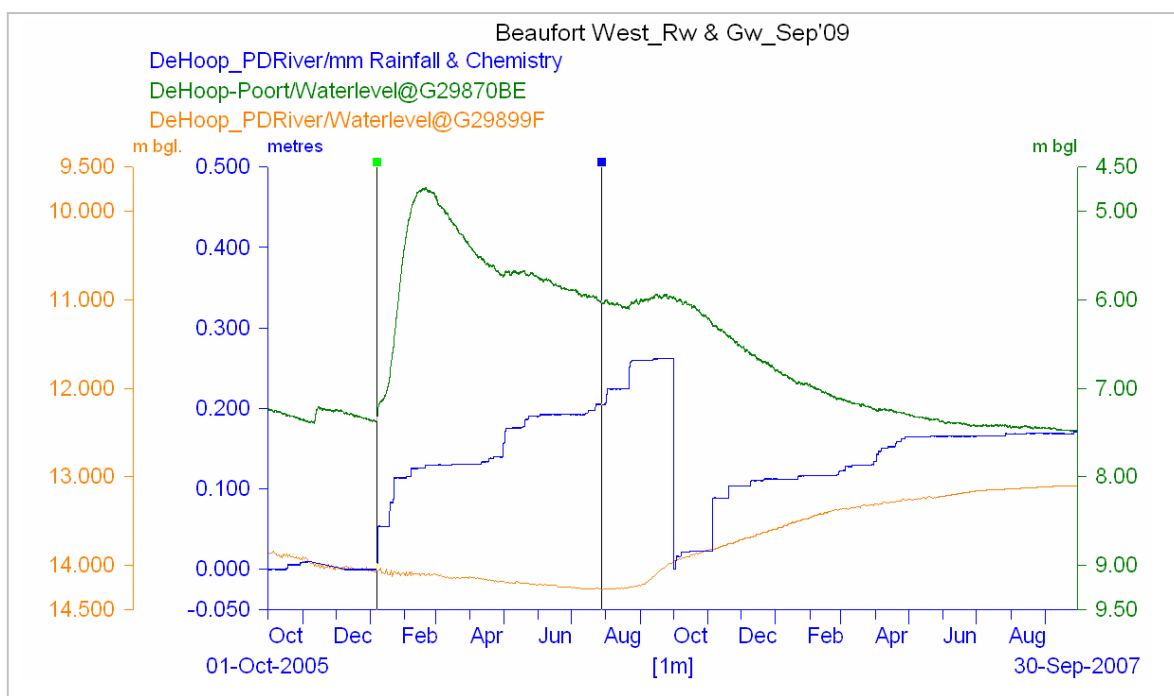


Figure 6.6. Water table responses in two different recharge cases in the Karoo environment against the local rainfall input over two HCs.

According to the classification of Xu and Beekman (2003, p. 83), monitoring site G29870BE can be correlated with Scenario b (hard rock terrain), whilst monitoring site G29899F corresponds to Scenario c (soil covered, weathered rock profile). Thus demonstrates the difference between (i) direct, effective recharge mechanisms with a unique hydrogeochemical signature, and (ii) Willemink's (1988) lateral feed recharge from surrounding direct-recharge-zone with a totally mixed hydrogeochemical signature.

When groundwater recharge estimations using hydrogeochemical tracers are performed, the recharge mechanism should be known/investigated beforehand. For example, in the case of using monitoring site G29899F in Figure 6.6, an IH cannot be visualized for this monitoring site area, as the actual water table/rainfall interaction lag time indicates a 202 day delay in an area with a relatively shallow water table (≈ 10 m bgl).

When utilizing hydrogeochemical-tracing methodologies, contributions of added tracer concentrations by dominant lateral flows from adjacent sub-reservoirs occur. Applying the CMB principle in the case of monitoring site G29899F, where the C_G value of $115 \text{ mg}\cdot\ell^{-1}$ is much higher than the C_G value of $36 \text{ mg}\cdot\ell^{-1}$ measured⁶⁷ at monitoring site G29870BE in the hard rock terrain (direct recharge area). With a local C_P at $0.8 \text{ mg}\cdot\ell^{-1}$, the combined R_T for the hard rock terrain is 1.8 mm (2% of $R_{\text{eff}}=91$ mm) and the peneplane area 0.6 mm (0.7% of a R_{eff} of 91 mm). The recharge ratio between the two sites is $\approx 3 : 1$; which correlates with the results of highly variable spatial recharge values observed by Nkotagu (1997) and De Vries and Simmers (2001).

Since potential recharge zones such as the hardrock terrains may represent a small portion of an aquifer system, their weighted recharge contribution to surrounding sub-reservoirs is significantly higher than the remaining areas with soil/regolith/vegetation cover where the R_T is significantly lower. Conditions like this, will give a total over-estimation of the effective recharge spatially, for example when a recharge value on Quaternary Catchment scale is to be estimated.

6.2.4 *Rainfall Intensities and Water Table Responses.*

Assessment of medium to long-term groundwater hydrographs from those spatially limited areas where direct, vertical recharge is possible. Firstly, two (2) outstanding patterns evolve, i.e. (i) a prominent, prolonged water table recession, followed by (ii) intermittent water table mounds with variable amplitudes. The latter comes mainly in two (2) formats, firstly small and short duration water table mounds which normally disappear within the long-term recession trend after a week or two. Secondly, prominent water table mounds

⁶⁷Harmonic mean from a population of 7 observations, Std. Dev. =0.11.

which result in a ASR, i.e. alters the aquifer storage status/sustainability for several years to come.

Rainwater infiltration is affected by natural conditions and man made constructions. In the urban environment, direct rainfall recharge is intercepted by storm run-off due to paved surfaces. Factors affecting rainwater infiltration under natural conditions may be considered as a three (3)-step sequence (Chow 1964), viz. surface entry, soil transmission, and storage capacity in the soil/regolith/UFWZ.

The amount (mm) of rainfall recorded over a specified time interval defines the rain rate or rainfall intensity (Stanger 1994). Obviously, there will be a substantial difference at the ground surface between a rain event of 45 mm over two (2) days compared to 45 mm over 6 hours in terms of creating depression storage, Hortonian overland flow and infiltration.

One of the useful applications of the hyetograph-hydrograph set is the ability to calculate rainfall intensities per rain event which is useful in specification of (i) effective rain events (R_{eff}), and (ii) initiating underdrainage flow to the water table interface. Preliminary rainfall depth-duration combinations were summarized from calculations for the southern African semi-arid region. These figures represent a lower limit for any significant groundwater recharge event to take place:

$$1.5\text{mm} \cdot \text{hr}^{-1} < R_{RT} \text{ and } R_{eff} > 40\text{mm} \quad (6-5)$$

where, R_{RT} donates the rain rate ($\text{mm} \cdot \text{hr}^{-1}$) and R_{eff} donates the effective rainfall depth.

The hyetograph-hydrograph set provides physical evidence of localized rain rates and duration of individual rainfall events. The short-term interval logging rainfall and water table data allows high-level assessment of these data sets and good correlations between the onset and durations of both state variables can be deducted.

Table 6.3 is a summary of rainfall intensities and rain durations of individual rain events over several recharging and non-recharging HCs and responding local water table fluctuations. It covers three different fractured hard rock types consisting of the Kraaipan Group-Mosita Granite Suite (Stella), Karoo Beaufort Group sediments (Beaufort West) and Karoo Letaba Group basalts (Taaiboschgroet).

Table 6.3. Rainfall intensities, duration and local water table responses calculated from hyetograph-hydrograph sets.

Geosites:	Basement shield rocks ¹ , Beaufort Group Sediments ² , Letaba Group Volcanics ³ .			Hydrological Years (Oct _n - Sep _{n+1}):	2003-2009	
Duration. (day)	Duration. (hrs)	Rain. (mm)	Rain Rate. (mm·hr ⁻¹)	Water Table Rebound Rate ⁴ (mm/d_for --days)	Time Lag between Rain Event and water table re- sponse (days and hrs)	
¹	2.00	48	157	3.3	240mm/d_0.2d	3days 10 hours
	0.44	10.5	110	10.5	30mm/d_31d ⁵	2days 12 hours
	0.33	8	50	6.3	18mm/d_29d	5days 7 hours
²	2.04	49	91	1.9	67mm/d_3d	-days 8 hours
	1.1	27.5	39	1.4	86mm/d_25d	-days 15 hours
	1.3	32	43	1.3	55mm/d_2.4d	-days 6 hours
	0.2	5.5	50	8.0	107mm/d_0.5d	-days 6 hours
	1.1	26.5	52	1.9	60mm/d_18d	3days 9 hours
	0.1	2	38	19.0	70mm/d_1d	0-day 1 hour
	0.8	19	110	5.8	80mm/d_17d	0-day 1 hour
³	1.69	40.5	63	1.56	6mm/d_16d	3-days 9 hours
	0.04	1	48	48.0		4-days 5 hours
	0.19	4.5	41	9.1	18mm/d_17d	-days 17 hours
	0.04	1.0	28	28.0		1day 12 hours
	0.42	10	103	10.3	725mm/d_2d	-day 2 hours

¹ Kraaipan Group and Mosita Granite Suite, Stella, Northern Cape (deep fractured/shallow weathered, water table range \approx -15 to -11 m);

² Karoo Supergroup, Beaufort sandstone/mudstone, Beaufort West, Western Cape (shallow fractured, water table range \approx -7.5 to -4.5 m);

³ Karoo Supergroup, Letaba Group basalts, Taaiboschgroet, Limpopo (shallow fractured/shallow weathered, water table range \approx -8.5 to -5.5 m);

⁴ Actual water table trend (mm·d⁻¹ rise/fall) over the rainfall event duration.

⁵ Recharge events extended to 910 days (or 2.5 years).

⁶ Water table Rise/Fall rate (mm·d⁻¹) - corresponds with Rain Rate.

The results reported in Table 6.3 of typical episodic rainfall events, illustrate the following conditions observed with the detailed hyetograph-hydrograph sets from where the constants in Eq. 6-5 were obtained:

- A close relationship between rain rate R_{RT} and the water table rebound rate (column 5), the highest recoded rebound rate (mm·d⁻¹) during the study period reported a rebound rate of 725 mm·d⁻¹ from a 10 hour - 103 mm rainfall event;

- Even low R_{RT} (1.3 to $1.4 \text{ mm}\cdot\text{hr}^{-1}$), but with rainfall depths between 40 and 45 mm instigate water table rebounds over short periods; and
- The data presented gives an overall range of the lag-times observed in hard rock recharge terrains.

In an example of rain rate applications, a close-up of the 2005-2006 hydrological season's hydrograph-hyetograph set on the Spitskopreen monitoring site is illustrated in Figure 6.7.

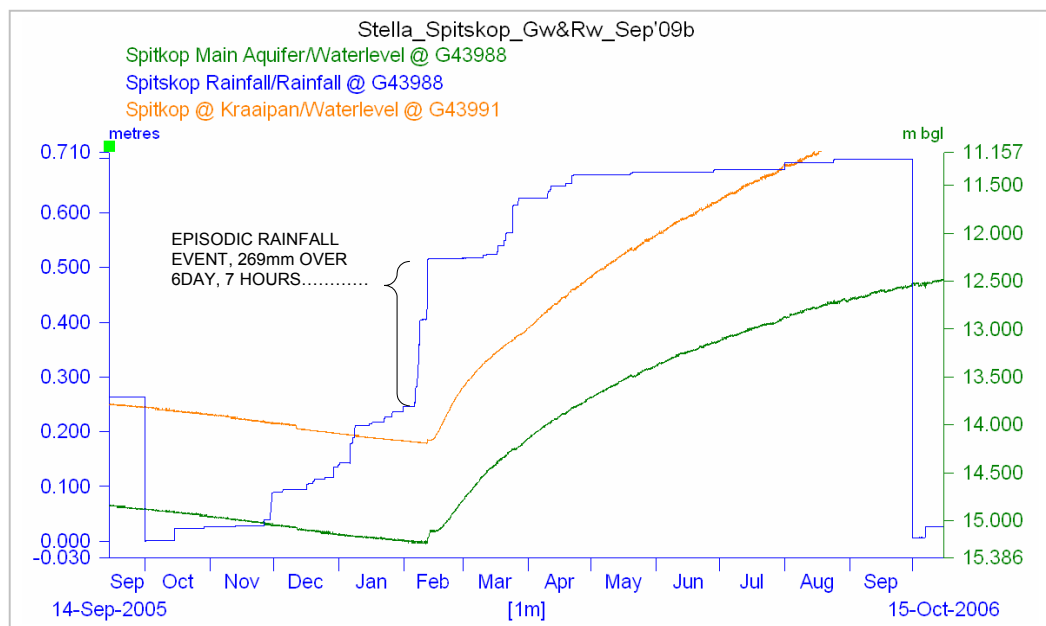


Figure 6.7. Hyetograph-hydrograph set for the 2005-2006 HC as observed on the Spitskopreen monitoring site, at Stella, Vryburg District.

The groundwater recharge initiating rain event confirms a typical rain-week scenario which started the 06 February 2005 at 02h00, it continued for a full six (6) days and eight (8) hours with a rainfall depth of 270 mm . A break of three (3) days and two (2) hours separated the two (2) rain events, a two (2) day eighteen (18) hour event of 157 mm , and a ten and a half ($10\frac{1}{2}$) hour event of 112 mm . It was the latter rain event that initiated an 835 day water table rebound (to peak at $\Delta h = 4.8 \text{ m}$) in the water table over the next two HCs. This rather long water table response time is indicative of a regional recharge event settling over the UFWZ aquifer system, which is probably a unique event for groundwater recharge cases. The actual initiating episodic rainfall event of six (6) days and eight (8) hours started this ASR event.

The wetting process of the UZR bulk matrix (i.e. the bypass macro-pores and micro-fracture medium) is required following prolonged drying-out periods. This results in a situation recurring in the semi-arid regions during both winter and summer dry periods when field capacity deficits develop in the unsaturated zone (Willemink 1988).

As soon as the new rainfall season starts, individual rain events taking place before an episodic event, all form part of a sequence of events that prepares the unsaturated zone for surplus rainfall infiltration. Without this process taking place, several HCs may pass before effective groundwater recharge occurs.

Long-term groundwater table responses report periods of prominent declining water table conditions running over long periods of time; in some cases for two (2) to five (5) consecutive years in a row (Figure 6.8)

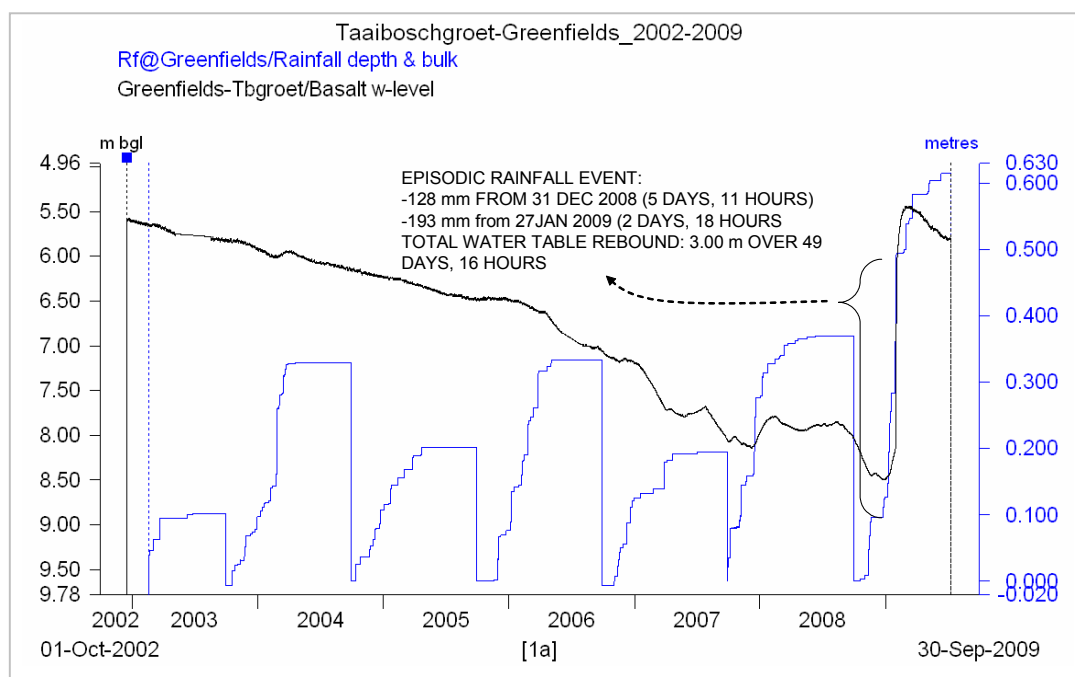


Figure 6.8. Hyetograph-hydrograph set for the 2002-2003 to 2008-2009 HC's as observed on the Greenfields monitoring site, at Taaiboschgroet, Alldays District, Limpopo Province.

In the case of the 2006-2007 hydrological season, several high rainfall intensities above the cut-off value of $1.5 \text{ mm} \cdot \text{hr}^{-1}$ were recorded, though the rain event was much less than the hypothetical 40 mm cut-off value (Eq. 6-5). This phenomenon indicates that the vol-

ume of recharging rainwater was not enough to bridge the field capacity requirement in the UZR to bring about groundwater recharge. The infiltrated rainwater was probably evaporated, used by the local vegetation, or absorbed by the rock medium (micro fractured portion). In the case of a rain-week condition, the field capacity requirement is probably bridged due to low ET rates (high relative humidity prevails for the same duration as the rain-week period).

Although the actual duration (hours or days) of rain events is built into the rain rate, the vadose zone and especially the UUZR seems to return to a deficit moisture condition after four (4) to six (6) days, due to excess ET, especially when the local rooting systems extends beyond the UFWZ (Willemink 1988). A complete new wetting process needs to be initiated which may consume even an episodic rainfall event within a rain-week condition (Figure 6.9).

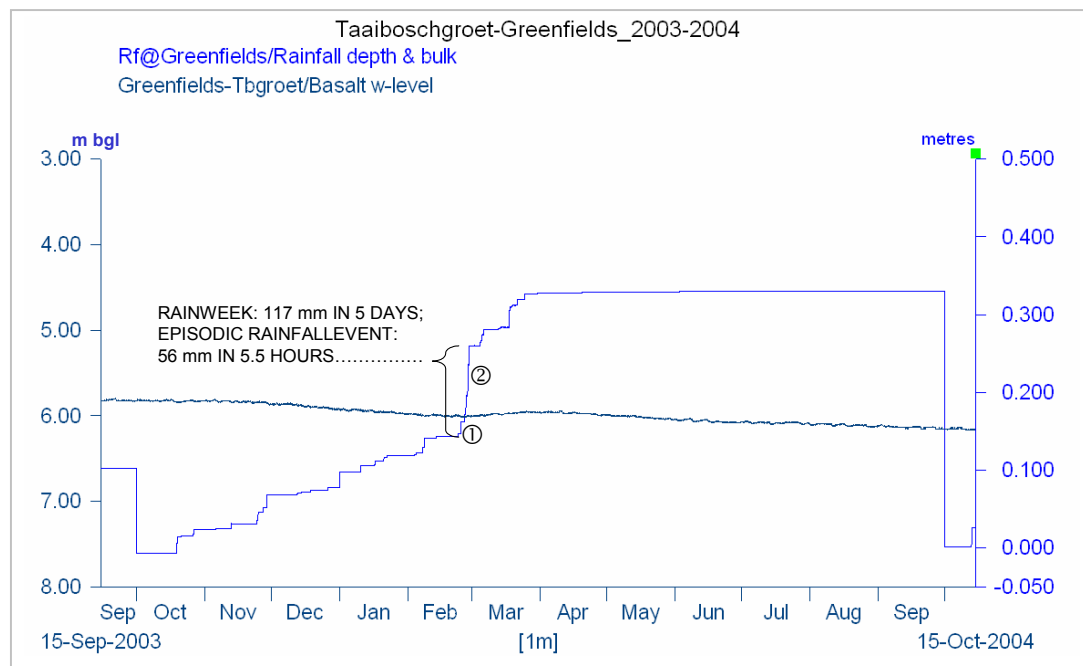


Figure 6.9. Hyetograph-hydrograph set for the 2003-2004 HC as observed on the Greenfields monitoring site, at Taaiboschgroet, Alldays District, Limpopo Province.

The upper limit of the rain rate and rainfall depth algorithm before Hortonian overland flow is generated has not been specified, due to landscape setting, local rolling terrains. It is

foreseen that once this limit has been exceeded, local depression storage will be created, which still keep the excess rainwater in the local area available for recharge.

Although the rain-week reported by the hyetograph at the end of February 2004, totals 117 mm in 5 days, including an episodic rainfall event of 56 mm in 5½ hours, the water table does not respond at all. This condition occurs especially when the local rooting system extends beyond the jointed and weathered profile (Gieske 1992). According to Willemink (1988), ET may already have depleted the moisture content in respect of field capacity within a short period (days) and the rooting zone start to dry-out. This status however requires a new recharge phase, thus a whole new wetting process of the UFWZ needs to be introduced by rainfall.

Within a few days, now with a different vegetation status (maximum water uptake period by plants in growing/production mode) the transpiration process becomes dominant and rainfall events smaller than the threshold specified by Eq. 6-5 is probably completely evapotranspired. In addition, desiccation cracks and microfractures at ground surface may have closed down affecting the direct infiltration of surplus rainwater.

6.2.5 Hydro-Lithologic Model of Hard Rock Recharge Terrains.

A conceptual model illustrating the concept of the direct groundwater recharge mechanism at fractured hard rock terrains has been constructed. It is based on field observations from the Karoo environment and the experimental monitoring terrains at Beaufort West were used given the level of hydrogeological information available. The model illustrates a geometry of secondary vertical and horizontal bypass features and matrix medium as observed in De Jagers Pass, ≈36 km northwest of Beaufort West.

This model portrays the vertical and horizontal flow paths and the Cl^- accession from vertical and lateral flux contributions along a flow path away from the hard rock terrain. This concept is drawn from hydrogeological and DTH-CC image logging (0-100 m) information obtained from the monitoring site at De Hoop Poort and Plaatdoorns, District Beaufort West (Figure 6.10).

The model demonstrates the concept of a hard rock relief and lower regions downstream towards a discharge area consisting of massive calcretes. The area in between represents the typical vegetated soil/regolith horizons as described in Section 4.4.2.1. All these areas were included in the monitoring site networks and in conjunction with the information obtained from the hard rock areas, an applicable differentiation between the various recharge modes could be drawn. Encircled values on the diagram report the actual measured long-term harmonic mean value of the Cl^- concentrations in the various local sites.

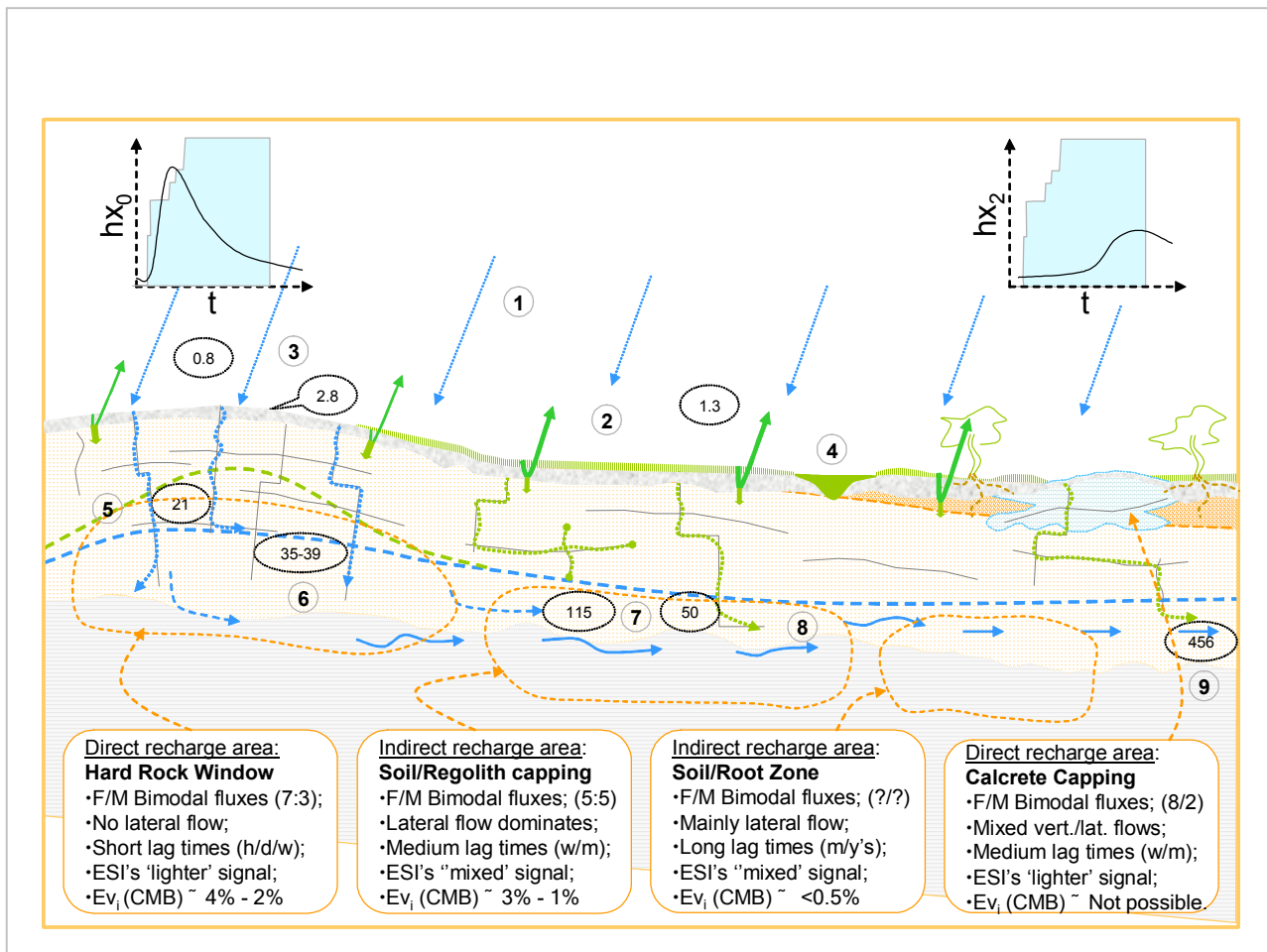


Figure 6.10. Hydrochemical conceptual model of groundwater recharge and the Cl^- flow path in an actual fractured hard rock terrain with adjacent soil/regolith cover area.

The illustration demonstrates the physical characteristics of direct and indirect groundwater recharge with specific reference to the CMB principle (showing the Cl^- concentration levels as physically observed at the experimental monitoring terrains).

These processes are:

- ① Showing the atmospheric hydrochemical contributions with rainwater Cl^- input consisting of episodic rainfall events ($0.3 - 0.7 \text{ mg}\cdot\ell^{-1}$) and normal rainfall events ($0.7\text{-}1.3 \text{ mg}\cdot\ell^{-1}$); dry Cl^- deposition $\approx 80 \text{ mg}\cdot\text{m}^2\cdot\text{y}^{-1}$ and wet Cl^- deposition $\approx 258 \text{ mg}\cdot\text{m}^2\cdot\text{y}^{-1}$;
- ② Hydrochemical enrichment processes at groundwater surface (depression storage) and in the UUZR that characterizes percolating water in excess of soil-moisture deficits (i.e. impact of ET). During this process a background Cl^- concentration is established in the hard rock recharge terrain which resembles the hydrochemical characteristics and concentrations in the rock matrix. Values are difficult to specify and can only be observed through dedicated hydrochemical profiling below the water table interface. Chloride values from as low as 5 to $12 \text{ mg}\cdot\ell^{-1}$ in mountainous terrains to 25 to $75 \text{ mg}\cdot\ell^{-1}$ in escarpments and peneplains were noted;
- ③ Chloride ion concentration of early season's surface run-off ($2.8 \text{ mg}\cdot\ell^{-1}$);
- ④ Local surface water runoff Cl^- concentration in local depressions ($30 \text{ mg}\cdot\ell^{-1}$);
- ⑤ Recharged rainwater migrating into the unsaturated zone as bypass flux through bypass flowpaths and creating a water table rebound which occupies part of the initial unsaturated zone. This phenomenon was observed at several sites following episodic rainfall events and is illustrated in Figure 5.14 ($21 \text{ mg}\cdot\ell^{-1}$);
- ⑥ Total (matrix and bypass flow mixture) Cl^- contribution to bulk water column after episodic recharge ($35\text{-}39 \text{ mg}\cdot\ell^{-1}$);
- ⑦ Total Cl^- contribution to groundwater in areas where direct recharge is lacking due to an effective soil/regolith cover instigating ET from the UUZR. Additional Cl^- may be added to the shallow groundwater system here by lateral flow in the aquifer from adjacent sub-reservoirs in addition to the local, direct contribution through diffuse recharge processes ($115\text{-}150 \text{ mg}\cdot\ell^{-1}$). At this stage using the CMB application should be questioned;
- ⑧ Some local areas exist where a thinner soil/regolith allow bypass flow to utilize macropore structures to drain the rainfall surplus to the SZ without ET (a thinner UUZR) and soil/matrix-moisture deficits ($50 \text{ mg}\cdot\ell^{-1}$).
- ⑨ Groundwater characterized by extreme high mineralization, although situated in effectively recharged areas due to its association with prominent calcrete capping. Any hydrochemical deductions in the case of calcrete overburden are therefore not advisable as it is

an evaporate itself and may contain elevated traces of connate salts included in the bulk carbonate mass.

Recharge estimations for the hard rock area are in the order of 4% for the macro-pore and 2% for the matrix flow component.

The hydrogeochemical flow path from rainwater into the aquifer system via the unsaturated zone is rather complex in terms of the actual recharge mechanism at the point of observation (Willemink 1988) (Section 6.2.3, Figure 6.6).

Although this conceptual model is biased to the Karoo environment, the same observations in terms of the hydrogeochemical characteristics of the rainwater-groundwater flow regime were observed at the Kuruman, Stella and Taaiboschgroet monitoring terrains. Heterogeneity from terrain to terrain is a physical factor as the hydrogeochemical regime is a factor of spatial variability. As was observed at the gross of the monitoring terrains, the concept is well established. The monitoring approach and identification of the direct recharge terrains is crucial to establish each terrain's hydrogeochemical diversity.

6.3 CONCEPTUAL FLOW REGIME AT DIRECT RECHARGE TERRAINS.

6.3.1 Introduction.

Physical response of the aquifer saturation levels following a specific recharge event provides an opportunity to qualify episodic recharge events. The magnitude of the response is (i) a factor of the rain intensity ($\text{mm}\cdot\text{hr}^{-1}$) and rainfall depth (mm), (ii) the hydraulic properties of the aquifer material and (iii) the regional flow regime and interconnectivity of the adjacent sub-reservoirs.

In terms of (ii) above, confined, hard rock aquifers characteristically portray significantly lower storage coefficients than their primary, soft rock equivalents. Storativities can therefore be an order of magnitude different. In the case of a fractured and weathered phreatic aquifer consisting of fractured hard rock material, the storativity is significantly higher than the underlying semi-confined hard rock parent rocks.

Aquifers with the same recharge mechanism, but with different storativity grading, will produce remarkably different water table mounds, i.e. Vaalian Ghaap Group dolomites versus

Permian-Triassic Beaufort Group sandstone/mudstone. It has been observed and demonstrated in hyetograph-hydrograph sets that water table mounds induced by single rain events in the Vaalian Ghaap Group dolomites (Kuruman area) can be as high as 20m at one time, whilst similar rainfall depths in the Palaeozoic Letaba Group basalt (Taaiboschgroet area) may be in the order of 3 meters.

6.3.2 *Enhancement of Episodic Recharge in Fractured Hard Rock Terrains.*

The bulk porous medium in fractured hard-rock terrains varies between primary (rock matrix) β_m and secondary (fracture) β_f porosities. Although porosities describes the total storage in aquifer systems, effective porosity influences the permeability coefficient of the flow medium to some degree which in the case of a fractured rock domain could be relatively high.

The hydraulic concept of a fractured rock mass therefore differ substantially from the bulk rock matrix concept due to the fact that the fracture itself acts like an elongated, open conduit, resulting in relatively high water flow velocities. These flow velocities seen in a fractured hard rock concept model will also vary between configurations of horizontal-vertical to vertical-horizontal fractures. DTH CC image logging reveales that horizontal fracture spacing quickly diminishes to only those associated with geological contacts in depth. Vertical fractures run much deeper, their apertures are several orders of magnitude smaller than the occasional horizontal fractures intersected.

Cook (2003) defines the hydraulic conductivity (K_f) of a planar fracture as:

$$K_F = (2b)^2 \left(\frac{\rho g}{12\mu} \right) \quad (6-6)$$

Where $2b$ is the fracture aperture (μm), ρ is the density of the water, g is the gravity acceleration and μ the viscosity of the water. The sum of evenly spaced fracture hydraulic conductivities ($\sum K_F = K$) is expressed as:

$$K_F = \left(\frac{(2b)^3}{12(2B)} \right) \frac{\rho g}{\mu} \quad (6-7)$$

where $2B$ represents the fracture spacings (expressed as intervals in metres).

With reference to Eq. 6.7 above, the mean groundwater flow rate or Darcy velocity q represents the volume of water that an aquifer transmits per unit cross-sectional area. For homogeneous porous media, this groundwater flow rate (q) can be associated with the groundwater velocity V_w by $q = V_w \cdot \phi$, where ϕ is the porosity of the porous media (Cook 2003). In the fractured hard rock domain, the groundwater flow rate q_f will be proportional to

$$q_f = V_{wf} \cdot \phi_F \approx V_{wf} \cdot dB \quad (6-8)$$

where V_{wf} is the water velocity in the fracture and ϕ_F the porosity of the fracture. The fracture porosity can be approximated by the product of the fracture spacing B , and the fracture aperture b (Cook 2003).

The groundwater flow rates through a fractured medium in comparison to a porous rock matrix (i.e., q_f vs q) can vary an order of magnitude or two (Box 6.1). The gross flow rate through the bulk rock is directly proportional to the fracture spacing B and fracture aperture b .

Box 6.1. Estimation of groundwater flow rates for fractured hard rocks with negligible matrix permeability (after Cook, 2003).

Case 1: Hydraulic Gradient $dh/dz = 10^{-1}$ and $\rho g/\mu = 8.6 \times 10^6 \text{ (m} \cdot \text{s)}^{-1}$

- Fracture Aperture $2b = 100 \text{ } \mu\text{m}$
- Fracture Spacing $2B = 0.5 \text{ m}$
- Matrix Porosity $\phi_M = 0.005$;
- Hydraulic Conductivity $K = 1.4 \text{E}^{-6} \text{ m} \cdot \text{s}^{-1}$ (or $0.12 \text{ m} \cdot \text{d}^{-1}$).
- Flow rate (Porous) $q = 5 \text{ m} \cdot \text{yr}^{-1}$
- Water Velocity Fracture $V_{wf} = 62 \text{ m} \cdot \text{d}^{-1}$

Although the estimations in Box 6.1 are based on approximated variables, the results highlight the difference between groundwater flux in porous medium versus fractured me-

dium, i.e. in the case of a hydraulic gradient $dh/dz = 10^{-1}$, the respective flows will be $0.01 \text{ m}\cdot\text{d}^{-1}$ versus $62 \text{ m}\cdot\text{d}^{-1}$.

The fracture water velocity calculated in Box 6.1 correlates with some of the field observations from hydrographs obtained from hard rock monitoring sites i.e. monitoring site G29870BE at the De Hoop Poort where the saturation level is on average 6.5 m bgl. The physical water table response time over an unsaturated thickness of $\approx 7.21 \text{ m}$ and the response time was 2 hrs, thus the $V_{wf} \approx 3.6 \text{ m}\cdot\text{h}^{-1}$ or $87 \text{ m}\cdot\text{d}^{-1}$.

Although the actual water flow velocity in fracture systems running through the unsaturated zone could be the order of several meters per day, once the fracture becomes saturated and field capacity is reached, the flow velocity will decrease dramatically and adjust according to the aquifer drainage flux governed by SDR.

6.3.3 *Hydraulic Characteristics of Water Table Rebound.*

The dynamic characteristics of an aquifer system are particularly reflected in seasonal and long-term fluctuations of the groundwater table. With reference to Figure 6.6, groundwater table fluctuations provide a measurable indicator for analyzing aquifer dynamics and diagnosing the influence(s) of environmental changes (De Vries 2000).

The water table behavior in direct recharge terrains is partially governed by aquifer storativity (S) and hydraulic conductivity (K). During a steady state condition the height of a groundwater rebound (mound) depends on (i) the recharge R_T , (ii) the hydraulic conductivity K, and (iii) the system dimension L. The hydraulic conductivity consists of a vertical (K_v) and horizontal (K_z) component which is highly variable in space due to the nature of the flow medium (rock mass and the fracture array).

De Vries (1974; 2000) suggests that the flow regimes in recharge and adjacent areas are governed by two parameters describing the groundwater flow through the UZR and finally the horizontal through-flow towards the discharge zone, and they are:

- (i) vertical flow resistance (VFR, Λ , in time - days; $\Lambda = b'/K'_v$), where b' and K'_v is the respective thickness and mean vertical permeability coefficient of the material through which the vertical flow occurs; and

(ii) horizontal (specific) drainage resistance (SDR), Υ , in time - days; $\Upsilon = \Delta h/R_R$), where Δh the hydraulic head represent between the recharge area centre and the discharge zone $x(0,L/2)$ and R_R the rainfall surplus ($\text{mm} \cdot \text{T}^{-1}$).

The SDR is proposed as one of the useful lumped parameters for assessment of the water table response in relation to rainfall induced water table fluctuations (De Vries 1974; 2000).

Given that in a recharge area where the primary topography is flat and the aquifer system resembles a linear reservoir model as depicted in Figure 4.10 (Section 4.5), the horizontal distance between the actual water table divide ($x=0$) and the discharge base (where the water table mound flattens to the regional water table gradient) is given as L . During an episodic recharge event the water table rebound is expanding vertically (Δh is increasing at the water table divide⁶⁸) which implies that the vertical influx of surplus rainwater is higher than the lateral discharge of the system to the adjacent/surrounding sub-reservoirs. De Vries (1974; 2000) describes this condition as:

$$\Delta h = \Upsilon D_D \quad (6-9)$$

where Δh is the water table head at the divide relative to the aquifer drainage base, Υ is the SDR, D_D is the mean areal discharge (which is rather difficult to establish where no physical flow occurs). Under steady state conditions, the recharge rate, $R_T \approx D_D$.

De Vries (1974; 2000) rewrites Eq. 6-9 in terms of the flow equation with the conservation of mass which gives:

$$\alpha S \frac{d\Delta h}{dt} = R_T - \frac{\Delta h}{\Upsilon} \quad (6-10)$$

where S is the storativity, R_T is the recharge and α is a factor, varying between 0.6 and 1.0 depending on the shape of the groundwater table.

⁶⁸At the centre of the hard rock window area.

De Vries (1974) specifies that the relationship between groundwater level rise, the rainfall per unit of time i , the time interval t and the average discharge D_D is given by

$$ti = tD_D + \Delta S \quad (6-11)$$

where ΔS is the change of groundwater storage per unit area as a result of changing groundwater tables.

If the groundwater table rises from $\Delta \bar{h}$ to Δh , the average flux through the phreatic surface during a recharge event is given by the relation:

$$D_D = \frac{\Delta h + \Delta \bar{h}}{2 \cdot Y} \quad (6-12)$$

where SDR, Y is specified in days.

The rise of the groundwater table following the rainfall event is considered to be superimposed on the annual average groundwater head, $\Delta \bar{h} = \bar{R}_R \cdot Y$.

Observations from the hyetograph-hydrograph sets portray graphically that rainfall surplus scenarios manifest under rainfall spells lasting three (3) to eight (8) days during a rain-week event and represents an instantaneous recharge pulse manifesting as a physical water table rebound from a few hours to maximum a few days later. This phenomenon has also been observed by groundwater studies elsewhere in southern Africa (Nyagwambo 2006). Logically, shallow aquifer systems will react almost immediately to the pulse recharge episode in the direct recharge terrain.

De Vries (1974) describes the water table behavior with daily interval increment and it yields:

$$\Delta(\Delta h) = \frac{H - \frac{\Delta \bar{h} \cdot t}{Y}}{\frac{t}{2Y} + S_y \cdot \alpha} \quad (6-13)$$

$$\text{where } H = c \left(\frac{t}{\Delta t} \right)^{(1-m)} \cdot \Delta t$$

obtained from the relation between frequency of exceedance (describing the occurrence of the episodic rain events) and precipitation amounts in $t/\Delta t$ days (preliminary values given by De Vries (1974). This is based on a range of frequency of exceedance, varying from 0.07% to 20%, S_y is the specific yield (0.1) and α is a factor (1.00 or 0.66) describing the geometry of the water table (0.66 for a parabolic water table). The values for H are determined from the frequency of exceedance (rainfall threshold) and the rainfall input in $t/\Delta t$ days given by De Vries (1974, p 179) for a range of rainfall inputs exceeding a particular input.

Values for H are only valid for $t < 180$ days. Application of Eq. 6-13 to illustrate the effect of drainage resistance by Gieske (1992) in semi-arid regions in Botswana and has specified a SDR T of 2500 days. In both cases the water level response in a water table aquifer system is theorized after a one (1) day rainfall event of 10 mm - needless to say that the depth to water table is only a few centimeters in this case study, thus the resulting recharge response from 10 mm rainfall only.

The mathematical expressions considered here were based on work done in the Botswana Kalahari by De Vries (1974; 2000) and Gieske (1992) and describe the water table response due to recharge-producing rainfall surplus as governed by the SDR of the aquifer system. The calculated Δh values for the different recharge zones i.e. the hard rock terrain (vertical recharge only) and the adjacent portions of the reservoirs where recharge derived by lateral groundwater flow only roughly simulate the water table response logged in the field.

The actual case is demonstrated by the De Hoop Poort monitoring site. The hydro-lithological model of this case is demonstrated in Figure 6.10 with specific reference to the hard rock terrain and the surrounding vegetated soil/regolith capped areas. The long-term hyetograph-hydrograph in Figure 6.6 illustrates the water table responses from two boreholes in the monitoring site area with totally different water table responses. In the case of G29870BE, the interaction between the episodic rain events and the water table behavior correlate within the short-term (in a matter of seven (7) days), and the water table from G29899F, 4.3 km from the former, does not correlate with episodic rain events in the same

manner as the hard rock area. It is believed that the unsaturated VFR in the G29899F terrain (soil/regolith covered plain) is significantly higher than the fractured hard rock terrain at G29870BE and surrounds.

In this case study, similar hydraulic parameters were used in both monitoring sites mentioned above. The main difference is the recharge modes; one is direct (G29870B) and the second one (G29899F) is most probably recharged at most laterally. From the time lags between episodic rain events and physical water table responses, SDR of 150 and 450 days were estimated. The $\Delta h/\Delta t$ resulting hydrograph produced over a period t , 365 days with a SDR of 150 days corresponds with the water table hydrographs generated by episodic rain events in the hard rock, direct recharge area (reference to insets in Figure 6.10). The simulated water table rebound is illustrated in Figure 6.11.

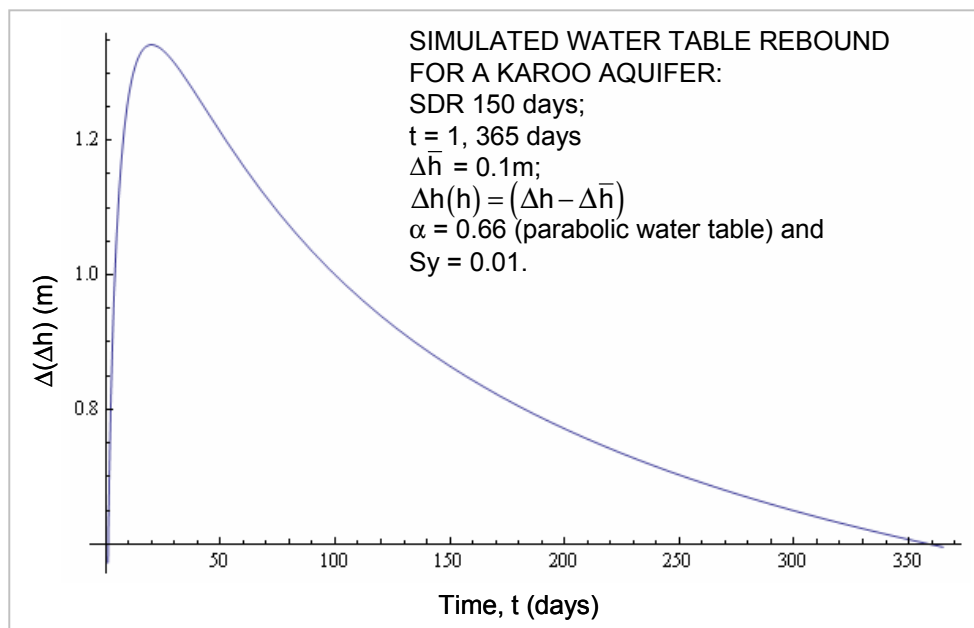


Figure 6.11. The theoretical water level response, $\Delta(\Delta h)$ over a period of 365 days from a precipitation rate of $10 \text{ mm} \cdot \text{d}^{-1}$.

The hydrograph simulation portrayed in Figure 6.11 corresponds with the measured hydrograph of monitoring site G29870BE, at De Hoop Poort and demonstrates the rather fast (<150 days) flow cycle of recharge-producing rainfall surplus through the hard rock terrain (Figure 6.5).

Applying the same algorithm at the G29899F monitoring site with SDR of 450 days, the resulting $\Delta h/\Delta t$ hydrograph shown in Figure 6.12 correspond with the concept proposed by Willemink (1988), i.e. where surrounding sub-reservoirs are subsequently recharged from a nearby hard rock terrain. The water table response is characterized by a much longer lag time between the rain event and the water table rebound and the aquifer systems gains water and reports an ASR condition.

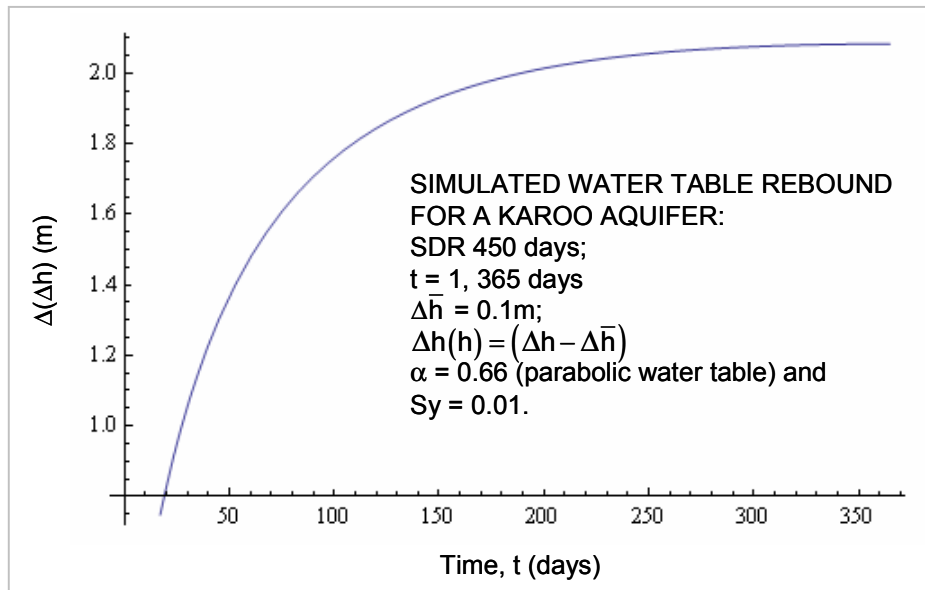


Figure 6.12. Showing a simulated water level response, $\Delta(\Delta h)$ over a period of 365 days from a precipitation rate of $10 \text{ mm} \cdot \text{d}^{-1}$.

This exercise demonstrates the effect of SDR where hard rock terrains act as direct recharge zones for surrounding sub-reservoirs. For an aquifer system with similar hydraulic parameters, but a different recharge mechanism (i.e., the indirect recharge areas illustrated in Figure 6.10) a higher SDR induces the hydrograph setting in Figure 6.7. This hydrograph format has been observed specifically at Stella during the 2005-2006 episodic recharge events. Other parameter changes like for example the storage values tend to influence the water table rebound increment (i.e. $\Delta(\Delta h)$). A difficult parameter to obtain is the value for H (in Eq. 6-13) as a significant set of rainfall data is required to calculate a reasonable representative frequency of exceedance for the said monitoring terrain (Section 6.1.2.1).

The application of the De Vries (1974) approach whereby a SDR value is specified for each monitoring site in a sparsely covered monitoring terrain should support identification of primary recharge terrains. Terrains where high SDR's occur might not classify as direct recharge terrains, but rather receiving sub-reservoirs (Willemink 1988). The resulting assessment will therefore, necessitates differentiating areas in direct recharge and/or non-direct recharge zones. Monitoring sites with high SDR values should not be primarily used as CMB sites due to the dominating lateral flow regime.

6.3.4 Hydrogeochemistry Characteristics of an Episodic Recharge Event.

The hydrochemical signal of an episodic rainfall event that is part of a rain-week condition is characteristically of a depleted nature (as observed over a 7 year period over six (6) experimental monitoring terrains). Atmospheric conditions during these rain-weeks are exceptionally humid (>80% RH), thus the hydrogeochemistry of both cloud water and the precipitating rainwater remain under equilibrium conditions. Minimum evaporation at the cloud base is taking place under these conditions and both Cl^- and ESI composition in the final precipitate is characterized by a depleted composition.

The Cl^- concentration is in the order of $0.4 \text{ mg}\cdot\text{l}^{-1}$ as has been observed at all the summer rainfall region's rainfall monitoring sites when reporting an episodic event. The RES unit specifically reported this phenomenon at the Pretoria East and Stella monitoring sites where Cl^- values from 16 samples over a period of one month varies between 0.1 and 0.6 were reported.

Recharge-producing rainfall surplus in the case of an episodic rainfall event will eventually have a depleted effect on the groundwater hydrochemistry soon after that particular recharge event. Such an event was recorded at the De Hoop Poort, G29870BE monitoring site at Beaufort West during the 2007-2008 HC (Figure 5.15). The sample collected at 6.5 m bgl, on 06-02-2008, was eight (8) days after an episodic rain event of 50 mm with a rain intensity of $8.0 \text{ mm}\cdot\text{hr}^{-1}$ and reported a groundwater Cl^- concentration of $21.8 \text{ mg}\cdot\text{l}^{-1}$. This is significantly lower than the medium-term background value of $\approx 38 \text{ mg}\cdot\text{l}^{-1}$.

Several other cases were noted where groundwater zones with Cl^- values varying $\pm 18\%$ from the mean background concentrations. Only a few cases were noted where higher

Cl⁻ spikes occur, thus indicating the presence of Cl⁻ enriched water in the groundwater profile. This phenomenon is expected, as rainfall events below the specifications set by Eq. 6-5 will introduce elevated Cl⁻ levels of into the unsaturated zone according to the principles governing the CMB application (Gieske 1992).

The ESI composition of the recharging rainwater from the bulk rainwater input over the early and peak rainfall season plots around $^{18}\delta = -3\text{‰}$, $^{2}\delta = -18\text{‰}$ on the Harmon Craig diagram. Most groundwater's ESI signatures in this study are relative more negative on the LMWL, i.e. $^{18}\delta = -6\text{‰}$, $^{2}\delta = -38\text{‰}$. Observations from episodic rainfall events are relatively depleted ($^{18}\delta = -10\text{‰}$, $^{2}\delta = -65\text{‰}$ to $^{18}\delta = -12\text{‰}$, $^{2}\delta = -78\text{‰}$) which indicates that a considerable portion of this rainwater in fact moves directly to the SZ (Figure 6.13).

This confirms that a considerable large contribution of bypass flow is taking place in these fractured hard rock terrains. It was noted by researchers that where direct groundwater recharge is enhanced by bypass infiltration, the isotopic composition of the episodic rainwater input and the groundwater should fall in the same range (Nkotagu 1997).

De Vries and Simmers (2002), mentions that bypass flow, received during the early stages of the summer season on a dry and cracked ground surface and/or during extraordinary high rainfall events may contribute to 90% of a regions annual recharge. These extraordinary high contributions is probably taking place in extreme hard rock cases like the TMG ortho-sandstones, in total bare rock conditions (no soil/regolith and UFWZ).

The comparison between rainwater input in peak 2006 ($^{18}\delta = -5.53\text{‰}$, $^{2}\delta = -37.0\text{‰}$), peak 2008 ($^{18}\delta = -6.33\text{‰}$, $^{2}\delta = -29.59\text{‰}$) and peak 2009 ($^{18}\delta = -4.24\text{‰}$, $^{2}\delta = -31.29$), and the groundwater around $^{18}\delta = -6\text{‰}$ and $^{2}\delta = -37\text{‰}$ is quite obvious and clearly signals the episodic rainfall input in 2006.

The information illustrated in Figure 6.13 reports the following hydrogeochemical scenario:

- Spitkopreen is the ESI composition of the early and peak rainwater collected during years with minimum episodic rainfall events, i.e., 2002-2003, 2004-2005 and 2006-2007;

- HC's with episodic events, represents ESI composition of the early and peak rainwater collected during years with prominent episodic rainfall events, i.e. 2003-2004, 2005-2006 and 2007-2008;

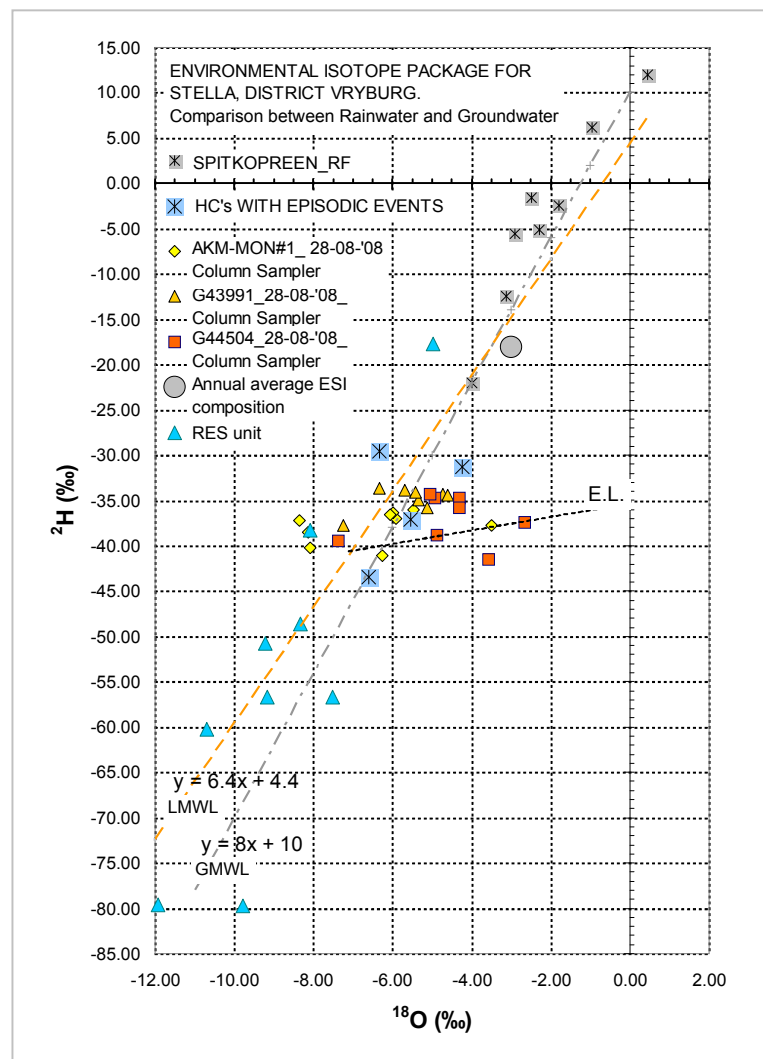


Figure 6.13. Comparison between the stable isotope composition of the 2002-2009 rainfall period and groundwater sampled from local boreholes where a water table mound of 2.84 m was recorded.

- AKM-MON#1 represents the ESI composition sampled on 28 August 2008 from a 2 m column in the Mosita granite at Stella which represents a hard rock terrain with <0.25 m soil/regolith cover;

- G43991 represents the ESI composition sampled on 28 August 2008 from a 2 m column in the Kraaipan Group at Stella which represents a hard rock terrain with limited soil/regolith cover;
- G 44504 represents the ESI composition sampled on 28 August 2008 from a 2 m column in the Mosita Granite Suite with thick soil/regolith cover. This site is situated close to several small depressions (pans). As indicated in Figure 6.13, the ESI composition reports a strong evaporation signature (E.L.) in this groundwater which is to be expected from the accumulation of rainwater in these depressions. The grouping of the sample points is also much wider than those from samples in boreholes G43991 and AKM-MON#1. It was noted (Google image assessments) that some of these pans once flooded can store the local run-off for extended periods; and
- RES unit represents the ESI composition of the rainwater sampled using the RES unit. Although these samples were only collected between December 2008 and January 2009 and out-of-phase with those presented in Figure 6.13, it still demonstrates the relatively depleted composition of individual cloud water samples.

Mook (2001) and Verhagen (2010) indicates that during prolonged rainfall events, i.e. the rain-week scenario, atmospheric conditions are remarkably different than during the normal isolated convection cell rainfall patterns normally encountered in the central South African region.

The relative humidity specifically plays a dominant role in the final hydrogeochemical composition of the rainwater, as the cloud water remains hydrogeochemically in equilibrium with the larger atmospheric mass with its unique hydrogeochemical character which probably is already considerably depleted during several rainout events along its migration pathway from its origin, the ITCZ and the equatorial ocean region.

To conclude, episodic rainfall events portray (i) the rain rate-depth configuration to effectively recharge and (ii) introducing a characteristic hydrogeochemical signature in the recharge-producing rainfall surplus and infiltrating rainwater.

6.4 RECHARGE ESTIMATES FOR DIFFERENT HYDROGEOLOGICAL TERRAINS.

6.4.1 *Introduction.*

A relatively diverse selection of experimental monitoring sites were developed for the generation of hydrological information required to investigate the role of episodic rainfall events, instigating groundwater recharge events of a similar episodic nature. Special attention to sites on mountainous regions and peneplains was put into effect in areas with different UFWZ characteristics based on the underlying parent rock types.

Statistical assessment of long-term rainfall data however revealed that episodic rainfall events above a certain rain rate and rainfall depth (Eq. 6-5), in fact occurs in an intermittent pattern, thus sustainable groundwater recharge could be graded as intermittent as well. Integrated hyetograph-hydrograph sets reported that ASR occurs during the peak interval in especially the summer rainfall regions.

Two (2) hydrochemical applications have been applied in this study, i.e., (i) CMB to evaluate the total groundwater recharge rate (R_T , $\text{mm}\cdot\text{yr}^{-1}$) by using C_P , C_G and R_{eff} with TC, and (ii) ESI's an indicator of multi-modal recharge regime.

The application of hydrogeochemical information on the one hand and high-frequency hyetograph-hydrograph information on the other hand, can be used to implement a dedicated rainwater-groundwater monitoring process. This procedure will support sampling time-dependant components of the hydrological cycle, based on the different rainfall intervals in winter and summer rainfall regions (i.e. dry, early and peak). This monitoring procedure generates a set of hydrogeological state variables which can be used to differentiate the rainwater (C_P) into three groups (C_D , C_{EP} and C_{PP}). These variables allow estimation of the groundwater recharge over specific intervals; in this case the dry, early and peak periods.

In the next section, this approach will be applied to the different experimental monitoring terrains and a quantification of the effective groundwater recharge per site will be presented.

6.4.2 Quantification of Episodic Recharge Events.

Estimation of the actual recharge event in terms of physical values (R_T , $\text{mm}\cdot\text{yr}^{-1}$, or Q_n , $\text{m}^3\cdot\text{yr}^{-1}$), requires additional parameters to be part of the monitoring attributes. Hydrometeorological attributes, especially specification of ET_A , on a daily interval can assign valuable information on the daily water balances as recommended by Willemink (1988). Application of the hydrogeochemical constituents requires a highly specialized monitoring programme which could become extremely costly when sampling is not governed by strict planning according to the behavior of the aquifer systems during episodic recharge episodes.

Comprehensive sampling of the rainwater and groundwater chloride concentrations allows for expansion of the recharge rate algorithm in three time related intervals over a specific HC, as illustrated:

$$\overline{R_T} = \frac{(\overline{P_D \cdot C_D}) + (\overline{P_{EP} \cdot C_{EP}}) + (\overline{P_{PP} \cdot C_{PP}})}{\overline{C_G}}, \quad (6-14)$$

Differentiated monitoring, as developed through this study, generates shorter series of hydrogeochemical data which allows differentiation of Eq. 6-14 in terms of the three tier periods over a HC; the following expression is suggested:

$$\overline{R_T} = \frac{(\overline{P_D \cdot C_{Pd}} + \overline{C_{Dd}})}{\overline{C_{Gd}}} + \frac{(\overline{P_{EP} \cdot C_{Pep}} + \overline{C_{Dep}})}{\overline{C_{Gep}}} + \frac{(\overline{P_{PP} \cdot C_{Ppp}} + \overline{C_{Dpp}})}{\overline{C_{Gpp}}}, \quad (6-15)$$

where:

R_T is the average recharge rate over a short-term period (one HC);

P_D , P_{EP} and P_{PP} are differentiated rainfall inputs over the dry, early and peak periods which can include an episodic rain event in either P;

C_{Pd} , C_{Pep} and C_{Ppp} are harmonic mean Cl^- concentrations ($\text{mg}\cdot\text{l}^{-1}$) in rainwater collected during the three tier period;

C_{Dd} , C_{Dep} and C_{Dpp} is the average annual dry Cl^- input ($\text{mg}\cdot\text{m}^2\cdot\text{y}^{-1}$), differentiated into the applicable three tier periods (in this case a daily Cl^- input is estimated and summed for each of the periods);

C_{Gd} is the average Cl^- concentration ($mg \cdot l^{-1}$) in the groundwater profile towards the end of the dry period i.e. towards the end of the recession period;

C_{Gep} is the average Cl^- concentration ($mg \cdot l^{-1} - Cl^-$) in the groundwater profile towards the end of Dec_n (also note that an episodic recharge event may have occurred during the early period); and

C_{Gpp} is the average Cl^- concentration ($mg \cdot l^{-1}$) in the groundwater profile towards the end of Mar_{n+1} (this period includes most of the episodic recharge events)

The dry atmospheric Cl^- deposition C_{Dd} needs special explanation in terms of Eq. 6-15 as this component is normally included in the wet deposition. In this study's case the measured dry Cl^- deposition, calculated on a daily interval is added with the first R_{eff} , depicted from the hyetograph-hydrograph set.

Application of Eq. 6-15 for some of the monitoring sites yields the total annual groundwater recharge estimations. Contribution of episodic recharge events may enhance a hydrological season's groundwater recharge in some cases in the order of 100% of the average annual recharge value.

For realistic comparison, Mazar's (1997) ET index (ET_{INDEX}) based on Cl^- as a hydrochemical marker, is also included. This algorithm reports the Cl^- ratio (as percentage - %) between local rainwater and groundwater and represents an index based on the impact of ET_A in a hydrogeological environment. The algorithm forms part of Eq. 6-15 (which completes the CMB application by incorporating effective rainfall R_{eff} and the dry Cl^- deposition C_D).

Observations of the lag time differences between individual rainfall events and water table responses in direct recharge terrains, and hydrogeochemical profiling below the water table interface, indicate that bypass recharge is more effective during the peak rainfall period in Jan_{n+1} to Mar_{n+1} . The hydrogeochemical signature during this period could therefore report the impact of bypass recharge. Comparing the groundwater Cl^- concentrations of the peak inputs on the one hand, and the actual water table response on the other hand as observed, indicates that the contribution of bypass recharge to groundwater systems in fractured hard rock terrains, may be as high as 60%.

6.4.2.1 Recharge Estimations for Some Experimental Monitoring Terrains.

The differential recharge estimations for monitoring terrains the semi-arid, summer rainfall region are presented based on application of Eq. 6-15. To illustrate the contribution of episodic rainfall events on the total annual groundwater recharge, a HC with prominent episodic rainfall events, i.e., 2007-2008, was used.

Box 6.2: Karoo Sedimentary Fractured Hard Rock Terrain.

The monitoring site consists of a fractured hard rock terrain in Karoo Supergroup mudstones. Vegetation is limited to typical savanna grassland with occasional scrubs/trees.

A thin (<200 mm) layer of regolith consisting of broken and decomposed mudstone fragments forms the ground surface. The local water table is between 5 and 7.5 m bgl.

These areas are highly responsive to rainfall events with duration and intensities above the observed rain rate of $1.5 \text{ mm} \cdot \text{h}^{-1}$ and rainfall depth of 45 mm (Figure 6.5).

The annual 2007-2008 HC recharge for this hard rock region is $\approx 4\%$ or $\approx 12 \text{ mm} \cdot \text{yr}^{-1}$ from an annual R_{eff} of 300 mm. The peak period, which includes the episodic rainfall events represents $\approx 63\%$ of R_T .

Box 6.2

DIFFERENTIAL ALGORITHM FOR Gwater RECHARGE ESTIMATIONS

For: De Hoop Poort 2007-2008 Hydrological Season's Base Line Chloride Input.

Recharge Mode: Karoo Fractured Hard Rock Terrain

'Dry' Chloride Spec		Dry Cl?	'Early' Chloride Spec		Dry Cl?		'Peak' Chloride Spec		Dry Cl?	P _A (mm)
P _D	C _{Pd}		P _{EP}	C _{Pep}	'Dry'	'Early'	P _{PP}	C _{Ppp}	'Peak'	
0	0	0	128	0.82	41	16	172	0.8	23	300
C _{Gd} = 55			C _{Gep} = 36				C _{Gpp} = 22			
0			161.96				160.6			
55			36				22			
. mm			4.5 mm				7.3 mm			R _T
. % per year			1.5 % per year				2.4 % per year			ET _{INDEX}

Total Gwater Recharge from Vertical Component is: 11.8 mm/y

Total Gwater Recharge as percentage of effective rainfall: 3.9 % per year

Table 6.4. Karoo fractured hard rock terrain, episodic recharge (2007-2008).		
Attribute	Quantify	Remarks
Rainwater Cl^- (peak), $\text{mg}\cdot\ell^{-1}$	0.8	Harmonic mean.
Groundwater Cl^- , $\text{mg}\cdot\ell^{-1}$	22	Bypass flow captured.
Recharge Mode	$R_{PR} : R_M$	Multi-modal in Beaufort mudstone.
Lag time (Rf to Wl) days/hours	7 hours	Bypass recharge dominates.

Box 6.3: Karoo Sedimentary Hard Rock Terrain with Soil/Regolith Cover.

The monitoring site is located on a SW dipping peneplain including a flood plain with streamline vegetation consisting of shrubs and trees.

The hyetograph-hydrograph set (Figure 6.6) reports no direct recharge features. The time lag between the local rainfall events and actual groundwater rebound is several months (181 days).

The ground surface consists of very fine flood-plain silt which probably blocks most of the fractures in the UFWZ.

Water table is around 10 to 13 m bgl and there are no short term (hours to days) responses to normal and episodic rainfall events. The local aquifer responds to long-term events only and is replenished by lateral drainage from surrounding hard rock outcrop areas.

Box 6.3

DIFFERENTIAL ALGORITHM FOR Gwater RECHARGE ESTIMATIONS

For: De Hoop Poort 2007-2008 Hydrological Season's Base Line Chloride Input.

Recharge Mode: Karoo Peneplain/Flood Plain with Soil/Regolith Cover.

'Dry' Chloride Spec		Dry Cl?	'Early' Chloride Spec		Dry Cl?		'Peak' Chloride Spec		Dry Cl? 'Peak'	P _A (mm)
P _D	C _{Pd}		P _{EP}	C _{Pep}	'Dry'	'Early'	P _{PP}	C _{Ppp}		
0	0	0	128	0.8	41	16	172	0.8	23	300
C _{Gd} = 150			C _{Gep} = 111				C _{Gpp} = 111			
0			159.4				160.6			
150			111				111			
. mm			1.4 mm				1.4 mm			
. % per year			.5 % per year				.5 % per year			R _T ET _{INDEX}

Total Gwater Recharge from Vertical Component is: 2.9 mm/y

Total Gwater Recharge as percentage of effective rainfall: 1. % per year

Table 6.5. Karoo fractured hard rock terrain with soil/regolith cover on peneplain, episodic recharge (2007-2008).

Attribute	Quantify	Remarks
Rainwater Cl^- , (peak), $\text{mg}\cdot\ell^{-1}$	0.8	Harmonic mean.
Groundwater Cl^- , $\text{mg}\cdot\ell^{-1}$	111	No indication of bypass flow
Recharge Mode	Lateral Flow	Little evidence of direct recharge.
Lag time (Rf to WI) days/hours	181 days	Soil/regolith covered area.

The annual recharge as percentage of R_{eff} of this site is low (1%) and represents 1% of R_{eff} , as indicated in Box 6.3, Groundwater recharge is mostly by lateral recharge from the surrounding hard rock terrains.

Currently one of the main aquifer systems supplying bulk water to the town of Beaufort West collapsed in terms of its sustainable use. In fact no ASR has occurred in the last 7 years at this site (Conrad 2010).

Box 6.4: Karoo: Highlands/Mountainous Terrains.

This monitoring site is situated in the Nuweveld Mountains in Karoo Supergroup MNDS. Characterised by depleted Cl^- values, mountainous terrains reports relatively low rain-water hydrochemical concentrations which is a result of (i) the higher elevation and (ii) the amount effect.

Box 6.4

DIFFERENTIAL ALGORITHM FOR Gwater RECHARGE ESTIMATIONS

For: Nuweveld Mountains 2007-2008 Hydrological Season's Base Line Chloride Input.

Recharge Mode: Karoo Fractured Hard Rock Terrain

'Dry' Chloride Spec		Dry Cl?	'Early' Chloride Spec		Dry Cl?		'Peak' Chloride Spec		Dry Cl?	P _A (mm)
P _D	C _{Pd}		P _{EP}	C _{Pep}	'Dry'	'Early'	P _{PP}	C _{Ppp}		
0	1	0	150	0.9	15	15	200	0.7	15	350
C _{Gd} = 15			C _{Gep} = 9.6				C _{Gpp} = 7.7			
0			165				155			
15			9.6				7.7			
. mm			17.2 mm				20.1 mm		R _T	
% per year			4.9 % per year				5.8 % per year		ET _{INDEX}	

Total Gwater Recharge from Vertical Component is: 37.3 mm/y

Total Gwater Recharge as percentage of effective rainfall: 10.7 % per year

Table 6.6. Karoo fractured hard rock terrain in Nuweveld Mountains, episodic recharge (2007-2008).

Attribute	Quantify	Remarks
Rainwater Cl^- (peak), $\text{mg}\cdot\ell^{-1}$	0.7	Harmonic mean.
Groundwater Cl^- , $\text{mg}\cdot\ell^{-1}$	7.3	Bypass flow captured
Recharge Mode	R_{PR}	Preferential in Karoo sand-stone/mudstone.
Lag time (Rf to Wl) days/hours	Hours	

Observations from the hyetograph-hydrograph set for this site reports irregular responses to local rain events. The UFWZ, once saturated may only act as a lateral through-flow system for a much larger flow regime, ending as base flow in the many rivulets and streams in mountainous regions. The actual recharge rate estimated in Box 6.4, therefore also includes that portion captured and discharged by interflow.

Characteristic shallow (<10m bgl) water table depths in specifically mountainous areas consisting of Karoo Supergroup formations is probably the result of impermeable beds creating purged water table conditions. The sustainability of these systems is well established by the higher rainfall input as observed in the Nuweveld Mountains.

Groundwater samples collected from a ephemeral spring at the Abrahamspoort monitoring site AT01, reports Cl^- values of around 5 to 8 $\text{mg}\cdot\ell^{-1}$, which correlates well with those observed in the Cl^- profiles in borehole AT01 (6.4 to 10.1 $\text{mg}\cdot\ell^{-1}$) some 30 m away.

The contribution of episodic recharge in this case is almost permanently as even some small rainfall events respond immediately as water table rebounds on the hydrographs. The recharge rate R_T is high ($\approx 11\%$) and has been observed in other high relief areas as well

High relief terrains, like the Nuweveld Mountains and Kuruman Hills, have relatively low groundwater Cl^- values (<15 $\text{mg}\cdot\ell^{-1}$); thus the recharge rates and values indicate relatively higher groundwater replenishment than the low-lying peneplains. The depth to water table does not have an impact on this as the groundwater Cl^- concentration at a monitoring terrain in the Kuruman Hills (BIF) falls between 4 and 18 $\text{mg}\cdot\ell^{-1}$ at ≈ 75 m bgl.

Box 6.5: Dolomitic Water Areas.

The monitoring site used for recharge estimations is situated on Vaalian Ghaap Plateau Group dolomites in the upper Kuruman River catchment (above the Kuruman A-Spring). It is typical dolomite hard rock terrain with virtually limited soil/regolith cover.

Box 6.5

DIFFERENTIAL ALGORITHM FOR Gwater RECHARGE ESTIMATIONS

For: Kuruman River Catchment 2007-2008 Hydrological Season's Base Line Chloride Input.

Recharge Mode: Ghaap Plateau Dolomite Hard Rock Terrain

'Dry' Chloride Spec		Dry Cl?	'Early' Chloride Spec		Dry Cl?		'Peak' Chloride Spec		Dry Cl?	P _A (mm)
P _D	C _{Pd}		P _{EP}	C _{Pep}	'Dry'	'Early'	P _{PP}	C _{Ppp}	'Peak'	
52	1	41	150	0.7	0	24	250	0.4	15	452
C _{Gd} = 25			C _{Gep} = 25				C _{Gpp} = 7.5			
93			129				115			
25			25				7.5			
3.7 mm			5.2 mm				15.3 mm			R _T
.8 % per year			1.1 % per year				3.4 % per year			ET _{INDEX}

Total Gwater Recharge from Vertical Component is: 24.2 mm/y

Total Gwater Recharge as percentage of effective rainfall: 5.4 % per year

Table 6.7. Dolomite hard rock terrain in Ghaap Plateau, Kuruman District, episodic recharge (2007-2008).

Attribute	Quantify	Remarks
Rainwater Cl ⁻ (peak), mg·ℓ ⁻¹	0.4	Harmonic mean.
Groundwater Cl ⁻ , mg·ℓ ⁻¹	7.5	Bypass flow captured.
Recharge Mode	R _{PR}	Bypass flow in KARST.
Lag time (Rf to WI) days/hours	12 to 48 hours	

Characteristically, the Ghaap Plateau, although fairly well vegetated with strong growers like shrubs, it portrays a rather barren landscape.

The Kuruman A-Spring is unique in the sense that it is recharged from two main sources, the Kuruman Hills and the Ghaap Plateau with distinctive different hydrochemical composition. The groundwater Cl⁻ concentration on the plateau is in the order of 20 to 25 mg·ℓ⁻¹, where as the spring's Cl⁻ concentration varies in a very narrow band between 4 and 8 mg·ℓ⁻¹.

Water table rebounds in dolomitic hard rock terrains respond almost immediate to rain events and water table mounds of 15 m within hours are quite common during especially episodic rain events (Figure 6.4).

The total groundwater recharge difference between the Ghaap Plateau dolomite (at 5%) and the adjacent banded ironstones of the Kuruman Hills (at maximum 15%) is considerably high (1:3); an important aspect to consider when large scale estimations for dolomitic terrains are performed.

The contribution of direct (vertical) recharge in dolomitic water terrains contributes to almost 100% of R_T due to the barren nature of these terrains. Hortonian run-off is a rare occasion and might occur in limited areas due to regolith cover. These areas are probably the best examples of close to 100% bypass flow contribution during recharge events. The lag time between an episodic rainfall event and the groundwater table rebound is <48 hours. Depending on the rain rate - rainfall depth, it can be <12 hours (observed from hyetograph-hydrograph sets).

The recharge rate R_T is high ($\approx 5\%$) in terms of other peneplain terrains ($\approx 1\%$). Episodic rainfall events contributes $\approx 58\%$ to R_T in dolomitic water areas.

Box 6.6: Basement Hard Rock with Local Hard Rock Windows.

The results from the experimental monitoring terrain at Stella, District Vryburg in the Northern Cape Province are used for presentation under this grouping.

The basement rock formation consists of the Mosita Granite ($\approx 25 \text{ km}^2$) characterized by its deep, fractured, pegmatitic composition and is situated $\approx 5 \text{ km}$'s south of Stella. The aquifer area is covered with soil/regolith, in places much more than 0.25 m. This relatively young (age still unknown to SACS) granite suite has most likely during its intrusion phase, intruded directly next to the Kraaipan Group BIF's.

The Swazian Kraaipan Group consists of highly fractured and jointed banded ironstone rocks which were deformed so that the succession is currently standing almost vertical. It forms a positive relief in the region and probably plays an important role in the local recharge mechanism as what could be observed at the Stella experimental monitoring ter-

rain. The latter forms a range of prominent north-south running hillocks in the Stella area, representing typical elevated, fractured hard rock terrains.

Box 6.6

DIFFERENTIAL ALGORITHM FOR Gwater RECHARGE ESTIMATIONS

For: Stella Area 2007-2008 Hydrological Season's Base Line Chloride Input.

Recharge Mode: Savanna Peneplain with Kraaipan Fractured Hard Rock Terrain.

'Dry' Chloride Spec		Dry Cl?	'Early' Chloride Spec		Dry Cl?		'Peak' Chloride Spec		Dry Cl? 'Peak'	P _A (mm)
P _D	C _{Pd}		P _{EP}	C _{Pep}	'Dry'	'Early'	P _{PP}	C _{Ppp}		
0	1	0	100	0.9	45	25	250	1	20	350
C _{Gd} = 75			C _{Gep} = 45				C _{Gpp} = 45			
0			160				270			
75			45				45			
. mm			3.6 mm				6. mm			
. % per year			1. % per year				1.7 % per year			
										R _T
										ET _{INDEX}
Total Gwater Recharge from Vertical Component is: 9.6 mm/y										
Total Gwater Recharge as percentage of effective rainfall: 2.7 % per year										

Table 6.8. Savanna peneplain with local hillocks consisting of Kraaipan Group BIF's (2007-2008).

Attribute	Quantify	Remarks
Rainwater Cl ⁻ (peak), mg·ℓ ⁻¹	0.9	Harmonic mean.
Groundwater Cl ⁻ , mg·ℓ ⁻¹	45	Bypass flow captured
Recharge Mode	R _M and R _{PR}	Multi-modal in GRNT.
Lag time (Rf to WI) days/hours	5 days 20 hours	

Direct recharge over the Mosita aquifer system itself is most likely not as high as indicated in Box 6.6; probably due to its rather high groundwater Cl⁻ concentration of ≈100 mg·ℓ⁻¹, where as the Kraaipan hard rock terrains have considerably less Cl⁻ concentration, i.e. from 12 to 40 mg·ℓ⁻¹.

The Mosita aquifer area is unique due to the presence of a large number of local depressions (pans). These pans seem to have quite different drainage factors, as some of them will drain out within a few days from being filled by local surface run-off (direct, but cluster recharge); others stay filled for several months before the water probably evaporates instead of infiltrate. The Cl⁻ concentration in one of these pans was ≈30 mg·ℓ⁻¹ a few weeks after it was filled by local run-off.

6.5 SUMMARY.

Box 6.7. Summary: Semi-Arid Regions of South Africa.

Box 6.7 represent a summary of the regional, semi-arid groundwater recharge using the average (HARmean) hydrochemical values from four monitoring sites (Beaufort West, Kuruman, Stella and Taaiboschgroet). These terrains can be classified as fractured hard rock terrains according to their bare rock outcrops. The data therefore represents the hydrochemical characteristics of peneplanes in the semi-arid regions.

Box 6.7

DIFFERENTIAL ALGORITHM FOR Gwater RECHARGE ESTIMATIONS

For: Semi-arid Regions 2007-2008 Hydrological Season's Base Line Chloride Input.

Recharge Mode: Hard Rock Regions, South Africa.

'Dry' Chloride Spec		Dry Cl?	'Early' Chloride Spec		Dry Cl?		'Peak' Chloride Spec		Dry Cl?	P _A (mm)
P _D	C _{Pd}		P _{EP}	C _{Pep}	'Dry'	'Early'	P _{PP}	C _{Ppp}		
10	1.5	34	100	0.8	0	34	150	0.4	20	260
C _{Gd} = 50			C _{Gep} = 39				C _{Gpp} = 20			
49			114				80			
50			39				20			
1. mm			2.9 mm				4. mm			
.4 % per year			1.1 % per year				1.5 % per year			R _T ET _{INDEX}
Total Gwater Recharge from Vertical Component is: 7.9 mm/y										
Total Gwater Recharge as percentage of effective rainfall: 3. % per year										

The background Cl⁻ concentration of 39 ±3 mg·ℓ⁻¹ for the groundwater used in this assessment is a mean (HARmean) value observed from the said experimental monitoring terrains. The contribution of dry Cl⁻ to the groundwater, which has been observed with the column sampling procedure, can be as high as 25% above the background Cl⁻ concentration. A value of 50 mg·ℓ⁻¹ Cl⁻ for this groundwater has been used which is rather high.

The groundwater Cl⁻ input during the peak period, which is dominated by episodic rainfall events varies between 15 and 25 mg·ℓ⁻¹ over the semi-arid region and is the result of the extremely low Cl⁻ concentration in the peak period's rainwater. A value of 0.4 mg·ℓ⁻¹ Cl⁻ is suggested for this period.

The annual recharge rate for semi-arid regions is 3% of R_{eff} which for the 2007-2008 HC represents 8 mm·yr⁻¹. This value is dependant of the ground surface conditions per re-

gion. As reported in Box 6.3, areas where interaction of a soil/regolith cover (>0.25 m) becomes a dominant factor, this value drops to 1% or less of R_{eff} or $\leq 3 \text{ mm}\cdot\text{yr}^{-1}$.

To conclude, the contribution of episodic rainfall input to the groundwater budget of local aquifer systems is in the order of 65% when included in a rain-week rainfall pattern. This is required to establish a ASR condition which drives the sustainability of particular aquifer systems.

Therefore, if a particular HC does not contain a rain-week rainfall pattern, the recharge to the groundwater system might not even support the medium-term requirement for sustainable supplies. The rainfall pattern scenario which currently occurs in the Beaufort West area is probably a typical example where the water demand completely overrides the effective recharge generated on the fractured hard rock terrains.

The occurrence rate of these rain-weeks with its associated episodic rainfall events for semi-arid regions, at 1 in 5 years requires measures for (i) dedicated conjunctive uses between local surface water and groundwater resources, and (ii) mind moving consideration and development for re-use of wastewater to augment the vulnerable local groundwater resources.

oooOOooo

7. CONCLUSIONS AND RECOMMENDATIONS: EPISODIC GROUNDWATER RECHARGE.

7.1 Background.

The study addresses various aspects of the semi-arid hydrological cycle with specific reference to the rainfall-groundwater interaction, i.e. groundwater recharge. The main driving factor behind this interaction is the hydro-climate, the ground surface conditions and the geo-character of the UZR.

Southern Africa's hydrometeorological status in the current inter-glacial period is fairly stable, although characterised by outstanding wet and dry cycles. The palaeo-climate throughout the current post-glacial period (i.e. the Holocene Epoch, ~10 000 yr BP) reveals a history of humid and dry cycles over much of southern Africa, especially the Kalahari-Karoo Basin of southern Africa (Partridge et al. 1990; Thomas and Shaw 1991).

Observations by De Vries (1984) indicate that for the Kalahari Basin, which is a semi-desert environment for many millennia, its current piezometric surface could be explained as a residual feature resulting from a Late Pleistocene water table head decay since the last pluvial period in southern Africa (~12 500 yr BP, Tankard et al. 1982).

Groundwater resources in the semi-arid region of southern Africa depends on rainwater recharge, whether direct or indirect. For long-term sustainable recharge, aquifer storage recharge is required as hyetograph-hydrograph sets justifiably links episodic rainfall with ASR. The maximum groundwater replenishment from these events occurs on hard rock terrains, where jointed and fractured rock material drives recharge-producing rainfall surplus to the water-table interface in a matter of hours/days. Interpretation of these recharge pulses can be considered with the use of rainwater/groundwater hydrogeochemical tracers and hyetograph-hydrograph responses.

Atmospheric processes in the semi-arid climate generate a specific hydrogeochemical signature for the incoming airborne moisture which ultimately reports in the rainwater at ground surface. Further physical processes in the lithosphere alter this signal before it is captured in the groundwater domain.

The HC contains a well established package of constants, parameters and state variables which can be observed in meticulous modes. Anthropogenic impacts on the state variables, for example, may influence the actual values to such a level that any analytical conclusion is doubtful. Special remote monitoring procedures were therefore investigated and implemented to allow for the generation of special short-term hydrological information around the aspect of rainfall input and groundwater recharge.

Several experimental monitoring terrains were selected where these monitoring procedures were implemented. In light with what constraints spatial conditions may induce on the data, these sites were selected in remote regions.

7.2 HYDROMETEOROLOGY CONDITIONS CONTROLLING EPISODIC RECHARGE EVENTS.

7.2.1 *Ground surface conditions.*

Development of *in situ* soil profiles in the semi-arid regions lacks the thick, mature profiles (>6 m) found in the semi-humid and humid areas. Colluvium/alluvium deposits in drainage valleys may reach more than 6 m, but is also colonized by deep rooted trees and scrubs with substantial rooting systems.

Evapotranspiration in this zone may in fact consume virtually all of the vertical rainwater recharge generated during a recharge-producing surplus rainfall event. Large communities of *Acacia Prosopis* in the drainage valleys of the Bushmanland region, Kenhardt, for example, have such a large requirement for water consumption that indirect recharges generated by flash floods in the drainage channel is consumed within a period of months (Fourie 2002, as observed at Rugseer, District Kenhardt, S29.374780°; 21.209673°, 806 m amsl).

Average daily summer temperatures in the semi-arid region are above 30°C; summer-winter extremes (highest-lowest) easily equal 49°C. Extreme surface temperatures⁶⁹ in the late summer, heavy transpiration by plants during their final seeding cycle and absence of rainfall during the winter months, instigate a significant dry-out of the UUZR and probably portions of the LUZR as well. This phenomenon resets the vadose zone in terms of field

⁶⁹ Temperature of 73°C was measured by the author on the Kalahari sand surface during February 1982.

capacity (near total deficit) which requires a complete new UZR wetting cycle when the following HC starts to enable future rainwater infiltration processes.

The role of wetting cycles in the UUZR and LUZR is extremely important for the generation of sufficient vertical flux in multi-modal recharge mechanisms. For example the status of field capacity in a dual porosity LUZR will influence the wetting process of macro-pores and may retard the vertical flux as a result (adopted from observations made by Cook (2003)).

7.2.2 Rainfall.

The semi-arid region in southern Africa falls into both summer and winter rainfall regions. Long-term variations in the annual rainfall totals vary substantially (+200%) as can be seen for example in the hyetograph-hydrograph set presented in Figure 6.3.

On a regional scale and apart from synoptic variations, spatial rainfall variations occur as a result of diverse orographic uplift around the southern African Great Escarpment. These are mostly winter rainfall occurrences originating from cold frontal systems, migrating inland. The summer rainfall systems are more isolated cases due to the convectional rainfall generation processes required. In addition, local ($<100 \text{ km}^2$) variations occur especially in the summer rainfall region due to the position and intensity of the low pressure Kalahari Trough, driving convective thunderstorm systems.

Although the summer rainfall season in the semi-arid region manifests as isolated convection cells, it varies from season to season due to long-term climate variations (the typical 3-4 year dry spells observed in southern Africa). Individual rainfall may vary up to 30% in a matter of 25 km^2 (observed by author on several monitoring sites with up to five (5) individual rainfall logging units spread over areas between 25 km^2 and 500 km^2).

For those semi-arid regions receiving the rainfall during the southern hemisphere winter period, the moisture originates in association with southern Atlantic frontal systems. Spatial variations are a factor of the local relief and distance from the coastline. Although rainfall depths in the winter rainfall region can be as high as $1000 \text{ mm} \cdot \text{yr}^{-1}$, rainfall on the lee side of the Great Escarpment is notably lesser.

7.2.2.1 The Narrative of Episodic Rainfall and Recharge Event(s).

Also referred to as extraordinary rainfall events, these are characterised by specific synoptic conditions, especially in the summer rainfall regions. Continuous rainfall logging reported sequences of rain events occurring over a period of three (3) to eight (8) days, i.e. the rain-week concept. In general, the rainfall pattern over a rain-week consists of several low (<25 mm) rainfall events and one or two extraordinary rainfall events, which may be as high as 50 to 100 mm respectively.

The hyetograph-hydrograph set of the Taaiboschgroet monitoring site, Limpopo Province, in Figure 7.1 illustrates two rain-week periods consisting of (i) 5 day 22½ hour (128 mm) event and (ii) a 2 day 15½ hour (193 mm) event with a 14 day 11½ hour (44 mm) period in between.

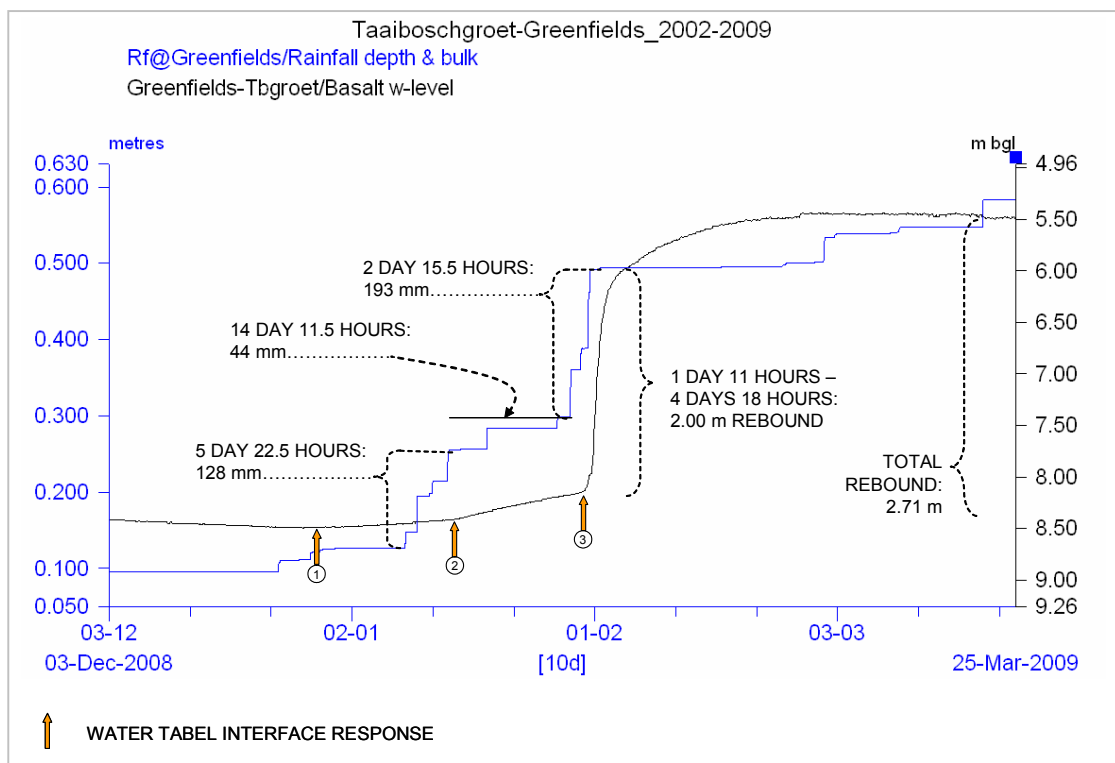


Figure 7.1. A rain-week scenario as it occurred from 29 - 31 January 2009 (2 days and 15½ hours) in the Taaiboschgroet area, Limpopo Province with a total rainfall of 193 mm.

The water table rebound in reaction to the second rain-week was 2.00 m which started 1 day 11 hours after the last rain-week and lasted for 4 days 18 hours at a rate $\pm 25 \text{ mm} \cdot \text{hr}^{-1}$.

The role of retaining field capacity and the degree that wetting of the LUZR play is also visible in the water table interface response as indicated in Figure 7.1. Three water table response indicators are shown in Figure 7.1; each responding a few days after a particular rainfall event. The 1st indicator corresponds with a groundwater recharge event initiated by a low impact rain event as a result of an earlier wetting phase in November 2008, when 79 mm fell over 4 days 13 hours. The 2nd indicator reports a slow, but consistent recharge event driven most probably 100% by a diffuse flow mechanism through the UZR. The UZR and LUZR is probably significantly wetted at this stage which was again augmented by the 44 mm rainfall event between the two rain-weeks.

Finally, the 3rd indicator announced the episodic recharge event which leads to a 2.71 m ASR event in this aquifer system. This pattern required for an ASR was observed in the Karoo fractured hard rock environment as well (Figure 6.5, Section 6.2.3).

An important aspect observed on this and several other hyetograph-hydrograph sets is the total lack of water table response to rainfall events later in the rainfall season, especially after ASR has occurred. For example, in this case, two events, one 28 days later (32 mm in 7 hours) and again 19 days later (36 mm in 4½ hours), physically did not produce any recharge, even considering that the water table interface was now 2.71 m closer to the ground surface. This is still an issue of uncertainty, although processes such as (i) interception by a very effective late season rooting system of the local vegetation and (ii) physical changes in the permeability of macro-pores and micro fractures in the rock matrix due to swelling of *in situ* clay minerals (Nkotagu 1997).

7.2.2.2 Frequency of Exceedance: Episodic Rain Events.

Long-term hyetograph-hydrograph sets from the experimental monitoring terrains show that the recurrence rate of episodic rain events is highly sporadic and may occur on occasion one or two times out of several hydrological seasons; thus the recurrence of a natural ASR event is extremely low. In the case of the Stella Area, Northern Cape Province and the Taaiboschgroet area, Limpopo Province, the hyetograph-hydrograph sets for both areas only reported an ASR in the 2005-2006 and 2008-2009 HCs respectively, whilst no ASR has occurred in the previous six (6) HCs (Figures 6.2 and 6.8).

Hyetograph-hydrograph sets indicate that during several HCs no evidence of physical water table rebounds occurred during above-average annual rainfall input, whereas the CRD methodology, for example would have simulated a groundwater recharge event. It seems therefore that a sound measure for sustainable aquifer resources lies in acknowledging the recurrence rates of these extraordinary rainfall events.

The rainfall data to perform frequency of exceedance, hence recurrence rates of rainfall events with a specific pattern, will be a good measure to assess the bridging period before the manifestation of a next ASR event.

7.2.2.3 Rainfall Rates and Design Rainfall Pattern.

Detailed assessment of rainfall depth and water table responses from six of the summer rainfall experimental monitoring terrains, produced a design rainfall pattern based on the rainfall intensities ($\text{mm}\cdot\text{hr}^{-1}$) and rainfall depths (mm). Eq. 6-5 (Section 6.2.4) specifies a rainfall intensity - rainfall depth threshold relationship of $1.5 \text{ mm}\cdot\text{hr}^{-1} - >40 \text{ mm}$.

The frequency of exceedance for a rain-week including a design rainfall pattern as per Eq. 6-5 for the Vryburg area for the peak rainfall months (Jan_n , Feb_n and Mar_n), is in the order of 0.04, 0.04 and 0.06, or on average 0.05 or 5%. Thus, for the total rainwater package, i.e. all rain events included and above the threshold value of 40-50 mm, the frequency of exceedance is 23%. A design rainfall pattern required for an ASR scenario based on the Vryburg rainfall pattern inevitably indicates its recurrence is only 23 years out of 100 years, or roughly 1 out of 5 years. This implies that although a groundwater resource might receive an ASR, the newly recharged volume needs to be managed over a period of approximately 5 years before an ASR will replenish the aquifer's sustainable storage.

This water resource control measure and crucial requirement for the medium-term management of rural water resources, is seldom adhered to by water boards and water users associations. It is not only the lower potential aquifer systems which are over-utilized, but even larger, higher potential aquifers like the dolomitic aquifers in South Africa, that fail severely after a few years of abstraction.

7.3 HYDROGEOCHEMICAL INDICATORS OF EPISODIC RECHARGE EVENTS.

7.3.1 *Monitoring Natural Rainwater Tracers.*

The summertime rainfall in southern Africa derives mostly from the Equatorial Indian Ocean, and migrates via the ITCZ and the Kalahari low pressure trough to the interior parts of southern Africa, carrying with it an alternating load of maritime salts and a specific ^2H and ^{18}O isotopic composition.

The hydrochemical composition of the winter rainwater is rather complex due to the high input of maritime aerosols along the coastal regions. These semi-arid areas have been omitted in this study, especially for the CMB application, as high intensity monitoring is required. Reference to the hydrogeochemical characteristics of the wintertime rainwater is high-lighted throughout the script (Table 7.1).

The values stated in Table 7.1 illustrate the differences between the summer and winter semi-arid region's Cl^- concentrations with regard to the larger continental effect and reports mean values in terms of (i) distance from the ocean, and (ii) elevations.

Rainout events along the flow path, addition of terrigenous dust, and evaporated moisture from the land surface alters the hydrogeochemical composition in several ways. Three distinctive intervals of the HC have been identified from dedicated rainwater monitoring, each interval reporting a measurable difference in the rainwater tracer composition.

This study inevitable confirms significant variations in the hydrochemical composition and specifically the Cl^- , NO_3^- and SO_4^{2-} concentrations. Seasonal variation of the Cl^- content, which is applied in the CMB application was traced b.m.o. the rainwater monitoring programme and it was found to vary between 0.7 and 1.5 $\text{mg}\cdot\ell^{-1}$. During rain-weeks and their associated episodic rainfall events, when the highest probability for groundwater recharge exists, the concentration drops down to just above the detection level of 0.1 $\text{mg}\cdot\ell^{-1}$.

These exceptionally low tracer values are due to the amount effect caused by high humidities and limited cloud water evaporation that manifests specifically during these rain-week scenarios. This is confirmed in Section 7.3.3.

Application of these tracers which forms part of the HC and describe certain facets of the hydrological processes in the HC, requires extremely dedicated monitoring and data collection. Although the concentrations and mutual compositions of these tracers can change due to climatic, atmospheric and topographical variations, they are relatively conservative under well managed monitoring procedures.

The hydrogeochemical data obtained from the monitoring infrastructure developed and implemented under this study, proves to be quite clean and unpolluted by secondary sources, as reported by the extreme low concentration of PO_4^- in the rainwater samples (values below detection levels, $<0.05 \text{ mg}\cdot\text{l}^{-1} \text{ PO}_4^-$).

Table 7.1. Chloride concentration in rainwater over a three tier interval of the HC for summer and winter rainfall in semi-arid regions, 2002 to 2009 (HARmean).			
Interval:	Chloride Ion	Interval:	Chloride Ion
Winter Rainfall Season ¹	$[\text{Cl}^-] \text{ mg}\cdot\text{l}^{-1}$	Summer Rainfall Season ²	$[\text{Cl}^-] \text{ mg}\cdot\text{l}^{-1}$
Early Winter [A, M, J] - n = 23	3.6 ^[0.4]	Early Summer [O, N, D] - n = 71	0.8 ^[0.1]
Peak Winter [J, A, S] - n = 24	2.7 ^[0.4]	Peak Summer [J, F, M] - n = 89	0.4 ^[0.1]
Dry Winter [O, N, D, J, F, M] - n = 30	6.8 ^[0.8]	Dry Summer [A, M, J, J, A., S] - n = 66	1.0 ^[0.2]
^[5.5] Standard Deviation from harmonic mean values.			
¹ 4 monitoring sites: Univ. Western Cape, Langebaan Road, Sandveld and Klein Karoo.			
² 6 monitoring sites: Beaufort West, Pretoria-East, Stella, Kuruman, Alldays and Northern Kalahari.			

7.3.2 Monitoring Natural Groundwater Tracers.

The ground surfaces in semi-arid, fractured hard rock terrains support multi-modal infiltration of recharge-producing rainfall surpluses once generated by a specific rainfall pattern. During extraordinary rainfall patterns such as the rain-weeks scenario's, conditions for bypass recharge are highly favourable, i.e. high rain rates and rainfall depths to generate recharge-producing rainfall surpluses.

The hydrogeochemical composition of the saturated UFWZ in hard rock regions contains water with depleted hydrogeochemical signatures (as observed with the differential sampling of 2 m water columns from below the water table interface). These signatures, point

towards dynamic recharge mechanisms which indicate considerable contribution by bypass flow conditions during recharge events.

Direct, vertical infiltration of rainwater in these hard rock regions with an underdrainage system containing an effective macropore network creates bypass flow conditions which may intercept a large portion (up to 65%) of the recharge-producing surplus rainfall and channel it through the UZR into the water table interface. In this case, the groundwater hydrogeochemistry will be more prominently marked by the rainwater chemistry input, especially when the incoming rainwater is also signalled by a distinctive composition, i.e. depleted Cl^- and ESI compositions (Figure 5.14).

Due to exceptional climatic conditions in semi-arid regions, a large percentage of certain rainfall events (i.e. $<1.5 \text{ mm}\cdot\text{hr}^{-1}$ rain rates - $<40 \text{ mm}$ depths), will evaporate/transpire within a short period, days (Willemink 1988). Once infiltrated, the remaining water will introduce elevated Cl^- and enriched ESI's in the groundwater profile as has been observed by a low ET_{INDEX} . These are probably the contribution by the slower matrix flux percolating through the porous/micro fractured part of the UURZ/LURZ (matrix flow) and marked by a low $\text{ET}_{\text{INDEX}}^{70}$.

The crucial aspect of this diverse water column, even over a 2 m interval, is its periodical change according to the rainfall seasons. During groundwater recharge events, layers with much lower ($\pm 50\%$ less than background values) Cl^- concentrations reside in the profile, which indicates significant contribution by bypass flux.

During steady state conditions and even when the aquifer saturation undergoes a recession phase, the hydrogeochemical profile is relatively stable (Figure 7.2).

The monitoring techniques applied in this study, generated rainwater and groundwater hydrogeochemical data probably never collected before. The sampling techniques used indicate intelligent anomalies in the groundwater profiles. It allows capturing and analysing re-

⁷⁰ A low ET_{INDEX} implies that extensive evapotranspiration of low rainfall events occur at ground surface (depression storage evaporation) and rooting zone (transpiration).

charged water introduced into the saturated water column during a water table rebound. In this study recharged water via local bypass flow mechanisms were sampled.

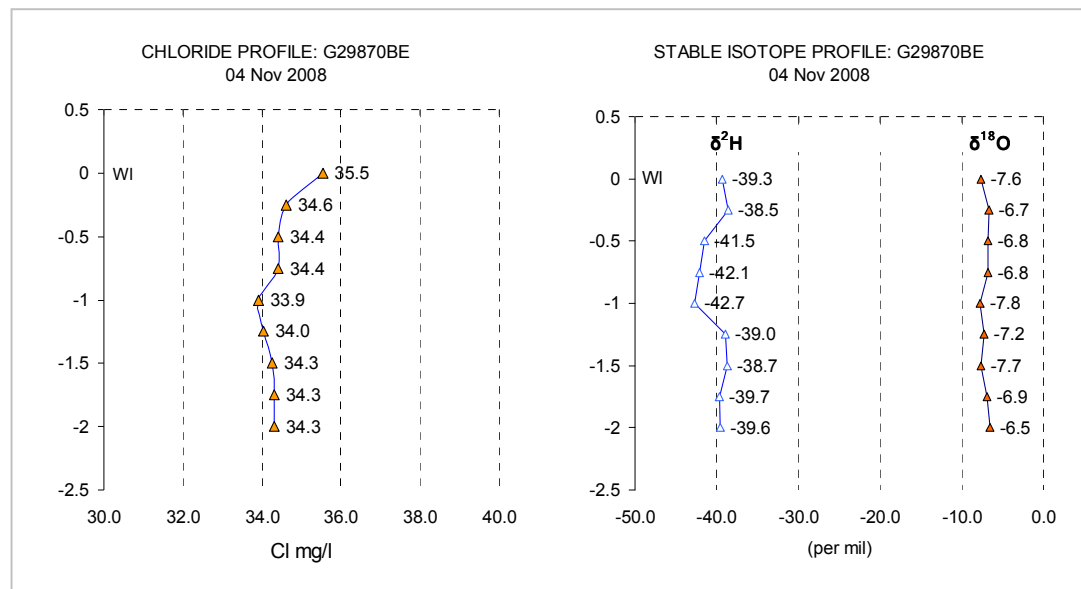


Figure 7.2. Chloride and ESI profile during steady state conditions in fractured hard rock terrain in Beaufort Group sandstone/mudstone at the De Hoop Poort monitoring site, Beaufort West District.

7.3.3 Environmental Isotopes.

The isotopic composition of the summer rainwater in southern Africa differs slightly from the GMWL which indicates a different fractionation of the isotopes since the moisture was evaporated from the Equatorial Indian Ocean. The long pathway from the ITCZ/ZAB/Equator is probably responsible for this slight deviation as the atmospheric moisture undergo several non-equilibrium rainout processes, along the migration path during rainout events.

It is specifically the *d-access* value which is lower and plots around 5.8‰ for South Africa as appose to the GMWL's 10‰.

The rainwater samples collected over time in the bulk sampling units is an accumulation of several highly variable rainfall events/depths over a specific interval and unfortunately does not report the characteristic isotopic composition of especially episodic rainout

events. Samples obtained from the RES unit reported extreme depleted values for both Cl^- and ESI's; thus indicating that the actual hydrogeochemical composition of the recharge-producing rainfall surplus is significantly different from those collected in bulk storage systems.

The ESI composition in groundwater tends to be rather depleted and correlates well with the characteristic depleted rainwater ESI composition of the episodic rainfall events. This phenomenon supports a strong bypass component through the UZR, thus bypassing the effects of ground surface/UUZR ET.

Although the groundwater ESI composition plots towards a depleted composition in relation to the average bulk rainwater ESI composition, the groundwater profile contains some indication of evaporated water as well (Figure's 5.12 and 5.14). The evaporated water contains a characteristic isotopic and hydrochemical composition which plots on a particular E.L. This phenomenon, confirms, that bypass flow is not solely driving groundwater recharge (up to 65%) in the fractured rock domain.

The multi-modal flow mechanism(s) in the UZR during episodic recharge events complicate the ESI tracer mode in the groundwater mound. In terms of the characteristic depleted hydrogeochemical composition of the incoming rainwater during episodic events, attempts to correlate this characteristic with the hydrogeochemical composition of the physical groundwater rebound, was found to be rather complex and probably site specific in most cases. It seems there is a slight phase shift (0.5 m) in the vertical plane which could probably be the result of a Cl^- memory in the UZR. This represents a situation where a portion of the groundwater with depleted ESI's correlates with the normal background Cl^- and *vice versa*.

To conclude, utilizing ESI's in conjunction with the hydrochemical tracers for tracking direct recharge terrains is quite useful and is probably the only application to identify multi-modal flux condition in the UZR recharging the UFWZ reservoir. The application calls for extreme dedicated sampling along with the hydrological regime incorporated in the three-tier HC interval approach.

This procedure requires a large number of individual samples/aliquots, which impacts on the long-term funding for monitoring programmes. The expenses for ESI analyses, however, have decreased since laser technology is applied instead of the traditional mass spectrometry methodologies.

7.4 HARD ROCK HYDROGEOLOGY IN DIRECT RECHARGE TERRAINS.

The climatic/ground surface conditions in the semi-arid regions favour the formation of hard rock terrains with shallow soil/regolith horizons, as appose to humid, climate regions, where deep weathering produces deep (>6 m) mature soils.

Hard rock terrains occur frequently in the form of low relief mounds. Local hills (hillocks) formed as a result of the Pan African II Erosion Cycle, vary from a few meters to several hundred meters high. These features can be classified as typical direct recharge terrains and their contribution varies from $\approx 4\%$ (hard rock terrains) and $\approx 13\%$ (mountains).

7.4.1 *Hard Rock Features.*

Semi-arid hard rock terrains are characterized by poorly developed (<0.25 m thick) or eroded A and B Horizons (soil/regolith) with erratic coverage in general.

Secondary macro pores i.e. joints/fractures are natural features in most hard rocks, due to secondary deformation caused by erosional unloading of the overburden and activation of bedding plane and transverse jointing. Whereas the former jointing pattern in combination with weathering processes may reach down to between 10 and 15 m bgl.

On close inspection of any bulk rock specimen, the jointed/fractured hard rock contains a mesh of micro-scale fractures. These features specify the bulk hydraulic characteristics of all aquifers and vary considerably according to the primary rock composition.

Generation of recharge-producing rainfall surpluses in the semi-arid hard rock environment is governed by the rainfall event configuration. In a rainfall event when the conditions satisfy the upper boundaries of Eq. 6-5 (rain rate $>1.5 \text{ mm}\cdot\text{hr}^{-1}$ - rainfall volume $>40 \text{ mm}$), surplus rainwater becomes available which will result in ground surface depression stor-

age. From here-on two processes are initiated, i.e. direct infiltration and surface run-off, where the later is a function of the rain rate and surface sloping.

The impact of Hortonian overland flow (or infiltration excess run-off) on the availability of recharge-producing rainfall surplus is difficult to assess on local scale. Notwithstanding the fact that a certain portion of recharge-producing rainfall surplus is removed from a site which might infiltrate a few meters down gradient and contribute to the underdrainage, local overland flows are probably by large supporting groundwater recharge on hard rock terrains.

Once depression storage materialize, (i) desiccation and tension cracks in the soil/regolith layer (if present) and (ii) vertical/oblique transverse fracture/joint sets will act as excellent flow paths, setting off vertical infiltration and underdrainage.

The fractured hard rock domain is characterized by a multi-modal vertical flux through the UZR, i.e. bypass flow through macro-pores and diffuse flow through a matrix consisting of micro-fractured bulk rock; both occurring in the UZR/UFWZ. This was observed through (i) rainfall-water table response times (hours/days), (ii) depleted Cl^- spikes and (iii) depleted ESI compositions in the upper 2-3 m of the groundwater profile.

7.4.2 Matrix Flow and Hydrochemistry Signal from Matrix Storage.

Matrix porosity is a secondary hydraulic attribute in most micro jointed rock formations. Figure 4.5 is a good example of micro-fracturing in Karoo Beaufort Group mudstones. The effectiveness of the fine matrix of joints/fractures in the bulk of any hard rock mass as a flow medium must be noted with sincerity and recognised as contributing to, but even representing the bulk porosity of most weathered jointed/fractured aquifer systems in South Africa.

Quantification of these matrix flow contributions in fractured hard rock aquifer requires a dedicated sampling procedure. The recharged water migrating through the rock matrix, reaches the saturated flow regime, after the water table rebound settles from the initial bypass flow contribution.

By implementing this principle in the monitoring programme, the recharged rainwater percolating through the matrix component of the multi-modal flow regime, can be sampled/analyzed. The CMB application indicates that the matrix flow component represents roughly between 40% and 50% of the total recharge input into the LUZR/SZ. This again may vary considerably on local scale.

Quantification of the matrix flow hydrochemical character was obtained with dedicated monitoring in the groundwater profile by comparing the background groundwater Cl^- concentrations, with the correlating rainwater Cl^- concentrations. The sampling period to obtain this background groundwater Cl^- value, was guided by the early water table recession onset as indicated on the particular hydrograph of the monitoring site.

Several cases were observed where elevated Cl^- spikes in the groundwater profile indicate an evaporative signature as the result of diffuse matrix flow mechanism, including a local ET cycle in the UUZR. This process is further supported the ESI composition indicated by a prominent (E.L.) plot (Figure 6.13).

7.4.3 Bypass Flow Mode in Vertical Recharge Cases.

Fracture flow velocities, based on observations of the lag-time between a specific rain event and the resulting water table response, as recorded in the hydrograph-hyetograph sets, indicate significant bypass flow during the first part of the rainy season.

Bypass flow conditions provides a significant opportunity for effective wetting of fracture/joint surfaces during the first recharge-producing rainfall surplus event (Figure 7.1, Section 7.2.2.1).

Lag-times in order of hours and days for water table depths up to 8 - 10 metres were observed in fractured hard rock terrains. The Karoo environment provides excellent examples of these conditions. Flow velocities of several meters per day (Box 6.1) were calculated using the method described by Cook (2003) and vertical fracture frequencies in the Karoo Beaufort Group sedimentary succession. This was supported by DTH-CC image logging of the LUZR where possible.

These images can be used to provide an indication of the ranges of joint/fracture apertures. The DTH-CC image logging results indicated that these apertures thin drastically a few meters below the UFWZ; although the joint/fracture can still be traced for tens of meters deeper. In the same manner, frequent horizontal jointing in the UFWZ diminishes over a few meters, although horizontal fracturing/jointing at the contact zone of different lithologies⁷¹ occurs frequently.

The stability of these secondary joint/fracture systems governs the effectiveness of bypass flow during a recharge-producing rainfall surplus scenario. The type of parent hard rock and its weathering process plays a crucial role, i.e. mudstone versus quartzite. In the case of inherent arenaceous parent rock types (ortho-sandstones, banded ironstones, felsic rocks and quartzites), these fracture/joint sets remains clean and may only get clogged if silt/clayey stuff infiltrates with the percolating rainwater from ground surface.

Limestone/dolomites, once jointed/fractured, represent the highest end of the bypass flow possibilities, as these features are always enlarged by the presence of carbonic acid in the infiltrating rainwater. These systems eventually form large swallows where surface run-off and rivulets drains into the underdrainage. Several examples of such conditions exist in the dolomitic water areas in South Africa and unfortunately contribute to the deterioration of these aquifer systems.

In the case of argillaceous and mafic rock types (mudstones, diamictites, basaltic lavas and granite-gneisses), secondary filling of joints and fractures with in situ decomposed rock material, was observed. (Willemink 1988; DTH-CC image logging by author). This natural clogging process seems to be significantly enhanced below the water table fluctuation zone as observed in the Karoo Letaba Formation lava in the Taaiboschgroet area, Limpopo Province (Verhagen et al. 2000).

7.4.4 Summary of Groundwater Recharge in Different Rock Types.

The experimental monitoring terrains used in this study cover a reasonable representative group of rock types and topographical features.

⁷¹For example between clastic sediments and dolerite intrusions (down to 500 m), basalts and sandstone (down to 220 m) and solo-rock fracturing 150 m.

The CMB application requires Cl^- values for rainwater (wet component), atmospheric out-fall (dry component) and groundwater recharge (residual component after ET_A). Although the rainwater Cl^- concentration differ substantially over a HC due to amount effects, regional differences were not high, even considering the geographical differences between the experimental monitoring terrains. The concept is illustrated in Figure 7.3.

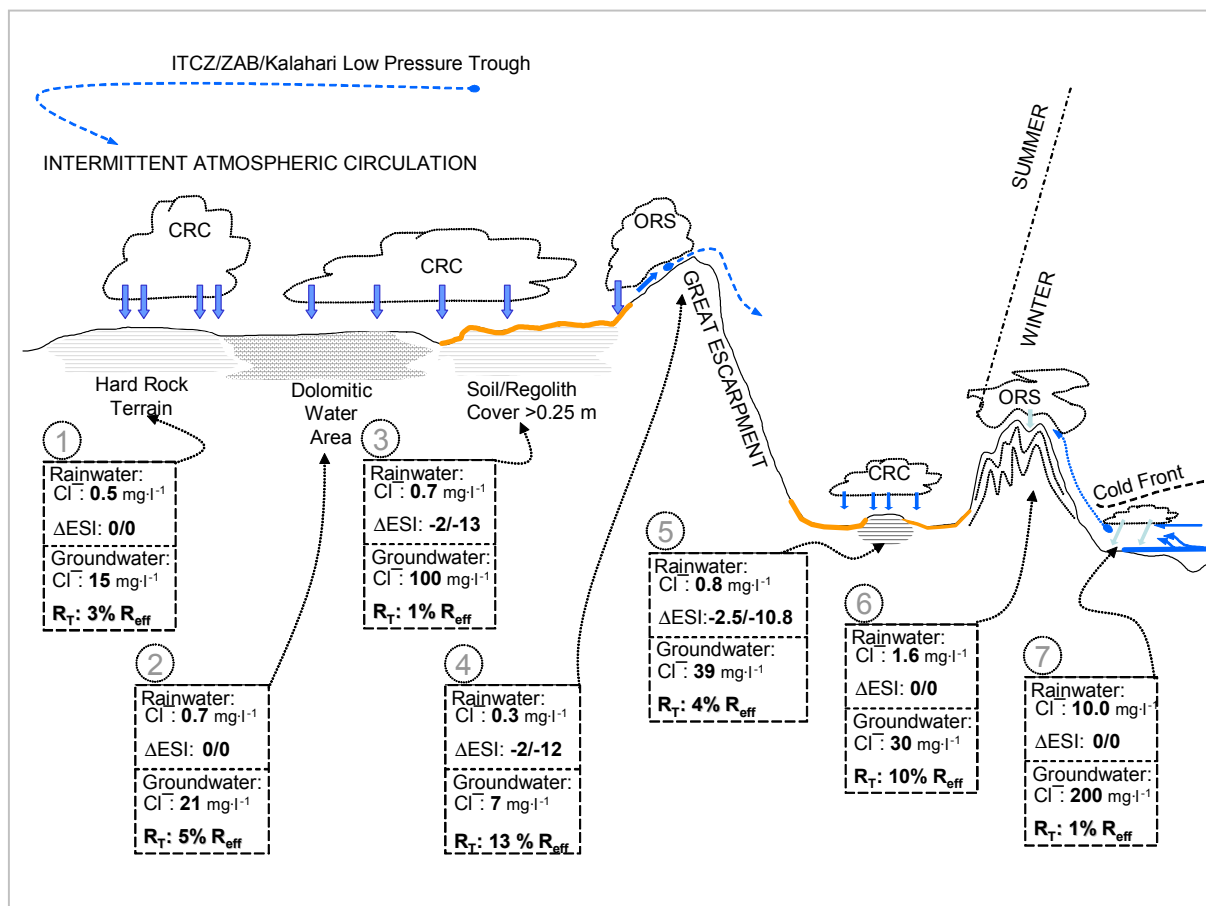


Figure 7.3. Flow diagram illustrating the peak rainwater and corresponding groundwater rebound Cl^- concentrations, the ESI variation between rainwater and groundwater and the estimated groundwater recharge as a percentage of R_{eff} .

The monitoring techniques applied in this study, generated rainwater and groundwater hydrogeochemical data probably never collected before. The sampling techniques used indicate intelligent anomalies in the groundwater profiles. It allows capturing and analysing recharged water introduced into the saturated water column during a water table rebound. In this study recharged water via local bypass flow mechanisms were sampled.

The concept is presented in the form of a generalized flow diagram with the different geological and topographical features and rainfall patterns. The diagram represents a section through the Great Escarpment, and report groundwater recharge as a percentage (%) of effective rainfall, R_T . The data presented in the diagram consists of the rainwater-groundwater Cl^- concentrations collected during the peak rainfall period

The rainfall patterns vary between convection rain cells (CRC's), orographic (uplift) rain systems (ORS) and frontal uplifts (West, South and East Coast Region of South Africa). The summer atmospheric moisture is generated at the ITCZ/ZAB and condensed by a combination of CRC's and large-scale convergence systems over the interior.

The different recharge responses are summarized as follows:

①: Fractured hard rock terrain as observed in the Karoo Supergroup, Letaba (Taaiboschgroet area) and Kraaipan Formation (Stella area). The Letaba basalts are forming low level ridges, and can be classified as a well weathered UFWZ of several meters (10 to 45 m). The Kraaipan Formation consists of a fractured hard rock BIF with a UFWZ of 10 to 15 m. Soil/regolith cover on the basalt is present near major drainages, rest of the area are sparsely covered by a thin soil/regolith layer (<0.25 m). The Kraaipan Formation consists of moderately elevated (15 m) bare rock surfaces with sparse vegetation cover.

②: Ghaap Plateau dolomite as observed in the catchment area of the Kuruman A-Spring. This is typical bare dolomitic terrain with virtually no soil/regolith cover.

③: Soil/regolith covered Karoo environment peneplains with underlying, horizontal mudstones and sandstone. Soil/regolith thicknesses are significantly larger than 0.25 m, in ravines. This is a complex soil condition, as it may contain a Na^+ rich top-soil which immediately seals during a rainfall event.

④: Elevated regions consisting of any kind of fractured hard rock formations mostly represented by the Great Escarpment and internal relicts of the African Erosion Surface, i.e. the Koranna-/Langeberg, Kuruman Hills mountain ranges and the Soutpansberg ranges. The data presented here is from the Nuweveld and Kuruman Hill mountain ranges in the Western and Northern Cape, respectively. The orographic rainfall patterns in the interior

regions produce rainwater that represents almost the final rainout product from either the ITCZ/ZAB or cold frontal systems.

⑤: This configuration represents a fractured hard rock terrain in a peneplain area which drives recharged groundwater to surrounding sub-reservoirs. This condition is explained in detail in Section 6.2.5 (Figure 6.10) and resembles the Karoo environment with its characteristic peneplains and low-level, hard rock hillocks.

⑥: Elevated regions along the coastal regions with moisture generated over the South Atlantic Ocean. In this case, the Kammanassie/Swartberg mountain ranges in the Western Cape are highlighted with hydrological data from the Vermaak River valley. This is a typical folded TMG ortho-sandstone region receiving winter rainfall. The characteristic elevated rainwater Cl^- concentration is indicative of the nearby oceanic moisture source.

⑦: Coastal regions receiving frontal rainfall introducing elevated Cl^- concentrations. Groundwater are characteristically saline (Na^+ , Cl^-) and direct recharge occurs on sandy coastal planes. The input from dry Cl^- deposition is quite high ($700\text{--}800 \text{ mg}\cdot\text{m}^2\cdot\text{y}^{-1}$) originating from maritime aerosols.

The method used to illustrate the isotopic signatures in the flow diagram, is based on the difference between the average rainwater and groundwater isotopic compositions as found in the Harmon Craig diagram, $^2\delta\text{‰}$ versus $^{18}\delta\text{‰}$ (Section 5.5.2). The 0/0 configuration, therefore, indicates that the groundwater represents a well balanced mixture with relation to the rainwater input.

Negative values ($-2.5\text{--}10.8$) indicate that the groundwater isotopic composition lies towards a relative more negative (depleted) isotopic composition than the rainwater itself. It was explained earlier that this phenomenon indicates a strong episodic recharge/bypass flow scenario as the episodic rainfall events portrays an even more negative (depleted) isotopic composition as the result of local amount effects in the cloud water.

The presentation illustrates the high diversity in rainwater-groundwater interactions in semi-arid regions which necessitate high-level monitoring procedures based on a realistic conceptual vision of the aquifer system.

7.5 EPISODIC GROUNDWATER RECHARGE.

Monitoring of the rainfall configuration over very short intervals (1 minute cycle sampling/storage) allows for the calculation of exact rain rates. From this information, it is possible to isolate episodic rainfall events and classify them according to the boundaries set by Eq. 6-5.

Corresponding water table interface rebounds were logged at thirty (30) to sixty (60) minute intervals, and allows for estimations of the exact time lag between a rainfall event and the water table rebound. The hyetograph-hydrograph sets confirm that all ASR events in direct recharge terrains are directly correlated with an episodic rainfall event.

Likewise, the hydrogeochemical correlation between rainwater input during episodic events and reporting in the SZ was frequently observed, regardless of what type of parent hard rock terrain is relevant.

7.5.1 Application of the CMB Methodology in the case of Episodic Recharge Events.

In its original format, the CMB application entails the Cl^- concentrations in rainwater (total MAP) and soil/regolith water from the UZR. Although moisture may be retained in the micro-fractures in the UZR, obtaining representative/un-evaporated samples from this zone is problematic and relies on the Cl^- values from the underlying SZ, which requires a different approach in terms of sampling in space and time.

This diversion from the traditional CMB application is probably applicable to only direct, hard rock recharge terrains, as lateral flow components in areas with a prominent lateral flow regime may produce a mixture between the vertical and lateral concentrations in the SZ.

Normally the recharge estimation is done by using annual averaged (mean or HARmean) values, or in some cases once-off measurements. The indication from the hyetograph-hydrograph sets illustrates that the groundwater recharge process is (i) mostly effective in direct recharge terrains and (ii) a ASR is initiated by episodic rainfall events.

The hydrogeochemical input during episodic events is quite different from annual values, as these events occur within a period of a few weeks. In fact, all the state variables in the CMB algorithm changes over a HC period, due to the drastic climatic conditions in the semi-arid environment; therefore any statistical approach using the total annual averages will not simulate the actual conditions in the geo-environment.

The differential recharge approach adopted in this study by using the measured hydrogeochemical compositions according to the rainfall-water table interaction (hyetograph-hydrograph sets), demonstrates that effective, short-term recharge events manifest as a specific occurrence (an episodic event) in the HC.

The application of the three tier algorithm requires dedicated monitoring. Although the monitoring exercise is (i) time consuming and (ii) relatively expensive, the data obtained is valuable and necessary for sustainable management of the aquifer system. Preliminary identification of a risk situation may save costly water supply augmentation programmes and allows the water supply authorities to manage a general groundwater recharge deficit (as currently the case with Beaufort West, Western Cape Province). Once a direct recharge terrain is characterised by this approach, recharge estimates from regional rainfall data is possible, i.e. whether an episodic recharge event has occurred or not.

Recharge estimates through application of the differential approach, based on the three tier intervals over the HC reports significant lower recharge values than those appearing in literature; especially on the peneplain areas. One good example here is the case of the original CRD method, where annual totals with a threshold value are used to calculate recharge. The hyetograph-hydrograph sets illustrate this appreciably well.

7.6 RECOMMENDATIONS.

The main requirement for estimating differential groundwater recharge is a sufficient collection period of hydrogeochemical, rainfall depths and water level data on an hourly interval. The data range should at least contain one well-monitored, episodic rainfall event in a series of HC's. The rainfall design assessment indicates that at least five (5) years of monitoring is required to capture one episodic event generating a groundwater recharge event.

A grouping of experimental monitoring terrains in the research area is required to differentiate between direct and indirect recharge terrains. Mapping of the hard rock terrains is required beforehand, to identify at least the direct recharge areas. Hard rock terrains consisting of surface limestone (calcretes) should be avoided, due to its hydrochemical complexities (elevated Cl^- and Na^+).

Availability of dedicated monitoring borehole(s) is always a problem when the groundwater development has already been completed. It is necessary, therefore, to include these boreholes in the budget requirements when a groundwater development programme is initiated. The geotechnical construction is quite simple, though, as these boreholes should only penetrate through the UZR and cover the long-term water table range in the UFWZ. In the summer rainfall regions, the best time during the HC for drilling dedicated monitoring boreholes is from 15 November_n to 15 January_{n+1}.

The construction of the monitoring boreholes should consist of a well-structured wellhead with sanitary seal protection for at least a depth of three (3) m bgl. The rest of the borehole should not be lined. If lining is necessary use at least a 50% overlapping vertical slot configuration. Borehole should not be foam-washed after completion. The best treatment is to use a small borehole pump for purging and cleaning afterwards.

The infrastructure (equipment, staff and funding) is highly important, especially when the monitoring terrain is situated in remote regions where special vehicles are required to reach these sites.

The application of the stage and column sampling technique in boreholes should be considered for application in the pollution study fields, due to undisturbed sampling capabilities of a rather simple piece of equipment.

The skim sampling method applied in the beginning of the study did not provide the dynamic data of the recharge profile as the column and stage sampling did. Its application for high-level recharge investigations alone is not recommended. The best sampling method for tracking (i) fast macropore flux and (ii) slow matrix flux in the physical recharge profile is the stage sampling technique. This requires a high-level technical input and monitoring skills, especially in remote regions, due to tracking of the water table interface to capture the full water table recovery cycle.

The column sampling technique is used for sampling the matrix flow component during the onset of the recession part of the water table trend.

Monitoring of pristine rainwater is crucial, especially when hydrogeochemical analyses are required. Special checks on the hydrochemical composition are necessary, i.e. to check for secondary pollution by bird/animal droppings, it is advised to analyze for PO_4^- at all times to evaluate for secondary pollution input.

Episodic rain events in semi-arid areas with soil cover do not generate the same magnitude of groundwater recharge as those areas with hard rock outcrops. This phenomenon puts a significant restriction on larger scale recharge estimations. Downscaling of recharge estimations according to the local soil cover area is to be acknowledged, therefore groundwater recharge estimations become a spatially based approach driven by a specific rainfall pattern (rain-week scenario).

Application of ESI's for groundwater recharge rate estimations in fractured hard rock terrains should be used to verify the status of multi-modal recharge, i.e. to qualify between bypass and diffused matrix flow conditions. It will support the identification of direct recharge terrains which should be protected against ground surface pollution. ESI profiling in the SZ can be used to identify the extend of pollution from local land use activities.

The collection of pristine rainwater and representative groundwater samples requires a highly technical approach such as the DWA rainfall logger/sampler unit and the stage and column-sampling units. Under no circumstances should water be pumped from the monitoring borehole, as blending between the upper, newly recharged groundwater and older water from the deeper, stagnant aquifer zone, which could be under sub-artesian pressure with a total different hydrochemical character, occurs.

The combination of hyetograph-hydrograph sets to plan for groundwater hydrogeochemical sampling programmes in the direct recharge terrains is recommended for water management institutions. The application of real time logging technology in this regard is highly appropriate in the sense of short-term recharge estimations. This application will for example, allow monitoring teams to plan monitoring runs on very short notice and will enable them to capture the peak input concentrations in the aquifer.

Rainfall data from long-term SAWS observation should be analyzed at quaternary catchment scale to obtain frequency of exceedance classifications. This classification allow estimation of critical management HCs, i.e. the number of HC's between episodic rainfall events driving an ASR condition when water restrictions should be considered.

Expansion of the rainwater-groundwater monitoring programmes needs to be considered by DWA Regional Offices with support from the SAWS and ARC. Application of special climate monitoring units like the Davis weather station should be promoted.

In terms of climate variability monitoring in South Africa, the rainwater-groundwater monitoring process developed through this study and incorporating the hydrology conditions in the UZR is required, if any knowledgeable conclusion(s) regarding climate variability scenarios is to be considered over 20 years from now.

To conclude, the CMB application still provides the most direct and a relatively economical method to generate a set of state variables required for the estimation of groundwater recharge. Development for automatic sampling of rainwater and groundwater during episodic events should be encouraged. Although the expansion of the initial R_T algorithm into the three-tier interval approach were applied, the control over short-term application of differential state variables is more effective. Atmospheric outfalls, influencing the dry Cl^- deposition, need to be investigated and probably require high-end technology to perform a differential sampling process between dry and wet Cl^- deposition in remote areas.

oooOOOooo

8. REFERENCES.

- Arid Zone Hydrology: *Investigations with Isotope Techniques* 1980, Proc. Adv. Group Meeting, Vienna, 6-9 November 1978, IAEA, Vienna.
- Balek, J 1988. 'Groundwater Recharge Concepts', in *Estimation of Natural Groundwater Recharge*, ed I Simmers, D. Reidel Publishing Co., pp. 3-9.
- Bean, JA 2003, 'A Critical Review of Recharge Estimation Methods used in Southern Africa', Unpublished PhD. thesis, University of the Free State, Bloemfontein.
- Beekman, HE Selaolo, ET & de Vries, JJ 1999, 'Groundwater recharge and resources assessment in the Botswana Kalahari,' *GRES II Executive summary and technical reports*, pp. 48.
- Bond, GW 1947, '*n Geochemiese Opname van die Grondwatervoorrade van die Unie van S.A*, Memorie no. 41, Dept van Mynwese, Geologiese Opname, Pretoria, RSA..
- Brandl, G 2002, *Geological and structural model for the Tshipise Fault Zone in the Alldays area, District Bochum*, Limpopo Province. Council for Geoscience, RSA.
- Bredenkamp, DB, Botha, LJ, Van Tonder, GJ & Van Rensburg, HJ 1995, *Manual on Quantitative Estimation of Groundwater Recharge and Aquifer Storativity*, Water Research Commission, South Africa.
- Butler, M 2010, *Personnal Communication*, Ithemba LABS, University of the Witwatersrand, Johannesburg, RSA.
- Chevallier, L, Goedhart, M & Woodford, A 2001, *The influences of dolerite sill and ring complexes on the occurrence of groundwater in Karoo fractured aquifers: A morpho - tectonic approach*, Water Research Commission, project 937/1/01,
- Chow, VT (ed.) 1964. *Handbook of Applied Hydrology. A Compendium of Water-resources Technology*, McGraw-Hill Inc., New York.
- Clarke, FW 1924, *Data of Geochemistry*. Bulletin 770. United States Geological Survey. Washington Governmental Printing Office.
- Conrad, J 2010, *Personnal Communication*, GEOSS, Pty (Ltd).
- Cook, PG 2003, *A Guide to Regional Groundwater flow in Fractured Rock Aquifers*, CSIRO, Land and Water Australia.
- Dansgaard, W 1964, Stable Isotopes in Precipitation, *Tellus*, vol.16, pp 436-469.
- De Villiers, E 2009. *Personnal Communication*. Private Consultant. Stella, Northern Cape.

- De Vries, JJ 1974, *Groundwater flow systems and stream nets in the Netherlands*, Ph.D. Thesis, Free University (Amsterdam). Rodopi N.V., The Netherlands.
- De Vries, JJ 1984, Holocene Depletion and Active Recharge of the Kalahari Groundwaters - a Review and an Indicative Model. *Journal of Hydrology*, vol. 70, pp. 221-232.
- De Vries, JJ 2000, Groundwater Level Fluctuations - The Pulse of the Aquifer, Evaluation and Protection of Groundwater Resources (Conference Wageningen), pp. 27-43.
- De Vries JJ & Simmers, I 2001, Groundwater Recharge: An Overview of Processes and Challenges, *Hydrology Journal* (2002), pp. 6-17.
- Department of Agricultural Development 1991, Grondklassifikasie. 'n Taksonomiese sisteem vir Suid Africa, Memior No. 15, pp. 261.
- Dooge, JCI 1959, A general theory of the unit hydrograph. *Journal of Geophysical Research*, vol. 64, no.2, pp. 241-256.
- Drever, JI 1997, *The geochemistry of natural waters - surface and groundwater environment*, Prentice Hall, New Jersey.
- DWAF, 2000. *Water use authorisation process, Individual applications*, Department of Water Affairs and Forestry, Edition 1, pp. 59.
- DWAF, 2003, National Geohydrological Map Series of the Department Water Affairs and Forestry, Pretoria, RSA.
- DWAF, 2004. National Water Resource Strategy, First Edition, September 2004, Pretoria, RSA.
- Dictionary of Geological Terms 1957, Revised Edition, American Geological Institute.
- Eriksson, E & Khunakasem, V 1969, Chloride concentration in Groundwater, *Recharge rate and rate of Deposition of Chloride in the Israel Coastal Plain*, *Journal of Hydrology*, vol. VII, no. 2, pp. 178-197.
- Fetter, CW 1988, *Applied Hydrogeology*, 2nd edn, Merrill Publishing Company, London.
- Fourie, SA & Mbatha, KD 2002, A complementary report on groundwater level monitoring to qualify the effect of eradication of the Sp Prosopis on the Rugseer River aquifer, Kenhardt, Northern.Cape Province, Dept Water Affairs, report no. GH3983.
- Freeze, RA & Cherry, JA 1979, *Groundwater*, Prentice Hall, Englewood Cliffs, New Jersey.
- Galy-Lacaux, C, Laouali, D, Descroix, L, Gorbron, N & Liousse, C 2008, Long term precipitation and wet deposition in a remote dry savanna site in Africa (Niger) *Atmospheric Chemistry and Physics Discussions*, pp. 5761-5812.
- Gehrels, JC & Peeters JEM 1998, The mechanism of soil water movement as inferred from ¹⁸O stable isotope studies, *Journal of Hydrological Sciences*, vol 43, no. 4, pp.579-594
- Gieske, A. 1992. *Dynamics of Groundwater Recharge. A case study in semi-arid Eastern Botswana*, Drukkerij Febodruk BV, Enschede, The Netherlands.

- Grünert, N 2003. *Namibia Fascination of Geology. (A Travel Handbook)*. Klaus Hess Publishers, Göttingen.
- Hawley, GH 1981, *The Condensed Chemical Dictionary*, VAN NOSTRAND REINHOLD COMPANY, New York.
- Harrington GA, Cook, PG & Herczeg, AL 2002, 'Spatial and temporal variability of ground water recharge in Central Australia: A tracer Approach'. *Groundwater*, vol. 40, no. 5, pp. 518-528.
- Hem, JD 1959, *Study and Interpretation of the Chemical Characteristics of Natural Water*. Geological Survey Water-Supply paper 1473. United States Government Printing Office, Washington, D.C.
- Hutton, JT 1958, Rainwater Analysis, *Commonwealth Scientific and Industrial Research Organization. Division of Soils*, Report 8/57.
- Johnston, CD 1987, Distribution of Environmental chloride in relation to subsurface Hydrology, *Journal of Hydrology*, vol. 94 (1987), pp. 67-88.
- Joseph, A, Frangi, JP & Aranyossy, JF 1992, Isotope characteristics of meteoric water and groundwater in the Sahelo-Sudanese Zone, *Journal of Geophysical Research*, vol. 97, no.D7, pp. 7543-7551.
- Keet, M 2009, *Personnal Communication*, Water Quality Management, Department of Water Affairs, Gauteng Region Office, Department of Water Affairs.
- Kendall, C & McDonnell, JJ 1998, *Isotope Tracers in Catchment Hydrology*, Elsevier, Amsterdam.
- Kent, LE 1949, *The Thermal Waters of the Union of South Africa and South West Africa*, Hortors Ltd, Johannesburg.
- Kessler, J & De Raad, SJ 1974, 'Analysing Rainfall Data. Drainage Principals and Applications', *International Institute for Land Reclamation and Improvement*, Publ. 16 - vol. 3, Wageningen, Netherlands.
- Kijne, JW 1974, Determining Evapotranspiration. Drainage Principles and Applications, *International Institute for Land Reclamation and Improvement*, publ. 16, vol. 3, Wageningen, Netherlands.
- King, LC 1942, *South African Scenery, A textbook of geomorphology*, Oliver and Boyd Ltd., London.
- Kirchner, J 2003, 'Changing Rainfall - Changing Recharge?', in *Groundwater Recharge Estimation in Southern Africa*, eds Y Xu and HE Beekman, Unesco Publishing, Paris, pp. 179-188.
- Lahee, FH 1952, *Field Geology*, 5th edn, McGraw-Hill Book Company, New York.

- Lancaster, IN 1988, 'The Pans of the Southern Kalahari, Botswana', Unpublished PhD Thesis, Univ. of Cambridge.
- Le Maitre, DC, Scott, DF & Colvin, C 2000, 'Information on interactions between groundwater and vegetation relevant to South African conditions: A review', in *Groundwater : Past Achievements and Future Challenges. Proceedings of the XXX IAH Congress on Groundwater*, eds O Silolo et al. A.A. Balkema, Rotterdam, pp. 959-962.
- Lerner, D 2003, 'Surface Water - Groundwater Interactions in the Context of Groundwater Resources', in *Groundwater recharge estimation in southern Africa*, eds Y Xu and HE Beekman, Unesco Publishing Paris, pp. 91-107.
- Lloyd, JW 1999, *Water Resources of Hard Rock Aquifers in arid and semi-arid Zones*. UNESCO, France.
- Masterton, WL & Slowinski, EJ 1977, *Chemical Principles*. W.B. Saunders Golden Sunburst Series.
- Mazor, E 1997, *Chemical and Isotopic Groundwater Hydrology. The Applied Approach, 2nd Edition*, Marcel Dekker Inc. New York.
- McCarthy, T & Rubidge, B 2005, *The Story of Earth and Life, A southern African perspective on a 4.6-billion-year journey*, Struik Publishers, Cape Town.
- McWhorter, DB & Sunada, DK 1977, *Groundwater Hydrology and Hydraulics*, Water Resources Publications, Fort Collins, Colorado.
- Mendelsohn, J, Jarvis, A, Roberts C & Robertson, T 2002, *Atlas of Namibia. A Portrait of the Land and its People*, Ministry of Environment and Tourism, Republic of Namibia, David Philip Publishers, Cape Town.
- Miller, T. G. 1994. *Living in the Environment. Principles, Connections and Solutions*. 8th edn, Wadsworth Publishing Co., California.
- Mook, WG 2000, *Environmental isotopes in the hydrological cycle, Principles and Applications*, , Technical Documents in Hydrology, no. 39, vol I, IHP-V.
- Mook, WG 2000, *Environmental isotopes in the hydrological cycle, Principles and Applications*, , Technical Documents in Hydrology, no. 39, vol IV, IHP-V.
- Mook, WG 2001, *Environmental isotopes in the hydrological cycle, Principles and Applications*, Technical Documents in Hydrology, no. 39, vol II, IHP-V.
- Mphepya, JN, Pienaar, JJ, Galy-Lacaux, C, Held, G & Turner, CR 2004, 'Precipitation chemistry in semi-arid areas of Southern Africa: A case study of a rural and an industrial site', *Journal of Atmospheric Chemistry*, vol. 47, pp. 1-24.
- Mphepya, JN, Galy-Lacaux, C, Lacaux, JP, Held, G & Pienaar, JJ 2006, 'Precipitation chemistry and wet deposition in Kruger National Park, South Africa', vol. 53, pp. 169-183.

- Muskat, M 1946, *The flow of homogeneous fluids through porous media*, McGraw-Hill Book Company, Inc., United State of America.
- Netterberg, F 1978, Dating and correaltion of calcretes and other pedocretes, *Trans. Geol. S. Afr.*, vol. 81, p. 379-391
- Netterburg, F 1980, Geology of South African calcretes: 1. Terminology, description, macrofeatures, and classification, *Trans. Geol.Soc. S. Afr.*, vol 83, p. 255-283.
- Nkotagu, H 1997, Application of environmental isotopes to groundwater recharge studies in semi-arid fractured crysalline basement area of Dodoma, Tanzania. *Journal of African Earth Sciences*, vol. 22, no. 4, pp 443-457.
- Nyagwambo, NL 2006, 'Groundwater Recharge Estimation and Water Resources Assessment in a Tropical Crystalline Basement Aquifer', unpublished PhD. thesis, Delft University of Technology.
- Park, RG 1983, *Foundations of Structural Geology*, Blackie and Son Limited, Glasgow.
- Partidge, TC & Maud RR 1987, 'Geomorphic evolution of southern Africa since the Mesozoic,' *South African Journal of Geology*, vol.42, no. 2, 179-208.
- Partridge, TC, Avery, DM, Botha, GA, Brink, JS, Deacon, J, Herbert, RS, Maud, RR, Scholtz, A, Scott, AS, Talma, AS & Vogel, JC 1990, 'Late Pleistocene and Holocene climatic change in Southern Africa', *South African Journal of Science*, vol. 86, pp. 302-306.
- Penver, P, Roy, C, Brundrit, GB, de Verdiere, AC, Freon, P, Johnson, AS, Lutjeharms, JRE & Shillington, FA 2001, 'A Regional hydro-Dynamic model of upwelling in the Southern Benguela', *South African Journal Of Science* , vol. 97, pp. 472-475.
- Price NJ 1966, *Fault and Joint Development in Brittle and Semi-brittle Rock*. Pergamon Press, New York.
- Rankama, K & Sahama, ThG 1949, *Geochemistry*. The University of Chicago Press, Chicago.
- Reason, CJC, Engelbrecht, F, Landman, WA, Lutjeharms, JRE, Piketh, S, Rautenbach, C de W, and Hewitson, BC 2006, 'A review of South African Research in atmospheric science and physical oceanography during 2005-2006,' *South African Journal of Science*, vol. 102, pp. 35-45.
- Republic of South Africa 1998, National Water Act (Act No. 36 of 1998), Government Gazette, vol. 398, no. 19182, Cape Town.
- Rouault, M, Florenchie, P, Faucherau, N & Reason, CJC 2003, 'South East Tropical Atlantic warm events and southern African rainfall', *Geophysical Research Letters*, vol. 30, no. 5, pp. CLI 9-1 - CLI 9-4.

- Rouault, M, Jobard I, White SA & Lutjeharms JRE 2001, 'Studying rainfall events over South Africa and adjacent oceans using the TRMM satellite', *South African Journal of Science*, vol. 97, pp. 455-460.
- Sami, K 1992, 'Recharge mechanisms and geochemical processes in a semi arid sedimentary basin, Eastern Cape, South Africa', *Journal of Hydrology*, vol 139, pp. 27-47.
- Sharma, ML & Hughes, MW 1985, 'Groundwater Recharge Estimation using chloride, Deuterium and Oxygen-18 Profiles in the Deep Coastal sands of Western Australia', *Journal of Hydrology*, vol. 81 No1/2, pp. 93-109.
- Selaolo, ET, Gieske, ASM & Beekman, HE 1994, 'Chloride Deposition and Recharge Rates for Shallow Groundwater Basins in Botswana', *Water Down Under '94*, Adelaide, Australia, pp. 501-506.
- Šimonič, M 2002, '*Geostatistical Analysis of the National Groundwater Quality Monitoring Programme*', Department of Water Affairs and Forestry, Pretoria.
- Šimonič, M 1993, '*Implementation of National Groundwater Quality Monitoring in South Africa*', Department of Water Affairs and Forestry, Pretoria.
- Smit, PJ 1977, 'Die Geohidrologie in die Opvanggebied van die Moloporivier in die Noordelike Kalahari', PhD. Thesis University of Pretoria.
- South African Weather Services, n.d. General introduction and southern hemisphere meteorology.
- South African Committee for Stratigraphy (SACS) 1980, *Stratigraphy of South Africa, Part 1, Lithostratigraphy of the Republic of South Africa, South West Africa/Namibia, and the Republics of Bophuthatswana, Transkei and Venda*, comp LE Kent.
- Stanger, G 1994, *Dictionary of Hydrology and Water Resources*. Lochan Publishing, Hallett Cove, Southern Australia.
- Sukhija, BS, Reddy, DV, Nagabhushanam, P & Hussain, S 2000, 'Natural groundwater recharge assessment: Role of preferential flow in semi-arid fractured aquifers', in *Groundwater : Past Achievements and Future Challenges. Proceedings of the XXX IAH Congress on Groundwater*, eds O Silolo et al. A.A. Balkema, Rotterdam, pp 331-336.
- Tankard, AJ., Jackson, MPA., Eriksson, KA, Hobday, DK, Hunter, DR & Minter, WEL 1982, *Crustal Evolution of Southern Africa. 3.8 Billion Years of Earth History*. Springer-Verlag, New York Heidelberg Berlin.
- Thomas, DSG & Shaw, PA 1991, *The Kalahari Environment*, Cambridge University Press, Cambridge.

- Ting, CS, Zhou,Y, De Vries, JJ & Simmers, I 1998, 'Development of a Preliminary Groundwater Flow Model for Water Resources management in the Pingtung Plain, Taiwan', *Ground Water*, vol. 36, no.1, pp. 20-36.
- Tredoux, G 2008, *Personnal Communication*. Natural Resources and the Environment, Council for Scientific and Industrial Research, Stellenbosch.
- Turner, BR (ed) 1979, *Geology of the uraniferous Beaufort Group near Beaufort West*, Guide Book, Geokongres 79, Geological Society of South Africa.
- Tyson, PD 1986, *Climatic change and variability in southern Africa*, Oxford University Press.
- Uil, H, van Geer, FC, Gehrels, JC & Kloosterman, FH 1999, *State of the art on monitoring and assessment of groundwaters*, UN/ECE Task Force on Monitoring and Assessment, vol. 4, Netherlands Institute of Applied Geoscience TNO, Delft, The Netherlands.
- Van der Merwe, CL 2008, 'Impact of scale dependence of aquifer parameters on sustainable borehole yield estimations,'. Unpublished M.Sc Thesis, Faculty of Natural and Agricultural Sciences, Department of Geohydrology, Univ. of the Free State, Bloemfontein South Africa.
- Van der Watt H & van Rooyen, TH 1990. A Glossary of Soil Science, pp. 356.
- Van Heerden, J & Hurry, L 1992, '*Southern Africa's Weather Patterns. An Introduction Guide*', Acacia Books, Pretoria.
- Van Lanen, HAJ 1998. Monitoring for Groundwater Management in (Semi-arid) Regions. Unesco Publishing, Paris.
- Van Tonder, GJ & Bean JA 2003, 'Challenges in Estimating Groundwater Recharge', in *Groundwater Recharge Estimation in Southern Africa*, eds Y Xu and HE Beekman, Unesco Publishing, Paris.
- Van Tonder, GJ & Xu, Y 2001, 'A Guide for the Estimation of Groundwater Recharge in South Africa', Institute for Groundwater Studies, University of the Free State.
- Van Wyk, E 2003, 'Establishment of Departmental National and Regional Hydrological Monitoring Committees (Groundwater)', Memorandum, Department of Water Affairs and Forestry:
- Vegter, JR 1995, 'An Explanation of a Set of National Groundwater Maps', Water Research Commission report TT74/95.
- Vegter, JR 2001, 'Groundwater Development in South Africa and an Introduction to the Hydrogeology of Groundwater Regions', Water Research Commission report TT134/00.
- Venter, BL 2004. *Personnal Communication*. Department of Water Affairs and Forestry. Pretoria.

- Verhagen, BTh 1984, 'Environmental isotope study of a groundwater supply project in the Kalahari of Gordinia', *Isotope hydrology 1983*, IAEA-SM-270/50, pp. 415-433.
- Verhagen, BTh, Butler MJ, Levin M & Van Wyk E 2000, 'Environmental isotopes assist in groundwater sustainability assessment of the Taaibosch fault zone, Northern Province, South Africa', in *Groundwater: Past Achievements and Future Challenges. Proceedings of the XXX IAH Congress on Groundwater*, eds O Silolo et al. A.A. Balkema, Rotterdam, pp 673-678.
- Verhagen, BTh, Bredenkamp, DB & Botha, LJ 2001, Hydrogeological and isotopic assessment of the response of a fractured multi-layered aquifer to long-term abstraction in semi-arid environment, Water Research Commission, project no. 565/1/01.
- Verhagen, BTh 2010, *Personal communication*, Professor Emiritus, School for Geosciences, University of the Witwatersrand, Johannesburg.
- Verhagen, BTh & Talma, S 2009, *Personal Communication*, Former Isotope Specialist, QUADRO Laboratory, Council for Scientific and Industrial Research.
- Vogel, JC & Van Urk, H 1975, 'Isotopic composition of groundwater in semi-arid regions of southern Africa,' *Journal of Hydrology*, vol. 25, p. 23-36.
- Walton, WC 1970, *Groundwater Resource Evaluation*, McGraw-Hill Book Company, New York.
- Wang, HF & Anderson, MP 1982, *Introduction to Groundwater Modeling. Finite Difference and finite Element Methods*, W.H. Freeman and Co. San Francisco.
- Weaver, JMC & Talma, AS 2005, 'Evaluation of Groundwater flow patterns in Fractured Rock Aquifers using CFCs and Isotopes', Water Research Commission, report no. 1009/1/03.
- Weaver, JMC & Talma, SA 2005, 'Cumulative rainfall collectors - A tool for assessing groundwater recharge', *Water SA*, vol. 31, no. 3, pp. 283-290.
- Wiegman, F. W., 2006. *Personal Communication*. VSA Geo-Consultants, Pretoria.
- Willeminck, J 1988, Estimating Natural Recharge of Groundwater by Moisture Accounting and Convolution, in: I. Simmers (ed.), *Estimation of natural groundwater recharge*, NATO ASI series C222, Reidel Publishing, Dordrecht, pp. 283-300.
- Woodford, AC & Chevallier, L 2002a, '*Regional characterization and mapping of the Karoo fractured aquifer systems - an integrated approach using geographical information systems and digital images*', Water Research Commission, report 653/1/02, Republic of South Africa.
- Woodford, AC & Chevallier, L (eds) 2002b, '*Hydrogeology of the Main Karoo Basin: Current Knowledge and Future Research Needs*', Water Research Commission Report TT 179/02, Republic of South Africa.

World Meteorological Organization 1989, *Management of groundwater observation programmes*, Operational Hydrological Report No. 31, WMO No. 705, World Meteorological Organization, Geneva, Switzerland.

Xu,Y & Beekman, HE (eds) 2003, *Groundwater Recharge Estimation in Southern Africa*, Unesco Publishing, Paris.

9. APPENDIXES.

Included in Attached DVD.

- 9.1 Appendix 1: Comprehensive Hydrological Assessment and Research Tool, CHART.
- 9.2 Appendix 2: Hydrological Instrumentation used in groundwater and rainfall monitoring in South Africa.
- 9.3 Appendix 3. Experimental Monitoring Terrains.
- 9.4 Appendix 4. Images Library
- 9.5 Appendix 5 Collection of Typical Hydrograph-Hyetograph information sets from a selection of Monitoring sites in South Africa.
- 9.6 Appendix 6. Summary of South African Weather Services rainfall information applied in assessment of *Frequency of Exceedance*.
- 9.7 Appendix 7. Application of the Vertical Flow and Horizontal Drainages Resistances.
- 9.8 Appendix 8. Long-term Hydrochemistry *Time-series* Trends in the vicinity of the Monitoring sites.
- 9.9 Appendix 9: CMB: Traditional Point - Depth Interval - Soil Moisture Method.
- 9.10 Appendix 10. Environmental Stable Isotopes Application for Characterizing Groundwater Recharge Mechanisms.
- 9.11 Appendix 11: A collection of Vertical Chloride (Cl^-) and Stable Isotope ($\delta^2\text{H}$ and $\delta^{18}\text{O}$) profiles from monitoring site's.
- 9.12 Appendix 12. Evaluation of Rainfall Intensities (R_{RT}) - Rain fall Depths (R_{eff}) versus Water Table Responses.
- 9.13 Appendix 13. Assessment of Case Studies on Episodic Recharge in Semi-Arid Environments.

End of Document.